# Dynamic Methods for the Prediction of Survival Outcomes using Longitudinal Biomarkers

by

Krithika Suresh

A dissertation submitted in partial fulfillment
of the requirements for the degree of
Doctor of Philosophy
(Biostatistics)
in the University of Michigan
2018

Doctoral Committee:

Professor Jeremy M.G. Taylor, Co-Chair
Professor Alexander Tsodikov, Co-Chair
Professor Edward L. Ionides
Professor Douglas E. Schaubel
Research Associate Professor Matthew J. Schipper

Krithika Suresh

ksuresh@umich.edu

ORCID iD: 0000-0001-7785-3536

To my family, my necessary and sufficient condition.

# ACKNOWLEDGEMENTS

This dissertation marks the completion of a wonderful and rewarding journey at the University of Michigan. During this time of intense learning, I grew considerably both on an academic and a personal level. To all the people who provided me with support, guidance, and encouragement, I would like to express my heartfelt gratitude.

First, I would like to thank my co-chairs, Jeremy Taylor and Alex Tsodikov, whose expertise and guidance have contributed greatly to my graduate experience. Jeremy has been an excellent academic advisor since my arrival at Michigan. He has encouraged me to pursue numerous opportunities to advance my learning and research. He is always generous with his time, whether to provide academic advice, discuss a research question, or read countless drafts of a manuscript. His insightful feedback and meticulous comments have been invaluable in shaping this dissertation. Alex has been instrumental in developing my knowledge of survival analysis. He has been a very patient teacher and inspired new ideas that have contributed greatly to my dissertation. I would also like to convey my sincere appreciation to my GSRA advisor, Matt Schipper, for his mentorship and words of encouragement. He has provided me with a multitude of opportunities that have helped me gain invaluable experience and confidence as a researcher. It has been a pleasure working with him and the UM Department of Radiation Oncology. In addition, I am grateful to the rest of my committee: Doug Schaubel and Ed Ionides, for their enthusiastic feedback and thought-provoking questions. Finally, to Tom Braun and Tim Johnson, who were excellent instructors and positive figures in the department.

My studies at Michigan were made so much more enjoyable because of my fellow

students, whose friendship has meant so much to me. I want to thank Nick Seewald, Allison Cullen Furgal, Lauren Beesley, Matthew Flickinger, Rebecca Rothwell, Marco Benedetti, Evan Reynolds, Mathieu Bray, Wenting Cheng, Emily Roberts, Kelly Speth, Lu Tang, Cui Guo, and Yilun Sun. I am especially grateful to Michelle Earley for all of the laughter during both the happy and difficult moments of the degree.

I am forever thankful to my amazing family for their unconditional love and support. My parents, Uma and Suresh, for instilling in me a passion for learning and always encouraging me to pursue my goals. My sister, Ragini, who is my biggest cheerleader, and a constant source of positivity, inspiration, and strength.

Lastly, I would like to thank my husband, John, for his unwavering confidence in me. Also, for his love, encouragement, and editing assistance that made finishing this dissertation possible.

# TABLE OF CONTENTS

# LIST OF FIGURES

**Figure**

# LIST OF TABLES

**Table**

# LIST OF APPENDICES

**Appendix**

# ABSTRACT

In medical research, predicting the probability of a time-to-event outcome is often of interest. Along with failure time data, we may longitudinally observe disease markers that can influence survival. These time-dependent covariates provide additional information that can improve the predictive capability of survival models. It is desirable to use a patient's changing marker information to produce updated survival predictions at future time points, which can in turn direct individualized care decisions. In this dissertation, we develop methods that incorporate time-dependent marker information collected during follow-up with the aim of dynamic prediction and inference.

In Chapter I, we compare two methods of dynamic prediction with a longitudinal binary marker, represented by an illness-death model. Joint modeling is a unified, principled approach that produces consistent predictions over time; however, it requires restrictive distributional assumptions and can involve computationally intensive estimation. Landmarking fits a Cox model at a sequence of prediction, or "landmark", times and is easily implemented, but does not produce a valid prediction function. We explore the theoretical justification and predictive capabilities of these methods, and propose extensions within the landmark framework to provide a better approximation to the true joint model.

In Chapter II, we present an approximate approach for obtaining dynamic predictions that combines the advantages of joint modeling and landmarking. We specify the marginal marker and failure time distributions conditional on surviving up to a prediction time, and use a Gaussian copula to link them over time with an association function. We use a single model for the time-to-event outcome from which the conditional survival is derived, achieving a greater level of consistency than landmarking. Estimation is conducted using a

two-stage approach that reduces the computational burden associated with joint modeling.

In Chapter III, we introduce a model that incorporates the effects of a partially observed marker on failure time. We consider the marker to represent an underlying stochastic risk process that accumulates over time until a failure is experienced. We model this increasing risk as a Lévy bridge process that has a multiplicative effect on the cumulative hazard. Using the mathematically tractable properties of the gamma process, we derive the marginal and conditional survival functions, and demonstrate estimation when the process is observed at the survival time. This approach can be extended to multiple measurement times, and applied to a variety of markers and disease settings where the correct marker distribution is not known or difficult to specify.

# INTRODUCTION

The primary goal of survival analysis is to analyze a time-to-event outcome with the aim of predicting or inferring about its probability of occurrence at a future time point. Traditional survival methods use covariates collected at a baseline time to model the risk of the survival event. However, there is also often interest in incorporating the effects of stochastic covariates that can change over time. With continued follow-up beyond baseline and increased interest in longitudinal studies, these covariates may be partially observed, providing additional information that could improve inference and produce more accurate survival predictions. In this dissertation, we consider dynamic survival models and prediction methods that incorporate the effects of longitudinally collected covariates on time-to-event outcomes.

In the first two chapters, we focus on the statistical task of dynamic prediction. Prediction models for a time-to-event outcome, such as relapse or death, are commonly used in clinical practice to quantify risk for a subject with a given set of characteristics. To tailor a patient's treatment strategy, clinicians can use these models to answer important questions, such as "What is the risk of the patient relapsing in the next 3 years?" However, traditional prediction models only inform clinicians on patient outcomes at a baseline time. Advancements in medical technology and treatments have led to improved patient survival, and thus allow for continued patient follow-up during which updated patient information (e.g., biomarker measurements, intermediate outcomes) is collected. Thus, given the patient is alive one year into treatment, their risk profile may have changed and the answer to the question above will be different. Dynamic prediction models incorporate time-varying patient information to produce an updated, more accurate risk

prediction for patients at follow-up times beyond baseline. This prediction plays a vital role in directing individualized clinical decisions for the patient.

Let $T$ be the time to the survival event and $Z(t)$ be the marker process that can be continuously or longitudinally observed. The aim of dynamic prediction is to develop a model from which, for a particular prediction time of interest, referred to as the "landmark time" $\tau$, and prediction window $s$, we can obtain the dynamic prediction $P(T > \tau + s | T > \tau, \bar{Z}(\tau))$, where $\bar{Z}(t)$ is the history of $Z$ up to time $\tau$. This is the conditional survival probability of surviving up to time $\tau + s$ given being alive at time $\tau$ and the up-to-date marker information at that time.

In Chapter I, we compare two methods for obtaining this dynamic prediction, namely *landmarking* (van Houwelingen, 2007; Zheng and Heagerty, 2005; Gong and Schaubel, 2013) and *joint modeling* (Taylor et al., 2005, 2013; Rizopoulos, 2011; Rizopoulos et al., 2013). This work was motivated by a condition described in Jewell and Nielsen (1993) that requires that the joint distribution of the marker process and survival time, $[T, Z]$, be specified to obtain a valid prediction function, from which the conditional survival prediction above can be derived. Joint modeling achieves this by specifying a model for the marker $[Z]$, and a model for the relationship between the marker and the hazard $[T|Z]$. Landmarking, however, is an approximate approach that specifies only a component of the joint distribution by modeling the residual time distribution conditional on the marker, $[T|T > \tau, Z(\tau)]$, directly at each $\tau$. Thus, it fails to produce predictions that are consistent with those at other time points. The benefit of landmarking is that it uses the Cox model to define the conditional residual time distribution and thus is easily implementable in standard software. Joint modeling requires the restrictive assumption of correctly specifying the joint distribution and can involve computationally intensive estimation. We explore the merits of the two approaches with the aim of identifying the effect that violating this consistency condition has on predictive performance, and the extent to which this justifies using an inconsistent model with easier estimation.

We examine the two methods in the context of a binary marker representing the occurrence of an intermediate event beyond baseline. The joint distribution of the marker and failure time is modeled with an irreversible illness-death model. We begin with this simple situation because it allows us to derive the form for the landmarking model from the true joint model to identify relationships that should be incorporated into the landmarking framework to provide a better approximation. We consider scenarios with one or two baseline covariates that have differential effects on the different transitions in both a Markov and a semi-Markov setting. We compare the predictive performance of the methods with a simulation study and demonstrate their application using a dementia data set where the marker is observed at regular measurement times, and a prostate cancer study where the marker is continuously observed.

By contrasting the joint modeling and landmarking approaches, we aim to identify whether by incorporating additional flexibility we can extend the landmark model to perform similarly to the joint model. Although landmarking does not constitute a unified approach to dynamic prediction, in situations where joint modeling can be too restrictive or cumbersome for estimation (e.g., sparse data), an approximate approach can be a sufficient, and perhaps necessary, alternative. However, beyond violating the consistency condition, there are other limitations of landmarking. It requires prespecifying the prediction times and prediction window, and its estimation relies on imputing marker values for individuals at prediction times at which they are not observed. Thus, although both methods exhibit good predictive performance, both have limitations that make them unsuitable or undesirable for use in certain situations.

In Chapter II, we introduce an alternative approximate approach for obtaining dynamic predictions that aims to combine the advantages of landmarking and joint modeling, overcome their limitations, and maintain good predictive performance. Describing the dependence between the the marker process and failure time distributions by specifying their joint distribution can be difficult and require restrictive assumptions. Thus,

we consider modeling the marginals for the marker at each landmark time and the failure time distribution, for which it can be easier to assess goodness-of-fit and identify the best-fitting models. In the dynamic prediction framework, we specifically model the marginal distributions conditional on being alive at a particular observation time, $Z_\tau = [Z|T > \tau]$ and $T_\tau = [T|T > \tau]$. We can specify these from a known class of models, for which established estimation and model selection techniques are available in standard software. To achieve a greater level of consistency than landmarking, we specify a marginal model for $[T]$ and then derive the conditional survival function from this single model. We then need a method by which we can link these marginals while accounting for their dependence, thus we consider a Gaussian copula (Song et al., 2009; Pitt et al., 2006).

Gaussian copulas, which stem from the field of quantitative finance, have been previously employed for modeling the joint distribution of marker and failure time processes (Rizopoulos et al., 2008a,b; Ganjali and Baghfalaki, 2015), but have yet to be applied in the area of dynamic prediction. With the copula, we can join the two marginals, $Z_\tau$ and $T_\tau$, together to give us a model for the joint distribution conditional on being alive at a particular time $\tau$, $[T, Z|T > \tau]$. The copula contains an association parameter that describes the dependence between the marginal distributions. The association will be negative if higher values of a continuous marker or having experienced the intermediate event represented by a binary marker are correlated with decreased time to the failure event. In certain disease settings, the association between $Z_\tau$ and $T_\tau$ might depend on baseline information and can also increase or decrease as we make predictions further away from baseline. Thus, we specify the association to be a flexible function of baseline covariates and observation time $\tau$. Estimation is performed using a two-stage approach commonly applied with copulas (Joe and Xu, 1996), where in the first stage estimates are obtained for the parameters from the marginal models and are then held fixed in the second stage to estimate the association function parameters. Using the tractable nature of Gaussian copulas, the desired distribution $[T|T > \tau, Z(\tau)]$ can then be computed.

This novel method for dynamic prediction aims to introduce a class of flexible models that overcomes the computational burden of estimation posed by joint modeling. In addition, it does not necessitate prespecifying the prediction times or horizon, as is required by landmarking. We describe our approach for both binary and continuous marker situations, and compare the predictive performance with joint modeling and landmarking using simulation studies. We demonstrate computing dynamic predictions with our proposed method in the binary setting using a prostate cancer data set, and in the continuous setting using a heart valve data set.

In Chapter III, we propose an alternative survival model specification for incorporating the effects of a partially observed covariate on survival. In cancer research, we are often faced with marked data, where we consider the marker to be an underlying stochastic process that is observed only at the survival time, giving us a current status observation and a cross-sectional surrogate (or "mark") of the latent stochastic process. With this very sparse data, the previously considered methods for dynamic prediction in this dissertation are inadequate. Both joint modeling and the copula approach require specifying a function for the marker trajectory or distribution, for which there may not be enough longitudinal observations to properly estimate. Landmarking will introduce bias into the estimates and predictions because it imputes the value of the marker at missing intermediate measurements. Thus, we consider modeling the marker as a stochastic process, allowing for more flexible behavior during periods in which the marker is not observed.

We consider the marker to represent an underlying stochastic risk process for each individual that accumulates over time until the person experiences the failure event. Thus, we can consider the problem in the context of a time-dependent frailty. Gjessing et al. (2003) present a generalization of proportional hazards frailty models where the frailty is considered to be a stochastic process and multiplicatively affects the hazard function. Continuous non-negative Lévy processes have been a popular choice for the frailty process due to the tractable form of their Laplace functional and their preservation of the non-

negative hazard function property. This poses a restriction of non-decreasing hazard rate. In addition, this framework assumes that the frailty process is completely unobserved.

To alleviate these limitations, we propose using the non-decreasing Lévy bridge process family more naturally as a multiplicative effect on the cumulative hazard function. We specifically consider a gamma process with mean and variance specified as a function of baseline covariates, and extend existing theory from a similar gamma bridge financial model for aggregate claims data (Hoyle, 2010; Brody et al., 2008) to a survival framework. Using the tractable nature of this process, we derive the marginal and conditional survival functions and describe the extension to multiple measurement times. By specifying a joint model, we also derive dynamic predictions of the marker value conditional on being alive at a particular time. The proposed survival model can be utilized for dynamic prediction, but also provides inference about covariate effects on both the survival probability and the marker behavior. The flexibility of this model specification allows it to be applied to a variety of marker and disease process settings where the correct marker distribution is not known or is difficult to specify. With a simulation study, we evaluate the effectiveness of our method for inference and its sensitivity to misspecification. We demonstrate its usage for survival and marker prediction using a motivating prostate cancer data set, where prostate-specific antigen (PSA) is modeled as a stochastic process that develops over time and can affect survival.

# CHAPTER I

# Comparison of Joint Modeling and Landmarking for Dynamic Prediction under an Illness-Death Model

## 1.1 Introduction

As survival outcomes for patients improve, there is additional follow-up information available and increased interest in predicting conditional survival for patients at a time beyond diagnosis or treatment. To achieve the most accuracy, prediction models should incorporate patient information that evolves over time and was collected during follow-up. The statistical task is to develop a technique that can quantify survival probability predictions at baseline, and produce updated risk predictions at future time points for patients who are still alive by including their new marker information.

Recent literature has explored obtaining dynamic predictions with the use of joint models for longitudinally measured markers and time-to-event outcomes (Taylor et al., 2005; Rizopoulos, 2011; Taylor et al., 2013; Rizopoulos et al., 2013). Joint modeling requires the specification of a model for the marker process, a model for the survival outcome, and a method by which to link the two models (Henderson et al., 2000). This is sufficient to obtain the joint distribution of the marker process and failure time, from which the residual time distribution can be easily derived at any landmark time of interest. Computing conditional survival probabilities from this distribution may involve

numerical integration and require substantial computation. Joint models require correct specification of the joint distribution of the marker process and the event time and can require computationally intensive techniques for estimation. To avoid making distributional assumptions about the marker process and to reduce the computational burden, approximate approaches for dynamic prediction have been developed that specify a model for only a component of the joint distribution of the marker and failure time processes.

One such approach to dynamic prediction is called "landmarking". This approach was first introduced in the context of clinical oncology by Anderson et al. (1983) as an alternative to a Cox model with a time-dependent covariate. In van Houwelingen (2007), the landmarking approach applies a simple Cox proportional hazards model to the data of individuals still alive at $\tau$, and the resulting estimates are used to predict the probability of surviving up to a fixed horizon, $\tau + s$. To link the landmark models, the estimated effects are allowed to change with landmark time in a smooth way. Since this method can be implemented using the Cox model, and since time is always measured from the original time origin, estimation can be conducted based on a partial log-likelihood method. Zheng and Heagerty (2005) proposed a similar approach called "partly conditional survival modeling", which describes landmarking in the context of resetting the clock at the landmark time. Gong and Schaubel (2013) combine landmarking and partly conditional methods to address the situation of dependent censoring.

The appeal of landmarking is that it avoids specifying the distribution of the stochastic marker process in time. However, as demonstrated by Jewell and Nielsen (1993), approximate approaches fail to produce predictions that are consistent (i.e., have a defined relationship) with predictions at other landmark times. Valid prediction functions require the definition of a model for the stochastic marker process and the functional relationship between the marker and the hazard at any given time. The residual time distribution, upon which predictions are based, is determined by the hazard at $w = \tau + s, s > 0$ conditional on event time $T > \tau$ and marker process $Z(\tau)$. The consistency condition proposed

by Jewell and Nielsen (1993) states that if the hazard function is determined by $Z(t)$ and denoted $h(t, Z(t))$, the hazard at all times $w > \tau$ cannot be arbitrarily chosen but must be computed from $h(w|\tau, Z(\tau)) = \mathrm{E}[h(w, Z(w))|T > \tau, Z(\tau)]$, where the expectation is with respect to the distribution of $Z$ between $\tau$ and $w$. Thus, specification of the marker process distribution is necessary to link the hazards over time to produce consistent predictions. Under the landmarking approach, the model for $h(w|\tau, Z(\tau))$ is chosen to have the form of a Cox regression, which can be easily fit using standard software. Thus, landmarking produces a sequence of best-fitting Cox models at each landmark time and there is no restriction on the predictions from each Cox model being consistent with those at earlier time points. Based on this violation of the consistency rule, an approach for prediction models that is based on modeling only the residual time may result in theoretically incorrect models.

It is well known that the residual time distribution based on a time-varying marker will depend on the stochastic process of the marker (Kalbfleisch and Prentice, 2011). Jewell and Kalbfleisch (1996) provided some specific examples of residual time distributions for additive models. Shi et al. (1996) showed that if the marker is following a Brownian motion then a reasonable approximation to the residual time distribution is based on the linear transformation model $(T-\tau)^{1/3} = g(Z(\tau)) + \epsilon$, where $g$ is a monotonic function and $\epsilon$ has a constant variance distribution. In discussing differences between a time-dependent Cox model and a landmarking approach, Putter and van Houwelingen (2016) showed that a proportional hazards assumption will not in general be valid for the landmarking model. Whether the lack of theoretical justification for the landmarking approach is a practical concern may depend on what landmarking models are used. Extensions in the landmark framework that increase flexibility may provide a sufficiently good approximation to the true residual time distribution.

The comparison of predictive performance between joint models and landmarking approaches has been recently explored in the statistical literature. Cortese et al. (2013)

compared predictions of cumulative incidence between a multi-state model and landmark approaches under competing risks, and found that the two modeling strategies had nearly identical predictive accuracy. Rizopoulos et al. (2013) demonstrated the superiority of the survival prediction accuracy of a joint model over landmarking under various functional forms of the association structure between a continuous longitudinal marker and failure time processes. Maziarz et al. (2017) proposed two models in the partly conditional modeling framework and compared them to a joint model by simulating data from a shared random-effects model. They showed that predictions obtained from partly conditional survival models are comparable to those from a joint model, but that partly conditional models have better computational efficiency.

We aim to contribute to this literature by contrasting landmark and joint models for dynamic prediction in the context of a binary longitudinal marker, represented by an illness-death model. In Section 1.2, we introduce notation for landmark and joint models and derive their predicted probabilities in the context of the illness-death model. Section 1.3 demonstrates that the landmark approach with a standard Cox model does not satisfy the consistency condition of Jewell and Nielsen (1993), and suggests extensions to provide a better approximation. Section 1.4 compares the performance of landmark and joint models using a simulation study. In Section 1.5, we apply these methods to cognitive aging data from the PAQUID study and metastatic clinical failure data from a prostate cancer study, and conclude with a discussion in Section 1.6.

## 1.2 Approaches for Dynamic Individualized Predictions

Let $\mathcal{D}_n = \{T_i^*, \delta_i, \mathbf{X}_i, \mathbf{Z}_i; i = 1, \ldots, n\}$ denote the observed data, where $T_i$ is the true event time, $C_i$ is the censoring time, $T_i^* = \min(T_i, C_i)$ is the observed event time, $\delta_i = \mathbf{1}(T_i \leq C_i)$ is the censoring indicator, $\mathbf{X}_i$ is the baseline covariate vector, and $\mathbf{Z}_i$ is the longitudinal marker vector, with $z_{il} = Z_i(t_{il})$ denoting the marker value at time $t_{il}, l = 1, \ldots, n_i$, for subject $i$.

The aim is to obtain a prediction probability for a new subject, $j$, from the same population, who has current marker and baseline covariate data available. Specifically, we are interested in obtaining a prediction probability of surviving up to time $\tau+s$, $s>0$, given that subject $j$ has survived up to time $\tau$, i.e.,

$$p_j(\tau+s|\tau) = \Pr(T_j \geq \tau+s|T_j > \tau, \mathcal{D}_n, \mathbf{X}_j, Z_j(\tau)) \tag{1.1}$$

where $Z_j(\tau)$ denotes the subject's marker value at time $\tau$. In this probability statement, $\tau$ is called the landmark time and $s$ is the prediction window. The dynamic nature of this prediction probability lies in its ability to be updated as new information for patient $j$ becomes available at time $\tau^* > \tau$, to produce the new prediction $p_j(\tau^*+s|\tau^*)$. Implicit in Eq.(1.1) is that the value of $Z$ is known for subject $j$ at time $\tau$. In practice this may not be the case. An alternative target of interest is to change Eq.(1.1) to condition on the known history of $Z$ up to time $\tau$ for subject $j$.

### 1.2.1 Joint Modeling

Joint modeling requires the full specification of the joint distribution of the longitudinal marker process and the survival data. The joint density is often factored into a product of the densities of $Z$ and $T|Z$, which requires specifying the model for the longitudinal marker process and a model for the event times with dependence on the defined marker process. As shown in Jewell and Kalbfleisch (1992) and Shi et al. (1996), once these distributions are specified the residual time distribution can be derived.

If $Z$ is a discrete random variable, joint modeling consists of formulating a process for the transitions between the states of $Z$ and defining the relationship between the covariate process and survival using a hazard function for $T$. This is sufficient to derive the joint distribution of $Z$ and $T$, from which the residual time distribution is then determined.

The irreversible illness-death model is the simplest example of discrete $Z$. In this model, $Z$ is binary with only two states {0,1}, all subjects start in state 0, and transitions

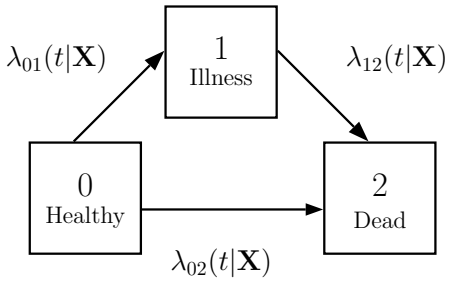


**Figure 1.1:** An irreversible illness-death model depicting three states, 0 (Healthy), 1 (Illness), and 2 (Dead), and the transition intensities between state $j$ and state $k$ ($\lambda_{jk}(t|\mathbf{X})$), where $\mathbf{X}$ is a vector of baseline covariates that can have transition-specific effects.

from state 1 to state 0 are not allowed. Let $T$ be the time to death, which is a terminal state. Then the joint distribution of $Z$ and $T$ can be described as a simple three-state illness-death model (0: Healthy, 1: Illness, 2: Dead), as shown in Figure 1.1. We then define the time-varying covariate process $Z(t) \in \{0, 1\}$ as an indicator of whether an individual has progressed from the "healthy" state to the "illness" state by time $t$. In this model, $\lambda_{jk}(t|\mathbf{X})$ describes the hazard of transitioning from state $j$ to state $k$ at time $t$ conditional on the baseline covariate vector $\mathbf{X}$, which can have a different effect on each transition. We assume that the clock does not reset once an individual has transitioned into the illness state, and thus $t$ is time since baseline. As well, we can model the rate of transition to be dependent on the duration in the current state for those in the ill state. Under the illness-death model, the residual time distribution conditional on $Z(\tau)$ is:

$$\begin{aligned}\Pr(T \geq \tau + s | T > \tau, \mathbf{X}, Z(\tau) = 0) &= \exp\left\{ -\int_{\tau}^{\tau+s} [\lambda_{02}(u|\mathbf{X}) + \lambda_{01}(u|\mathbf{X})]\, \mathrm{d}u \right\} \\ &+ \int_{\tau}^{\tau+s} \exp\left\{ -\int_{\tau}^{v} [\lambda_{02}(u|\mathbf{X}) + \lambda_{01}(u|\mathbf{X})]\, \mathrm{d}u \right\} \lambda_{01}(v|\mathbf{X}) \exp\left\{ -\int_{v}^{\tau+s} \lambda_{12}(u|\mathbf{X})\, \mathrm{d}u \right\} \mathrm{d}v \end{aligned} \tag{1.2}$$

$$\Pr(T \geq \tau + s | T > \tau, \mathbf{X}, Z(\tau) = 1) = \exp\left\{ -\int_{\tau}^{\tau+s} \lambda_{12}(u|\mathbf{X})\, \mathrm{d}u \right\} \tag{1.3}$$

In Eq.(1.2) the first term represents the probability that the individual remained in state 0 from time $\tau$ to $\tau + s$, and the second term is the probability the individual transitioned from state 0 to 1 at time $v \in (\tau, \tau + s)$ and then remained in state 1 from time $v$ to $\tau + s$.

The observed data is given as $\mathcal{D}_n = \{T_i^*, \delta_i, \mathbf{X}_i, \mathbf{Z}_i, V_i; i = 1, \ldots, n\}$, where in addition to the previously described notation, $V_i$ is the known, exact transition time from state 0 to state 1 for the $i$th individual if they have transitioned. Thus, using a joint model approach, the full likelihood can be written as

$$\begin{aligned} L = \prod_i & \exp\left[-\left\{1 - Z_i(T_i^*)\right\}\left\{\Lambda_{01}(T_i^*|\mathbf{X}_i) + \Lambda_{02}(T_i^*|\mathbf{X}_i)\right\}\right] \lambda_{02}(T_i^*|\mathbf{X}_i)^{\delta_i(1-Z_i(T_i^*))} \\ & \times \exp\left[-Z_i(T_i^*)\left\{\Lambda_{01}(V_i|\mathbf{X}_i) + \Lambda_{02}(V_i|\mathbf{X}_i)\right\}\right] \lambda_{01}(V_i|\mathbf{X}_i)^{Z_i(T_i^*)} \\ & \times \exp\left[-Z_i(T_i^*)\left\{\Lambda_{12}(T_i^*|\mathbf{X}_i) - \Lambda_{12}(V_i|\mathbf{X}_i)\right\}\right] \lambda_{12}(T_i^*|\mathbf{X}_i)^{\delta_i Z_i(T_i^*)} \end{aligned}$$

where $\Lambda_{ij}(t|\mathbf{X}) = \int_0^t \lambda_{ij}(u|\mathbf{X})\,\mathrm{d}u$ is the cumulative hazard. Using the likelihood, parameter estimates of the joint model can be obtained, from which the desired residual time distribution in Eqs.(1.2) and (1.3) are computed. Since it is unlikely that the exact transition times are observed in practice, this likelihood can be adjusted to accommodate interval-censored observation times (Commenges, 2002). Alternatively, a semi-Markov model, for which the transition to death from the illness state depends on the duration in the illness state, can be fit (Foucher et al., 2010).

### 1.2.2 Landmarking

Landmarking describes the approach in which models are proposed and estimation is conducted at a set of prediction times of interest, defined as landmark times. There are several models and estimation methods that exist within the landmarking framework. After a model is selected and fit, the required residual time distribution given by Eq.(1.1) can be calculated.

The idea behind landmarking is to pre-select a landmark time, $\tau$, at which there is interest in making a prediction. Given access to a database of patient information, if we were interested in predicting survival up to time $\tau + s$ for patients still alive at $\tau$, we could select all the patients in the database alive at $\tau$ and estimate the probability of

survival at $\tau + s$ using a survival model (e.g., Cox proportional hazards model). We may also be interested in considering many landmark times, $\tau_1, \tau_2, \ldots, \tau_L$, and developing a prediction model for each. To do this we construct a prediction data set for each landmark time, $\tau_l$, which consists of individuals still alive at $\tau_l^-$, with administrative censoring at a pre-specified horizon, $t_{\text{hor}} = \tau_l + s$. These landmark data sets are then stacked to create a "super prediction data set" to which the landmark models are applied. We note that with the selection of multiple landmark times, the same patient contributes to the estimation of many of the predicted residual time distributions. It is also necessary that every subject have a value of $Z$ at every landmark time. In practice this may not be the case, and $Z$ must be imputed from a model for $Z$, or more commonly by using the last-observation-carried-forward (LOCF) approximation, which will be the method used in this chapter.

In the most basic application of landmarking, we fit a separate model to each landmark data set and estimate a landmark-specific effect of the marker for predicting survival between $\tau$ and a fixed horizon $t_{\text{hor}} = \tau + s$. The **basic landmark model** is given as

$$h(t|\tau, Z(\tau), \mathbf{X}) = h_0(t|\tau) \exp\{\beta_\tau Z(\tau) + \boldsymbol{\zeta}'\mathbf{X}\} \quad \text{for } \tau \leq t \leq t_{\text{hor}}$$

where, the dependence of the baseline hazard on $\tau$ can be modeled by estimating a different baseline hazard for each $\tau$, i.e., $h_0(t|\tau) = h_{0\tau}(t)$.

As an alternative, we can apply a "super prediction model" to the stacked super data set and allow the regression coefficients to depend on landmark time in a smooth, parametric way, such as with a linear or a quadratic function. This **super model** is defined as

$$h(t|\tau, Z(\tau), \mathbf{X}) = h_0(t|\tau) \exp\{\beta(\tau) Z(\tau) + \boldsymbol{\zeta}'\mathbf{X}\} \quad \text{for } \tau \leq t \leq t_{\text{hor}} \tag{1.4}$$

where $\beta(\tau) = \sum_j \gamma_j f_j(\tau)$, with basis functions $f_j(\tau)$ and parameters $\gamma_j$. This model

can be fit to the stacked super data set using a Cox model with stratification on $\tau$ and interaction terms $Z(\tau) * f_j(\tau)$. For estimation we maximize a pseudo-partial log-likelihood, which is the sum over the partial log-likelihoods corresponding to the Cox models fit to each of the landmark data sets.

Instead of assuming a different baseline hazard for each $\tau$, we can further extend this model to allow the baseline hazard to change smoothly with landmark time. Thus, the **extended super model** is given by

$$h(t|\tau, Z(\tau), \mathbf{X}) = h_0(t) \exp\{\theta(\tau) + \beta(\tau) Z(\tau) + \boldsymbol{\zeta}' \mathbf{X}\} \quad \text{for } \tau \leq t \leq t_{\text{hor}} \tag{1.5}$$

where $\theta(\tau) = \sum_j \eta_j g_j(\tau)$, with basis functions $g_j(\tau)$ and parameters $\eta_j$. In this model, $g_j(\tau)$ are now covariates. The pseudo partial log-likelihood for this model differs slightly from the one for the model in Eq.(1.4). Details are given in van Houwelingen (2007).

This landmark super model can be generalized further. In Eq.(1.5), the effect of $Z$ depends on $\tau$ but it does not depend on $t$; thus, it still has a proportional hazards structure. For some applications it may be more appropriate to assume that the effect of $Z$ depends on the time $t - \tau$ and to include a term $Z(\tau)\omega(t - \tau)$, where $\omega(s)$ is a smooth function of $s$. Thus, we can use the **non-proportional hazards extended super model** given by

$$h(t|\tau, Z(\tau), \mathbf{X}) = h_0(t) \exp\{\theta(\tau) + \beta(\tau) Z(\tau) + \omega(t-\tau) Z(\tau) + \boldsymbol{\zeta}' \mathbf{X}\} \quad \text{for } \tau \leq t \leq t_{\text{hor}} \tag{1.6}$$

## 1.3 Landmark Cox model construction corresponding to the Illness-Death model

We now consider landmarking when $Z$ is a binary covariate process. Under the landmark approach, when making a prediction for a new subject at landmark time $\tau$, we use all available information at that landmark time. This method does not directly incorporate possible future transitions to illness. Since landmarking uses the LOCF approximation,

if the marker process covariate, $Z_i$, is 0 at the time of the individual's last observation $t_{il}$ before $\tau$, then we set $Z(\tau) = 0$. Thus, it is implicitly assumed the individual does not transition to the illness state between $t_{il}$ and $\tau$. Under the joint modeling approach, when predicting for a new individual we integrate over all possible paths of an individual through the illness-death model, including the individual possibly progressing to illness state after their last inspection but before $\tau$. Thus, for individuals with $Z(t_{il}) = 0$, if there is interest in predicting for landmark times far later than $t_{il}$, joint modeling can be expected to provide a better prediction than landmarking.

We can also demonstrate that the standard landmark approach uses a model that is not compatible with the illness-death model. To model the residual time distribution in a landmarking framework with binary $Z$, we consider the super landmark model in Eq.(1.4). If the proportional hazards assumption in the landmark Cox model is to hold then it is necessary that $\beta(\cdot)$ in Eq.(1.4) does not depend on $t$. We will investigate whether it is possible under the illness-death model to achieve a form for $\beta(\cdot)$ that is independent of $t$. If not, then we will examine how $\beta(\tau)$ can be generalized to better approximate the correct residual time distribution.

For the purposes of our derivation, we reparameterize the hazard in Eq.(1.4) as follows:

$$h(t|\tau, Z(\tau), \mathbf{X}) = h_0(t|\tau) \exp\left\{\beta(\tau)(1 - Z(\tau)) + \boldsymbol{\zeta}'\mathbf{X}\right\} \tag{1.7}$$

We can then define the residual time distribution for the Cox-type landmark model as surviving to time $\tau + s$, $s > 0$, given the individual was alive at landmark time $\tau$ with an illness indicator $Z(\tau)$. From Eq.(1.7), this can be written as

$$\Pr(T \geq \tau + s | T > \tau, \mathbf{X}, Z(\tau)) = \exp\left[ - \int_{\tau}^{\tau+s} h_0(u|\tau) \exp\left\{\beta(\tau)(1 - Z(\tau)) + \boldsymbol{\zeta}'\mathbf{X}\right\} \, \mathrm{d}u \right] \tag{1.8}$$

### 1.3.1 Equating residual time distribution

To determine the form for $\beta(\tau)$ and $h_0(t|\tau)$ in Eq.(1.7) that corresponds to the illness-death model, we equate the appropriate residual time distributions for the two models. Starting with the situation where the individual transitioned to the illness state by time $\tau$, it is required that Eq.(1.8) for $Z(\tau) = 1$ and Eq.(1.3) are equal, hence

$$\exp\left\{-\int_{\tau}^{\tau+s} h_0(u|\tau)\exp(\boldsymbol{\zeta}'\mathbf{X})\,\mathrm{d}u\right\} = \exp\left\{-\int_{\tau}^{\tau+s}\lambda_{12}(u|\mathbf{X})\,\mathrm{d}u\right\}$$

$$\implies h_0(u|\tau)\exp(\boldsymbol{\zeta}'\mathbf{X}) = \lambda_{12}(u|\mathbf{X}) \quad \forall\tau \tag{1.9}$$

Thus, the hazard for the Cox-type model in the landmark approach conditional on being in the illness state is equivalent to the transition intensity from illness to death. Notice that it has the same form for all landmark times.

For the situation where the individual has not yet transitioned to illness, we require that Eq.(1.8) for $Z(\tau) = 0$ and Eq.(1.2) are equal, thus

$$\exp\left\{-\int_{\tau}^{\tau+s} h_0(u|\tau)\exp(\beta(\tau)+\boldsymbol{\zeta}'\mathbf{X})\,\mathrm{d}u\right\} = \text{Eq.(1.2)}$$

$$\implies \beta(\tau)+\boldsymbol{\zeta}'\mathbf{X} = \log\left[-\frac{\log\{\text{Eq.(1.2)}\}}{\int_{\tau}^{\tau+s}h_0(u|\tau)\,\mathrm{d}u}\right]$$

Substituting in the value for $h_0(u|\tau)$ from Eq.(1.9):

$$\implies \beta(\tau)+\boldsymbol{\zeta}'\mathbf{X} = \log\left[-\log\{\text{Eq.(1.2)}\}\right] - \log\left\{\int_{\tau}^{\tau+s}\lambda_{12}(u|\mathbf{X})\,\mathrm{d}u\right\} \tag{1.10}$$

which is the form for the covariate effects from the landmark Cox regression model that corresponds to an illness-death model. Notice that the required form for $\beta(\tau)$ given on the right-hand side of Eq.(1.10) is quite complicated since it involves Eq.(1.2), which

is composed of two additive terms. Also, notice that it is dependent on both $s$ and $\tau$, which violates the form of the simple Cox regression model desired for the landmark setting, i.e., $\beta(\cdot)$ dependent only on $\tau$. Thus, a landmark approach with a proportional hazards assumption is not the correct method when the true data generative model is an illness-death model.

If $\lambda_{12}(u|\mathbf{X}) = \lambda_{12,0}(u)\exp\{\boldsymbol{\alpha}_{12}'\mathbf{X}\}$, then $\boldsymbol{\zeta} = \boldsymbol{\alpha}_{12}$. The form of $\mathbf{X}$ on the right-hand side of Eq.(1.10) is not linear in $\mathbf{X}$ and furthermore, it depends on three separate linear combinations, $\boldsymbol{\alpha}_{01}'\mathbf{X}, \boldsymbol{\alpha}_{02}'\mathbf{X}$, and $\boldsymbol{\alpha}_{12}'\mathbf{X}$, rather than one. If there are several baseline covariates, the covariate vector can be different for each transition, which will also not be captured by the linear form of $\mathbf{X}$ in the Cox model. This suggests that the landmark Cox models should include more flexible forms for $\mathbf{X}$, such as $\boldsymbol{\zeta}(\boldsymbol{\tau})'\mathbf{X}$, or an interaction, such as $\boldsymbol{\phi}'\mathbf{X}Z(\tau)$.

We now consider special cases for the transition intensities to identify situations in which the derived forms for the landmark Cox baseline hazard and covariate effects provide good approximations of the residual time distribution under the illness-death model.

#### 1.3.1.1 Constant and equal baseline transition intensities

Under the simplest situation of constant and equal baseline transition intensities, $\lambda_{jk}(t|\mathbf{X}) = \psi\exp\{\boldsymbol{\alpha}_{jk}'\mathbf{X}\}$, we obtain the following form for the baseline hazard and covariate effects under the Cox landmark model from Eqs.(1.9) and (1.10),

$$
\begin{aligned}
h_0(t|\tau,\mathbf{X})\exp(\boldsymbol{\zeta}'\mathbf{X}) &= \psi\exp(\boldsymbol{\alpha}_{12}'\mathbf{X}) \\
\beta(\tau) + \boldsymbol{\zeta}'\mathbf{X} &= \log\left[-\log\left(\exp\left\{-\psi s(e^{\boldsymbol{\alpha}_{02}'\mathbf{X}} + e^{\boldsymbol{\alpha}_{01}'\mathbf{X}})\right\}\right.\right. \\
&\qquad \left.\left. + \frac{\exp\left(\boldsymbol{\alpha}_{01}'\mathbf{X} - \psi s e^{\boldsymbol{\alpha}_{12}'\mathbf{X}}\right)\left\{1 - \exp\left\{-\psi s\left(e^{\boldsymbol{\alpha}_{02}'\mathbf{X}} + e^{\boldsymbol{\alpha}_{01}'\mathbf{X}} - e^{\boldsymbol{\alpha}_{12}'\mathbf{X}}\right)\right\}\right\}}{e^{\boldsymbol{\alpha}_{02}'\mathbf{X}} + e^{\boldsymbol{\alpha}_{01}'\mathbf{X}} - e^{\boldsymbol{\alpha}_{12}'\mathbf{X}}}\right)\right] \\
&\qquad - \log[\psi s e^{\boldsymbol{\alpha}_{12}'\mathbf{X}}]
\end{aligned}
$$

The form for the covariate effects does not resemble a structure that is implementable within a standard Cox regression in the landmark approach. Also, $\beta(\tau)$ is dependent on $s$ and violates the form of a simple Cox regression model in the landmark setting, which assumes that $\beta$ depends only on $\tau$.

#### 1.3.1.2 Proportional hazards transition intensities

For the situation with proportional hazards transition intensities, we define the transition intensity for $j \to k$ as $\lambda_{jk}(t|\mathbf{X}) = \lambda_{jk,0}(t)\exp\{\boldsymbol{\alpha}'\mathbf{X}\}$, where $\lambda_{jk,0}(t)$ is the baseline transition intensity for the $j \to k$ transition, such that $\lambda_{02,0}(t) = \lambda(t), \lambda_{01,0}(t) = \gamma\lambda(t), \lambda_{12,0}(t) = \eta\lambda(t)$. We denote the cumulative hazard $\Lambda(t) = \int_0^t \lambda(u)\,\mathrm{d}u$. Then from Eqs.(1.9) and (1.10), we derive

$$
\begin{aligned}
h_0(t|\tau,\mathbf{X})\exp(\boldsymbol{\zeta}'\mathbf{X}) =& \eta\lambda(t)\exp(\boldsymbol{\alpha}'\mathbf{X}) \\
\beta(\tau) + \boldsymbol{\zeta}'\mathbf{X} =& \log\left[-\log\left(\frac{1-\eta}{1+\gamma-\eta}\exp\left\{-(1+\gamma)e^{\boldsymbol{\alpha}'\mathbf{X}}[\Lambda(\tau+s)-\Lambda(\tau)]\right\}\right.\right. \\
&\left.\left. +\frac{\gamma}{1+\gamma-\eta}\exp\left\{-\eta e^{\boldsymbol{\alpha}'\mathbf{X}}[\Lambda(\tau+s)-\Lambda(\tau)]\right\}\right)\right] \\
&- \log\left[\eta e^{\boldsymbol{\alpha}'\mathbf{X}}\{\Lambda(\tau+s)-\Lambda(\tau)\}\right]
\end{aligned}
$$

In this scenario, the form of the covariate effects also does not have a Cox proportional hazards structure. Here, $\beta(\tau)$ is dependent on both $\tau$ and $s$, unless $\lambda(t)$ is a constant. As the flexibility of the transition hazards in the illness-death model is increased, we find that the corresponding form of the covariate effects under the landmark approach is not consistent with a Cox regression model and depend on both $\tau$ and $s$. Allowing the effect of the baseline covariates to vary with transition, the forms of the baseline hazard and covariate effects are even more complicated.

#### 1.3.1.3 Short prediction horizon

Since we are typically most interested in short term predictions, we also consider whether the Cox model in the landmark framework approximately satisfies a proportional hazards assumption for small time horizons of interest. Thus, we explored obtaining a simpler form of the derived residual time distribution using the Taylor approximation. Taking the second-order Taylor expansion of log(Eq.(1.2)) and log(Eq.(1.3)) about $s = 0$, we get the following approximation of the residual time distribution for small $s$

$$\Pr(T \geq \tau + s | T > \tau, \mathbf{X}, Z(\tau) = 0) \approx \exp\left\{ -\lambda_{02}(\tau|\mathbf{X})s \right.$$
$$\left. -\frac{1}{2}\left[\lambda'_{02}(\tau|\mathbf{X}) - \lambda_{02}(\tau|\mathbf{X})\lambda_{01}(\tau|\mathbf{X}) + \lambda_{01}(\tau|\mathbf{X})\lambda_{12}(\tau|\mathbf{X})\right] s^2 \right\}$$
$$\Pr(T \geq \tau + s | T > \tau, \mathbf{X}, Z(\tau) = 1) \approx \exp\left\{ -\lambda_{12}(\tau|\mathbf{X})s - \frac{1}{2}\lambda'_{12}(\tau|\mathbf{X})s^2 \right\}$$

Taking the derivative of the negative log of these equations, and denoting $t = \tau + s$, gives us the hazard functions

$$h(t|T \geq \tau, \mathbf{X}, Z(\tau) = 0) = \lambda_{02}(\tau|\mathbf{X}) - [\lambda'_{01}(\tau) - \lambda_{02}(\tau|\mathbf{X})\lambda_{01}(\tau|\mathbf{X}) + \lambda_{01}(\tau|\mathbf{X})\lambda_{12}(\tau|\mathbf{X})](t - \tau)$$
$$h(t|T \geq \tau, \mathbf{X}, Z(\tau) = 1) = \lambda_{12}(\tau|\mathbf{X}) + \lambda'_{12}(\tau|\mathbf{X})(t - \tau)$$

These hazards do not have the form of proportional hazards. Thus, to achieve consistency between the illness-death model and the landmark approach we need a broader class of landmark models that accommodates the derived form of the hazards and contains the Cox proportional hazards model as a special case.

Based on the derivations in this section, we conclude that Cox proportional hazards within the landmark framework is not an appropriate model for the residual time distribution arising from an illness-death model. We have shown that in plausible scenarios the covariate effects are a function of both $\tau$ and $s = t - \tau$ and that the effect of baseline covariates is unlikely to be well described by a simple, single linear combination. For the more likely but complicated scenario of an illness-death model with transition-specific base-

line intensities and covariate effects, the associated $h_0(t|\tau, \mathbf{X})$ and $\beta(\tau)$ are non-standard and the super landmark model does not provide a good theoretical approximation of the residual time distribution. Thus, we use a simulation study to explore the performance of extensions within the landmark framework that accommodate non-proportional hazards, coefficient effects of $Z$ as a function of $\tau$ and $s$, more complex forms for the baseline covariate effects $\mathbf{X}$, and interactions between $Z$ and $\mathbf{X}$.

## 1.4 Simulation Study

The aims of our simulation study were to compare the predictive performance of joint and landmarking models in the context of illness-death data, and to evaluate whether increased landmark model flexibility provides a better approximation to the true model.

### 1.4.1 Data Generation and Structuring

Five hundred simulations of $n = 500$ subjects were run for each scenario. Defining the states as {0: Healthy, 1: Ill, 2: Dead}, the ages at illness onset and death without illness were generated from

$$\lambda_{jk}(t_i|\mathbf{X}_i) = \left(\frac{\rho_{jk}}{\kappa_{jk}}\right)\left(\frac{t_i}{\kappa_{jk}}\right)^{\rho_{jk}-1} \exp\left\{\boldsymbol{\alpha}'_{jk}\mathbf{X}_i\right\} \quad \text{for } j = 0, k = 1, 2 \tag{1.11}$$

For the transition intensity from illness to death ($1 \to 2$), we generate data under two different models: (1) Markov, where the transition intensity depends only on current time and (2) semi-Markov ("clock-reset"), where the transition depends on duration in the illness state. Under the Markov model, $\lambda_{12}(t|\mathbf{X})$ is given as in Eq.(1.11). Under the semi-Markov model, given the known transition time $V$, the transition intensity from illness to death is specified as $\lambda_{12}^{SM}(t|\mathbf{X}, V) = \lambda_{12}(t - V|\mathbf{X})$.

We choose the transition intensity shape and scale parameters such that $\lambda_{12}(t) > \lambda_{02}(t) > \lambda_{01}(t)$ [$\rho_{jk} = 1.15$ for all $j \to k$; $\kappa_{01} = 20; \kappa_{02} = 12.5; \kappa_{12} = 10$]. We simulate

a binary baseline covariate, $X$, that has a stronger effect on death in ill subjects, with $\alpha_{01} = 0.5, \alpha_{02} = 0.5, \alpha_{12} = 2$. We explored simulating the exposure prevalence of $X$ from 5% to 50%, but present only the results for 40% due to the similarity of results under other percentages. We simulate right-censoring from an exponential distribution with mean 80 and apply administrative censoring at time 20 to achieve a 15% censoring rate. We simulate marker measurement under two patterns of observation: (1) the marker process is continuously observed (then the exact transition time from "healthy" to "ill" is observed) and (2) the value of the marker is observed at random inspection times. Under the scenarios where the marker, $Z$, is measured at inspection times, inter-inspection times are exponentially distributed with rate 0.5.

We assume that there is interest in dynamic prediction for the first five years following baseline. Thus, we use an equally spaced grid of landmark times from time 0 to time 5, every 0.2 years. The endpoint of interest is death within a prediction window of $s = 1, 3, 5$ years from the prediction time. To structure the data as a super data set, we create a landmark data set for each $\tau$, with administrative censoring at $\tau + s$, and stack the landmark data sets. We also structure the data as a longitudinal data set for the setting with simulated inspection times. In this data set, each patient contributes a row for each of their inspection times $(t_{il}, l = 1, \ldots, n_i)$, with administrative censoring of their event times at $t_{il} + s$.

### 1.4.2 Joint Models

Under the joint modeling approach, we fit both Markov and semi-Markov models. Defining $\lambda^{W}_{jk,0}(t)$ and $\lambda^{Cox}_{jk,0}(t)$ as the baseline hazards of a Weibull model and Cox proportional hazards model, respectively, we fit the parametric and semiparametric joint models (MM), (MMCox), (MSM), (MSMCox), and (SMM) shown in Table 1.1.

For (MM) we fit a Markov illness-death model with Weibull hazard transition intensities. (MMCox) fits the model with semiparametric transition intensities using a Cox

**Table 1.1:** Joint models fit in the simulation study.

| **Model** | **Baseline hazard** | **Transition intensity** $\forall j \to k$ | **Label** |
|---|---|---|---|
| **Markov** $\lambda_{jk}(t\|X)$ | Parametric | $\lambda^{W}_{jk,0}(t)\exp\{\alpha_{jk}X\}$ | (MM) |
| | Semiparametric | $\lambda^{Cox}_{jk,0}(t)\exp\{\alpha_{jk}X\}$ | (MMCox) |
| **Markov,** $V^*$ $\lambda_{jk}(t\|X,V^*)$ | Parametric | $\lambda^{W}_{jk,0}(t)\exp\{\alpha_{jk}X+\gamma V^*\mathbf{1}(j=1,k=2)\}$ | (MSM) |
| | Semiparametric | $\lambda^{Cox}_{jk,0}(t)\exp\{\alpha_{jk}X+\gamma V^*\mathbf{1}(j=1,k=2)\}$ | (MSMCox) |
| **Semi-Markov** $\lambda_{jk}(t\|X,V^*)$ | Parametric | $\lambda^{W}_{jk,0}(t-V^*\mathbf{1}(j=1,k=2))\exp\{\alpha_{jk}X\}$ | (SMM) |

proportional hazards model. These models are extended to (MSM) and (MSMCox) to account for the effect of the observed transition time, $V^*$, by including it as a covariate. For (SMM) we fit a semi-Markov illness-death model.

Estimation is conducted using methods described in Section 1.2.1 with the `R` packages `SmoothHazard` for (MM) (Touraine et al., 2013), `mstate` for (MMCox) and (MSMCox) (de Wreede et al., 2011), and the function `optim` for the optimization of the likelihood for (MSM) and (SMM) using the quasi-Newtonian algorithm, the code for which is available in the Supporting Information materials. We plug in the resulting estimates ($\hat{\lambda}_{jk}$) into $1-$Eq.(1.2) and $1-$Eq.(1.3) to produce dynamic predictions of death within $s$ years for landmark time $\tau_l$. Note that for the models that are conditional on $V^*$, we replace $\lambda_{12}(u|\mathbf{X})$ with $\lambda_{12}(u|\mathbf{X},v)$ in Eq.(1.2) and $\lambda_{12}(u|\mathbf{X})$ with $\lambda_{12}(u|\mathbf{X},V)$ in Eq.(1.3).

### 1.4.3 Landmark models

Motivated by the derivations in Section 1.3 and based on the equations in Section 1.2.2, we fit the landmark models (LM1), (LM2), (LM3), and (LM4) given in Table 1.2 to the simulated data, where $\beta(\tau)=\beta_0+\beta_1\tau+\beta_2\tau^2$, $\theta(\tau)=\theta_1\tau+\theta_2\tau^2$, $\omega(s)=\omega_1 s+\omega_2 s^2$.

For estimation, under the super data set structuring, the $\tau$'s in (LM1-LM4) correspond to the chosen grid of landmark (prediction) times. Under the longitudinal data structuring, only (LM2), (LM3), and (LM4) apply, and the $\tau$'s represent the inspection times. The landmark data sets are created using the `dynpred` package in `R` (Putter, 2015).

**Table 1.2:** Landmark models fit in the simulation study.

| Model | Hazard | Label[2] |
|---|---|---|
| **LM**[1] $h(t\|\tau, Z(\tau), X)$ | $h_{0\tau}(t)\exp\{\beta(\tau)Z(\tau)+\zeta X\}$ | (LM1) |
| | $h_0(t)\exp\{\theta(\tau)+\beta(\tau)Z(\tau)+\zeta X\}$ | (LM2) |
| | $h_0(t)\exp\{\theta(\tau)+\beta_0 Z(\tau)+\omega(t-\tau)Z(\tau)+\zeta X\}$ | (LM3) |
| | $h_0(t)\exp\{\theta(\tau)+\beta(\tau)Z(\tau)+\omega(t-\tau)Z(\tau)+\zeta X\}$ | (LM4) |
| **LM,** $V^*$ $h(t\|\tau, Z(\tau), X, V^*)$ | $h_{0\tau}(t)\exp\{\beta(\tau)Z(\tau)+\gamma V^* Z(\tau)+\zeta X\}$ | (LSM1) |
| | $h_0(t)\exp\{\theta(\tau)+\beta(\tau)Z(\tau)+\gamma V^* Z(\tau)+\zeta X\}$ | (LSM2) |
| | $h_0(t)\exp\{\theta(\tau)+\beta_0 Z(\tau)+\omega(t-\tau)Z(\tau)+\gamma V^* Z(\tau)+\zeta X\}$ | (LSM3) |
| | $h_0(t)\exp\{\theta(\tau)+\beta(\tau)Z(\tau)+\omega(t-\tau)Z(\tau)+\gamma V^* Z(\tau)+\zeta X\}$ | (LSM4) |
| **LM, Interaction** $h(t\|\tau, Z(\tau), \mathbf{X})$ | $h_0(t)\exp\{\theta(\tau)+\beta(\tau)Z(\tau)+\boldsymbol{\zeta}'\mathbf{X}+\boldsymbol{\phi}'\mathbf{X}Z(\tau)\}$ | (LMInt2) |
| | $h_0(t)\exp\{\theta(\tau)+\beta_0 Z(\tau)+\omega(t-\tau)Z(\tau)+\boldsymbol{\zeta}'\mathbf{X}+\boldsymbol{\phi}'\mathbf{X}Z(\tau)\}$ | (LMInt3) |
| | $h_0(t)\exp\{\theta(\tau)+\beta(\tau)Z(\tau)+\omega(t-\tau)Z(\tau)+\boldsymbol{\zeta}'\mathbf{X}+\boldsymbol{\phi}'\mathbf{X}Z(\tau)\}$ | (LMInt4) |

[1] LM: landmark model; [2] (*1): Super model; (*2): Extended super model; (*3): Extended super model, non-proportional hazards; (*4): Extended super model, non-proportional hazards, covariate effects are a function of landmark time

In (LM1) we fit a simple Cox model with a different baseline hazard for each $\tau$. Thus, this approach can only be applied when we pre-specify the landmark times and construct the super data set based on these landmark times. In (LM2), we still fit a simple Cox model, but parameterize the baseline hazard to depend smoothly on $\tau$, resulting in decreased model flexibility but allowing us to fit the model to our longitudinal data set. In (LM3), we propose a model that allows for non-proportional hazards by including the covariates $\omega(s)Z(\tau)$ that are a function of $s = t - \tau$, to accommodate time-varying effects of our covariate process. In (LM4), we extend the Cox model to include both $\beta(\tau)$ and $\omega(t-\tau)$, since in Section 1.3 we showed that under the illness-death model the form for the covariate effects for the Cox regression model in the landmark framework was a function of both $s$ and $\tau$.

Under the semi-Markov model for generating data, modeling complications arise due to the change in time scale between the transitions. Thus, for simplicity, we can incorporate the dependency of transition on the observed illness time, $V^*$, by including it as a covariate in the landmark models. Thus, we modify the models (LM1-LM4) to be conditional on

$V^*$ with parameter $\gamma$, and fit the models (LSM1), (LSM2), (LSM3), and (LSM4) given in Table 1.2.

After obtaining the estimates from these parameterizations $(\hat{\beta}, \hat{\theta}, \hat{\zeta}, \hat{\omega}, \hat{\gamma})$, we compute the dynamic predictions of death within a window of $s$ years at the pre-specified landmark times, $\tau_l$, using the following equation

$$\Pr(T \leq \tau_l + s | T > \tau_l, Z(\tau_l), X, V) = 1 - \exp\left\{ - \int_{\tau_l}^{\tau_l + s} h(u | Z(\tau_l), X, V\hat{\beta}, \hat{\theta}, \hat{\omega}, \hat{\zeta}, \hat{\gamma}) \, \mathrm{d}u \right\}$$

In addition, to the basic scenario of a single baseline covariate, we also evaluated the performance of landmark models when the baseline covariate vector varies by transition. We generate data with two binary baseline covariates, $X_1$ that has a stronger effect on death in ill subjects $[\alpha_{01,1} = \alpha_{02,1} = 0.5, \alpha_{12,1} = 2]$ and $X_2$, which has no effect on death $[\alpha_{01,2} = 1, \alpha_{02,2} = \alpha_{12,2} = 0]$. We fit the joint models (MM) and (MMCox) with the covariates $X_1$ and $X_2$. We modify $\zeta X$ in models (LM1-LM4) to $\boldsymbol{\zeta}'\mathbf{X}$ where $\boldsymbol{\zeta} = (\zeta_1, \zeta_2)$ and $\mathbf{X} = (X_1, X_2)$ are the parameter and baseline covariate vectors, respectively. We also fit the additional models (LMInt2), (LMInt3), and (LMInt4), given in Table 1.2, that include an interaction term with illness status and parameter vector $\boldsymbol{\phi} = (\phi_1, \phi_2)$.

### 1.4.4 Performance Comparison Metrics

The dynamic predictions produced at the sequence of landmark times are compared to the true death probabilities. These are obtained by using the true shape and scale parameters to get the true transition intensities and then using numerical integration to compute the true death probability within window $s$ from Eqs.(1.2) and (1.3), replacing $\lambda_{12}(u|\mathbf{X})$ with $\lambda_{12}(u|V^*, \mathbf{X})$ when generating under the semi-Markov model. For each landmark time, we compute the bias and variance of the dynamic predictions under the landmark approaches and joint model.

To assess the discrimination and calibration of these dynamic predictions, we use

the dynamic analogues of weighted area under the curve (AUC) and Brier score that account for censored data, denoted $\text{AUC}(\tau, s)$ and $\text{BS}(\tau, s)$, respectively, for landmark time $\tau$ and fixed prediction window $s$ (Blanche et al., 2015). Since BS depends on the cumulative incidence of death in $(\tau, \tau + s]$, we used a standardized version that results in an $R^2$-type measure that compares how well the predictions perform compared to a null model that assumes that all subjects have the same predicted risk of death regardless of subject-specific information, $\text{BS}_0(\tau, s)$. We denote this scaled measure $R^2(\tau, s) = 1 - \text{BS}(\tau, s)/\text{BS}_0(\tau, s)$.

To make comparisons between the different models, we compute AUC and $R^2$ using the prediction probabilities from the true models, denoted $\text{AUC}_{\text{True}}$ and $R^2_{\text{True}}$, respectively. We then report the relative measures $\Delta\text{AUC} = \text{AUC} - \text{AUC}_{\text{True}}$ and $\Delta R^2 = R^2 - R^2_{\text{True}}$ for each of the models, with a higher value indicating better performance.

For cross-validation, in each simulation all of the described models were fit to a training data set, created by randomly selecting 4/5 of the simulated individuals. The remaining 1/5 individuals were treated as the validation data set, from which predicted conditional death probabilities within the window $(\tau, \tau + s]$ were obtained for those still alive at time $\tau$.

### 1.4.5 Simulation Results

Figure 1.2 compares the performance of the landmark model (LM1) and the joint model (MM) under a Markov assumption with a single baseline covariate for the various prediction windows, $s = 1, 3, 5$. The joint model performs better than the landmark model across all of the prediction windows in terms of all of the considered metrics. For $Z = 0$, as the prediction window increases, the bias and variance of the joint model increases, with the reverse effect for $Z = 1$. There is no pattern of performance for the landmark model (LM1) across $s$. However, within each prediction window, the relationship between the performance of the different landmark models was consistent. Thus, we present the

remaining simulation results for a single prediction window, $s = 3$. As well, we will focus on $Z = 1$ for reporting the bias and variance since the absolute bias of the models is higher than for $Z = 0$.

We compare the landmark and joint models in Figure 1.3, which depicts the performance of the models for $Z = 1, X = 1, s = 3$ for a continuously observed marker. Across all the landmark times, the joint models perform the best in terms of bias, variance, $\Delta$AUC and $\Delta R^2$, and thus give more accurate predictions than the landmark models. Within the joint models, the semiparametric model (MMCox) performs almost as well as the parametric model under which the data was generated, (MM), and both outperform the landmark models, which can have high absolute bias. In comparing the landmark models, model (LM3), which includes time-varying effects, has the lowest variance, but has the highest bias for early landmark times. The bias for model (LM3) decreases with increasing landmark time, while it increases for the other landmark models. Model (LM4), which incorporates both landmark and residual time, performed similarly to the simpler landmark models (LM1) and (LM2). All the landmark models had similar $\Delta$AUC and $\Delta R^2$. Thus, incorporating additional flexibility into the landmark models did not translate into less deviation from the true predicted probabilities or substantially better predictive performance. Due to their similar performance to (LM4), for the remaining figures we omit the results of (LM1) and (LM2).

In Figure 1.4, we compare the different methods of data structuring. When the marker is continuously observed there is more information available than when the process is observed at inspection times, and thus performance is better across all the metrics. Within the inspection times simulations, with the exception of the bias for the landmark model with non-proportional hazards, the longitudinal data set outperformed the super data set across all four performance metrics for all the landmark models. Since this relationship persisted in our simulation results, and it is unlikely that markers are observed continuously in practice, we will only present the results from the "longitudinal data set,

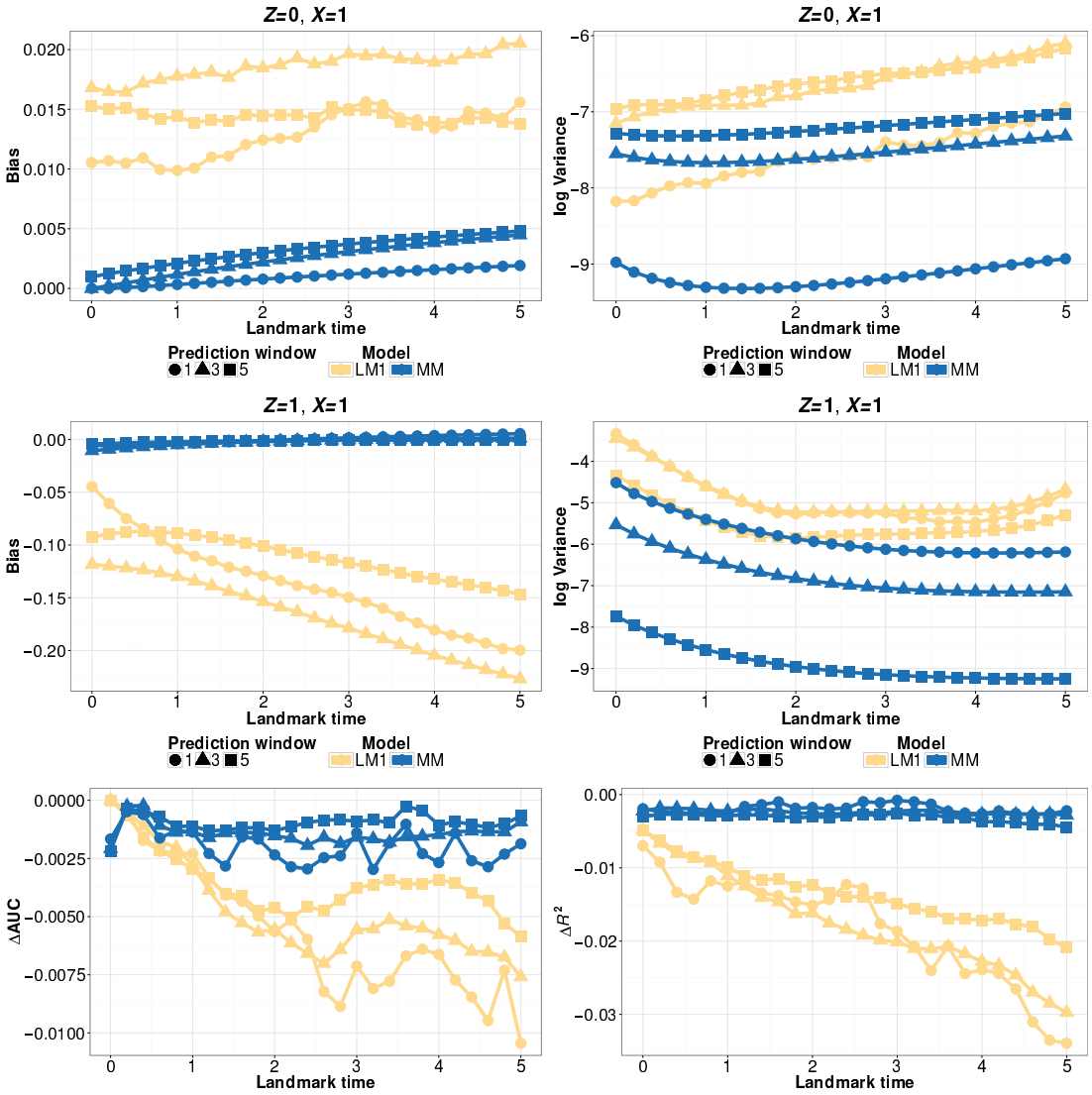


**Figure 1.2:** Simulation estimates for bias (upper-left), variance (upper-right), $\Delta$AUC (bottom-left), and $\Delta R^2$ (bottom-right) for predicted probability $P(T \leq \tau + s | T > \tau, Z(\tau), X)$ for $s = 1, 3, 5$-year prediction windows from joint model (MM) and landmark model (LM1), under a Markov illness-death model with a single baseline covariate and continuously observed marker measurement.

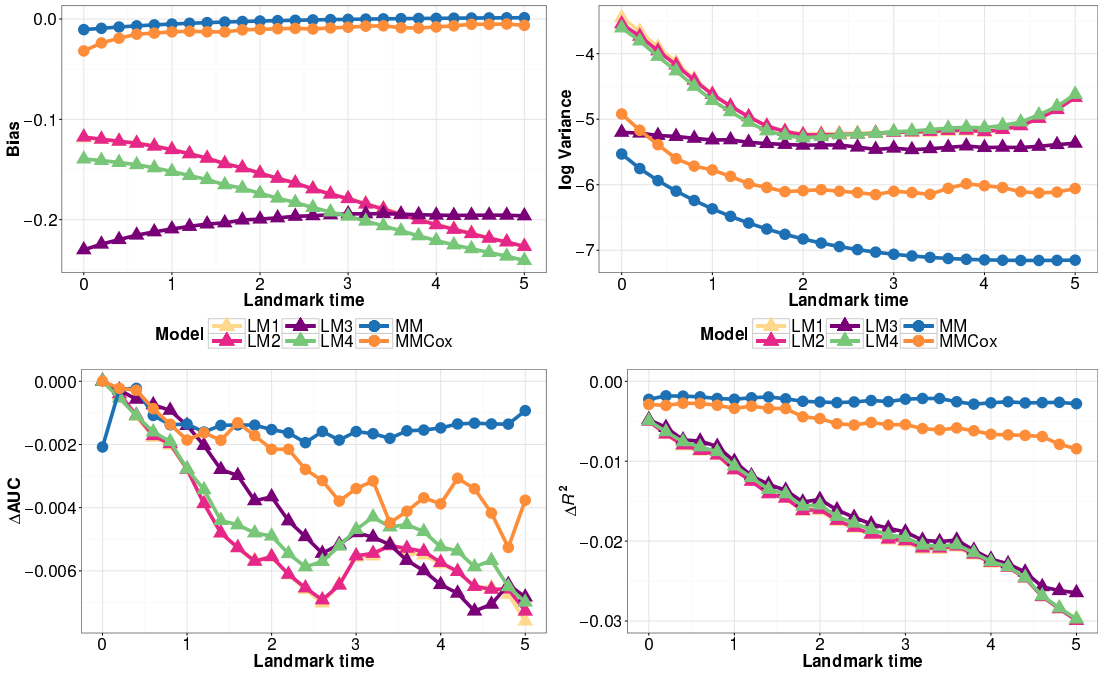


**Figure 1.3:** Simulation estimates for bias (upper-left) and variance (upper-right) for $Z(\tau) = 1, X = 1$, $\Delta$AUC (bottom-left), and $\Delta R^2$ (bottom-right) for predicted probability $P(T \leq \tau + 3|T > \tau, Z(\tau), X)$ from the joint models (MM), (MMCox) and landmark models (LM1-LM4), under a Markov illness-death model with a single baseline covariate and continuously observed marker measurement.

inspection times marker measurement" scenarios in the rest of our comparisons.

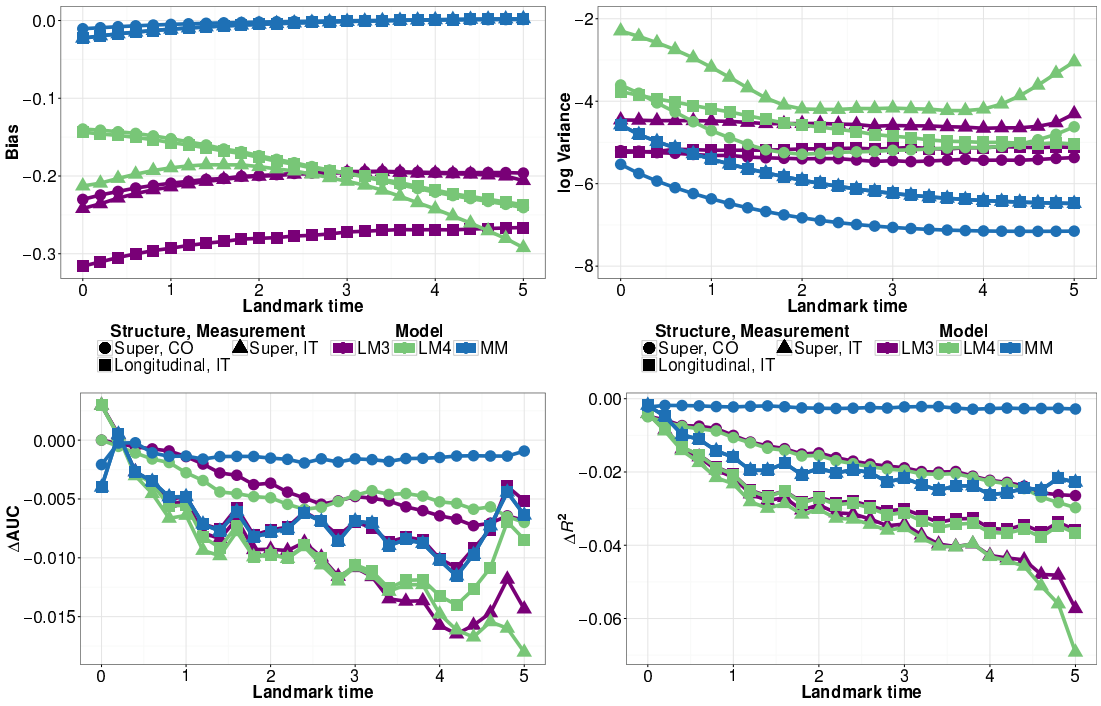


**Figure 1.4:** Simulation estimates for bias (upper-left) and variance (upper-right) for $Z(\tau) = 1, X = 1$, $\Delta$AUC (bottom-left), and $\Delta R^2$ (bottom-right) for predicted probability $P(T \leq \tau + 3 | T > \tau, Z(\tau), X)$ from joint model (MM) and landmark models (LM3), (LM4) fit to data structured as a super or longitudinal data set, under a Markov illness-death model with a single baseline covariate and continuously observed (CO) or inspection time (IT) marker measurement.

Figure 1.5 shows the results from models that condition on observed illness time applied to data generated from a Markov illness-death model. Among the joint models, parametric Markov model (MM) and semiparametric (MMCox) had similar performance. The joint models that condition on $V^*$, (MSM) and (MSMCox), had nearly identical performance to their corresponding Markov models, and still have better performance metrics than the landmark models. The semi-Markov model (SMM) had almost identical predictive performance to (MM), and had similar bias to the other joint models and the lowest variance for early landmark times. The performance of the landmark models (LSM3) and (LSM4) did not significantly change by conditioning on $V^*$. Thus, when simulating under a Markov assumption, conditioning on observed illness does not affect model performance.

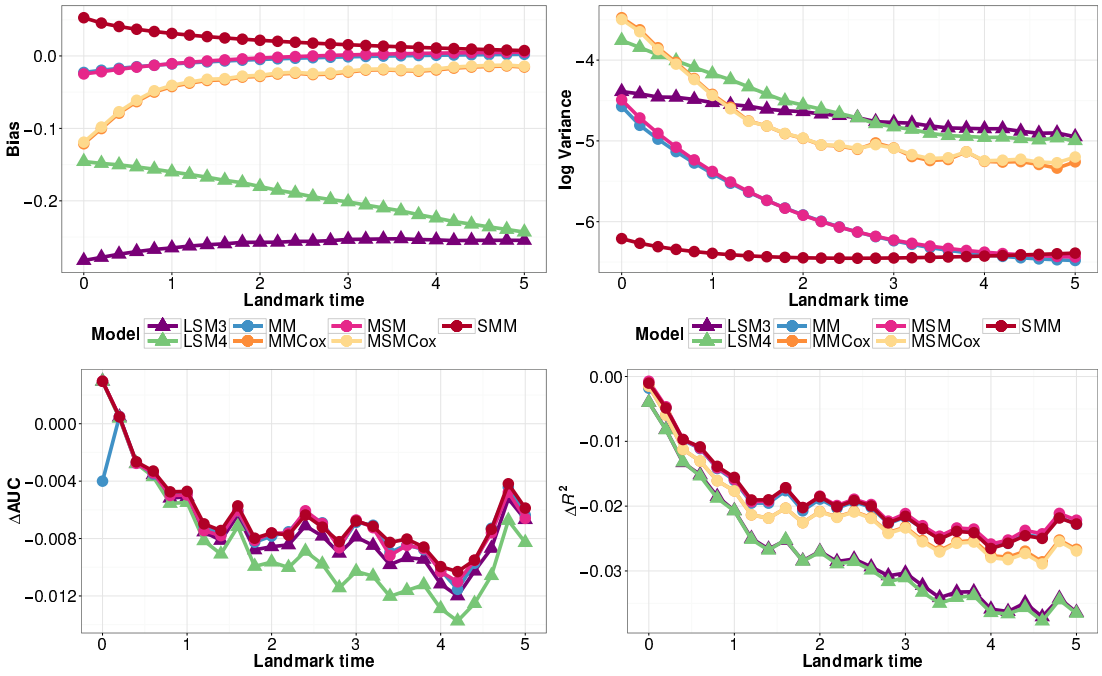


**Figure 1.5:** Simulation estimates for bias (upper-left) and variance (upper-right) for $Z(\tau) = 1, X = 1$, $\Delta$AUC (bottom-left), and $\Delta R^2$ (bottom-right) for predicted probability $P(T \leq \tau + 3 | T > \tau, Z(\tau), X)$ from joint models (MM), (MMCox), (MSM), (MSMCox), (SMM) and landmark models (LSM3), (LSM4) fit to a longitudinal data set, under a Markov illness-death model with a single baseline covariate and inspection time marker measurement.

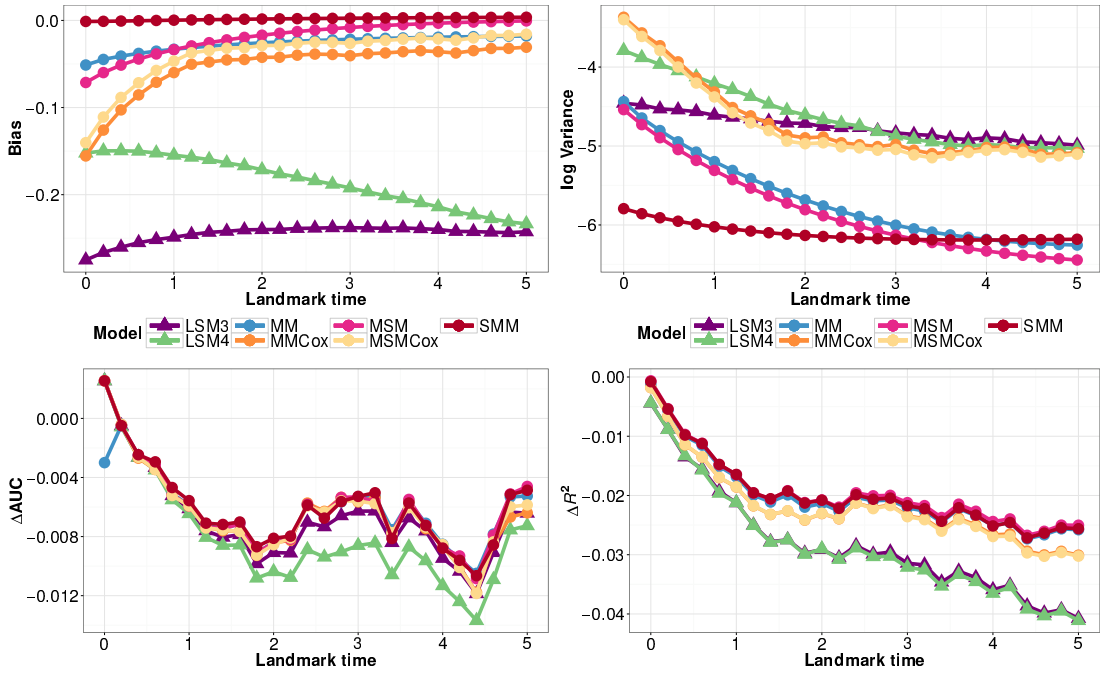


**Figure 1.6:** Simulation estimates for bias (upper-left) and variance (upper-right) for $Z(\tau) = 1, X = 1$, $\Delta$AUC (bottom-left), and $\Delta R^2$ (bottom-right) for predicted probability $P(T \leq \tau + 3 | T > \tau, Z(\tau), X)$ from joint models (MM), (MMCox), (MSM), (MSMCox), (SMM) and landmark models (LSM3), (LSM4) fit to a longitudinal data set, under a semi-Markov illness-death model with a single baseline covariate and inspection time marker measurement.

In Figure 1.6, we fit these same models to data generated under a semi-Markov illness-death model. The predicted probabilities for determining the bias and variance were computed given $V = 2\tau/3$, for landmark time $\tau$. The results were very similar to those in Figure 1.5. The (SMM) model performed the best, with the models that account for transition time performing marginally better than their counterparts, but with a greater distinction than in Figure 1.5. Since the gains are minimal, but existent, when conditioning on the observed illness time in our particular situation, there is an indication that these models will outperform the Markov models in other simulation scenarios.

Finally, we consider the situation where we simulate two baseline covariates with different effects on each transition. From Figure 1.7, we see that by including the interaction term $\mathbf{X}Z(\tau)$, the performance of the landmark models is on par with the joint models in terms of bias. The landmark models with the interaction term have lower variance, better

$\Delta R^2$, and similar $\Delta$AUC than those without the interaction. Thus, including an interaction term in the landmark Cox model captures the effect of baseline covariate vectors that differ by transition better than a linear function of $\mathbf{X}$ and provides a much better approximation to a joint model.

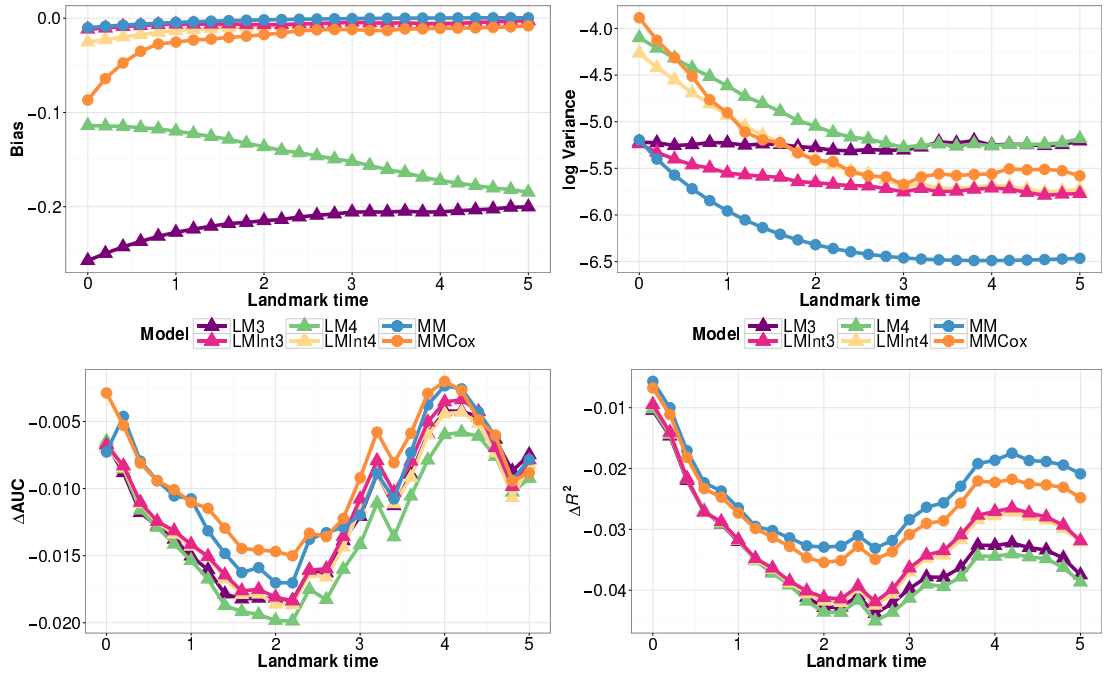


**Figure 1.7:** Simulation estimates for bias (upper-left) and variance (upper-right) for $Z(\tau) = 1, X_1 = 1, X_2 = 1$, $\Delta$AUC (bottom-left), and $\Delta R^2$ (bottom-right) for predicted probability $P(T \leq \tau + 3 | T > \tau, Z(\tau), \mathbf{X})$ from joint models (MM), (MMCox) and landmark models (LM3), (LM4), (LMInt3), (LMInt4) fit to a longitudinal data set, under a Markov illness-death model with two baseline covariates and inspection time marker measurement.

Overall, based on the set of scenarios considered, the simulation results show that joint modeling gives better performance than landmarking. The difference is generally quite small, with the exception of bias for which the landmarking approach can have high absolute bias. The results suggest that more general landmark models than the simplest (LM1) can improve performance and that given inspection time data, using a longitudinal structure for the landmark data set produces better predictions than a super data set. The results also indicate that misspecification of the joint model did not affect predictive performance.

## 1.5 Applications to Real Data

In this section, we apply landmarking and joint models to data from two different studies that can be modeled with an illness-death model and have information collected beyond baseline on a binary time-dependent covariate. The large PAQUID study on cognitive aging provides interval-censored inspection time data for transition time to the illness state and allows us to use cross-validation to compare the predictive performance of the methods under longitudinal and super data structures. We also apply the models to data from a prostate cancer study with continuously observed time to clinical failure to compare the coefficient interpretations and dynamic predictions produced under the two approaches.

### 1.5.1 PAQUID Study of Cognitive Aging

We evaluate the predictive abilities of landmark and joint models using data collected by the PAQUID study. The Personnes Agées QUID (PAQUID) Study is a large, prospective cohort study of cognitive and physical aging (Dartigues et al., 1992). We use data from the R package `SmoothHazard` (Touraine et al., 2013) on a random subset of 1000 subjects from the original study, which consisted of 3,777 individuals aged 65 years and older living in southwestern France. Subjects had 10 visits over 20 years, at which they were assessed for dementia. The longitudinal data set was created using interval-censored observations and the approximate visit times 1, 3, 5, 8, 10, 13, 15, 17, 20 years from the initial visit.

There were 186 subjects that were diagnosed with dementia. Of the 724 deaths, 597 died without a dementia diagnosis and 127 died after diagnosis. We model the data as an illness-death model with the states, "alive without dementia", "alive with dementia", and "dead". The baseline covariates are age at study entry (median 74; IQR 69-79), gender (female: 58%, male: 42%), and primary school diploma status (with diploma: 76%, without diploma: 24%).

This data represents the typical data set for which there is interest in determining the probability of death at a given landmark time beyond baseline of study enrollment. It involves a high-risk group of individuals for which there is future information, i.e., dementia diagnosis, that can affect their risk of death and thus must be incorporated into prediction models to produce accurate and updated prediction probabilities. This study also involves diagnosis updates at inspection times, which allows us to evaluate the landmark models by structuring the data as both a super data set and a longitudinal data set. The large size of the data set allows us to perform cross-validation to prevent overfitting when assessing model performance.

We fit both landmark and joint models as in the simulation study. The subject-specific predictions were computed at the landmark times $\tau = 0, 1, 3, 5, 8, 10$ years for a prediction window of $s = 3, 5, 7$ years. The estimates for assessing predictive accuracy were obtained by performing cross-validation based on repeated random sub-sampling. The data was split into 2/3 training data, to which the models were fit, and AUC and $R^2$ were computed for predictions from the remaining 1/3 validation data. This procedure was repeated 500 times. We present the averaged dynamic AUC and $R^2$ values under the super and longitudinal data structure for $s = 5$, since the other prediction windows showed similar patterns.

Fitting the model (MM) to the full data, we find that the baseline covariates of diploma status and gender have different effects for each of the transitions. Having a diploma has a significant effect on reducing risk of developing illness ($0 \to 1$), and males have increased risk of death ($1 \to 2$, $0 \to 2$). Thus, we consider landmark models with an interaction term. The landmark models performed similarly so we only present the results for models (LM3) and (LMInt3). In Figure 1.8, we evaluate the inclusion of an interaction and compare the different data structures. The model with the interaction has better predictive performance under both structures, with the longitudinal data set having higher AUC at earlier time points. We investigate the performance of joint Markov

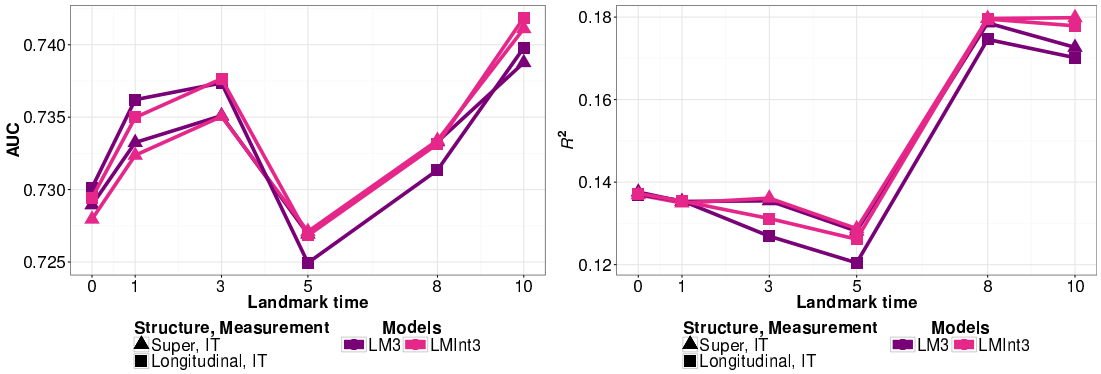


**Figure 1.8:** PAQUID data estimates for the cross-validated prediction accuracy measure AUC (left) and $R^2$ (right) for predicted probability $P(T \leq \tau + 5 | T > \tau, Z(\tau), \mathbf{X})$ from landmark models (LM3), (LMInt3), fit to inspection time (IT) marker measurement data structured as a longitudinal or super data set.

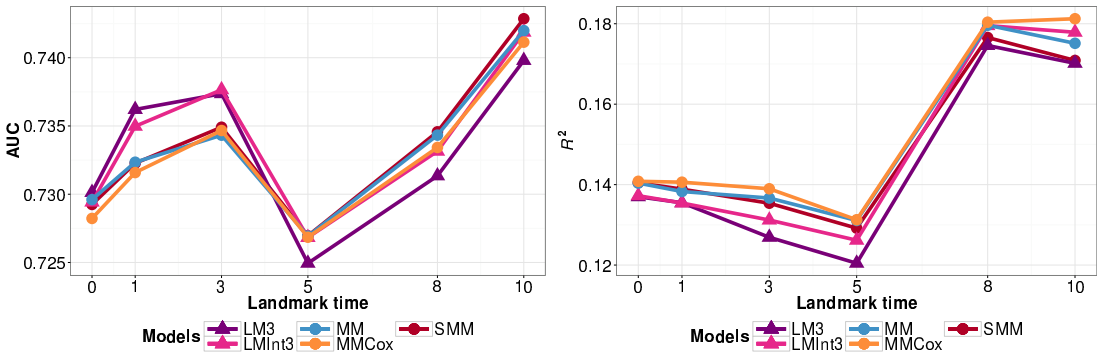


**Figure 1.9:** PAQUID data estimates for the cross-validated prediction accuracy measure AUC (left) and $R^2$ (right) for predicted probability $P(T \leq \tau + 5 | T > \tau, Z(\tau), \mathbf{X})$ for joint models (MM), (MMCox), (SMM) and landmark models (LM3), (LMInt3), fit to a longitudinal data set.

and semi-Markov models under the longitudinal data structuring in Figure 1.9 and notice that the landmarking models have higher AUC at earlier landmark times, but that joint models (MM) and (MMCox) perform consistently better in terms of $R^2$. The joint semi-Markov model, (SMM), performs similarly to the other joint models in terms of both AUC and $R^2$.

Based on this real data analysis, the predictions had similar accuracy under the different data structures. Extensions to the landmark models that incorporate $s$ and $\tau$ as covariates did not increase flexibility enough to produce significant improvement in model performance. However, the inclusion of an interaction between baseline covariates and

$Z(\tau)$ produces more accurate predictions. The joint models had marginally better or equivalent performance at the landmark times than the landmark models. The models that conditioned on transition time as a covariate did not provide a better fit; however, the semi-Markov model (SMM) performed similarly to the Markov models, and may outperform these models in a situation where the Markov assumption does not hold.

### 1.5.2 Prostate Cancer Study

We present the analysis results and dynamic predictions obtained from fitting the landmark and joint models to data from a prostate cancer study conducted at the University of Michigan. The data set is composed of 745 patients with clinically localized prostate cancer who were treated with radiation therapy. We measure time from start of treatment, considering metastatic clinical failure (CF) as a time-dependent binary covariate. The states of our illness-death model are "alive without clinical failure", "alive with clinical failure", and "dead". The median follow-up time was 9 years, and 52 patients experienced clinical failure. Out of 188 deaths, 154 died before and 34 died after experiencing clinical failure. The pretreatment prognostic factors measured at baseline are age (median 69; IQR 63-74), $\log(\text{PSA}+1)$ (PSA ng/ml; median 8; IQR 5-12), Gleason score treated as a continuous covariate with a score of 7="3+4" and 7.5="4+3" (median 7; IQR 6-7.5), prostate cancer stage (T1: 57%, T2-T3: 43%), and comorbidities (0: 55%, 1-2: 37%, $\geq$3: 8%).

We use landmark and joint models to obtain predicted probabilities of death within 5 years for landmark times $\tau = 0, 1, \ldots, 8$ years. We assume that the marker is continuously observed, and structure the data as a super data set. The coefficient estimates from fitting the joint models are given in Table 1.3. The parametric and semiparametric Markov models (MM) and (MMCox), respectively, have similar estimates for the different transitions. The (MSM) model incorporates clinical failure time as a covariate for the $1 \rightarrow 2$ transition, which is not significantly different than 0 and thus the Markov as-

**Table 1.3:** Coefficient estimates for joint models applied to prostate cancer data.

| | | **MM** | | **MMCox** | | **MSM** | | **SMM** | |
|---|---|---|---|---|---|---|---|---|---|
| Transition | Covariate | Coef. | SE | Coef. | SE | Coef. | SE | Coef. | SE |
| $0 \to 1$ | Age | 0.013 | 0.019 | 0.014 | 0.019 | 0.012 | 0.018 | 0.012 | 0.018 |
| | log(PSA + 1) | 0.424 | 0.173 | 0.431 | 0.172 | 0.422 | 0.173 | 0.422 | 0.173 |
| | Gleason score | 0.740 | 0.156 | 0.753 | 0.159 | 0.740 | 0.156 | 0.741 | 0.156 |
| | Stage T2-T3 | 0.798 | 0.349 | 0.767 | 0.349 | 0.799 | 0.349 | 0.796 | 0.349 |
| | Comorbidities 1-2 | 0.053 | 0.302 | 0.061 | 0.302 | 0.054 | 0.302 | 0.054 | 0.301 |
| | Comorbidities >=3 | 0.263 | 0.497 | 0.271 | 0.497 | 0.264 | 0.496 | 0.263 | 0.496 |
| $0 \to 2$ | Age | 0.077 | 0.013 | 0.080 | 0.013 | 0.076 | 0.013 | 0.076 | 0.013 |
| | log(PSA + 1) | 0.204 | 0.126 | 0.193 | 0.127 | 0.205 | 0.125 | 0.205 | 0.125 |
| | Gleason score | 0.135 | 0.093 | 0.174 | 0.095 | 0.136 | 0.093 | 0.136 | 0.093 |
| | Stage T2-T3 | 0.051 | 0.169 | -0.030 | 0.172 | 0.051 | 0.169 | 0.051 | 0.169 |
| | Comorbidities 1-2 | 0.678 | 0.181 | 0.700 | 0.182 | 0.679 | 0.181 | 0.678 | 0.181 |
| | Comorbidities >=3 | 1.426 | 0.236 | 1.491 | 0.238 | 1.425 | 0.236 | 1.425 | 0.236 |
| $1 \to 2$ | Age | 0.049 | 0.024 | 0.043 | 0.025 | 0.050 | 0.024 | 0.048 | 0.023 |
| | log(PSA + 1) | -0.238 | 0.260 | -0.183 | 0.319 | -0.263 | 0.270 | -0.293 | 0.271 |
| | Gleason score | 0.574 | 0.206 | 0.612 | 0.229 | 0.584 | 0.209 | 0.580 | 0.202 |
| | Stage T2-T3 | 0.059 | 0.475 | 0.207 | 0.508 | 0.105 | 0.488 | 0.078 | 0.478 |
| | Comorbidities 1-2 | -0.927 | 0.421 | -1.005 | 0.451 | -0.942 | 0.424 | -0.873 | 0.400 |
| | Comorbidities >=3 | -0.507 | 0.646 | -0.555 | 0.708 | -0.453 | 0.659 | -0.330 | 0.596 |
| | Time of CF ($V$) | | | | | -0.036 | 0.089 | | |
| Log-likelihood | | | -966.4 | | -1182 | | -966.4 | | -966.1 |
| AIC | | | 1969 | | 2399 | | 1971 | | 1968 |

sumption does not appear to be violated. This is further demonstrated by the estimates for the $1 \to 2$ transition in (SMM), which are very similar to the estimates from the (MM) model. The effects of the baseline covariates vary across the different transitions. Increased age significantly increases risk of death ($0 \to 1, 0 \to 2$), higher PSA, Gleason score, and Stage T2-T3 indicate increased risk of developing clinical failure ($0 \to 1$), and among those with clinical failure, higher Gleason score increases risk of death and those with 1-2 comorbidities have decreased risk of death ($1 \to 2$).

We present the results from fitting the landmark models in Table 1.4. In (LM3) we accommodate non-proportional hazards by considering clinical failure as a time-varying covariate. The effect of clinical failure decreases as the landmark time at which the prediction is made increases. (LM4), which (LM2) and (LM3) are nested within, has the highest log-likelihood of the models and the lowest AIC, indicating better fit. Since the joint models show that the baseline covariates have differential effects on risk of death be-

fore or after clinical failure, we present the results from (LMInt4), a model with interaction terms between clinical failure and the baseline covariates. The log-likelihood for (LMInt4) is higher than model (LM4) and it has a lower AIC even with the penalization for including six more covariates. Increased age, PSA, Gleason score, and number of comorbidities were all significantly associated with increased risk of death. The only significant interaction was with comorbidities, where those with clinical failure had a significantly decreased risk of death if they had 1-2 comborbidities compared to no comorbidities, as was seen in the joint models. The coefficients for the baseline covariates for the landmark models do not always properly capture the effect of the baseline covariates on risk. For example, the coefficient for Gleason score in (LM4) is averaged over those with and without clinical failure and thus, is much lower than the effect on the $1 \rightarrow 2$ transition but much higher than the effect for the $0 \rightarrow 2$ transition in the joint models. As well, the effect of stage, which is significant for the $0 \rightarrow 1$ transition in the joint models but has a small effect on the transitions to death, is not properly reflected by (LMInt4), where the effect of stage on risk of death is quite high for those who experience clinical failure.

In Figure 1.10 we present the predicted probabilities from the landmark and joint models, some of which have been omitted due to similar results, for two individuals in the data set. The pattern of the predictive probabilities for these specific patients is similar to that of the other patients in the data set with the same final clinical failure status, who experience death. Individual A has increased risk of death due to his high PSA and number of comorbidities, thus his predicted probability of death becomes quite high as landmark time increases and he dies before experiencing clinical failure. We see that for this patient, the predicted probabilities from the landmark models and the semiparametric Markov model (MMCox) track together and the predicted probabilities for all the models are similar. Individual B is young, but has other baseline variables that characterize him as high risk. Their effect is particularly seen after the patient experiences clinical failure, after which his predicted probability of death greatly increases and he dies within 2 years.

**Table 1.4:** Coefficient estimates for landmark models applied to prostate cancer data.

| | | **LM2** | | **LM3** | | **LM4** | | **LMInt4** | |
|---|---|---|---|---|---|---|---|---|---|
| | Covariate | Coef. | SE | Coef. | SE | Coef. | SE | Coef. | SE |
| $\beta(\tau)$ | CF | 3.317 | 1.204 | 2.065 | 0.279 | 3.921 | 1.210 | 3.406 | 2.972 |
| | CF$*\tau$ | -0.439 | 0.427 | | | -0.460 | 0.409 | -0.220 | 0.374 |
| | CF$*\tau^2$ | 0.020 | 0.034 | | | 0.021 | 0.033 | 0.006 | 0.031 |
| $\omega(\tau)$ | CF$*(t-\tau)$ | | | -0.513 | 0.190 | -0.562 | 0.175 | -0.341 | 0.188 |
| | CF$*(t-\tau)^2$ | | | 0.082 | 0.051 | 0.093 | 0.045 | 0.062 | 0.049 |
| $\theta(\tau)$ | $\tau$ | -0.056 | 0.018 | -0.043 | 0.019 | -0.069 | 0.023 | -0.073 | 0.022 |
| | $\tau^2$ | 0.004 | 0.001 | 0.001 | 0.002 | 0.004 | 0.002 | 0.004 | 0.002 |
| $\zeta$ | Age | 0.080 | 0.012 | 0.080 | 0.012 | 0.080 | 0.012 | 0.082 | 0.013 |
| | log(PSA + 1) | 0.227 | 0.111 | 0.234 | 0.110 | 0.227 | 0.111 | 0.246 | 0.112 |
| | Gleason score | 0.292 | 0.091 | 0.288 | 0.091 | 0.289 | 0.091 | 0.269 | 0.094 |
| | Stage T2-T3 | 0.040 | 0.168 | 0.054 | 0.168 | 0.042 | 0.167 | 0.057 | 0.171 |
| | Comorbidities 1-2 | 0.414 | 0.171 | 0.395 | 0.171 | 0.420 | 0.170 | 0.474 | 0.174 |
| | Comorbidities $\geq$3 | 1.214 | 0.248 | 1.207 | 0.247 | 1.214 | 0.247 | 1.230 | 0.252 |
| $\zeta Z(\tau)$ | CF*Age | | | | | | | -0.015 | 0.024 |
| | CF*log(PSA + 1) | | | | | | | -0.577 | 0.366 |
| | CF*Gleason score | | | | | | | 0.336 | 0.252 |
| | CF*Stage T2-T3 | | | | | | | 0.372 | 0.655 |
| | CF*Comorbidities 1-2 | | | | | | | -1.116 | 0.457 |
| | CF*Comorbidities $\geq$3 | | | | | | | -0.148 | 0.708 |
| Log-likelihood | | -11135 | | -11143 | | -11132 | | -11118 | |
| AIC | | 22292 | | 22308 | | 22289 | | 22273 | |

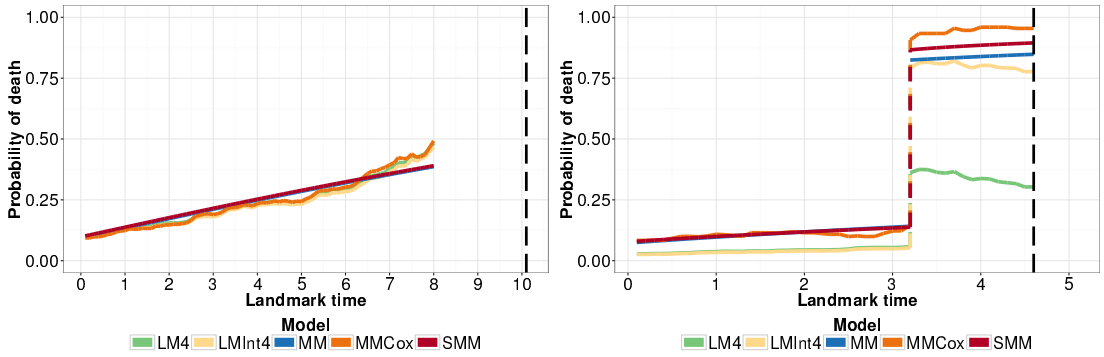


**Figure 1.10:** Predicted probability of death within 5 years, $P(T \leq \tau + 5 | T > \tau, Z(\tau), \mathbf{X})$ for two individuals in the prostate cancer data set. Individual A (left) is 60 years old at baseline, with PSA 19.7 ng/mL, Gleason score 7.5 ("4+3"), T1 Stage, 6 comorbidities, and does not experience clinical failure but dies 10 years from baseline. Individual B (right) is 54 years old at baseline, with PSA 16 ng/mL, Gleason score 9, T2 Stage, zero comorbidities, and experiences clinical failure at time 3 before dying at time 4.6 years from baseline. Black dashed line indicates time of death.

The predictions from the joint models (MM) and (SMM) are very similar both before and after clinical failure. Prior to clinical failure, the prediction probabilities from the landmark models are lower than those from the joint models by an amount that is not insignificant. After clinical failure, the landmark model without interactions (LM4) does not perform well for predicting death. Thus, the landmark models require interactions between the time-dependent binary covariate and the baseline covariates to capture the differential effects of the covariates on the different transitions.

## 1.6 Discussion

Models that can incorporate updated time-dependent marker information to revise survival predictions are vital for identifying high-risk subjects and making timely clinical decisions. In this chapter, we have compared the theoretical justification and predictive capabilities of two such dynamic prediction approaches: joint modeling and landmarking.

We contribute to the existing literature that compares these two approaches by investigating them under an illness-death model. We focused on a survival model with a binary time-dependent covariate, which is the simplest example of a joint model, to demonstrate

that even in this basic situation a Cox model in the landmark framework is not theoretically valid. With more complicated forms of the marker process, we can expect that the discrepancies between the performance of joint models and landmarking will be even greater, and that the inclusion of flexible forms in landmark models, as were suggested in this chapter, and better informed imputations of the marker value at landmark times, will be even more important. In our simulation study, we demonstrate that joint modeling produces more accurate predictions than landmarking. We simulate data under a joint model since the landmark model provides an approach to describe the data, but is not a data-generating model. Thus, to provide a fair comparison we also consider misspecified models within the joint modeling framework, particularly a semi-Markov model and a Markov model with a non-smooth baseline hazard. In addition, we compared the performance of the approaches to real data from the PAQUID study and concluded that the joint models performed marginally better than the simple landmark models.

Joint modeling and landmarking have different approaches to predicting the future for a subject. Joint modeling achieves this by directly modeling the longitudinal variable and integrating over the possible paths the variable might take, and thus uses the possibly strong relationship between the longitudinal variable and the event of interest to make the prediction. Landmarking is an approach which, in essence, obtains the empirical distribution of future event times among people similar to the person of interest. Estimation of this empirical distribution is achieved through a descriptive model of the residual times based on a finite number of parameters. Since the residual time distribution is determined by the stochastic process for the longitudinal variable, landmarking does depend implicitly on the stochastic process. The data provides information about the stochastic process of the longitudinal variable, which is exploited in the joint modeling approach but ignored in the landmarking approach. Using data from the prostate cancer study, we demonstrated that the simple landmark models do not properly capture the effects of the baseline covariates, averaging their effect on predictive probability over both individuals

who have experienced "illness" and those who have not. The joint models compute the predicted probability by considering all possible paths through the illness-death model, allowing the effect of the baseline covariate to vary depending on the state in the process. The use of more flexible landmark models and interactions between the baseline covariates and the time-dependent "illness" indicator helps to mitigate this issue.

While the landmarking approach is appealing because it does not require specification of a longitudinal model, the derivations in this chapter suggest that simple forms for the landmark models are unlikely to fit well, and the form of the landmark models may need to include non-proportional hazards and interactions. Thus, just as with joint models, considerable effort may be needed to obtain a good fitting model. One difference between joint models and landmarking is in setting up the data. For joint models, the likelihood is derived from the observed data and there are no choices to make. With landmarking there are choices to make that will change the predictions, which include the number and values of the landmark times, what time horizon to use when administratively censoring the data in the super data set, and how to impute $Z(\tau)$.

To avoid using LOCF, we proposed a longitudinal data structure based on inspection times and demonstrated that in our situation it performed better than or as well as the super data set proposed by van Houwelingen and Putter (2011). Alternatively, we can specify a longitudinal model for $Z$ and impute a sensible value for $Z(\tau)$ for each subject, as was done by Maziarz et al. (2017). This approach has some similarity to the two-stage procedure of fitting a joint model in Bycott and Taylor (1998), which is known to have small bias and be more computationally convenient than a full joint model likelihood approach. They accomplish this by specifying the longitudinal marker process as a random effects model plus stochastic process and using the fit of this model to obtain less variable imputes of $Z(\tau)$ for each subject, which are then used as covariates in a time-varying Cox model.

In our opinion, joint modeling provides a more unified and principled approach that

also satisfies the consistency criteria. It could even be enhanced by the incorporation of external information. If the stochastic process can be well characterized, then we might expect the predictions to be more accurate, including for longer prediction windows. In situations where the stochastic process can be well estimated from the available data, joint modeling is likely to perform better. In situations where it is harder to estimate, e.g., sparse longitudinal data or many longitudinal variables, then the empirical performance of landmarking might provide a good enough approximation.

# CHAPTER II

# A Gaussian Copula Approach for Dynamic Prediction of Survival with a Longitudinally Measured Marker

## 2.1 Introduction

To obtain accurate, individualized survival predictions at a given point in time beyond treatment or diagnosis, prediction models must be able to utilize patient information that is collected during follow-up. The dynamic prediction at a prediction time of interest, $\tau$, can be obtained as the survival probability $\Pr(T > \tau + s | T > \tau, Z(\tau))$ for a patient that is still alive at time $\tau$, based on their updated marker value, $Z(\tau)$ or marker history at that time point, $\bar{Z}(\tau) = \{Z(u), u \leq \tau\}$, $u \leq \tau$. Thus, dynamic prediction methods require incorporating time-dependent marker information, $Z(t)$, into a model for the failure time, $T$, to obtain the conditional distribution $[T|T > \tau, Z]$.

In joint modeling, we specify a model for the marker process, $Z(t)$, and a model for the failure time that links it to the marker process, $T|Z$, e.g., a survival model with hazard $h(t|Z(t))$. From these two models, the joint distribution $[T, Z]$ can be derived. Thus, joint modeling produces a valid prediction function from which we can obtain consistent predictions that have a defined, meaningful relationship with predictions obtained from the model at other time points (Jewell and Nielsen, 1993). Another advantage of

joint modeling is that it is able to handle irregular marker measurements, and can produce a dynamic prediction at any prediction time of interest. The dynamic predictions obtained from joint modeling at time $\tau$ for surviving up to time $w = \tau + s$ involve integrating the conditional hazard $h(t|\tau, Z(\tau))$ from $\tau$ to $w$, which requires knowledge of the distribution of future values of the marker process beyond the current measurement $\{Z(t), \tau \leq t \leq w\}$. Thus, utilizing joint modeling for predictions requires the full, correct specification of the marker process, which can be difficult and involves making specific distributional assumptions. In addition, the marker model may be difficult to estimate when there are sparse longitudinal measurements, and misspecification of this model can result in biased predictions. A practical disadvantage of this method is that it can require computationally intensive methods for both estimation, particularly when using shared parameter joint models, and the calculation of the dynamic predictions, which involves numerical integration.

Landmarking requires directly specifying a survival model for $[T|T > \tau, Z(\tau)]$ by looking at the empirical failure time distribution at fixed time points, $\tau$, conditional on being alive at $\tau$ and having marker value $Z(\tau)$ (Anderson et al., 1983; van Houwelingen, 2007; Zheng and Heagerty, 2005; Gong and Schaubel, 2013). Thus, at each $\tau$, we obtain the best-fitting model for $T$ using information from individuals alive at $\tau$ and their marker information $Z(\tau)$. Estimation of this empirical distribution is accomplished by using a Cox regression to model the hazard $h(t|\tau, Z(\tau))$, where the covariate and baseline hazard effects can be restricted to vary smoothly with $\tau$. The dynamic survival predictions can be directly computed as $\Pr(T > \tau + s|T > \tau, Z(\tau)) = \exp\left\{-\int_{\tau}^{\tau+s} h(t|\tau, Z(\tau))\,\mathrm{d}t\right\}$. The advantages of this method are that it avoids having to specify the distribution of the marker process and can be easily implemented in standard software. A disadvantage of landmarking is the numerous decisions required by the method. To conduct estimation, landmarking requires prespecifying the prediction times of interest, referred to as landmark times. For simple landmarking models, computing dynamic predictions is restricted

to these time points. Since a model for the marker process is not specified, landmarking also requires selecting an imputation method for marker values at landmark times at which individuals do not have observations. As well, the landmarking approach does not satisfy the consistency criteria described in Jewell and Nielsen (1993), since it directly models the conditional hazard $h(t|\tau, Z(\tau))$ and does not derive it from the joint distribution of failure time and marker processes, as in joint modeling. In previous work (Suresh et al., 2017), we demonstrated that under a binary marker process, landmarking results in a theoretically incorrect model. However, by increasing model flexibility we were able to show that landmarking could provide a sufficient approximation to a joint model.

There has been much literature proposing alternative joint modeling methods for dynamic prediction (Rizopoulos et al., 2014; Andrinopoulou et al., 2015; Andrinopoulou and Rizopoulos, 2016; Njagi et al., 2016); however, they still require strong distributional assumptions and computationally intensive techniques for estimation. Similarly, extensions have been suggested within the landmarking framework that aim to overcome its limitations, but as a result require increased computation or modeling assumptions (Nicolaie et al., 2013; Parast and Cai, 2013; Huang et al., 2016; Rizopoulos et al., 2017; Ferrer et al., 2017). There are several benefits of using an ad-hoc approach, such as landmarking, for dynamic prediction. In comparison to joint modeling, it is a simpler method that does not require assumptions about the marker distribution and does not impose a computational burden on estimation or calculating predicted probabilities. However, its violation of the Jewell and Nielsen (1993) consistency criteria makes it a less attractive option since the behavior of predictions over time are not restricted to have a sensible relationship.

In this paper, we propose an approximate method for dynamic prediction that requires specifying the marginal models $Z|T > \tau$ and $T|T > \tau$ for individuals alive at time $\tau$, and then uses a bivariate Gaussian copula to model the joint distribution $(Z, T)|T > \tau$, conditional on being alive at $\tau$. From this joint distribution we can directly compute the dynamic predictions. Like landmarking, this method does not produce a comprehensive

probability model; however, we maintain a greater level of consistency in our predictions by specifying a single model for $T$, and then deriving the model for $T|T > \tau$, which will be consistently defined for all $\tau$. Unlike joint modeling, we do not require a flexible specification of the marker process using random effects that can lead to complex estimation. Instead, to enable easy estimation we specify the marginal distribution of the longitudinal data at each $\tau$, allowing the mean and variance of the distribution to change smoothly with $\tau$. We use two-stage estimation to first estimate the parameters from the marginal models, and then hold them fixed in the joint likelihood to estimate the association parameters. Estimation is conducted using likelihood-based methods, which allow for standard methods of model checking and validation.

Rizopoulos et al. (2008a) and Rizopoulos et al. (2008b) described copulas for the joint modeling of longitudinal marker and failure time processes. They proposed using the copula as a reparameterization of a shared random-effects model. The copula models the joint distribution of the random effects of the marker process and the frailty term of the survival process with a single association parameter. The authors considered various dependence structures between the two processes by exploring different copulas. Our aim is to use the copula to directly model the association between survival and marker data, with the dependence specified as a flexible, smooth function of time. We assume simple, but flexible, models for the marginal distributions, which avoids the complexity of random effects estimation. Although there are a variety of copulas to choose from, we consider the Gaussian copula because it is flexible, analytically tractable, and allows for the convenient derivation of marginal and conditional distributions.

An alternative approach within the copula framework could be to use a multivariate copula to obtain a fully specified joint model for $T$ and $Z$ measured at fixed time points $\tau_1, \tau_2, \ldots, \tau_k$, given by $(T, Z_{\tau_1}, Z_{\tau_2}, \ldots, Z_{\tau_k})$, as described by Ganjali and Baghfalaki (2015). This model makes use of an individual's entire longitudinal marker history, $\bar{Z}$, to make predictions. However, there are several aspects of the model specification

that do not recommend its use for dynamic prediction. This approach will not accommodate situations that involve irregular measurement times that vary by individual, which is common in practice. While EM algorithm estimation is used to handle unbalanced data, this involves imputing the values of the marker for time points beyond the individual's censoring or event time. Another important restriction of this multivariate copula approach is that the covariance matrix can greatly increase in dimension as the number of measurement times increase. The authors make an exchangeable correlation assumption to reduce the number of parameters to be estimated; however, our aim is to keep the association structure flexible to accommodate changing dependence over time.

We aim to describe a new method for dynamic prediction using a novel Gaussian copula approach. In Section 2.2, we introduce the model and discuss a two-stage approach for estimation of the Gaussian copula's marginal and association parameters. We consider the situation of both a binary marker (illness-death model) and continuous marker. In Section 2.3, we explore the performance of our method under both of these situations using simulation studies and in Section 2.4 we demonstrate using our method to obtain dynamic predictions with two real-world applications. Section 2.5 ends with a discussion of the advantages and limitations of our method and future directions.

## 2.2 Method

Our proposed method for dynamic prediction specifies the marginal distributions of the marker data and the survival outcome and uses a copula to model the association between the two outcomes over time. The intuition behind this approach is that we can specify a simpler model for each of the marginals that imposes fewer restrictive assumptions on the marginal distributions, and then model their correlation using a copula with a time-varying association structure. While copulas are most commonly use in financial applications, recent statistical literature has shown the applications of copulas for specifying the joint distribution of mixed outcomes (Song et al., 2009), time-to-event outcomes

(Emura et al., 2018), and joint modeling (Ganjali and Baghfalaki, 2015; Rizopoulos et al., 2008a,b).

In the bivariate situation, the joint distribution $F_{X,Y}$ of two random variables can be related to the corresponding marginal distributions $F_X$ and $F_Y$ using a copula $C$, defined by

$$F_{X,Y}(x, y) = C(u, v; \rho)$$

where $u$ and $v$ are the realizations of the probability integral transforms $U = F_X(X) \sim \text{Unif}(0, 1)$ and $V = F_Y(Y) \sim \text{Unif}(0, 1)$, and $\rho$ is a measure of the dependence between $F_X$ and $F_Y$. Sklar (1959) states that such a $C$ exists and that if $F_X$ and $F_Y$ are continuous, $C$ is unique. Thus, this approach allows us to specify the marginal distributions of the marker data and time-to-event process and then model their association using the copula. The copula is a flexible way of specifying this association since there is no restriction on the marginal distributions, which do not have to be specified parametrically.

### 2.2.1 Copula Model and Estimation

Let $\mathcal{D}_n = \{T_i^*, \delta_i, \mathbf{X}_i, \mathbf{Z}_i; i = 1, \ldots, n\}$ denote the observed data, where $T_i$ is the true event time, $C_i$ is the censoring time, $T_i^* = \min(T_i, C_i)$ is the observed event time, $\delta_i = \mathbf{1}(T_i \leq C_i)$ is the censoring indicator, $\mathbf{X}_i$ is the baseline covariate vector, and $\mathbf{Z}_i$ is the longitudinal marker vector, with $z_{il} = Z_i(\tau_{il})$ denoting the marker value at time $\tau_{il}, l = 1, \ldots, n_i$, for subject $i$.

The dynamic prediction of interest is the predicted probability of surviving up to time $\tau + s$, $s > 0$, given that a new subject $j$ has survived up to time $\tau$, i.e.,

$$p_j(\tau + s|\tau) = \Pr(T_j \geq \tau + s|T_j > \tau, \mathcal{D}_n, \mathbf{X}_j, Z_j(\tau)) \tag{2.1}$$

where $Z_j(\tau)$ denotes the subject's marker value at time $\tau$.

In the context of dynamic prediction with a time-to-event outcome and a longitudinal

marker, we are interested in specifying the marginal distributions of $T$ and $Z$ for each landmark time $\tau$. Thus, we are restricting the models for $T$ and $Z$ to be conditional on the patient being alive at time $\tau$, and are specifically interested in modeling the marginals of the conditional survival time $T|T > \tau$ and marker data $Z|T > \tau$, denoted by $T_\tau$ and $Z_\tau$, respectively. A Gaussian copula is then used to link the survival time distribution and the marker data at all time points, allowing us to compute the dynamic predictions from an overall model.

We begin by considering the situation of a continuous marker process. Let $F_{T_\tau}$ and $F_{Z_\tau}$ be the marginal distributions of the time-to-event outcome and continuous marker data, respectively, conditional on the individual being alive at time $\tau$. Both of the marginals can be conditional on baseline covariates $\mathbf{X}$, i.e., $F_{T_\tau|\mathbf{X}}$ and $F_{Z_\tau|\mathbf{X}}$; however, we shall omit them from the following model specification for brevity. Then the joint distribution $F_{T_\tau,Z_\tau}$ is defined by a Gaussian copula as

$$F_{T_\tau,Z_\tau}(t,z) = \Phi_2\left(\Phi^{-1}\left\{F_{T_\tau}(t)\right\}, \Phi^{-1}\left\{F_{Z_\tau}(z)\right\}; \rho_\tau\right) \tag{2.2}$$

where $\Phi$ is the standard normal distribution, $\Phi_2$ is the standard bivariate normal distribution, and $\rho_\tau = \rho(\tau)$ is the correlation, which is specified as a smooth function of landmark time and possibly baseline covariates $\mathbf{X}$. The joint density is then given by

$$\begin{aligned} f_{T_\tau,Z_\tau}(t,z) = \Pr(T_\tau = t, Z_\tau = z) &= \frac{\partial^2}{\partial t \partial z} F_{T_\tau,Z_\tau}(t,z) \\ &= \frac{f_{T_\tau}(t) f_{Z_\tau}(z)}{\sqrt{1-\rho_\tau^2}} \exp\left\{-\frac{\rho_\tau^2(q_1(t)^2 + q_2(z)^2) - 2\rho_\tau q_1(t) q_2(z)}{2(1-\rho_\tau^2)}\right\} \end{aligned}$$

where $q_1(t) = \Phi^{-1}(F_{T_\tau}(t))$ and $q_2(z) = \Phi^{-1}(F_{Z_\tau}(z))$, and $f_{T_\tau}$ and $f_{Z_\tau}$ are the marginal densities of $T_\tau$ and $Z_\tau$, respectively. This is the likelihood contribution of individuals who at time $\tau$ are alive and have observed marker value $z$, and at time $t$ have an observed event. For individuals who are are alive at time $\tau$, but are censored at time $t$, the joint

density is given by

$$\begin{aligned}\Pr(T_\tau > t, Z_\tau = z) &= \frac{\partial}{\partial z}\left[F_{Z_\tau}(z) - F_{T_\tau, Z_\tau}(t, z)\right] \\ &= f_{Z_\tau}(z) - \Phi\left(\frac{q_1(t) - \rho_\tau q_2(z)}{\sqrt{1-\rho_\tau^2}}\right) f_{Z_\tau}(z) \\ &= \Phi\left(-\frac{q_1(t) - \rho_\tau q_2(z)}{\sqrt{1-\rho_\tau^2}}\right) f_{Z_\tau}(z)\end{aligned}$$

Let $\boldsymbol{\theta}$ be the parameter vector containing both the marginal and association parameters of interest. Thus, the likelihood contribution for an individual $i$ at measurement time $\tau_{il}$ is given by

$$L_{il}(\boldsymbol{\theta}) = f_{T_{\tau_{il}}, Z_{\tau_{il}}}(t_i, z_{il}; \boldsymbol{\theta})^{\delta_i} \Pr(T_{\tau_{il}} > t_i, Z_{\tau_{il}} = z_{il}; \boldsymbol{\theta})^{1-\delta_i} \tag{2.3}$$

where $t_i$ is the time at which individual $i$ has the event or was censored (i.e., last observed time).

We construct a pseudo-likelihood by assuming working independence between measurements at different time points. Thus, we construct the likelihood by multiplying each individual's contribution at each measurement time as if they were independent to get the pseudo-likelihood $PL(\boldsymbol{\theta}) = \prod_{i=1}^{n} \prod_{l=1}^{n_i} L_{il}(\boldsymbol{\theta})$. If we were to specify a full likelihood then we would have to take into account the association between the multiple measurements on each individual, which would require the specification of several conditional distributions. The purpose of a pseudo-likelihood is to replace a numerically complex joint density by a simpler function. In a longitudinal framework, the observations from the same individual at different time points are not typically independent; however, in order to avoid the computational complexity and burden of specifying the full likelihood distribution of each individual $i$, $f_{T_{\tau_{i1}}, \ldots, T_{\tau_{in_i}}, Z_{\tau_{i1}}, \ldots, Z_{\tau_{in_i}}}$, we use a pseudo-likelihood where we explicitly model the association between the two processes measured for each individual, but do not specify the correlation structure of each of the processes themselves between the different measurement time points. This strategy is appropriate in our framework since we are in-

terested in the association between the two processes but we consider the correlation due to repeated measurements a nuisance. Arnold and Strauss (1991) found that maximizing a pseudo-likelihood produces consistent and asymptotically normal estimates.

Due to the number of parameters associated with both the marginal models and the association structure, direct maximization of this pseudo-likelihood may still be computationally difficult. Thus, we further simplify the pseudo-likelihood by using a method of inference functions for margins (IFM), where the marginal parameters are first estimated from the marginal models and then held fixed in the pseudo-likelihood to obtain the estimates for the association parameters. Joe and Xu (1996) showed that with IFM the estimate for $\boldsymbol{\theta}$ is consistent and asymptotically normally distributed.

The standard errors for the marginal survival model can be obtained in the same way as with a standard Cox or parametric survival model (Andersen and Gill, 1982). Robust standard errors for the marginal marker model are computed using a sandwich estimator (Zeger and Liang, 1986; Long and Ervin, 2000). Following arguments presented in existing literature (Shih and Louis, 1995; Joe and Xu, 1996; Prenen et al., 2017; Song, 2007), we describe two-stage parametric variance estimation for the association parameters in Appendix A.1, with the extension to semiparametric variation following from arguments presented in Prenen et al. (2017) and Spiekerman and Lin (1998). The analytic standard errors of the association parameter vector are complicated since they need to account for the variability from the estimates from the marginal models. Thus, in practice the standard errors are estimated using a resampling scheme, such as jackknife (Joe and Xu, 1996) or bootstrapping (Efron and Tibshirani, 1994).

Once the parameter estimates $\hat{\boldsymbol{\theta}}$ have been obtained using the IFM method, we can

compute the dynamic prediction of interest from Eq.(2.1) as,

$$\begin{aligned}
\Pr(T \geq \tau + s | T \geq \tau, Z(\tau) = z; \hat{\boldsymbol{\theta}}) &= \Pr(T_\tau \geq \tau + s | Z_\tau = z; \hat{\boldsymbol{\theta}}) \\
&= \frac{\Pr(T_\tau \geq \tau + s, Z_\tau = z; \hat{\boldsymbol{\theta}})}{\Pr(Z_\tau = z; \hat{\boldsymbol{\theta}})} \\
&= \frac{\dfrac{\partial}{\partial v}\left[F_{Z_\tau}(v; \hat{\boldsymbol{\theta}}) - F_{T_\tau, Z_\tau}(t, v; \hat{\boldsymbol{\theta}})\right] |_{t=\tau+s, v=z}}{f_{Z_\tau}(z; \hat{\boldsymbol{\theta}})} \\
&= \Phi\left(-\frac{\hat{q}_1(\tau + s) - \hat{\rho}_\tau \hat{q}_2(z)}{\sqrt{1 - \hat{\rho}_\tau^2}}\right) \qquad (2.4)
\end{aligned}$$

where $\hat{q}_1(\tau + s) = \Phi^{-1}(F_{T_\tau}(\tau + s; \hat{\boldsymbol{\theta}}))$, $\hat{q}_2(z) = \Phi^{-1}(F_{Z_\tau}(z; \hat{\boldsymbol{\theta}}))$, and $\hat{\rho}_\tau = \rho(\tau; \hat{\boldsymbol{\theta}})$.

For the situation where the continuous marker is not observed at the prediction time, we consider instead using the value $\hat{q}_2(z) = \Phi^{-1}(F_{Z_{\tau^*}}(z; \hat{\boldsymbol{\theta}}))$ in our prediction, where $\tau^*$ is the time at which the marker was last observed. That is, we compute the quantile of the marker distribution at the time at which the marker was observed and carry that forward to the prediction time of interest, rather than carrying the marker value to a new time at which the marker distribution is different. Carrying forward the marker value might be particularly problematic for situations with sparse data. For example, if a person's marker value is in the 10th percentile of the marker distribution at the time it is measured, it is intuitive that they will remain in that percentile, rather than the percentile that corresponds to the marker distribution at the new prediction time, which can be far in the future.

### 2.2.2 Modeling copula components

In choosing the models for the components of our copula, we want to consider simple, flexible, but possibly misspecified models that can serve as a good approximation to the true models. The aim is to avoid placing restrictive assumptions on the models, and allow for easy estimation that can be readily implemented in standard software.

#### 2.2.2.1 Modeling the continuous marker data

Instead of specifying a mixed effects model for the continuous marker data, as is the case with joint modeling, we describe the behavior of the marker using a marginal model, where the mean and variance can be specified as a function of landmark time $\tau$ and baseline covariates $\mathbf{X}$. We define the model $Z_\tau = \mu(\tau, \mathbf{X}, \boldsymbol{\gamma}_\mu) + \epsilon_\tau$, where $\boldsymbol{\gamma}_\mu$ is a vector of regression coefficients, $\mu(\tau, \mathbf{X}, \boldsymbol{\gamma}_\mu)$ is a function of landmark time, baseline covariates, and regression coefficients, and $\epsilon_\tau$ is an error term that is independently distributed. We consider a linear regression for $Z_\tau$, where we model $\mu(\tau, \mathbf{X}, \boldsymbol{\gamma}_\mu)$ as a smooth parametric function of landmark time, and $\epsilon_\tau \sim N(0, \sigma_Z^2)$, where $\sigma_Z^2 = g(\tau, \mathbf{X}, \boldsymbol{\gamma}_\sigma)$ and $\boldsymbol{\gamma}_\sigma$ is a vector of regression coefficients. From this model we can obtain an interpretation of the population-averaged effects of the baseline covariates on the marker process, and how these effects change with landmark time.

#### 2.2.2.2 Modeling the failure time data

We model the time-to-event outcome, $F_T$, and then compute the conditional survival $F_{T_\tau}$ from this model as

$$F_{T_\tau}(t) = \frac{F_T(t) - F_T(\tau)}{1 - F_T(\tau)}$$

To model the time-to-event outcome distribution, we can consider using a non-parametric method, such the Kaplan-Meier or Nelson-Aalen estimators. However, these two methods do not lend themselves to the inclusion of multiple baseline covariates. Thus, we propose modeling the failure time using a Cox model that can be extended to accommodate non-proportional hazards or additional flexibility,

$$h(t) = h_0(t) \exp\{d(t, \mathbf{X}, \boldsymbol{\nu})\}$$

where $h_0(t)$ is the baseline hazard, $\boldsymbol{\nu}$ is a vector of regression coefficients, and $d(t, \mathbf{X}, \boldsymbol{\nu})$ is a function of baseline covariates, regression coefficients, and possibly time, to allow for non-

proportional hazards or time-varying covariate effects. The marginal distribution of the time-to-event outcome is then given by $F_T(t) = 1 - S(t) = 1 - \exp\left\{-\int_0^t h(u)\,\mathrm{d}u\right\}$. From this model we can also obtain the interpretation of the effect of the baseline covariates on the risk of death.

#### 2.2.2.3 Modeling the association

Once we define the marginals $F_{T_\tau}$ and $F_{Z_\tau}$, we can use the copula defined in Eq.(2.2) to describe the joint distribution at landmark time $\tau$. To model the association between the two marginals, we define the association $\rho_\tau$ as a function of landmark time and baseline covariates $\mathbf{X}$. Since we must restrict $\rho_\tau \in (-1, 1)$, we re-parameterize using Fisher's z-transformation $\eta_\tau = \log\{(1 + \rho_\tau)/(1 - \rho_\tau)\}/2$. We then define $\eta_\tau = \eta(\tau, \mathbf{X}, \boldsymbol{\xi})$ as a function of landmark time $\tau$, baseline covariates $\mathbf{X}$, and regression coefficients $\boldsymbol{\xi}$. Thus, from the association function we can evaluate the extent of the correlation between the time-to-event outcome and the marker process, and how that relationship changes with landmark time.

#### 2.2.2.4 Modeling the copula

For the purposes of this chapter, we consider a Gaussian copula due to its tractable nature, and easy implementation in standard software. However, there are other choices of copulas that have differing strengths of dependence in the distribution tails. Like the Gaussian copula, the Student's t copula is also symmetric. It has an additional parameter for degrees of freedom that controls the strength of the tail dependence. This copula is both upper- and lower-tail dependent, which allows for joint extreme events and can be beneficial if we expect our distribution to have heavy tails. The Clayton and Gumbel copulas are Archimedean copula that are lower-tail and upper-tail dependent, respectively. We present the derivation of our model for these three alternative copulas in Appendix A.2, and consider the performance of the Student's t copula in our simulation study.

### 2.2.3 Copula model for binary marker data

In medical research, we are often faced with information on the occurrence of an intermediate event (e.g., recurrence), which can inform about the patient's survival or other time-to-event outcomes. These intermediate events can be considered as a binary marker process, and modeled as an irreversible illness-death model. We consider the covariate process $Z(t) \in \{0, 1\}$ as a time-dependent indicator of whether the individual has progressed from the "healthy" to "illness" state by time $t$. Thus, we are now interested in modeling the joint distribution of a binary marker and a continuous time-to-event outcome. A Gaussian copula, as was described in the previous section, is applicable only when linking two continuous outcomes. Joint modeling strategies for mixed outcomes using a copula approach were explored by Song et al. (2009). We use an extension of their model for mixed polychotomous and continuous outcomes, as described by de Leon and Wu (2011). The authors propose using a latent variable formulation of the discrete outcome to transform it into a continuous one, after which a parametric Gaussian copula can be used to model the time-varying association between the two continuous outcomes.

#### 2.2.3.1 Model for mixed bivariate copula

We introduce the notation, $Z^* \sim F_{Z^*}$, as an unobserved continuous latent process underlying our discrete marker process $Z$. For patient $i$, the observed $Z_i$ is related to $Z_i^*$ through

$$Z_i = \begin{cases} 0, & \text{if } Z_i^* \in (-\infty, 0) \\ 1, & \text{if } Z_i^* \in [0, \infty) \end{cases}$$

We then define the joint distribution $F_{T_\tau, Z_\tau^*}$ as in Eq.(2.2) replacing $Z_\tau$ with $Z_\tau^*$,

$$F_{T_\tau, Z_\tau^*}(t, z) = \Phi_2 \left( \Phi^{-1} \left\{ F_{T_\tau}(t) \right\}, \Phi^{-1} \left\{ F_{Z_\tau^*}(z) \right\}; \rho_\tau \right) \tag{2.5}$$

Thus, the marginals $F_{T_\tau}$ and $F_{Z_\tau^*}$ are absolutely continuous distributions. We can

define the mean of $F_{Z^*_\tau}$ as $E(Z^*_\tau) = \mu(\tau, \mathbf{X}; \boldsymbol{\gamma})$, which is a function of landmark time and baseline covariates, with parameters $\boldsymbol{\gamma}$ associated with the marginal distribution of $Z$. For identifiability, we assume that $Z^*$ has unit variance (or scale). The pseudo-likelihood is then

$$\begin{aligned} PL = \prod_{i=1}^{n}\prod_{j=1}^{n_i} & \Pr(T_{\tau_{ij}} = t_i, Z_{\tau_{ij}} = 0)^{I(Z_{\tau_{ij}}=0)\delta_i} \cdot \Pr(T_{\tau_{ij}} \geq t_i, Z_{\tau_{ij}} = 0)^{I(Z_{\tau_{ij}}=0)(1-\delta_i)} \\ & \Pr(T_{\tau_{ij}} = t_i, Z_{\tau_{ij}} = 1)^{I(Z_{\tau_{ij}}=1)\delta_i} \cdot \Pr(T_{\tau_{ij}} \geq t_i, Z_{\tau_{ij}} = 1)^{I(Z_{\tau_{ij}}=1)(1-\delta_i)} \\ = \prod_{i=1}^{n}\prod_{j=1}^{n_i} & \Pr(T_{\tau_{ij}} = t_i, Z^*_{\tau_{ij}} < 0)^{I(Z^*_{\tau_{ij}}<0)\delta_i} \cdot \Pr(T_{\tau_{ij}} \geq t_i, Z^*_{\tau_{ij}} < 0)^{I(Z^*_{\tau_{ij}}<0)(1-\delta_i)} \\ & \Pr(T_{\tau_{ij}} = t_i, Z^*_{\tau_{ij}} \geq 0)^{I(Z^*_{\tau_{ij}}\geq 0)\delta_i} \cdot \Pr(T_{\tau_{ij}} \geq t_i, Z^*_{\tau_{ij}} \geq 0)^{I(Z^*_{\tau_{ij}}\geq 0)(1-\delta_i)} \end{aligned}$$

where the likelihood contribution is given by one of the following for an individual at measurement time $\tau$ who:

- Has the event at time $t$ and does not have the intermediate event by time $\tau$

$$\Pr(T_\tau = t, Z^*_\tau < 0) = \frac{\partial}{\partial t} F_{T_\tau, Z^*_\tau}(t, 0) = \Phi_2\left(\frac{q_2(0) - \rho_\tau q_1(t)}{\sqrt{1-\rho^2_\tau}}\right) f_{T_\tau}(t)$$

- Is alive or censored at time $t$ and does not have the intermediate event by time $\tau$

$$\Pr(T_\tau \geq t, Z^*_\tau < 0) = F_{Z^*_\tau}(0) - F_{T_\tau, Z^*_\tau}(t, 0)$$

- Has the event at time $t$ and has the intermediate event at/before time $\tau$

$$\Pr(T_\tau = t, Z^*_\tau \geq 0) = \frac{\partial}{\partial t}[F_{T_\tau}(t) - F_{T_\tau, Z^*_\tau}(t, 0)] = \Phi_2\left(-\frac{q_2(0) - \rho_\tau q_1(t)}{\sqrt{1-\rho^2_\tau}}\right) f_{T_\tau}(t)$$

- Is censored or still alive at time $t$ and has the intermediate event at/before time $\tau$

$$\Pr(T_\tau \geq t, Z_\tau^* \geq 0) = [1 - F_{Z_\tau^*}(0)] - F_{T_\tau}(t) + F_{T_\tau, Z_\tau^*}(t, 0)$$

where $q_1(t) = \Phi^{-1}(F_{T_\tau}(t))$ and $q_2(z) = \Phi^{-1}(F_{Z_\tau^*}(z))$.

Two-stage estimation using the pseudo-likelihood can be conducted via IFM as described in the previous section to obtain parameter estimates $\hat{\boldsymbol{\theta}}$, and the dynamic predictions can be computed as

$$\begin{aligned}
\Pr(T \geq \tau + s | T \geq \tau, Z(\tau) = 0; \hat{\boldsymbol{\theta}}) &= \Pr(T_\tau \geq \tau + s | Z_\tau = 0; \hat{\boldsymbol{\theta}}) \\
&= \frac{F_{Z_\tau^*}(0; \hat{\boldsymbol{\theta}}) - F_{T_\tau, Z_\tau^*}(\tau + s, 0; \hat{\boldsymbol{\theta}})}{F_{Z_\tau^*}(0; \hat{\boldsymbol{\theta}})} \\
\Pr(T \geq \tau + s | T \geq \tau, Z(\tau) = 1; \hat{\boldsymbol{\theta}}) &= \Pr(T_\tau \geq \tau + s | Z_\tau = 1; \hat{\boldsymbol{\theta}}) \\
&= \frac{[1 - F_{Z_\tau^*}(0; \hat{\boldsymbol{\theta}})] - F_{T_\tau}(\tau + s; \hat{\boldsymbol{\theta}}) + F_{T_\tau, Z_\tau^*}(\tau + s, 0; \hat{\boldsymbol{\theta}})}{1 - F_{Z_\tau^*}(0; \hat{\boldsymbol{\theta}})}
\end{aligned}$$

#### 2.2.3.2 Modeling the binary marker data

Under the true illness-death model, we can write out the distribution of the marker process conditional on surviving up to time $\tau$ as

$$\begin{aligned}
\Pr(Z = 0 | T \geq \tau, \mathbf{X}) &= \frac{\Pr(Z = 0, T \geq \tau | \mathbf{X})}{\Pr(T \geq \tau | \mathbf{X})} \\
&= \frac{e^{-\int_0^\tau \lambda_{01}(u|\mathbf{X}) + \lambda_{02}(u|\mathbf{X})\, \mathrm{d}u}}{e^{-\int_0^\tau \lambda_{01}(u|\mathbf{X}) + \lambda_{02}(u|\mathbf{X})\, \mathrm{d}u} + \int_0^\tau e^{-\int_0^v \lambda_{01}(u|\mathbf{X}) + \lambda_{02}(u|\mathbf{X})\, \mathrm{d}u} \lambda_{01}(v|\mathbf{X}) e^{-\int_v^\tau \lambda_{12}(u|\mathbf{X})\, \mathrm{d}u}\, \mathrm{d}v} \\
\Pr(Z = 1 | T \geq \tau, \mathbf{X}) &= 1 - \Pr(Z = 0 | T \geq \tau, \mathbf{X})
\end{aligned}$$

where $\lambda_{ij}(t|\mathbf{X})$ represents the hazard of transitioning from state $i$ to state $j$ (0: Healthy, 1: Ill, 2: Dead), with transition-specific baseline covariate effects. Since the form of this distribution as a function of $\mathbf{X}$ does not correspond to a known distribution, we consider a misspecified model for the marker data that can serve as a good approximation of the

true model but allows for easy estimation. As in the previous section, we want to specify a simple, flexible model, where the mean is a function of landmark time $\tau$ and baseline covariates $\mathbf{X}$. We can define the latent model $Z_\tau^* = \mu(\tau, \mathbf{X}, \boldsymbol{\gamma}) + \epsilon_\tau$ where $\boldsymbol{\gamma}$ is a vector of regression coefficients, $\mu(\tau, \mathbf{X}, \boldsymbol{\gamma})$ is a function of the landmark time, baseline covariates, and regression coefficients, and $\epsilon_\tau$ is an error term that is independently, and identically distributed.

- If $\epsilon_\tau$ is normally distributed $N(0, \sigma^2)$, then $Z_\tau^* \sim N(\mu(\tau, \mathbf{X}, \boldsymbol{\gamma}), \sigma^2)$ and $Z_\tau$ is a probit model, where $\sigma^2 = 1$ for identifiability.
- If $\epsilon_\tau$ has a logistic distribution, then $Z_\tau$ will be a standard logistic regression.
- If $\epsilon_\tau$ is non-standardized Student t-distributed $t(0, 1, v)$ (mean 0, scale 1, and df $v$), then $Z_\tau^* \sim t(\mu(\tau, \mathbf{X}, \boldsymbol{\gamma}), 1, v)$, where we fix unit scale for identifiability.

Modeling the time-to-event process and the association can be performed in the same way as described in the previous section.

## 2.3 Simulation Study

We conduct a simulation study for both the situations of a binary and a continuous marker process to evaluate the predictive performance of our proposed method in comparison to the existing methods of joint modeling and landmarking.

### 2.3.1 Performance Comparison Metrics

To assess the performance of the dynamic predictions produced under the different models, we focus on a prediction window, $s$, during which it is of medical importance to assess whether or not the individual has the event of interest. We evaluate the discrimination and calibration of the methods for the interval $(\tau, \tau + s]$ using dynamic analogues of weighted area under the curve (AUC) and Brier score (BS), which account for censoring

(Blanche et al., 2015). We denote these measures as $\text{AUC}(\tau, s)$ and $\text{BS}(\tau, s)$, respectively, and use the following definitions

$$\text{AUC}(\tau, s) = \Pr(p_i(\tau + s|\tau) > p_j(\tau + s|\tau) | D_i(\tau, s) = 1, D_j(\tau, s) = 0, T_i > \tau, T_j > \tau)$$

$$\text{BS}(\tau, s) = \mathbb{E}\left[(D(\tau, s) - p(\tau + s|\tau))^2 | T > \tau\right]$$

where $D_i(\tau, s) = I(\tau < T_i \leq \tau + s)$ and $p_i(\tau + s|\tau)$ is the dynamic prediction of interest given in Eq.(2.1).

Since BS depends on the cumulative incidence of death in $(\tau, \tau + s]$, we use a standardized version that produces an $R^2$-type measure that compares how well the predictions perform relative to a null model that does not take into account subject-specific information, $\text{BS}_0(\tau, s)$. We denote this scaled measure as $R^2(\tau, s) = 1 - \text{BS}(\tau, s)/\text{BS}_0(\tau, s)$. To make comparisons between the different models, we compute AUC and $R^2$ using the predicted probabilities from the true models, denoted $\text{AUC}_{\text{True}}$ and $R^2_{\text{True}}$, respectively. We then report the relative measures $\Delta\text{AUC} = \text{AUC}_{\text{True}} - \text{AUC}$ and $\Delta R^2 = R^2_{\text{True}} - R^2$ for each of the models, where a lower value indicates better performance.

To ensure that our method is not consistently predicting higher or lower than the true probabilities, we also evaluate calibration using the root mean squared prediction errors (RMSEs) between the true conditional survival probabilities and the predictions obtained from each of the different models considered. In addition, for the binary marker situation, for each landmark time we compare the bias and variance of the dynamic predictions under the various approaches.

Five hundred simulations of 1000 subjects were run for each scenario. Five hundred of these subjects were randomly selected to create a training data set, to which the model were fit. The performance metrics were then computed for predictions from the remaining 500 patients who compose the validation data set.

### 2.3.2 Simulation: Continuous marker process

In the situation of a continuous marker process, we simulate patients who have been followed for a period of 15 years, for whom longitudinal biomarker measurements are available at baseline. We simulate marker measurement under two patterns of observation: (1) the marker process is observed every year for 14 years following baseline, and (2) the value of the marker is observed at random inspection times. Inter-inspection times are exponentially distributed with rate 0.5 and 1, to simulate under situations with more sparsely collected marker measurements. We simulate a binary baseline covariate $X$ that has prevalence of 50%. We generate the longitudinal marker measurements using a linear mixed effects model.

$$z_i(t) = m_i(t) + \epsilon_i(t) = \alpha_0 + \alpha_1 t + \alpha_2 X + \alpha_3 X t + b_{i0} + b_{i1} t + \epsilon_i(t)$$

where $\epsilon_i(t) \sim N(0, \sigma^2_\epsilon)$ and $\mathbf{b}_i \sim N(\mathbf{0}, \mathbf{D})$.

To generate the survival times, we use the following joint model

$$h_i(t|m_i(t)) = h_0(t) \exp\{\omega_2 X_i + \phi m_i(t)\}$$

with $h_0(t) = \exp\{\omega_0\}\omega_1 t^{\omega_1 - 1}$ as the Weibull baseline hazard. We let $\alpha_0 = -3, \alpha_1 = 1, \alpha_2 = -0.8, \alpha_3 = 0.5, \omega_1 = 1.4, \omega_2 = 0.5, \gamma_1 =$, $\mathbf{D}=\begin{pmatrix} 1 & 0.5 \\ 0.5 & 1 \end{pmatrix}$. Since $\phi$ describes how the survival process is affected by the longitudinal biomarker, we vary the correlation between the two processes and consider $\phi = 0.5$ and 1.5. Since $\sigma^2_\epsilon$ describes the noisiness of the marker process, we simulate under the values $\sigma_\epsilon = 0.6$ and 1.2. We generate right-censoring from a Uniform(0,15) distribution. Under the various scenarios considered, we vary the value of $\omega_0$ to achieve a censoring rate of about 45%. We are interested in dynamic predication for the first five years following baseline, thus we consider landmark times $\tau = 0, 1, \ldots 5$. We present results for a prediction of failure within a window of

$s = 3$ years beyond the prediction time.

#### 2.3.2.1 Models

The joint, landmark, and copula models fit to the continuous marker data are shown in Table 2.1. We consider shared random effects models for the joint models, where (JM) is the model from which the data is simulated under and (JM2) is a misspecified model. For both, we fit a mixed effects model for the longitudinal marker process; however, in (JM2) we misspecify the functional form by incorrectly modeling the time relationship. The landmark models considered are the super model (LM1) and the extended super model (LM2) from Chapter I. For additional flexibility, we also include an interaction between the marker value and the baseline covariates in the (LMInt*) models, which was found to improve performance in Chapter I. Recall that for (LM1) and (LMInt1) we create a landmark data for each prediction time of interest with administrative censoring at the prediction horizon, and stack them to form a super data set to which we fit the models. We do not consider the landmark models with non-proportional hazards since there was no evidence of improved performance.

To identify the modeling structure for the copula components, we examine diagnostic plots and test goodness-of-fit, as demonstrated in Appendix A.3.1. We fit a population-averaged model to the longitudinal data, and from the loess curve plotted to the marker trajectories, we identify that a basis spline for landmark time with an interaction with the baseline covariate is the best-fitting function for the marginal mean. Also, we allow the variance of the population-averaged model to increase with time. We use this structure for the mean in all of the copula models considered. We model the failure time data parameterically (W: Weibull) or semiparametrically (C: Cox) and include the effect of the baseline covariate $X$. In (C*1), we model the association as a function of time, the baseline covariate, and their interaction. In models (C*2) we model the association more flexibly using a basis spline for landmark time. Finally, (C*3) has the same model

components as (C*1), which are instead joined using a Student's t copula with 4 degrees of freedom to identify whether the heavier tails of this copula provide a better fit to the data.

**Table 2.1:** Summary of models fit in the continuous marker simulation study.

| Class | Model | Label |
|---|---|---|
| **Joint Model** (Correctly specified) | $h_i(t\|m_i(t)) = h_0(t)\exp\{\phi_1 X_i + \phi_2 m_i(t)\}$<br>$m_i(t) = \alpha_0 + \alpha_1 t + \alpha_2 X + \alpha_3 Xt + b_{i0} + b_{i1}t$<br>$z_i(t) = m_i(t) + \epsilon_i(t)$ | (JM) |
| **Joint Model** (Misspecified) | $h_i(t\|m_i(t)) = h_0(t)\exp\{\omega_2 X_i + \phi m_i(t)\}$<br>$m_i(t) = \alpha_0 + \alpha_1 t^3 + Xt^3 + b_{i0} + b_{i1}t$<br>$z_i(t) = m_i(t) + \epsilon_i(t)$ | (JM2) |
| **Landmark Models** | $h_{0\tau}\exp\{\beta(\tau)Z(\tau) + \alpha X\}$ | (LM1) |
| | $h_{0\tau}\exp\{\beta(\tau)Z(\tau) + \alpha_1 X + \alpha_2 XZ(\tau)\}$ | (LMInt1) |
| | $h_0(t)\exp\{\theta(\tau) + \beta(\tau)Z(\tau) + \alpha X\}$ | (LM2) |
| | $h_0(t)\exp\{\theta(\tau) + \beta(\tau)Z(\tau) + \alpha_1 X + \alpha_2 XZ(\tau)\}$ | (LMInt2) |
| **Copula Models** | $C$: Gaussian copula<br>$\mu_Z = \gamma_{\mu 0} + \gamma_{\mu 1}X + \sum_{k=1}^3 \gamma_{\mu 2k}B_k(\tau) + \sum_{k=1}^3 \gamma_{\mu 3k}B_k(\tau)X$<br>$\sigma_Z^2 = \gamma_{\sigma 0} + \gamma_{\sigma 1}\tau + \gamma_{\sigma 2}X$<br>$\eta_\tau = \xi_0 + \xi_1\tau + \xi_2 X + \xi_3 X\tau$<br>$h(t) = h_0(t)\exp\{\nu X\}$; $h_0(t)$ modeled nonparametrically | (CC1) |
| | $h(t) = h_0(t)\exp\{\nu X\}$; $h_0(t)$ modeled as Weibull hazard | (CW2) |
| | $C$: Gaussian copula<br>$\mu_Z = \gamma_{\mu 0} + \gamma_{\mu 1}X + \sum_{k=1}^3 \gamma_{\mu 2k}B_k(\tau) + \sum_{k=1}^3 \gamma_{\mu 3k}B_k(\tau)X$<br>$\sigma_Z^2 = \gamma_{\sigma 0} + \gamma_{\sigma 1}\tau + \gamma_{\sigma 2}X$<br>$\eta_\tau = \xi_0 + \sum_{i=1}^3 \xi_{1k}B_k(\tau) + \xi_2 X$<br>$h(t) = h_0(t)\exp\{\nu X\}$; $h_0(t)$ modeled nonparametrically | (CC2) |
| | $h(t) = h_0(t)\exp\{\nu X\}$; $h_0(t)$ modeled as Weibull hazard | (CW2) |
| | $C$: Student's t (df=4)<br>$\mu_Z = \gamma_{\mu 0} + \gamma_{\mu 1}X + \sum_{k=1}^3 \gamma_{\mu 2k}B_k(\tau) + \sum_{k=1}^3 \gamma_{\mu 3k}B_k(\tau)X$<br>$\sigma_Z^2 = \gamma_{\sigma 0} + \gamma_{\sigma 1}\tau + \gamma_{\sigma 2}X$<br>$\eta_\tau = \xi_0 + \xi_1\tau + \xi_2 X + \xi_3 X\tau$<br>$h(t) = h_0(t)\exp\{\nu X\}$; $h_0(t)$ modeled nonparametrically | (CC3) |
| | $h(t) = h_0(t)\exp\{\nu X\}$; $h_0(t)$ modeled as Weibull hazard | (CW3) |

#### 2.3.2.2 Results

We simulate under the scenarios described in Table A.5 and present the results for all three methods in Appendix A.4, Tables A.6-A.17. The landmarking models with the interaction perform similarly to their counterparts without the interaction. Thus,

this effect does not seem to have as much importance as it did in the binary setting in Chapter I. In Figure 2.1 (Scenario 1a), we compare the performance of all three methods. The copula model with semiparametric hazard (CC1) performs better than the parametric version (CW1). The model (CC1) outperform the landmark models (LM1) and (LM2) across all metrics, with the model (CW1) having similar RMSE and $\Delta R^2$, but higher AUC (i.e., lower $\Delta$AUC). The copula models have lower or similar RMSE, $\Delta$AUC and $\Delta R^2$ than the misspecified joint model (JM2) at earlier time points. However, at later time points the performance of (JM2) is on par with the model from which the data is generated (JM).

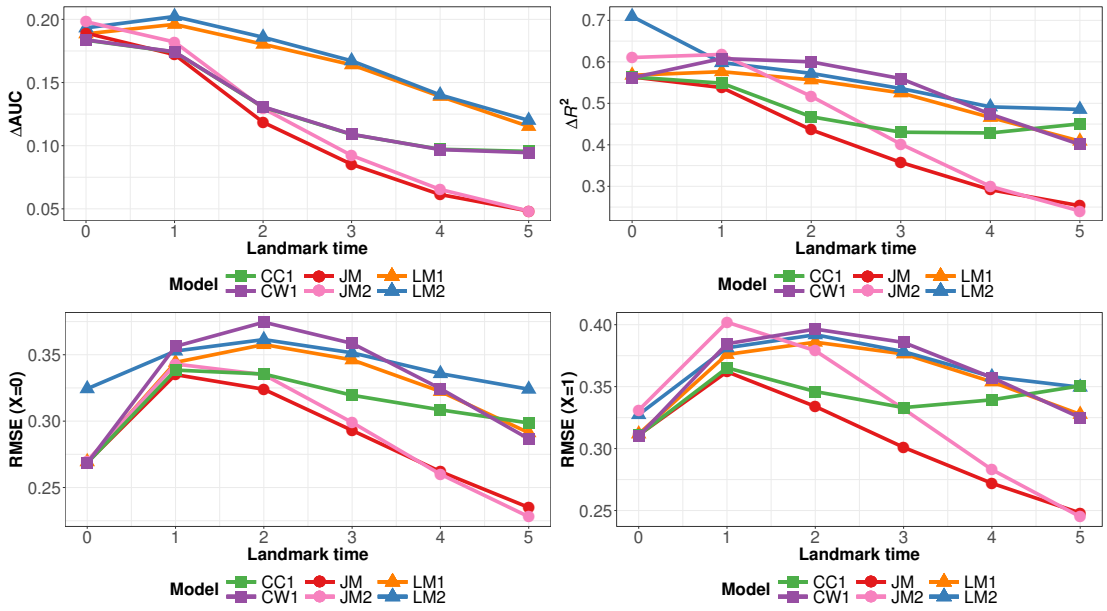


**Figure 2.1:** Simulation estimates for continuous marker Scenario 1a ($\sigma_\epsilon = 0.6$, $\phi = 0.5$, inter-inspection rate 0.5) for $\Delta$AUC (top-left) and $\Delta R^2$ (top-right), and RMSE for $X = 0$ (bottom-left) and $X = 1$ (bottom-right) for predicted probability $P(T \leq \tau + 3 | T > \tau, Z(\tau), X)$ from copula models (CC1), (CW2), joint models (JM), (JM2) and landmark models (LM1), (LM2).

In Figure 2.2 (Scenario 1a), we compare the performance of the different copula models. All the copula models have very similar AUC. In terms of the other metrics, We see that the Weibull models (CW*) do not have as good performance as the Cox models (CC*), with higher $\Delta R^2$ and RMSE. In comparing (C*1) and (C*2) we find that changing the

association structure results in similar performance. This suggests that choosing a flexible form for the association function is sufficient as long as well-fitting models are chosen for the marginal marker and failure time distributions. The (C*3) models that use the Student's t copula have similar performance to the (C*1) and (C*2) model, with slightly better performance in scenarios with more frequent measurement times.

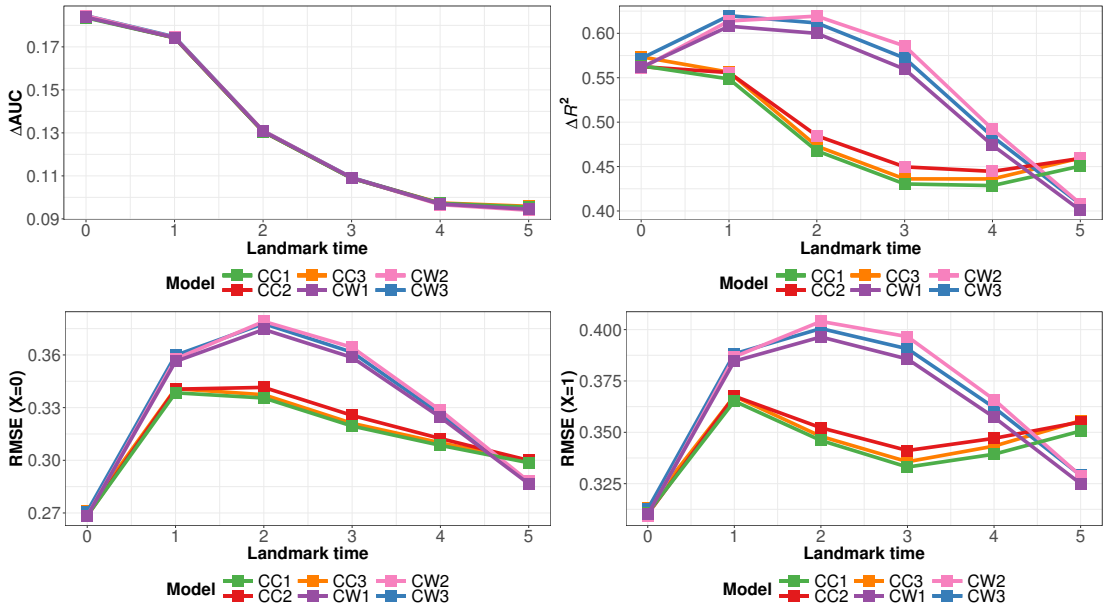


**Figure 2.2:** Simulation estimates for continuous marker Scenario 1a ($\sigma_\epsilon = 0.6$, $\phi = 0.5$, inter-inspection rate 0.5) for $\Delta$AUC (top-left) and $\Delta R^2$ (top-right), and RMSE for $X = 0$ (bottom-left) and $X = 1$ (bottom-right) for predicted probability $P(T \leq \tau + 3 | T > \tau, Z(\tau), X)$ from copula models (CC1), (CC2), (CC3), (CW1), (CW2), (CW3).

As the rate of inspection times increase (Scenarios *b), the RMSE decreases for all the models, with the copula models still performing better than (LM2) and (LMInt2), and marginally better or similar to (LM1) and (LMInt1). With a fixed inspection time (Scenarios *c), all the models have similar AUC that is on par with the joint models, as demonstrated in Figure 2.3 (Scenario 1c). Model (LM1) has lower RMSE than the copula model at later inspection times. However, it has comparable $\Delta$AUC and $\Delta R^2$. The copula models still outperform (LM2), which has a smaller improvement in RMSE and $\Delta R^2$ compared to the other models.

As the parameter $\phi$ that represents the association between the marker process and the

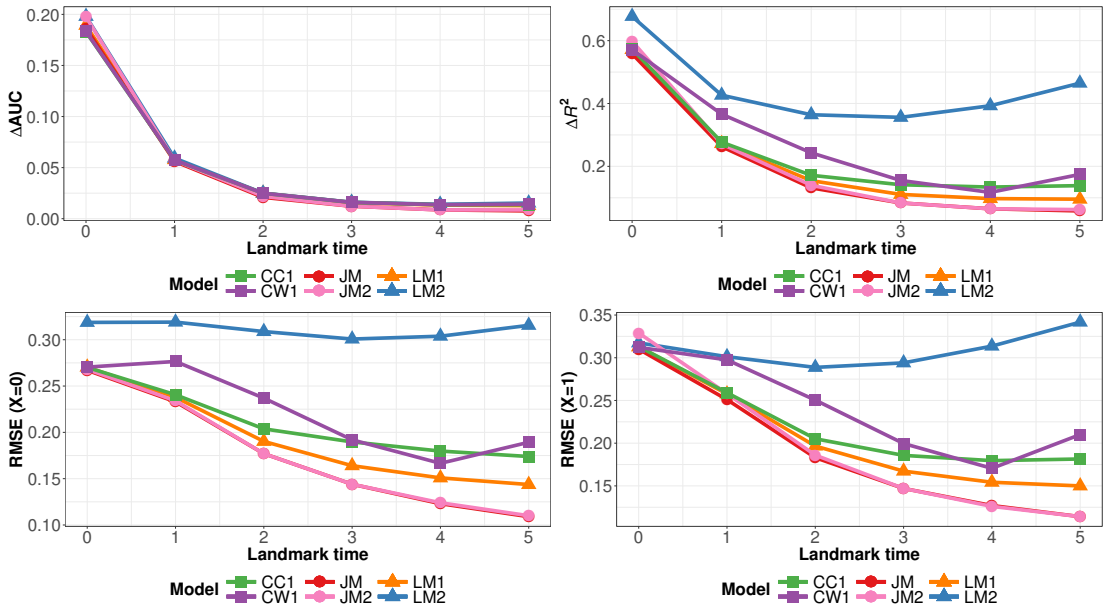


**Figure 2.3:** Simulation estimates for continuous marker Scenario 1c ($\sigma_\epsilon = 0.6$, $\phi = 0.5$, fixed inspection every year) for $\Delta$AUC (top-left) and $\Delta R^2$ (top-right), and RMSE for $X = 0$ (bottom-left) and $X = 1$ (bottom-right) for predicted probability $P(T \leq \tau + 3 | T > \tau, Z(\tau), X)$ from copula models (CC1), (CW2), joint models (JM), (JM2) and landmark models (LM1), (LM2).

hazard increases (Scenario 1 vs. 2, and 3 vs. 4), the copula model has better performance than the landmarking models. With increasing measurement error $\sigma_\epsilon$ (Scenarios 1 vs. 3, and 2 vs. 4), the RMSE for all the models increase, with the copula model having similar RMSE as the (LM1) model, but higher AUC and BS.

In general, we find that the performance of the copula model is good across all of the metrics considered. It has consistently better performance than the landmark model that allows the baseline hazard to be a function of landmark time, and outperforms the landmark model with stratified hazards when there are irregular measurement times. The copula model performs similarly to the joint model from which the data is generated and the misspecified joint model at earlier prediction times. It also appears to be robust to the choice of association function if the marginal models are well chosen, and is able to maintain good prediction with varying levels of measurement error ($\sigma_\epsilon$) and association ($\phi$) between the marker and survival process.

### 2.3.3 Simulation: Binary marker process

In the situation of a binary marker process, we simulate patients from an illness-death model. Defining the states as {0: Healthy, 1:Ill, 2:Dead}, the ages of illness onset and death without illness were generated from

$$\lambda_{jk}(t_i|\mathbf{X}_i) = \left(\frac{\rho_{jk}}{\kappa_{jk}}\right)\left(\frac{t_i}{\kappa_{jk}}\right)^{\rho_{jk}-1}\exp\{\boldsymbol{\alpha}'_{jk}\mathbf{X}_i\} \quad \text{for } j=0, k=1,2$$

For transition intensity from illness to death ($1 \to 2$), we generate data under two different models: (1) Markov, where the transition intensity depends only on current time, i.e., $\lambda_{12}(t|\mathbf{X})$, and (2) semi-Markov ("clock-reset"), where the transition depends on duration in the illness state i.e., $\lambda_{12}(t-V|\mathbf{X})$, where $V$ is the known transition time.

We choose the transition intensity shape and scale parameters such that $\lambda_{12}(t) > \lambda_{02}(t) > \lambda_{01}(t)$ [$\rho_{jk} = 1.15$ for all $j \to k$, $\kappa_{01} = 15$; $\kappa_{02} = 12.5$; $\kappa_{12} = 10$], to achieve 25% of patients developing illness. We simulate a binary covariate $X$ with prevalence 50%, that has a stronger effect on death in ill subjects, with $\alpha_{01} = 0.5$, $\alpha_{02} = 0.5$, $\alpha_{12} = 2$. We generate right-censoring from a Uniform(0,15) distribution to achieve a 50% censoring rate. We simulate marker measurement under two patterns of observation: (1) the marker process is continuously observed, and (2) the value of the marker is observed at random inspection times. Inter-inspection times are exponentially distributed with rate 0.5 and 1, to simulate both frequent and more sparsely collected marker measurements.

In addition to the basic scenario of a single baseline covariate, we also evaluated the performance of landmark models when the baseline covariate vector varies by transition. We generate data with two binary baseline covariates $X_1$ that has a stronger effect on death in ill subjects [$\alpha_{01,1} = \alpha_{02,1} = 0.5, \alpha_{12,1} = 2$] and $X_2$, which has no effect on death [$\alpha_{01,2} = 1, \alpha_{02,2} = \alpha_{12,2} = 0$]. We are interested in the dynamic prediction of failure at the landmark times $\tau = 0, 1, \ldots, 5$, for a prediction window of 3 years beyond the prediction time.

#### 2.3.3.1 Binary Marker Models

As described in Chapter I, we fit Markov and semi-Markov models, shown in Table 2.2. Recall, (MM) is a Markov illness-death model with Weibull transition intensities. (MSM) accounts for the effect of the observed transition time on the risk of death for those in the illness state. (MMCox) and (MSMCox) are their semiparametric counterparts. (SMM) is a parametric semi-Markov ("clock-reset") illness-death model, where the risk of transition to death after illness depends on the duration of time the individual has spent in the illness state. We also consider the flexible landmark models introduced in Chapter I that can be fit to unbalanced longitudinal data and do not require super data set structuring. (LM3) is the extended super landmark model and allows for non-proportional hazards. (LM4) allows the covariate effects of illness status to be a function of both landmark time ($\tau$) and residual time ($t - \tau$). (LMInt3) and (LMInt4) extend these models to include an interaction term between illness status and the baseline covariates. Recall, that in Chapter I these interaction models were found to have significantly improved performance over the regular landmarking models, especially when there were multiple baseline covariates with differential effects for the different transitions.

To identify the functional forms of the copula models we examine goodness-of-fit statistics and perform model selection, as outlined in A.3.2, A.3.4, and A.3.3. We present the results from six flexible copula models, with the model for the failure time data modeled either parametrically (W: Weibull) or semiparametrically (C: Cox) and including the baseline covariate $X$. In model (B*1), we model both the association and the mean of the continuous latent process underlying the binary marker as a function of time and the baseline covariate. In (B*2), we increase the flexibility by including an interaction between the baseline covariate and time in the model for the mean of the latent process. In (B*3), we consider an interaction between the baseline covariate and time in both the model for the marker and for the association. We also considered more flexible forms for the mean and association using splines and higher order terms, but found that the

**Table 2.2:** Summary of models fit in the binary marker simulation study.

| Class | Model | Label |
|---|---|---|
| **Markov** | $\lambda^W_{jk,0}(t)\exp\{\alpha_{jk}X\}$ for $j \to k$ transition | (MM) |
| **Markov,** $V^*$ | $\lambda^W_{jk,0}(t)\exp\{\alpha_{jk}X + \gamma V^* \mathbf{1}(j=1,k=2)\}$ | (MSM) |
| **Semi-Markov** | $\lambda^W_{jk,0}(t - V^* * \mathbf{1}(j=1,k=2))\exp\{\alpha_{jk}X\}$ | (SMM) |
| | $\lambda^W_{jk,0}(t)$ modeled as Weibull hazard | |
| **Markov** | $\lambda^{Cox}_{jk,0}(t)\exp\{\alpha_{jk}X\}$ for $j \to k$ transition | (MMCox) |
| **Markov,** $V^*$ | $\lambda^{Cox}_{jk,0}(t)\exp\{\alpha_{jk}X + \gamma V^* \mathbf{1}(j=1,k=2)\}$ | (MSMCox) |
| | $\lambda^{Cox}_{jk,0}(t)$ modeled nonparametrically | |
| **Landmark Models**[1] | $h_0(t)\exp\{\theta(\tau) + \beta_0 Z(\tau) + \omega(t-\tau)Z(\tau) + \alpha X\}$ | (LM3) |
| | $h_0(t)\exp\{\theta(\tau) + \beta_0 Z(\tau) + \omega(t-\tau)Z(\tau) + \alpha_1 X + \alpha_2 XZ(\tau)\}$ | (LMInt3) |
| | $h_0(t)\exp\{\theta(\tau) + \beta(\tau) Z(\tau) + \omega(t-\tau)Z(\tau) + \alpha X\}$ | (LM4) |
| | $h_0(t)\exp\{\theta(\tau) + \beta(\tau) Z(\tau) + \omega(t-\tau)Z(\tau) + \alpha_1 X + \alpha_2 XZ(\tau)\}$ | (LMInt4) |
| **Copula Models** | $C$: Gaussian copula | |
| | $\mu_{Z^*} = \gamma_0 + \gamma_1\tau + \gamma_2 X$ | |
| | $\eta_\tau = \xi_0 + \xi_1\tau + \xi_2 X$ | |
| | $h(t) = h_0(t)\exp\{\nu X\}$; $h_0(t)$ modeled nonparametrically | (BC1) |
| | $h(t) = h_0(t)\exp\{\nu X\}$; $h_0(t)$ modeled as Weibull hazard | (BW1) |
| | $C$: Gaussian copula | |
| | $\mu_{Z^*} = \gamma_0 + \gamma_1\tau + \gamma_2 X + \gamma_3 X\tau$ | |
| | $\eta_\tau = \xi_0 + \xi_1\tau + \xi_2 X$ | |
| | $h(t) = h_0(t)\exp\{\nu X\}$; $h_0(t)$ modeled nonparametrically | (BC2) |
| | $h(t) = h_0(t)\exp\{\nu X\}$; $h_0(t)$ modeled as Weibull hazard | (BW2) |
| | $C$: Gaussian copula | |
| | $\mu_{Z^*} = \gamma_0 + \gamma_1\tau + \gamma_2 X$ | |
| | $\eta_\tau = \xi_0 + \xi_1\tau + \xi_2 X + \xi_3 X\tau$ | |
| | $h(t) = h_0(t)\exp\{\nu X\}$; $h_0(t)$ modeled nonparametrically | (BC3) |
| | $h(t) = h_0(t)\exp\{\nu X\}$; $h_0(t)$ modeled as Weibull hazard | (BW3) |

[1] $\beta(\tau) = \beta_0 + \beta_1\tau + \beta_2\tau^2$; $\theta(\tau) = \theta_1\tau + \theta_1\tau^2$; $\omega(s) = \omega_1 s + \omega_2 s^2$

additional flexibility did not improve fit or performance.

#### 2.3.3.2 Binary Marker Simulation Results

We simulate under the scenarios outlined in Table A.18 and present the results comparing the three methods for dynamic prediction in Appendix A.5, Tables A.19-A.27. First, we simulate under a Markov assumption with a single baseline covariate. In Figure 2.4, we present the results from the inspection time measurement setting (Scenario 1a). As expected, the joint model from which the data were simulated (MM) has the best predictive performance. We find that the copula model has better RMSE for both values of the binary baseline covariate than the misspecified Cox model with semiparametric baseline hazards (MMCox) and the landmark models (LM3) and (LMInt3). We present the bias for $X = 1, Z = 1$ (i.e., those in the illness group with baseline covariate $X = 1$), and find that as the landmark time increases the bias for the copula model worsens. At the later time points there are very few individuals in this group (3% at LM=5), demonstrating that the copula model does not fit the data well at later time points for groups that have sparse data at those times. The copula model has low variance and BS relative to the other models, and comparable AUC. The performance of the copula model fit with a semiparametric Cox model for the marginal survival time distribution (BC*) has higher RMSE than the semiparametric version (BW*) but performs similarly or slightly better for the other performance metrics. As the inspection time increases (Scenario 1b, 1c), the performance of the landmark model with the interaction and semiparametric Markov model improve to be on par with the copula model. The copula and other models consistently outperform the landmark model without the interaction term.

For the semi-Markov simulation setting, we compare the copula model with landmark models and joint models that condition on the observed transition to illness. We present the results for the unbalanced measurement setting in Figure 2.5 (Scenario 2a). We find that the copula model has better performance than the landmark models and the

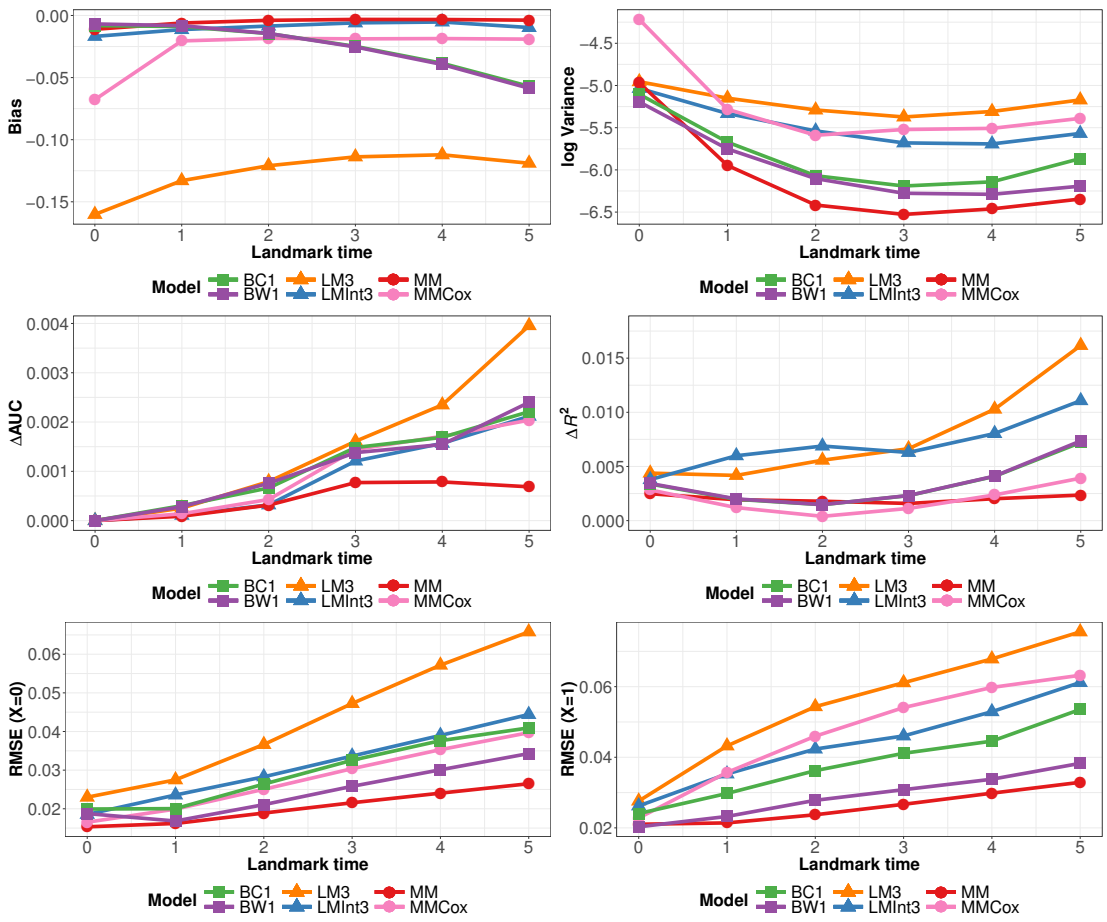


**Figure 2.4:** Simulation estimates for binary marker Scenario 1a for bias (upper-left) and variance (upper-right) for $Z(\tau) = 1, X = 1$, $\Delta$AUC (middle-left), and $\Delta R^2$ (middle-right), and RMSE for $X = 0$ (bottom-left) and $X = 1$ (bottom-right) for predicted probability $P(T \leq \tau + 3 | T > \tau, Z(\tau), X)$ from copula models (BC1), (BW1), joint models (MM), (MMCox) and landmark models (LM3), (LMInt3), under a Markov illness-death model with one baseline covariate and inspection time marker measurement.

semiparametric semi-Markov model (MSMCox). It has low variance and Brier score and has an AUC comparable with that of (SMM). As the inspection time increases (Scenario 2b, 2c), the performance of (MSMCox) improves, but the copula model still outperforms the landmark models across all the metrics.

Finally, we generate data under a Markov model with two baseline covariates that have differing effects for the different transitions. From Figure 2.6, in the setting with inspection time measurement (Scenario 3a) we see that the copula model has low variance and Brier score compared to the landmark models, and comparable RMSE to the landmark model

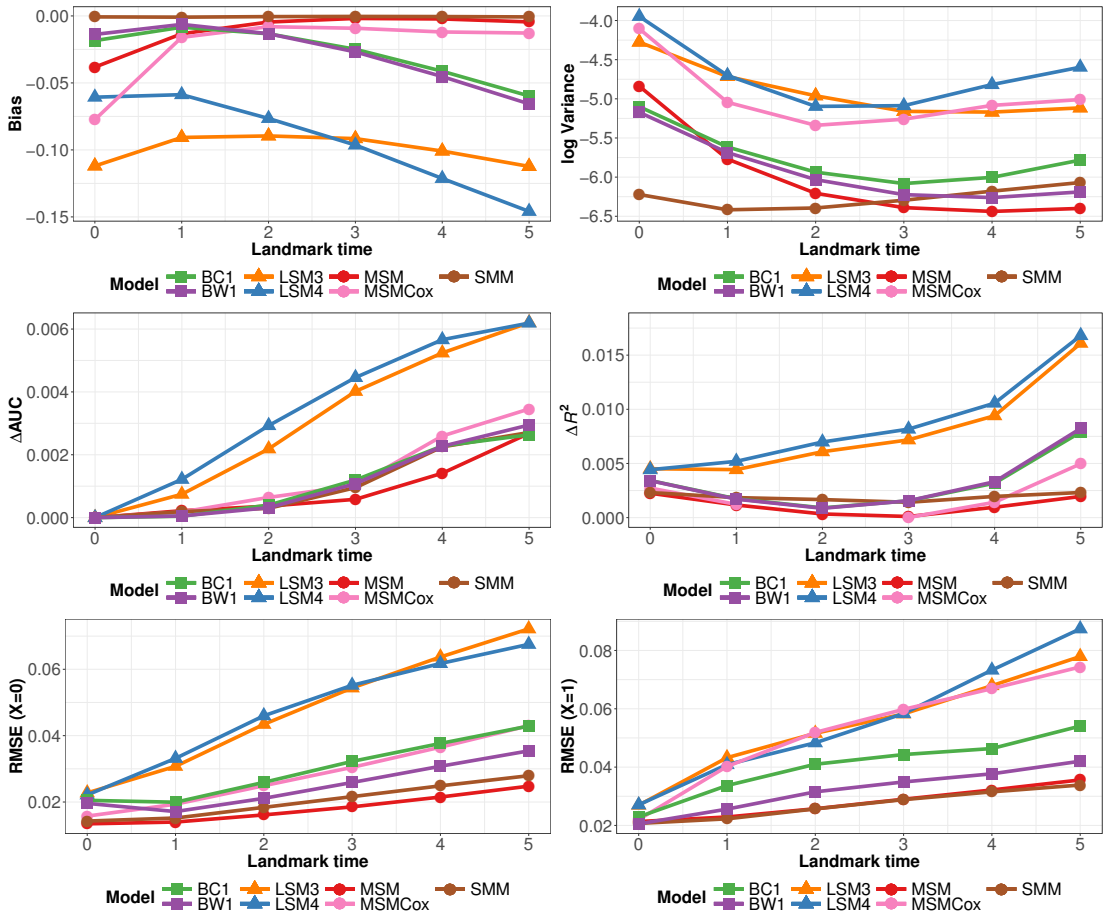


**Figure 2.5:** Simulation estimates for binary marker Scenario 2a for bias (upper-left) and variance (upper-right) for $Z(\tau) = 1, X = 1$, $\Delta$AUC (middle-left), and $\Delta R^2$ (middle-right), and RMSE for $X = 0$ (bottom-left) and $X = 1$ (bottom-right) for predicted probability $P(T \leq \tau + 3 | T > \tau, Z(\tau), X)$ from copula models (BC1), (BW1), joint models (MSM), (MSMCox), (SMM), and landmark models (LSM3), (LSM4), under a semi-Markov illness-death model with one baseline covariate and inspection time marker measurement.

with the interaction and the semiparametric Markov model. We present bias for the group $X_1 = 1, X_2 = 1, Z = 1$, and find that for the copula model the bias increases with landmark time. Again, we find that this is associated with few people being in that group at later times, preventing the copula from estimating the marginal distributions well at those times.

Overall, the copula model has good predictive performance across all the metrics, performing better than landmark models and misspecified Markov models with less frequent inspection times, and on par with other models with a continuously observed binary

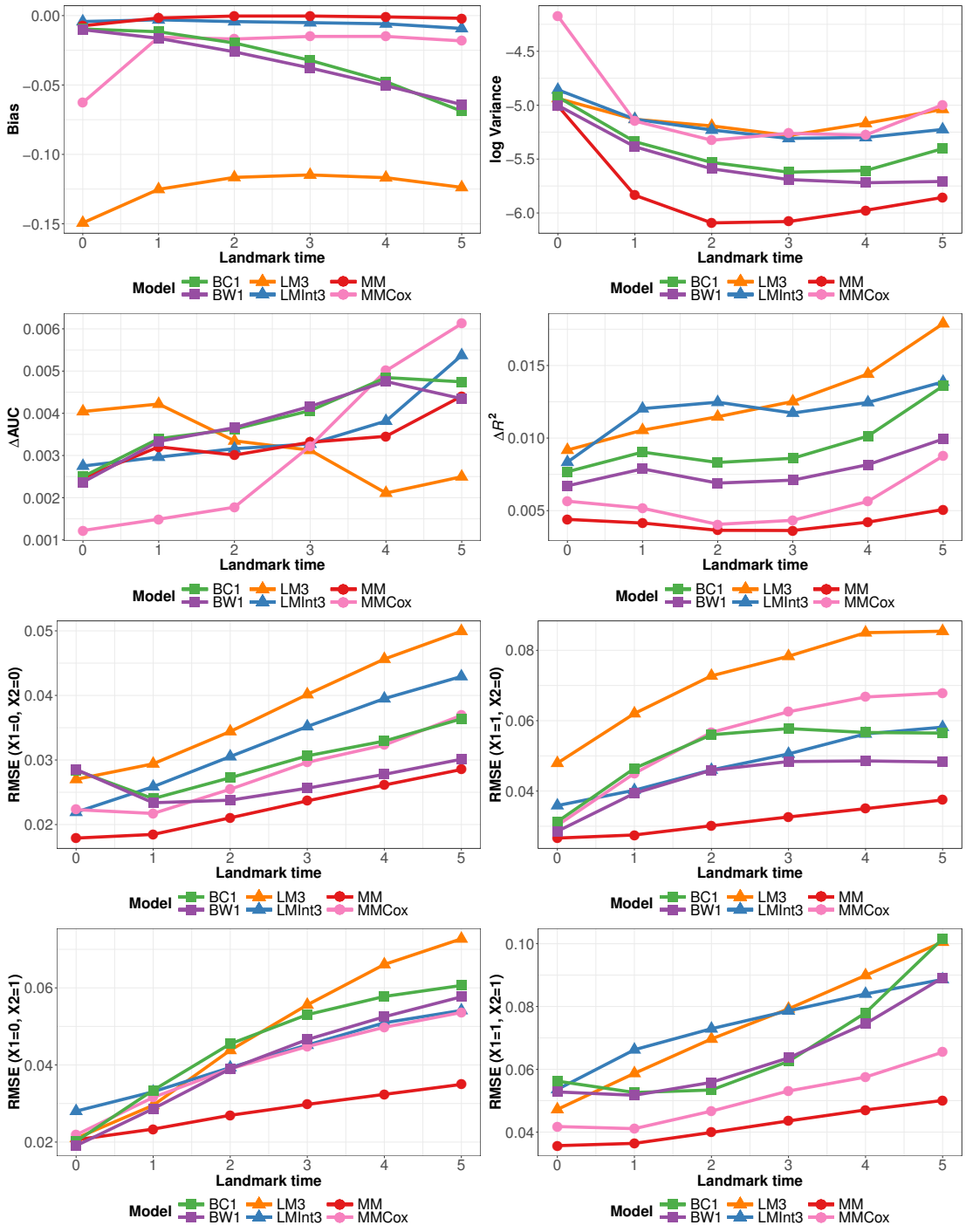


**Figure 2.6:** Simulation estimates for binary marker Scenario 3a for bias and variance for $Z(\tau) = 1, X_1 = 1, X_2 = 1$, $\Delta$AUC, and $\Delta R^2$, and RMSE for predicted probability $P(T \leq \tau + 3 | T > \tau, Z(\tau), \mathbf{X})$ from copula models (BC1), (BW1), joint models (MM), (MMCox) and landmark models (LM3), (LMInt3), fit to data structured as a longitudinal data set, under a Markov illness-death model with two baseline covariates.

marker. The copula model consistently outperforms the landmark model without the interaction term indicating that it has better predictive performance than the simpler landmark models that do not include the flexibility introduced in Chapter I. The bias for the copula model can be high for groups at times where there is little data observed; however, from RMSE we see that overall performance of the copula model by baseline covariate is better or comparable to the flexible landmark and misspecified Markov models.

## 2.4 Application

In this section, we apply our proposed copula method to both a heart valve and prostate cancer data set, to produce dynamic predictions using a longitudinally measured continuous and binary marker, respectively.

### 2.4.1 Continuous marker process: Aortic Heart Valve Study

To demonstrate the ability of the copula method to produce dynamic predictions using a continuous marker, we use data from an observational study that followed 248 patients who received an aortic valve replacement with the aim of comparing the efficacy of two artificial heart valves: homograft or stentless (Lim et al., 2008; Philipson et al., 2017). Longitudinal measurements of the left ventricular mass index (LVMI) were collected after surgery (baseline time), with an average of 3.68 and a maximum of 10 measurements per patient. Long-term buildup of left ventricular muscle mass can result in a fatal heart attack, thus there is interest in using a patient's changing LVMI to predict their future risk of death. The baseline covariate information used in the models considered were: type of implanted aortic prosthesis (homograft: 53%, stentless: 47%), age (median: 68; IQR: 59-75), and gender (male: 71%, female: 29%).

In Figure 2.7a we examine the survival curves by stent type and see a significantly higher survival probability for those who received the stentless valve compared to those who received the homograft valve. We examine the fit of a Cox model to the failure time

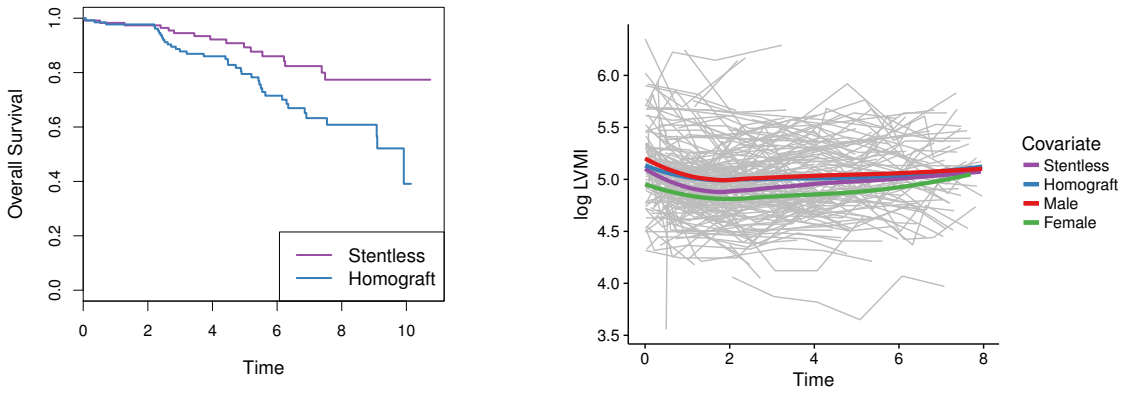


**(a)** Overall survival curves **(b)** Longitudinal log(LVMI) trajectories

**Figure 2.7:** Summary plots for heart valve data. (a) Overall survival curves by valve type. (b) Longitudinal log(LVMI) marker measurements for individuals over time with loess curves by valve type and gender.

data and find no violation of the proportional hazards assumption for any of the baseline covariates. Figure 2.7b depicts the longitudinal log(LVMI) observations per patient and from the loess curves we see that there is a decrease in mean log(LVMI) in the first year, after which it appears to be increasing with time. Thus, we consider a non-linear relationship, with possible interactions between the covariates and time. Selecting the best fitting model using backwards selection with AIC, we identify the population-averaged model for $Z_\tau$ as the main effects model with a basis spline effect for landmark time and constant variance $\sigma^2$. We considered more flexible forms for the association function including interactions and splines, but found that the results are similar to simpler forms. Thus, we fit the following copula model

$$
\begin{aligned}
&C: \text{ Gaussian copula} \\
&h(t) = h_0(t)\exp\{\boldsymbol{\nu}'\mathbf{X}\} \\
&\mu_Z = \gamma_0 + \boldsymbol{\gamma}_1'\mathbf{X} + \sum_{k=1}^{3}\gamma_{2k}B_k(\tau) \\
&\eta_\tau = \xi_0 + \boldsymbol{\xi}_1'\mathbf{X} + \xi_2\tau
\end{aligned}
$$

**Table 2.3:** Coefficient estimates and standard errors for copula model applied to heart valve data.

| | Covariate | Coef. | SE |
|---|---|---|---|
| | Age/10 | 1.029 | 0.184 |
| $\boldsymbol{\nu}$ | Female | -0.042 | 0.299 |
| | Homograft | 0.026 | 0.314 |
| | Intercept | 5.200 | 0.073 |
| | Age/10 | -0.013 | 0.011 |
| | Female | -0.178 | 0.029 |
| $\boldsymbol{\gamma}$ | Homograft | 0.079 | 0.027 |
| | $B_1$ | -0.527 | 0.149 |
| | $B_2$ | 0.425 | 0.258 |
| | $B_3$ | -0.481 | 0.385 |
| | Intercept | -1.085 | 0.818 |
| | Age/10 | 0.148 | 0.118 |
| $\boldsymbol{\xi}$ | Female | -0.035 | 0.200 |
| | Homograft | -0.210 | 0.194 |
| | $\tau$ | -0.038 | 0.044 |

where $\mathbf{X}$ is a vector of baseline covariates with age, valve type, and gender, $h_0(t)$ is modeled nonparametrically, and $B_k$ is a B-spline for a natural cubic spline with boundary knots at 0 and 10 years. The parameter estimates for the copula model are given in Table 2.3, and the standard errors were computed using bootstrapping. From the marginal model for $T$ we find that the age has a significant positive effect on time to death, while the effect of gender or stent type was not significant. From the marginal model for $Z$, females have a lower average log(LVMI) than males, and those with the homograft valve have a higher average log(LVMI) than those with the stent valve. There was a significant cubic spline effect for time on average log(LVMI). For females and those who received the homograft valve, the association between the risk of death and increased log(LMVI) is negative indicating decreased time to death.

We also apply the joint modeling and landmarking approaches to the data set for comparison. We fit a joint model with a random intercept and slope, and the flexible landmark model with non-proportional hazards and an interaction between the marker and baseline covariates. In Figure 2.8, we compare the predicted survival curves with

the empirical Kaplan-Meier estimators for patients still alive at one year. We present the curves by type of heart value (homograft vs. stentless), male gender, and whether the patient has a log(LVMI) $\leq 5$ vs. $> 5$ (median log(LVMI) at 1 year). Since the three methods model continuous log(LVMI), we use the 25th (4.7) and 75th (5.2) percentile values of log(LVMI) to obtain predictions, and median age. We see that our approach and joint modeling track each other closely and are similar to the empirical Kaplan-Meier curves. The landmark model curve splays out from the Kaplan-Meier curve for the higher range of log(LVMI).

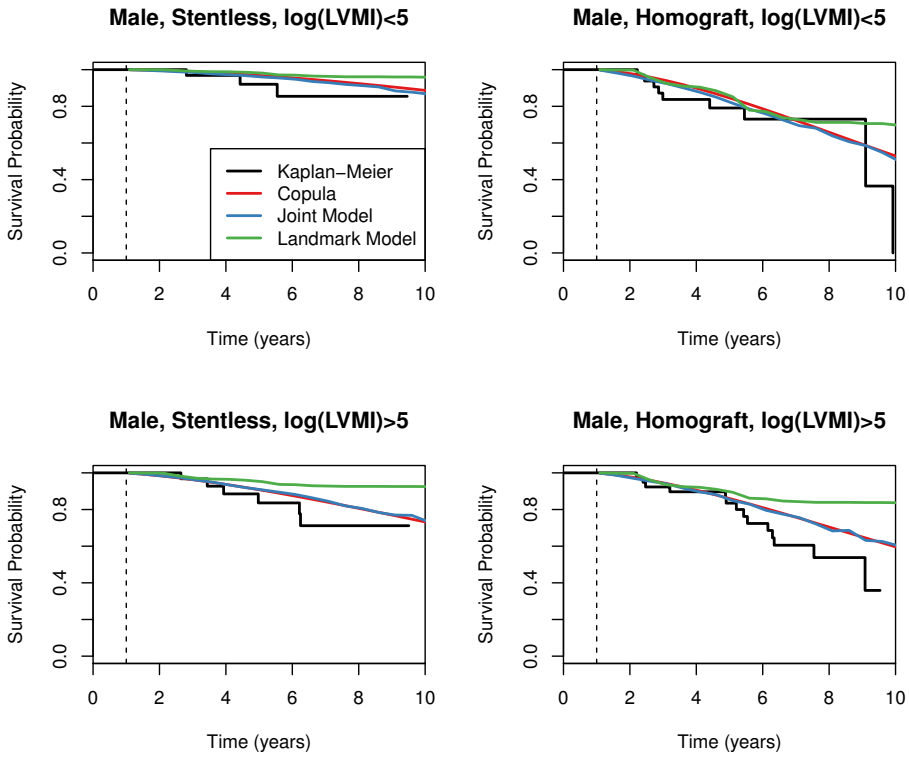


**Figure 2.8:** Prediction of future survival probability for patients at risk at 1 year post baseline by log(LVMI) range and valve type using the fourth methods: (1) Kaplan-Meier estimators, (2) proposed copula approach; (3) joint modeling, and (4) landmarking.

In Figure 2.9, we depict the predicted survival probabilities for two patients in the data set as their continuous marker value changes. Individual A is a younger male, who received the stentless valve, and has lower log(LVMI) that is increasing over time. Individual B is older, received the homograft valve, and has a steady, but higher log(LVMI) with a sudden

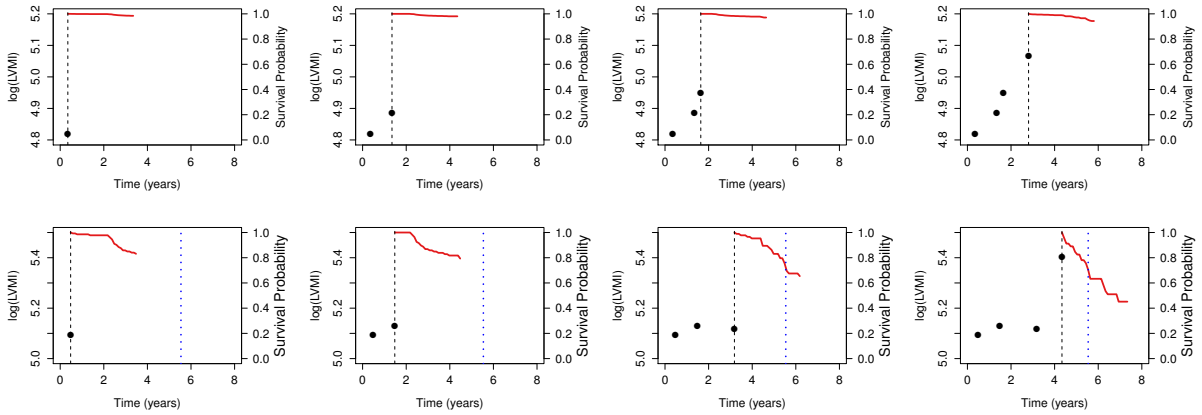


**Figure 2.9:** Predicted survival probabilities for risk of death within 3 years from the copula model for two patients in the heart valve data set. Individual A (top) is male, 59 years old at baseline, received the stentless valve, and does not die before the end of the study. Individual B (bottom) is male, 78 years old at baseline, received the homograft valve and died at 5.4 years after baseline. Blue dotted line indicates time of death.

increase at the last measurement. Since Individual A is a relatively low-risk patient we see that their predicted probability of death is low, with risk of death increasing as their log(LVMI) increases. Individual B is at higher risk due to their increased age at baseline, and their risk of death in the next 3 years increases greatly after their log(LVMI) spikes suddenly at 4 years, and they eventually die at 5.4 years from baseline. These predicted probability plots can be used by clinicians to monitor a patient's prognosis following valve replacement to identify if the patient's changing log(LVMI) is putting them at high risk for future death and further interventions must be implemented.

### 2.4.2 Binary marker process: Prostate Cancer Study

Returning to the prostate cancer study in Chapter I, we demonstrate and assess the use of the copula model for obtaining dynamic predictions using a binary marker. Recall, 745 patients with clinically localized prostate cancer were treated with radiation therapy. Patients were followed from start of treatment (baseline) and monitored for the occurrence of metastatic clinical failure (CF), treated as a time-dependent binary covariate. The aim is to use the intermediate CF information to predict a patient's future risk of death.

The states of the illness-death model are then "alive without clinical failure", "alive with clinical failure", and "dead". The median follow-up time was 9 years, and 52 patients experienced CF. Out of 188 deaths, 154 died before and 34 died after experiencing clinical failure. The pretreatment prognostic factors measured at baseline are age (median 69; IQR 63-74), log(PSA + 1) (PSA ng/ml; median 8; IQR 5-12), Gleason score treated continuously with a score of 7="3+4" and 7.5="4+3" (median 7; IQR 6-7.5), prostate cancer stage (T1: 57%, T2-T3: 43%), and comorbidities (0: 55%, 1-2: 37%, ≥3: 8%).

We obtain predicted probabilities of death within 5 years for landmark times $\tau = 0, 1, \ldots, 8$ years. We assume that the marker is continuously observed, and for fitting the landmark and copula models we structure the data as a super data set, with the LOCF assumption at each of the landmark times. In Chapter I, Tables 1.3 and 1.4, we present the parameter estimates from the joint and landmark models, respectively. We found that the effects of the baseline covariates vary across the different transitions. The landmark models with an interaction between the baseline covariates and CF status, (LMInt3) and (LMInt4), produced predicted probabilities similar to the joint models, (MM) and (MMCox). The landmark models without an interaction, (LM3) and (LM4), were not able to properly capture the effect of the baseline covariates on the risk of death after a patient experiences CF.

After performing model selection and assessing goodness-of-fit, we fit the following copula model

$$
\begin{aligned}
&C: \text{ Gaussian copula} \\
&h(t) = h_0(t) \exp\{\boldsymbol{\nu}\mathbf{X}\} \\
&\mu_{Z^*} = \gamma_0 + \boldsymbol{\gamma}_1\mathbf{X} + \sum_{k=1}^{3} \gamma_{2k} B_k(\tau) \\
&\eta_\tau = \xi_0 + \boldsymbol{\xi}_1\mathbf{X} + \sum_{i=1}^{3} B_k(\tau, \boldsymbol{\xi}_2)
\end{aligned}
$$

where $B_k$ is a B-spline for a natural cubic spline with boundary knots at 0 and 10 years. We

consider models where $h_0(t)$ is modeled nonparametrically (CopCox) and parametrically with a Weibull baseline hazard (CopWeib).

We evaluate the fit of the Cox model to the failure time data, and find that there is no violation of the proportional hazards assumption for any of the baseline covariates. We assess the fit of the probit model to the binary marker and identify that no covariate transformation is required. The model for the association parameter function was chosen to be a flexible function of landmark time and baseline covariates.

The parameter estimates for the components of the copula model are given in Table 2.4. Robust standard errors were computed for the marginal marker model coefficient estimates, and standard errors for the association parameters were computed using bootstrapping. For the marginal model for time to death, increased age, PSA, Gleason score, and number of comorbidities are significantly associated with increased risk of death. These were the results obtained from the landmark models fit in the previous chapter. From the marginal model for the binary marker data, increased age, Gleason score, and Stage T2-T3 were associated with increased probability of developing CF. These were the relationships observed in the joint models fit in Chapter I. Unlike the copula model, the landmark models are not able to evaluate the effect of the baseline covariates on the risk of CF. The bootstrapped association parameter standard errors are large due to the incorporation of the estimation uncertainty of the first-stage parameters. But negative association parameter estimates suggest that increasing Gleason score and Stage T2-T3 result in more negative association between the latent variable underlying CF and time to death, indicating that patients with those characteristics have high negative association between CF and death (i.e., decreased time to death). Similarly, the positive coefficient for having 1-2 comorbidities compared to 0 comorbidities indicates positive association between CF and time to death, and thus decreased risk of death. This relationship was also demonstrated in the landmark models with interactions in Chapter I.

In Figure 2.10, we return to the two individuals in the data set for whom we presented

**Table 2.4:** Coefficient estimates and standard errors for copula model applied to prostate cancer data with binary marker.

| | | **CopCox** | | **CopWeib** | |
|---|---|---|---|---|---|
| | Covariate | Coef. | SE | Coef. | SE |
| $\boldsymbol{\nu}$ | Age | 0.073 | 0.012 | | |
| | log(PSA+1) | 0.263 | 0.110 | | |
| | Gleason Score | 0.311 | 0.084 | | |
| | Stage T2-T3 | 0.043 | 0.158 | | |
| | Comorbidities 1-2 | 0.472 | 0.163 | | |
| | Comorbidities $\geq 3$ | 1.228 | 0.217 | | |
| $\boldsymbol{\gamma}$ | Intercept | -6.152 | 1.074 | | |
| | Age | 0.002 | 0.012 | | |
| | log(PSA+1) | 0.267 | 0.075 | | |
| | Gleason Score | 0.220 | 0.109 | | |
| | Stage T2-T3 | 0.245 | 0.175 | | |
| | Comorbidities 1-2 | 0.096 | 0.188 | | |
| | Comorbidities $\geq 3$ | -0.120 | 0.280 | | |
| | $B_1$ | 2.523 | 0.553 | | |
| | $B_2$ | 1.416 | 0.371 | | |
| | $B_3$ | 1.713 | 0.323 | | |
| $\boldsymbol{\xi}$ | Intercept | -0.498 | 2.332 | -0.283 | 2.069 |
| | Age | 0.005 | 0.016 | 0.007 | 0.015 |
| | log(PSA+1) | 0.024 | 0.228 | -0.020 | 0.192 |
| | Gleason Score | -0.151 | 0.191 | -0.147 | 0.171 |
| | Stage T2-T3 | -0.314 | 0.396 | -0.285 | 0.384 |
| | Comorbidities 1-2 | 0.230 | 0.312 | 0.225 | 0.284 |
| | Comorbidities $\geq 3$ | -0.117 | 0.402 | -0.006 | 0.311 |
| | $B_1$ | 1.789 | 2.219 | 1.105 | 1.871 |
| | $B_2$ | 0.050 | 0.888 | -0.079 | 0.765 |
| | $B_3$ | 1.207 | 1.266 | 0.825 | 1.059 |

predicted probabilities in the previous chapter. Recall, Individual A had increased risk of death due to risk factors (high PSA and number of comorbidities), and Individual B was at low risk of death but has some baseline covariates that indicate increased probability of CF (high PSA and Gleason, Stage T3) and that also increased the risk of death after experiencing CF. In the probability plots, the predictions from the copula models are very similar to the joint model and the landmark model with the interaction (LMInt4). Unlike the landmark model without the interaction (LM4), the copula model is able to take into account the differential effects of the baseline covariates on the different transitions, which is demonstrated by the large increase in predicted probability of death after CF for Individual B, similar to that of the joint models (MM) and (MMCox). There is no difference in the predicted probabilities for (CopCox) and (CopWeib) for Individual A, but we see that the predictions from (CopWeib) are lower than (CopCox) in Individual B after they experience CF. In Figure 2.11, we present the association functions for the two individuals. Individual B has more negative association between time to death and CF than Individual A. As landmark time increases the association becomes more positive and approaches zero, thus indicating that as time from treatment increases the predicted probability of death relies less on an individual's CF status. This is also demonstrated in the effect of the interaction between CF and landmark time in the landmark models where as landmark time increases the effect of CF on the risk of death decreases.

## 2.5 Discussion

Dynamic models that incorporate the effects of time-dependent covariates on the risk of survival are essential for making important, personalized clinical decisions about an individual's care. While there are two popular statistical methods for dynamic prediction, landmarking and joint modeling, they both have limitations that we address by presenting an alternative approximate method that has useful advantages and good predictive performance.

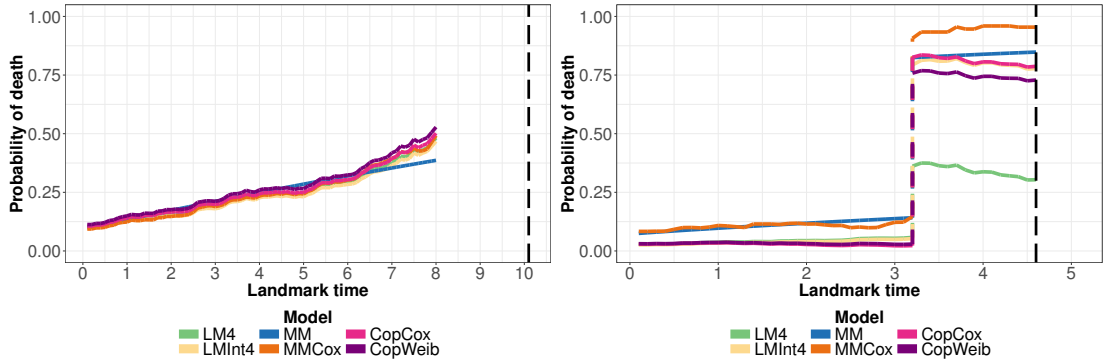


**Figure 2.10:** Predicted probability of death within 5 years, $P(T \leq \tau+5|T > \tau, Z(\tau), \mathbf{X})$ for two individuals in the prostate cancer data set for landmark, joint, and copula models. Individual A (left) is 60 years old at baseline, with PSA 19.7 ng/mL, Gleason score 7.5 ("4+3"), T1 Stage, 6 comorbidities, and does not experience clinical failure but dies 10 years from baseline. Individual B (right) is 54 years old at baseline, with PSA 16 ng/mL, Gleason score 9, T2 Stage, zero comorbidities, and experiences clinical failure at time 3 before dying at time 4.6 years from baseline. Black dashed line indicates time of death.

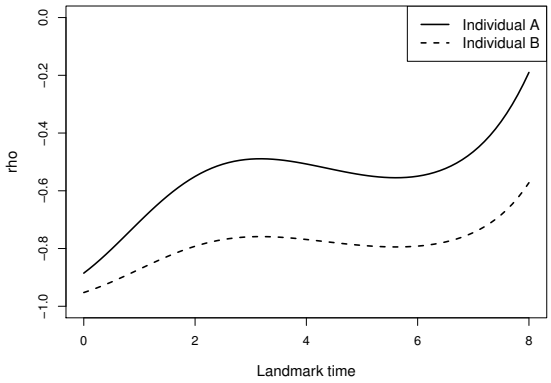


**Figure 2.11:** Association functions from (CopCox) for Individual A (solid) and Individual B (dashed) from the prostate cancer data set.

In this chapter, we propose the use of a copula-based approach for incorporating longitudinally collected marker information in predicting an individual's future survival. First, we specify from a well established class of models the marginal distributions of the marker (e.g., linear regression, generalized linear model) and the failure time (e.g., Cox, cure model). This allows us to apply standard goodness-of-fit tests and variable selection techniques to identify the best-fitting marginal models. From these marginals, we can also perform inference on the survival and marker outcomes using baseline covariate information to draw useful clinical conclusions. Second, we define the joint distribution of the survival time and marker conditional on being alive at a particular prediction time. This formulation allows us to easily derive the dynamic prediction of interest. We present our modeling framework for both a binary and a continuous marker process and demonstrate its predictive performance and ability using a simulation study and an application to real data.

There are several advantages of our approach over the existing joint model and landmarking methods. In comparison to landmarking, the copula model does not require the creation of a landmark data set, instead only using marker information available at measurement times. This allows us to avoid prespecifying landmark times and imputing unobserved marker values at these times, which can introduce bias. As well, it can accommodate unbalanced data and irregular marker measurement times. We also do not need to fix a time horizon for prediction, and can obtain predictions for a new patient at any continuous time point beyond baseline. As well, since we specify a unified time-to-event model from which we derive the conditional survival, we maintain a greater level of consistency in our predictions than landmarking. As in joint modeling, we specify a model for the marker; however, since we are modeling the population-averaged trajectory, rather than allowing for individual-specific random effects, we are able to specify a simpler model than a shared random effects or frailty model that can require complex and computationally-intensive estimation. In principle, it is easier to check goodness-of-fit for

marginal models; thus, by specifying them independently we are able to minimize bias at this stage.

A limitation of our proposed method is that it relies heavily on the availability of data at prediction times of interest for it to properly model the joint distribution between the marker and failure time. In the continuous marker setting, although the copula performs better than landmarking with increased measurement error, it's predictive performance is similar when there are fixed, common measurement times. In the binary marker simulations, we demonstrate that as the number of people in a particular group decreases at later time points the bias of the predictions increases. This indicates the need for model validation to be performed before the copula prediction model that is trained on a particular data set can be applied to a new set of individuals. As well, with the different models for the marginals and the association, there are several parameters to be estimated. The two-stage approach results in large standard errors for the association parameters, due to the estimation variability of the marginal model parameters. However, we found that the copula model performance is robust to the choice of association function, and thus we consider a flexible form rather than performing variable selection for the association parameters.

Using a copula framework provides the potential for several extensions to more complicated data structures. In this chapter, we consider an irreversible illness-death model, but the use of the copula to model the distribution of the latent marker process over time suggests an easy extension to the reversible illness-death model (e.g., illness represents hospitalization). We can then include as a covariate the number of reversals a patient has experienced by a particular landmark time to account for their increased risk of future illness and/or death. In addition, we can consider extensions to a multivariate Gaussian copula to accommodate multiple longitudinal markers. Thus, rather than specifying a full joint model for the different marker processes, it is easier to consider modeling their marginal behavior and using a flexible form for the copula association function to model

their joint distributions. This model structure can also help identify the size and direction of the correlation between the various longitudinal markers. Such an approach can greatly increase the dimension of the parameter space, so care should be taken to choose more parsimonious models for the marginal components and simpler association functions for the resulting correlation matrix.

While joint modeling and landmarking are popular in current literature, our copula-based approach provides an alternative method for dynamic prediction that has good predictive performance and easy estimation. By choosing more flexible and complicated models for the marginals we could potentially further decrease the bias introduced by fitting a misspecified model. Future work will focus on extending the copula framework for dynamic prediction to address more complex data forms and applications.

# CHAPTER III

# Dynamic Risk Modelling with a Partially Observed Covariate using Lévy-based Bridge Processes

## 3.1 Introduction

In cancer research, we are often interested in predicting a patient's risk of some future time-to-event outcome. Survival data can be thought of as a coarsened representation of a more complex underlying stochastic process that leads to these survival events. For example, suppose that all men are born with some genetic risk of prostate cancer. Due to lifestyle and changing biological factors, they then accumulate additional risk over their lifetime until some of them develop prostate cancer. This developing risk can depend on observable biomarker processes that change over time, such as prostate-specific antigen (PSA). These time-dependent markers can be considered as stochastic processes (Taylor et al., 1994; Jewell and Kalbfleisch, 1996; Shi et al., 1996). With increasing interest in conducting longitudinal studies, these stochastic markers are often partially observed at discrete measurement times. In cancer studies, we often have marked endpoints, where the stochastic marker is only observed at the survival time, providing us with a cross-sectional observation (mark) of the latent marker process. Thus, there is interest in using a joint analysis to model the effect of this limited marker process information on the time-to-event outcome.

Joint models for longitudinal-survival data specify submodels for the longitudinal marker and the survival process, and a mechanism by which to link the two (Tsiatis and Davidian, 2004). The most common form of a joint model, as discussed in Chapter II, involves modeling the longitudinal marker as a mixed-effect model and the hazard conditional on the marker value using a Cox proportional hazards model. This method requires the functional form for the marker trajectories to be specified, which restricts the marker behavior of individuals in the population to follow a similar pattern and ignores biological variability. To overcome this limitation, others have modeled the individual marker trajectories more flexibly using a stochastic process, such as an Ornstein-Uhlenbeck or Gaussian process (Taylor et al., 1994; Wang and Taylor, 2001; Henderson et al., 2000); however, these methods still rely on the restrictive assumption of proportional hazards.

Yashin and Manton (1997) proposed a general stochastic process model using a Gaussian diffusion process to link unobserved or partially observed stochastic variables with a hazard. This hazard rate is described as a time-dependent quadratic function of the stochastic marker, which can be restrictive if we do not believe that the hazard is U- or J-shaped. The effect of the marker on mortality risk is also based on the particular marker and disease process being studied, which relies on prior knowledge. Estimation is conducted using a maximum likelihood approach that involves solving stochastic differential equations and may be challenging to implement.

Using the sparse longitudinal information from marked data, it can be difficult and restrictive to develop a joint analysis for the marker and time-to-event outcome that properly models the trajectory of the biomarker over time and its effect on survival. Thus, we model the continuous marker as a flexible stochastic process that changes over time and possibly influences survival. Compared to existing methods, we propose a model specification that avoids restricting the behavior of the hazard rate and can be applied to a variety of marker and disease settings. We take advantage of the tractable nature of our model to perform estimation using a maximum likelihood based method, allowing

us to avoid the computational burden and complexity often associated with other joint modeling approaches.

In this chapter, we specify a joint model that incorporates the effects of a partially observed stochastic covariate on the risk of a time-to-event outcome, with the aim of predicting both survival and marker behavior. In Section 3.2, we describe the construction of our submodels for the longitudinal marker and survival processes. In Section 3.3, we introduce notation and describe our model formulation and estimation under three scenarios of marker observation. In Section 3.4, we examine the performance of our model in simulation studies. In Section 3.5, we look at an application of our model to prostate cancer data to demonstrate its ability to obtain predicted survival probabilities. Finally, in Section 3.6 we discuss the merits and limitations of our proposed method, and outline potential future developments.

## 3.2 Developing the Joint Model

### 3.2.1 Modeling Survival

Let $T$ be the survival time for the event of interest, $\mathbf{X}$ be a vector of baseline covariates, and $Z_t$ be a time-dependent covariate that is observed continuously or partially observed at discrete time points. Survival conditional on baseline covariates is often modeled using a Cox proportional hazards model

$$S(t|\mathbf{X}) = \exp\left\{-\int_0^t h_0(s)\exp\{\boldsymbol{\beta}'\mathbf{X}\}ds\right\} = \exp\{-\exp\{\boldsymbol{\beta}'\mathbf{X}\}H_0(t)\} = e^{-H(t|\mathbf{X})} \quad (3.1)$$

where $h_0(t)$ and $H_0(t)$ represent the baseline hazard and baseline cumulative hazard, respectively, $H(t|\mathbf{X})$ is the cumulative hazard, and $\boldsymbol{\beta}$ represents the vector of regression parameters for the baseline covariates $\mathbf{X}$, which can contain $Z_0$. To increase flexibility, survival models have been extended to include a frailty, a random effect that accounts

for the effects of unobserved heterogeneity due to the dissimilarity of individuals (Vaupel et al., 1979). At baseline, a frailty $W_i$ is drawn from a distribution of non-negative random variables for each individual $i$ and applied multiplicatively to the baseline hazard. The frailty determines whether an individual's risk is increased ($W_i > 1$) or decreased ($W_i < 1$). The marginal survival function is obtained by integrating over the distribution of the frailty $W$, and thus is characterized by the Laplace transform of $W$, $\mathbb{E}_W[e^{-sW}]$, evaluated at $s = H(t|\mathbf{X})$. The marginal survival is then given as

$$S(t|\mathbf{X}) = \mathbb{E}_W\left[\exp(-W\exp\{\boldsymbol{\beta}'\mathbf{X}\}H_0(t)|\mathbf{X})\right] = \mathbb{E}_W\left[e^{-WH(t|\mathbf{X})}\right]$$

where $H_0(t)$ is the deterministic cumulative baseline hazard, $H(t|\mathbf{X})$ is the cumulative hazard, and $W$ is the frailty random variable that is typically drawn from a parametric family, such as gamma or compound Poisson (Vaupel et al., 1979; Aalen, 1992).

Since we expect that an individual's risk can develop dynamically over time, we consider a generalization of the proportional hazard frailty models where an individual's frailty is treated as a stochastic process, $W_t$. With process-based frailty models, we specify the survival function as the expectation over the distribution of the unobserved time-dependent frailty. The marginal survival function is thus an average over all the possible histories $W[0,t]$ of the process and is characterized by the Laplace functional, $E_{W[0,t]}\left[e^{-\int_0^t W_s f(s)\,\mathrm{d}s}\right]$ for function $f(s) = h(s|\mathbf{X})$, and is given by

$$S(t|\mathbf{X}) = \mathbb{E}_{W[0,t]}\left[\exp\left\{-\int_0^t W_s h_0(s)\exp\{\boldsymbol{\beta}'\mathbf{X}\}\,\mathrm{d}s\right\}|\mathbf{X}\right] = \mathbb{E}_{W[0,t]}\left[e^{-\int_0^t W_s h(s|\mathbf{X})\,\mathrm{d}s}\right] \quad (3.2)$$

where $W_s$ is the time-varying frailty, $W[0,t]$ is the history of $W_s$, $s \in [0,t]$, and $h(s|\mathbf{X}) = h_0(s)\exp\{\boldsymbol{\beta}'\mathbf{X}\}$. Thus, the development of statistical estimation and inference methodology is facilitated by the availability of a tractable form of the Laplace functional or characteristic functional of the frailty process.

Gjessing et al. (2003) therefore modeled $W_t$ as a non-negative Lévy process. Lévy pro-

cesses are a class of stochastic processes with independent, stationary increments (Bertoin, 1998). The family of Lévy processes contains the familiar Wiener processes, Gaussian processes, compound Poisson processes, gamma processes, etc. Yashin and Manton (1997) defined the hazard rate of their model using a Gaussian process, which was squared to preserve a non-negative hazard rate. By using a Lévy process, Gjessing et al. (2003) assumes that the individual hazard increases in jumps rather than risk developing as a diffusion process. Thus, with this specification it is not sufficient to use a Lévy process that is restricted to be positive (i.e., squaring or exponentiating a Lévy process that can take on negative values), but requires that the process have non-negative increments. The class of non-negative Lévy processes leaves a sub-family of Lévy subordinators, i.e. non-decreasing processes that represent the compound Poisson processes and their limits, and excludes the Gaussian members of the Lévy family. The use of Lévy subordinators provides a tractable form for Eq.(3.2), from which the population survival and hazard can be derived. This process is required to be non-negative since it acts multiplicatively on the hazard function and must preserve the non-negative hazard function property. However, this places restrictions on the behavior of the hazard. It assumes that all individuals have proportional hazards and the use of an increasing Lévy process requires that an individual's hazard rate be increasing over time.

Putter and Van Houwelingen (2015) also describe dynamic frailty models using Lévy processes. The time-dependent frailty $W_t$ is constructed from many independent frailty components $X(u, v)$ that contribute to the hazard only if $u \leq t$ and $v \geq t$, i.e., the time period after which they are "born" and before they "die". Thus, the frailty components are constructed using a compound birth-death process and are specified as a Lévy process in two dimensions. The parameters of this model are estimated using the expectation-maximization algorithm on the full likelihood for a multivariate survival time formulation, which can be computationally slow. We are interested in the univariate survival setting, thus allowing us to use likelihood methods of estimation that do not pose as much of a

computational burden.

In both the Gjessing et al. (2003) and Putter and Van Houwelingen (2015) applications, the frailty process is fully unobserved or unobservable and therefore their methods are based on the marginal survival model, which is difficult to evaluate. Suppose instead that the frailty $W_t$ is the marker process that is observed at time points $\tau_1, \tau_2, \ldots$, but is a latent process during intervals where it is unobserved $(0, \tau_1), (\tau_1, \tau_2)$, etc. In the simplest case, $W_t$ is the marker process, but in general, $W_t$ is a function of the marker. Since the process is observed only at measurement times, we model $W_t$ as a non-decreasing Lévy bridge process scaled by its final value. A bridge is a stochastic process that has a known value at some fixed future time point (Fitzsimmons et al., 1993). A Lévy bridge is a Lévy process that is defined over a finite interval, and the initial and terminal values of the process are known at baseline.

While in the dynamic frailty framework the non-negative Lévy process is applied multiplicatively to the hazard, to alleviate the restriction of increasing hazards we propose using the non-decreasing Lévy bridge process more naturally as a multiplicative effect in the cumulative hazard function. Peng and Huang (2007) explored a similar class of models to extend the standard proportional hazards model so that temporal covariate effects are applied directly to the cumulative hazard function, i.e., $S(t|\mathbf{X}) = \exp\{-H(t|\mathbf{X})\} = \exp\{-\exp(h_0(t) + b_0(t)'X)\}$, where $H(t|\mathbf{X})$ is the cumulative hazard function, $h_0(t)$ is an unspecified function, $\mathbf{X}$ is a vector of covariates, and $b_0(t)$ is a vector of unknown time-varying regression coefficients. This formulation relaxes the proportional hazards assumption, and interpretation of covariate effects is performed directly on the survival function. However, restrictions must be placed on the time-dependent covariates to ensure the cumulative hazard is non-decreasing. In our approach, the time-dependent covariates enter into the model through the Lévy bridge, and by taking advantage of its increasing nature we do not require additional restrictions.

Using the formulation in Eq.(3.2) with $W_t$ as a scaled Lévy bridge process, we apply the

effect of the stochastic process multiplicatively in the cumulative hazard. To compute the marginal survival we average over the unobserved stochastic process between observations. Thus, our approach enjoys greater tractability and convenience from being able to obtain the survival function from the Laplace transform of the Lévy bridge process rather than the Laplace functional

$$S(t|\mathbf{X}) = \mathbb{E}[\exp\{-W_t H(t)\}|\mathbf{X}] \tag{3.3}$$

where $H(t)$ is defined as the *conditional cumulative hazard*. If $W_t = w \ \forall t$ is known, then the survival function is given as $S(t|W_t = w) = e^{-wH(t)}$, and can be specified as a Cox model as in Eq.(3.1). Thus, $H(t)$ represents the cumulative hazard of the proposed survival model, conditional on the marker process being a known constant. If $W_t$ is completely observed, the cumulative hazard of our model is $W_t H(t)$, which is necessarily non-decreasing.

### 3.2.2 Modeling the Marker Process

We assume that the risk of the time-to-event outcome is associated with an underlying stochastic process $\{W_t\}_{0\leq t\leq\infty}$ that takes the form

$$W_t = U_{t\tau} V_\tau \tag{3.4}$$

where $\{U_{t\tau}\}_{0\leq t\leq\tau}$ is a Lévy bridge over the interval $[0, \tau]$ from 0 to 1, and scaled by $V_\tau$, the final value of the process at time $\tau$. This process is applied multiplicatively to the cumulative hazard, and the survival function is specified as in Eq.(3.3).

The motivation for this construction is two-fold. First, by considering a non-negative Lévy bridge process, we represent the accumulation of risk over time using an increasing process. This allows us to apply the effect of the stochastic marker multiplicatively to the cumulative hazard to model its effect directly on survival while satisfying its non-decreasing behavior.

Second, in the development of a model where the marker is partially observed, we average over the trajectory of the partially observed stochastic process in intervals where the process is not observed. This can be computationally difficult if, conditional on the observed marker values, this average does not have a tractable form. We consider a process in the family of Lévy processes for which the required survival functions have an analytically tractable form. The gamma process is often used to model stochastic processes due to the convenience of its distributional properties (Gjessing et al., 2003; Putter and Van Houwelingen, 2015; Lawless and Crowder, 2004). The gamma bridge process has been proposed in financial mathematics as a model for aggregate claims data, and derivations of useful properties are available from existing literature (Brody et al., 2008; Hoyle, 2010). Thus, this process is suited for describing the accumulation of risk represented by the time-varying covariate, and we extend these methods to survival analysis.

Within this framework, we model the dynamic frailty $\{W_t\}_{0\leq t\leq\infty}$ as a scaled gamma process, with growth rate $\mu$ and spread $\sigma$. The process has independent increments such that $W_0 = 0$ and $W_t$ has a gamma distribution with mean $\mu t$ and variance $\sigma^2 t$. Then, $U_{t\tau}$ is the gamma bridge and by special properties of the process, $U_{t\tau}$ is independent of $V_\tau$. Thus, we can imagine that $U_{t\tau}$ is the part of the risk process that has no information about the final observed value $V_\tau$, but provides a flexible way for us to model the unknown behavior of the process in between measurement times. The Laplace transform of a gamma bridge is the familiar beta distribution (Brody et al., 2008). Thus, the resulting construction in Eq.(3.3) is a tractable survival model from which closed-form expressions for the conditional and marginal survival and hazards can be derived.

Our proposed survival model in Eq.(3.3) and our marker model in Eq.(3.4) fully specifies a joint model of the marker process and survival time, where the process is chosen to have a distributional form such that averaging over the unobserved marker process is simplified. This provides us with a stochastic process model that can be used to predict future survival for a patient given their partially observed marker history.

## 3.3 Model Construction

We describe our model under three different marker observation scenarios: (1) The marker process is completely observed, (2) The marker is only observed at the survival time, (3) The marker process is observed indirectly with measurement error. Estimation is conduction using maximization of the likelihood and standard errors are obtained using numerical differentiation. We extend our model formulation to the situation with multiple marker measurement times. In addition, we consider more flexible parametric forms for the conditional cumulative hazard, and demonstrate the ease with which these can be implemented in our model formulation. We present the general formulas in the body of the paper, and describe the derivations under the gamma process example in Appendix B.1.

### 3.3.1 Completely observed process

Let $Y_i$ and $C_i$ denote the true event time and censoring time, respectively. Let $T_i = \min(Y_i, C_i)$ denote the observed survival time, and $\delta_i = I(Y_i \leq C_i)$ be the event indicator. Let $\mathbf{X}$ be a vector of baseline covariates, that can include the baseline value of the marker process. Let $\{W_t\}_{0 \leq t \leq T}$ be the Lévy process representing the marker. Suppose that $W_t$ is completely observed. Our observed data is then $\mathcal{D}_n = \{T_i, \delta_i, \mathbf{X}_i, \bar{W}_{T_i}; i = 1, \ldots n\}$, where $\bar{W}_\tau = W[0, \tau]$ is the history of $W_t$ from time 0 until time $\tau$. The survival function is then

$$S(t) = e^{-\Lambda(t)} = e^{-H(t)W_t}$$

where $\Lambda(t)$ is the cumulative hazard of our survival model, and $H(t)$ is the conditional cumulative hazard. We can incorporate baseline covariates $\mathbf{X}$ into $H(t)$ and $W_t$ and specify the survival function conditional on $\mathbf{X}$, $S(t|\mathbf{X})$; however, we exclude $\mathbf{X}$ in the following

model specifications for brevity. The corresponding hazard function is then given by

$$d\Lambda(t) = W_t dH(t) + H(t)dW_t$$

Estimation is then conducted by maximizing the log-likelihood

$$l = \sum_{i=1}^{n} \left\{ \delta_i \log[d\Lambda(T_i|\bar{W}_{T_i}) S(T_i|\bar{W}_{T_i})] - (1-\delta_i)\Lambda(T_i|\bar{W}_{T_i}) \right\}$$

### 3.3.2 Marker observed at survival time

If we have marked data, then we observe $W_t$ only at the survival time. Let $\tau$ be the marker measurement time. Let $\{U_t\}_{0\leq t\leq\tau}$ be a Lévy process that is defined on the finite time horizon $[0,\tau]$, and let $\{U_{t\tau}\}_{0\leq t\leq\tau}$ be a Lévy bridge starting at zero and ending at one at time $\tau$. Thus, we write the frailty process $W_t$ as a bridge process $U_{t\tau}$ that is scaled by the value of the process at time $\tau$, $V_\tau$, as in Eq.(3.4). We assume that $W_t$ is a scaled gamma process with mean $\mu t$ and variance $\sigma^2 t$. For the purposes of derivation, we use the reparameterization $m = \mu^2/\sigma^2$ and $\kappa = \sigma^2/\mu$, where $m$ can be considered as a "standardized" growth rate and $\kappa$ as a scale. Then the gamma bridge $U_{t\tau}$ has a beta distribution with parameters $\alpha = mt$ and $\beta = m(\tau - t)$ for $0 \leq t \leq \tau$ (Brody et al., 2008). The survival conditional on $V_\tau$ is then obtained by averaging the effect of the unobserved trajectory of the gamma bridge on survival over the interval $[0,\tau]$. Thus, the conditional survival for $0 \leq t \leq \tau$ is the Laplace transform of $U_{t\tau}$ and is given by

$$S(t|V_\tau) = \mathbb{E}_{W_t}[e^{-H(t)W_t}|V_\tau] = \mathbb{E}_U[e^{-H(t)U_{t\tau}V_\tau}|V_\tau] = M(mt, m\tau, -H(t)V_\tau)$$

where $M$ is Kummer's confluent hypergeometric function of the first kind (Hoyle, 2010). The baseline covariates $\mathbf{X}$ can be included in all of the model parts $\mu$, $\sigma^2$, and $H(t)$.

For individuals who do not experience the event of interest and $V_\tau$ is not observed,

the marginal survival is obtained by averaging over the distribution of $V_\tau$,

$$S(t) = \mathbb{E}_{V_\tau}[\mathbb{E}_U[e^{-H(t)U_{t\tau}V_\tau}]] = 1 + \sum_{k=1}^{\infty}\prod_{r=1}^{k}\frac{\alpha+r-1}{\alpha+\beta+r-1}\frac{(-1)^k p_k H^k(t)}{k!}$$

where $p_k = \mathbb{E}[V_\tau^k]$ is the $k$th moment of $V_\tau$. We assume that $V_\tau$ arises from the same gamma process as $W_t$, i.e., $V_\tau$ is a gamma random variable with mean $\mu\tau$ and variance $\sigma^2\tau$, thus the marginal survival is given by

$$S(t) = (1 + \kappa H(t))^{-mt} \tag{3.5}$$

which is the Laplace transform of a gamma random variable with mean $\mu t$ and variance $\sigma^2 t$, as expected. Detailed derivations are given in Appendix B.1.

Suppose that the marker process is only observed at the event time. Let $V_\tau = v_\tau$ be the observed value of the marker at time $\tau$, and let $W_{T_i} = v_{T_i}$ if $\delta_i = 1$. Using observed data $\mathcal{D}_n$, estimation is then conducted by maximizing the log-likelihood

$$l = \sum_{i=1}^{n}\Big\{\delta_i \log[d\Lambda(T_i|v_{T_i})S(T_i|v_{T_i})g_{V_{T_i}}(v_{T_i})] + (1-\delta_i)\log[S(T_i)]\Big\}$$

where the conditional survival given the observed marker value $S(t|v)$ is from Eq.(B.2), the conditional hazard of the survival model $d\Lambda(t|v)$ is given in Eq.(B.3), the marginal survival $S(t)$ is from Eq.(3.5), and $g_{V_T}(v)$ is the density of a gamma random variable with mean $\mu T$ and variance $\sigma^2 T$.

If the marker process was observed for everyone at the survival time (i.e., we observe the marker measurement for both those who do and do not experience the event), then we let $v_\tau$ be the observed value of the marker at time $\tau$, and $W_{T_i} = v_{T_i}$ for all $i$. Using observed data $\mathcal{D}_n$, we then maximize the log-likelihood

$$l = \sum_{i=1}^{n}\Big\{\delta_i \log[d\Lambda(T_i|v_{T_i})S(T_i|v_{T_i})g_{V_{T_i}}(v_{T_i})] + (1-\delta_i)\log[S(T_i|v_{T_i})g_{V_{T_i}}(v_{T_i})]\Big\} \tag{3.6}$$

### 3.3.3 Marker measured indirectly

Suppose that the marker measurement obtained is subject to some "error", i.e., we only observe marker value $Z_\tau$, which is some surrogate of $V_\tau$. We define $Z_t|V_t$ as a white noise process plus mean $V_t$, which is the true value of the process at time $t$. Thus, $Z_t|V_t$ at any two time points are not correlated. Under the assumption that given $V_\tau$, $T \perp Z_\tau$, the conditional survival distribution is obtained by averaging the survival function $S(t|V_\tau)$ over the regression $Z_\tau \sim V_\tau$, and given by

$$G(t|Z_\tau = z) = \frac{\mathbb{E}_{V_\tau}[S(t|V_\tau) \times f_{Z_\tau|V}(z|V_\tau)]}{\mathbb{E}_{V_\tau}[f_{Z_\tau|V}(z|V_\tau)]}$$

We denote the conditional survival function for our measurement-error model by $G(t|z)$ and the cumulative hazard as $\Phi(t)$. The general and gamma process derivation for this conditional survival probability are given in Appendix B.1.2. We are interested in distributions for $Z_\tau|V_\tau$ that have mean $V_\tau$ and thus consider compound gamma distributions for which there are closed-form expressions for the conditional survival function. We introduce an additional parameter $\gamma$ in the variance of the measurement error that measures the extent to which the assumption that the marker is measured with error is necessary. We present the derivations for the conditional survival function for $Z_\tau|V_\tau$ with gamma distribution mean $V_\tau$ and variance $V_\tau^2/\gamma$, and normal distribution mean $V_\tau$ and variance $1/\gamma^2$ in Appendices B.1.2.1 and B.1.2.2, respectively. Thus, as $\gamma$ increases the variance of the measurement error decreases and the observed value goes to the true value. Although the marginal distributions for $Z_\tau$ under both of these measurement-error models contain special functions, they have closed-form expressions. However, the normal distribution error density contains the parabolic cylinder function and produces numerical complications due to its approximation in standard software. Thus, we consider the performance of the gamma measurement-error model in the remainder of this chapter and expect that future work will expand model evaluation to other measurement-error models as well.

If the marker process is only observed at the event time, let $Z_\tau = z_\tau$ be the observed value of the marker at time $\tau$, and let $W_{T_i} = z_{T_i}$ if $\delta_i = 1$. With observed data $\mathcal{D}_n$, estimation is conducted by maximizing the log-likelihood

$$l = \sum_{i=1}^{n} \left\{ \delta_i \log \left[ d\Phi(T_i|z_{T_i}) G(T_i|z_{T_i}) f_{Z_{T_i}}(z_{T_i}) \right] + (1-\delta_i) \log \left[ S(T_i) \right] \right\}$$

where the conditional survival given the observed marker value $G(t|z)$ is from Eq.(B.5), the conditional hazard of the survival model $d\Phi(t|z)$ is given in Eq.(B.6), the marginal survival $S(t)$ is from Eq.(3.5), and $f_{Z_T}(z)$ is the density of the observed marker value at $T$ given in Eq.(B.4).

If we observe the marker process for everyone at their survival time, then we let $z_\tau$ be the observed value of the marker at time $\tau$, and $W_{T_i} = z_{T_i}$ for all $i$. Using observed data $\mathcal{D}_n$, we maximize the log-likelihood

$$l = \sum_{i=1}^{n} \left\{ \delta_i \log \left[ d\Phi(T_i|z_{T_i}) G(T_i|z_{T_i}) f_{Z_{T_i}}(z_{T_i}) \right] + (1-\delta_i) \log \left[ G(T_i|z_{T_i}) f_{Z_{T_i}}(z_{T_i}) \right] \right\} \quad (3.7)$$

In an alternative specification, we can present the likelihood as

$$\begin{aligned} l = \sum_{i=1}^{n} \delta_i \log & \left[ \mathbb{E}_{V_{T_i}} \left[ d\Lambda(T_i|v_{T_i}) S(T_i|v_{T_i}) f_{Z_{T_i}|V_{T_i}}(z_{T_i}|v_{T_i}) \right] \right] \\ & + (1-\delta_i) \log \left[ \mathbb{E}_{V_{T_i}} \left[ S(T_i|v_{T_i}) f_{Z_{T_i}|V_{T_i}}(z_{T_i}|v_{T_i}) \right] \right] \end{aligned}$$

where we specify the contributions conditional on $V_{T_i}$ and take the expectation with respect to the unobserved random variable. We derive the likelihood in this form in Appendix B.1.3 and demonstrate that the result is the same as with the specification in Eq.(3.7).

### 3.3.4 Modeling the Conditional Cumulative Hazard

Due to modeling the marker process effect as multiplicative in the conditional cumulative hazard rather than in the hazard rate as in traditional survival models, we have additional flexibility in specifying the conditional cumulative hazard function to match the marginal behavior of the data. While we can choose parametric models for the conditional cumulative hazard, such as exponential, Weibull, or gamma, we can also consider more flexible parametric or non-parametric models, as is demonstrated in our application to prostate cancer data in Section 3.5. If we believe that there is unobserved heterogeneity in the population, we can also consider modeling the conditional cumulative hazard using a univariate frailty model, where a random effect is drawn at baseline for each individual and remains fixed for the individual's lifetime. This frailty is distinct from the frailty process specified for our marker. The derivation of the conditional and marginal survival functions for a gamma bridge marker process and a gamma frailty for the conditional cumulative hazard are demonstrated in Appendix B.4.

### 3.3.5 Multiple marker measurements and dynamic prediction

So far, we have developed our model for the situation of a single observed marker measurement for each individual, which is observed jointly with survival data at the survival time. Here, we set up the framework for extending our model specification to multiple measurement times with the aim of developing a model and estimation for dynamic prediction. We derive the conditional survival for two measurement times, which can be extended to additional measurement times in the same way. We can also extend the conditional survival function to incorporate multiple marker measurements to use a patient's longitudinal marker history to make more accurate predictions at time points beyond baseline. Derivations for the marginal survival and hazard functions will follow from arguments similar to those presented in Appendix B.1, and will be explored in future work.

Suppose that we observe the marker process at two time points $\tau$ and $s$, with values $V_\tau$ and $V_s$, respectively. Recall that the conditional survival for one measurement time $\tau$ for $0 \leq t \leq \tau$ is given by

$$S(t|V_\tau) = \mathbb{E}_U \left[ e^{-H(t)U_{t\tau}V_\tau} | V_\tau \right] = M(mt, m\tau, -H(t)V_\tau)$$

If we consider the situation where we observe the marker at another measurement time $s$ before $\tau$, then the conditional survival for $0 \leq s \leq t \leq \tau$ is

$$\begin{aligned} S(t|V_\tau, V_s) &= \mathbb{E}_{W_t} \left[ e^{-H(t)W_t} | V_\tau, V_s \right] \\ &= \mathbb{E}_B \left[ e^{-H(t)(V_s + B_{t\tau}(V_\tau - V_s))} | V_\tau, V_s \right] \\ &= e^{-H(t)V_s} \, \mathbb{E}_B \left[ e^{-H(t)B_{t\tau}(V_\tau - V_s)} | V_\tau, V_s \right] \\ &= e^{-H(t)V_s} M(m(t-s), m(\tau - s), -H(t)(V_\tau - V_s)) \end{aligned}$$

where $B_{t\tau}$ is a gamma bridge from 0 to 1 on the interval $[s, \tau]$ and thus has a beta distribution with parameters $\alpha = m(t-s)$ and $\beta = m(\tau - t)$. Notice that if we have $s = 0$, then our formula reduces to the survival function conditioning on $V_\tau$.

Suppose the marker value at time $s$ is not observed, i.e., we are interested in making predictions for a person beyond their last observed marker value. The general formula for the future predicted survival for $0 \leq \tau \leq t$ is given by

$$\begin{aligned} S(t|V_\tau = v) &= \int_v^\infty P(T > t | V_\tau = v, V_t = y) f_{V_t|V_\tau}(y|v) \, \mathrm{d}y \\ &= \int_v^\infty e^{-yH(t)} \frac{1}{\Gamma(m(t-\tau))\kappa^{m(t-\tau)}} (y - v)^{m(t-\tau)-1} e^{-\frac{(y-v)}{\kappa}} \, \mathrm{d}y \\ &= e^{-H(t)v} (1 + \kappa H(t))^{-m(t-\tau)} \end{aligned}$$

Thus, the future survival prediction is the marginal survival probability of surviving

up to time $t$ with marker value $v$ multiplied by the marginal survival for a gamma process on the interval $[\tau, t]$. With increasing $v$, future survival probability worsens, as expected.

Combining these results, the dynamic prediction of survival at time $\tau$ for the prediction horizon $\tau + s$ is given by

$$\begin{aligned} S(\tau + s | V_\tau = v, T > \tau) &= \frac{P(T > \tau + s, V_\tau = v)}{P(T > \tau, V_\tau = v)} \\ &= \frac{\int_v^\infty P(T > \tau + s, V_\tau = v, V_t = y)\, \mathrm{d}y}{S(\tau|v) f_{V_\tau}(v)} \\ &= \frac{\int_v^\infty P(T > \tau + s | V_\tau = v, V_t = y) f_{V_t|V_\tau}(y|v) f_{V_\tau}(v)\, \mathrm{d}y}{M(m\tau, m\tau, -vH(\tau)) f_{V_\tau}(v)} \\ &= \frac{\displaystyle\int_v^\infty e^{-yH(\tau+s)} \frac{1}{\Gamma(ms)\kappa^{ms}} (y - v)^{ms-1} e^{-\frac{(y-v)}{\kappa}}\, \mathrm{d}y}{e^{-vH(\tau)}} \\ &= e^{-(H(\tau+s)-H(\tau))v} (1 + \kappa H(\tau + s))^{-ms} \end{aligned} \tag{3.8}$$

In Appendix B.2, we derive the conditional survival probabilities under the measurement-error model.

### 3.3.6 Marker Prediction

In addition to modeling the effect of the marker on the survival, we may be interested in the behavior of the marker conditional on the survival data and observed marker measurements. This can help identify patterns in the marker process over time. We present the derivation of the following formulas in Appendix B.3.

#### 3.3.6.1 True marker value observed

Suppose that we observe the true marker value at time $\tau$, $V_\tau$. For $0 \le t \le \tau \le T$,

$$\begin{aligned} \mathbb{E}[W_t | T > \tau, V_\tau = v] &= \frac{\int P(T > \tau | W_t, V_\tau) q(W_t | V_\tau) g(V_\tau) W_t\, \mathrm{d}W_t}{\int P(T > \tau | W_t, V_\tau) q(W_t | V_\tau) g(V_\tau)\, \mathrm{d}W_t} \\ &= \frac{tv}{\tau} \end{aligned} \tag{3.9}$$

where the probability distribution of $W_t|V_\tau$ when $0 \leq t \leq \tau$ is given by the beta distribution scaled by the value of $V_\tau$. Thus, the expected value is the ratio of the time spent in the interval scaled by the value of the marker at the end of the interval.

For $0 \leq \tau \leq t \leq T$,

$$\begin{aligned}\mathbb{E}[W_t|T > t, V_\tau = v] &= \frac{\int P(T > t|W_t, V_\tau)q(W_t|V_\tau)g(V_\tau)W_t \, \mathrm{d}W_t}{\int P(T > t|W_t, V_\tau)q(W_t|V_\tau)g(V_\tau) \, \mathrm{d}W_t} \\ &= v + \frac{\kappa m(t-\tau)}{1 + \kappa H(t)} \end{aligned} \tag{3.10}$$

where $W_t|V_\tau$ for $0 \leq \tau \leq t$ is gamma distributed with mean $V_\tau + \mu(t-\tau)$ and variance $\sigma^2(t-\tau)$, and $S(t|W_t, V_\tau) = S(t|W_t) = e^{-H(t)w}$. Thus, the mean marker value at time $t > \tau$ is the marker at $\tau$ plus the mean value of the marker over the interval $[t, \tau]$ scaled by the Laplace transform of a gamma random variable with shape 1 and scale $\kappa$. The second term represents the competition between the mean value of the process beyond $\tau$ and the conditional survival. As $t$ increases, the mean value of the process increases; however, the conditional cumulative hazard in the denominator also increases. This captures the effect that over time those with high values of $W_t$ experience failure, leaving healthier individuals with lower marker values in the population. Thus, if $H(t)$ increases faster than $(t-\tau)$ the average conditional marker behavior can increase and then decrease, even though the marker process for each individual is increasing. This phenomenon is similar to that of the population average hazard in cure models that can decrease over time due to the increasing proportion of less frail individuals.

#### 3.3.6.2 Marker observed with measurement error

Suppose that we observe the marker at time $\tau$ with gamma measurement error. For $0 \leq t \leq \tau \leq T$,

$$
\begin{aligned}
&\mathbb{E}[W_t|T>\tau, Z_\tau = z] \\
&= \frac{\int P(T>\tau, W_t, Z_\tau) W_t \,\mathrm{d}W_t}{\int P(T>\tau, W_t, Z_\tau)\,\mathrm{d}W_t} \\
&= \frac{\int_0^\infty \left[\int_0^v S(\tau|v) q(w|v) f(z|v) g(v) w \,\mathrm{d}w\right] \mathrm{d}v}{\int_0^\infty \left[\int_0^v S(\tau|v) q(w|v) f(z|v) g(v) \,\mathrm{d}w\right] \mathrm{d}v} \\
&= \frac{t}{\tau}(\gamma z)^{\frac{1}{2}} \left(H(t) + \frac{1}{\kappa}\right)^{-\frac{1}{2}} \frac{K_{\gamma - m\tau - 1}\left(2\sqrt{\left(H(t)+\frac{1}{\kappa}\right)(\gamma z)}\right)}{K_{\gamma - m\tau}\left(2\sqrt{\left(H(t)+\frac{1}{\kappa}\right)(\gamma z)}\right)}
\end{aligned}
\tag{3.11}
$$

where $S(\tau|V_\tau) = e^{-H(\tau)V_\tau}$, $q(W_t|V_\tau)$ is the beta distribution scaled by $V_\tau$, $g(V_\tau)$ is the gamma distribution with shape $m\tau$ and scale $\kappa$, and the distribution $f(Z_\tau|V_\tau)$ depends on the measurement-error model. Notice that this has a similar form to Eq.(3.9), where instead of $v$ we have a function of $z$ representing the value of $v$ measured with error.

For $0 \le \tau \le t \le T$,

$$
\begin{aligned}
\mathbb{E}[W_t|T>t, Z_\tau = z] &= \frac{\int P(T>t, W_t, Z_\tau) W_t \,\mathrm{d}W_t}{\int P(T>t, W_t, Z_\tau)\,\mathrm{d}W_t} \\
&= \frac{\int_0^\infty \left[\int_0^\infty S(t|w) q(w|v) f(z|v) g(v) w \,\mathrm{d}w\right] \mathrm{d}v}{\int_0^\infty \left[\int_0^\infty S(t|w) q(w|v) f(z|v) g(v) \,\mathrm{d}w\right] \mathrm{d}v} \\
&= (\gamma z)^{\frac{1}{2}} \left(H(t) + \frac{1}{\kappa}\right)^{-\frac{1}{2}} \frac{K_{\gamma - m\tau - 1}\left(2\sqrt{\left(H(t)+\frac{1}{\kappa}\right)(\gamma z)}\right)}{K_{\gamma - m\tau}\left(2\sqrt{\left(H(t)+\frac{1}{\kappa}\right)(\gamma z)}\right)} + \frac{\kappa m (t-\tau)}{1+\kappa H(t)}
\end{aligned}
\tag{3.12}
$$

where $S(t|W_t) = e^{-H(t)W_t}$, $q(W_t|V_\tau)$ is the gamma distribution with mean $V_\tau + \mu(t-\tau)$ and variance $\sigma^2(t-\tau)$, $g(V_\tau)$ is the gamma distribution with shape $m\tau$ and scale $\kappa$, and $f(Z_\tau|V_\tau)$ is the measurement-error model. Notice that is has the same form as in Eq.(3.10), where $v$ is replaced with the same function of $z$ as in Eq.(3.11).

#### 3.3.6.3 Marker value not observed

If the value of the marker is not observed at any measurement time, $\forall t \geq 0$

$$\begin{aligned} \mathbb{E}[W_t|T > t] &= \frac{\int P(T > t|W_t)q(W_t)W_t \, \mathrm{d}W_t}{\int P(T > t|W_t)q(W_t) \, \mathrm{d}W_t} \\ &= \frac{\kappa m t}{(1 + \kappa H(t))} \end{aligned} \tag{3.13}$$

This is the second element in Eq.(3.10), which represents the behavior of the marker after the observed marker measurement. We use these formulas to demonstrate the behavior of the marker process in the data application in Section 3.5.

## 3.4 Simulation study

Simulations were conducted to evaluate the estimation of the proposed survival model. We simulate our data from both the situation when the marker is measured without error and when we assume that we observe a surrogate of the marker measured with error. We fit the models with and without measurement error to evaluate the performance of the generating model and a misspecified model. We simulate under sample sizes of $n = 200, 300, 500$ and perform 500 replications. Standard errors were obtained numerically from the Hessian matrix evaluated at the estimated parameter values.

We simulate a binary baseline covariate $X$, with a prevalence of 30%. We simulate the marker process $W_t$ from a gamma process with mean $\mu t$ and variance $\sigma^2 t$, where $\mu = \exp\{\mu_0 + \mu_1 X\}$ and $\sigma^2 = \exp\{\eta_0 + \eta_1 X\}$. The baseline hazard is assumed to be exponential with rate $\exp\{\beta_0 + \beta_1 X\}$. The true parameter values are chosen to be $\mu_0 = -1.1, \mu_1 = 0.3, \eta_0 = -2.1, \eta_1 = 0.5, \beta_0 = -3.6, \beta_1 = 0.6$. Failure times are generated from the model $S(t) = e^{-H(t)W_t}$ and the censoring distribution is Unif(0, $c$), where we consider a censoring horizon of $c = 20, 30, 50$ to achieve censoring rates of 40%, 30%, 20%, respectively. A detailed description of the how the gamma marker process and event times were simulated is given in Appendix B.5.

For the simulations with measurement error, we generate the observed marker value from a gamma distribution with mean at the true value $V_T$ and variance $V_T/\exp(\gamma)$, where $T$ is the survival time and $\gamma$ represents the measurement error. Values of $\gamma$ were chosen based on the scale of $V_T$, and we consider $\gamma = 1, 2, 3$ to simulate small, medium, and large measurement error.

In Tables 3.1 and 3.2 we present the results from data simulated without measurement error and fit with same model. We see that the bias is small even for smaller sample sizes. The coverage probabilities for the intercept parameters $\mu_0$ and $\eta_0$ are lower than the 95% nominal level; however, the coverage probability of the other parameters corresponding to the baseline covariate $(\mu_1, \eta_1)$ and the parameters associated with the conditional cumulative hazard $(\beta_0, \beta_1)$ approach the nominal value.

**Table 3.1:** Simulation results for the parameters associated with the stochastic marker process from a gamma bridge survival model with no measurement error fit to marker data simulated from a gamma bridge process with no measurement error.

| | | $\mu_0$ | | | | $\mu_1$ | | | | $\eta_0$ | | | | $\eta_1$ | | | |
|---|---|---|---|---|---|---|---|---|---|---|---|---|---|---|---|---|---|
| **n** | **%Cens** | Est[1] | SE[2] | ESD[3] | CP[4] | Est | SE | ESD | CP | Est | SE | ESD | CP | Est | SE | ESD | CP |
| **200** | **20** | -1.13 | .031 | .030 | 84.6 | .290 | .062 | .063 | 93.5 | -2.17 | .131 | .134 | 91.1 | .447 | .244 | .250 | 94.3 |
| **200** | **30** | -1.12 | .032 | .033 | 88.1 | .286 | .064 | .062 | 94.8 | -2.16 | .132 | .137 | 92.5 | .449 | .246 | .259 | 92.1 |
| **200** | **40** | -1.12 | .034 | .034 | 89.3 | .290 | .067 | .069 | 92.5 | -2.15 | .133 | .133 | 93.1 | .450 | .248 | .255 | 93.7 |
| **300** | **20** | -1.13 | .025 | .022 | 83.4 | .291 | .050 | .050 | 94.5 | -2.16 | .107 | .107 | 90.7 | .457 | .199 | .200 | 93.9 |
| **300** | **30** | -1.12 | .026 | .025 | 87.9 | .285 | .052 | .051 | 94.7 | -2.16 | .107 | .116 | 89.5 | .452 | .200 | .212 | 92.7 |
| **300** | **40** | -1.12 | .028 | .028 | 88.3 | .284 | .055 | .058 | 91.3 | -2.15 | .109 | .111 | 92.9 | .447 | .202 | .203 | 93.7 |
| **500** | **20** | -1.13 | .019 | .019 | 72.8 | .286 | .039 | .040 | 92.1 | -2.16 | .083 | .082 | 89.6 | .455 | .154 | .153 | 92.9 |
| **500** | **30** | -1.13 | .020 | .021 | 77.0 | .289 | .041 | .039 | 94.9 | -2.16 | .083 | .084 | 87.9 | .471 | .155 | .161 | 93.5 |
| **500** | **40** | -1.12 | .022 | .022 | 84.0 | .284 | .043 | .042 | 93.9 | -2.15 | .084 | .085 | 89.3 | .452 | .156 | .157 | 93.9 |

[1] Est: Average of the parameter estimates over 500 simulations
[2] SE: Average of estimated standard errors
[3] ESD: Empirical standard deviation of parameter estimates
[4] CP: Coverage probability of the proportion of simulations that the 95% confidence interval contains the true parameter values

In Tables 3.3 and 3.4 we examine the results for simulating from a measurement-error model and fitting the same model. The coverage probabilities for the mean parameters are improved compared to the model without measurement error. The bias of the variance parameters $(\eta_0, \eta_1)$ is high and the standard errors are large. The bias is low and coverage probabilities approach 95% for the conditional cumulative hazard parameters $(\beta_0, \beta_1)$. The bias and coverage probabilities are better for smaller values of $\gamma$. The coverage

**Table 3.2:** Simulation results for the parameters associated with the conditional cumulative hazard from a gamma bridge survival model with no measurement error fit to marker data simulated from a gamma bridge process with no measurement error.

| | | $\beta_0$ | | | | $\beta_1$ | | | |
|---|---|---|---|---|---|---|---|---|---|
| **n** | **%Cens** | Est[1] | SE[2] | ESD[3] | CP[4] | Est | SE | ESD | CP |
| **200** | **20** | -3.60 | .094 | .094 | 95.1 | .614 | .168 | .169 | 95.5 |
| **200** | **30** | -3.60 | .102 | .101 | 94.8 | .614 | .178 | .172 | 95.8 |
| **200** | **40** | -3.61 | .117 | .120 | 94.5 | .612 | .196 | .198 | 94.1 |
| **300** | **20** | -3.60 | .077 | .076 | 95.9 | .604 | .137 | .140 | 94.7 |
| **300** | **30** | -3.60 | .084 | .084 | 94.1 | .601 | .145 | .143 | 95.2 |
| **300** | **40** | -3.61 | .096 | .094 | 95.8 | .611 | .160 | .161 | 94.1 |
| **500** | **20** | -3.60 | .059 | .060 | 95.3 | .602 | .106 | .105 | 94.7 |
| **500** | **30** | -3.60 | .065 | .065 | 95.2 | .600 | .112 | .115 | 95.8 |
| **500** | **40** | -3.60 | .074 | .071 | 95.8 | .608 | .123 | .117 | 96.8 |

[1] Est: Average of the parameter estimates over 500 simulations
[2] SE: Average of estimated standard errors
[3] ESD: Empirical standard deviation of parameter estimates
[4] CP: Coverage probability of the proportion of simulations that the 95% confidence interval contains the true parameter values

probabilities improve towards the nominal level as censoring rate decreases.

We present the results of the misspecified models in Appendix B.6. In Tables B.1 and B.2 we generate under a model with no measurement error but fit a measurement-error model. We find similar coverage probabilities and bias for all the parameters as when fitting the model without measurement error in Tables 3.1 and 3.2. The standard errors are slightly larger for the variance parameters $(\eta_0, \eta_1)$ in this setting. We expect a large estimate for $\gamma$ relative to the observed marker value at the survival time and find that the estimate is fairly consistent across all levels of sample size and censoring. The standard errors of $\gamma$ are also large, and there is not good agreement between the empirical standard deviation and the standard errors. This is likely a result of fitting a more complicated model and attempting to estimate a parameter for which there is little information available in the data.

In Tables B.3 and B.4 we generate under a measurement-error model but fit a model without measurement error. We find that the bias of the variance parameters $(\eta_0, \eta_1)$ are lower compared to when we fit the measurement-error model (Tables 3.3 and 3.4). The standard errors of all the parameters are also lower. This possibly a result of numer-

**Table 3.3:** Simulation results for the parameters associated with the stochastic marker process from a gamma bridge survival model with no measurement error fit to marker data simulated from a gamma bridge process with no measurement error.

| | | | $\mu_0$ | | | | $\mu_1$ | | | | $\eta_0$ | | | | $\eta_1$ | | | |
|---|---|---|---|---|---|---|---|---|---|---|---|---|---|---|---|---|---|---|
| **n** | log($\gamma$) | **%Cens** | Est[1] | SE[2] | ESD[3] | CP[4] | Est | SE | ESD | CP | Est | SE | ESD | CP | Est | SE | ESD | CP |
| **200** | **0.0** | **20** | -1.14 | .095 | .096 | 91.2 | .297 | .176 | .174 | 95.0 | -2.51 | .617 | .670 | 92.8 | .325 | 1.11 | 1.08 | 94.2 |
| **200** | **0.0** | **30** | -1.13 | .096 | .100 | 90.8 | .277 | .176 | .181 | 92.9 | -2.57 | .585 | .651 | 94.2 | .367 | 1.04 | 1.09 | 94.9 |
| **200** | **0.0** | **40** | -1.14 | .098 | .107 | 91.3 | .299 | .181 | .181 | 95.4 | -2.54 | .561 | .559 | 94.7 | .405 | 1.00 | .937 | 97.1 |
| **200** | **0.7** | **20** | -1.13 | .072 | .068 | 91.4 | .288 | .132 | .133 | 94.3 | -2.41 | .477 | .522 | 95.8 | .352 | .819 | .851 | 96.9 |
| **200** | **0.7** | **30** | -1.13 | .073 | .075 | 93.7 | .287 | .135 | .137 | 95.2 | -2.44 | .451 | .487 | 96.0 | .380 | .766 | .870 | 96.9 |
| **200** | **0.7** | **40** | -1.13 | .075 | .079 | 92.2 | .285 | .138 | .138 | 95.4 | -2.45 | .410 | .470 | 94.1 | .405 | .725 | .797 | 96.0 |
| **200** | **1.1** | **20** | -1.13 | .062 | .060 | 91.9 | .286 | .115 | .119 | 94.1 | -2.35 | .408 | .467 | 94.9 | .364 | .665 | .745 | 96.0 |
| **200** | **1.1** | **30** | -1.13 | .063 | .063 | 92.1 | .282 | .117 | .118 | 93.8 | -2.38 | .385 | .435 | 95.5 | .425 | .637 | .719 | 96.1 |
| **200** | **1.1** | **40** | -1.12 | .065 | .070 | 92.2 | .280 | .120 | .125 | 93.8 | -2.37 | .356 | .368 | 93.6 | .402 | .588 | .697 | 94.7 |
| **300** | **0.0** | **20** | -1.13 | .077 | .076 | 92.1 | .287 | .142 | .143 | 93.1 | -2.48 | .504 | .538 | 92.3 | .366 | .894 | .922 | 94.6 |
| **300** | **0.0** | **30** | -1.12 | .079 | .081 | 92.3 | .279 | .144 | .145 | 94.8 | -2.49 | .476 | .501 | 94.6 | .374 | .841 | .857 | 96.1 |
| **300** | **0.0** | **40** | -1.13 | .080 | .078 | 93.6 | .280 | .148 | .147 | 94.6 | -2.54 | .457 | .509 | 90.5 | .432 | .793 | .873 | 96.7 |
| **300** | **0.7** | **20** | -1.13 | .059 | .056 | 92.2 | .286 | .108 | .109 | 94.6 | -2.40 | .395 | .442 | 93.5 | .388 | .654 | .738 | 96.5 |
| **300** | **0.7** | **30** | -1.13 | .060 | .063 | 91.3 | .293 | .111 | .108 | 94.7 | -2.42 | .358 | .397 | 93.8 | .454 | .602 | .625 | 97.2 |
| **300** | **0.7** | **40** | -1.13 | .061 | .063 | 91.7 | .283 | .113 | .117 | 93.3 | -2.39 | .326 | .354 | 90.2 | .447 | .564 | .597 | 95.2 |
| **300** | **1.1** | **20** | -1.13 | .051 | .049 | 91.7 | .290 | .094 | .094 | 94.9 | -2.36 | .341 | .388 | 93.0 | .441 | .548 | .588 | 96.6 |
| **300** | **1.1** | **30** | -1.13 | .052 | .054 | 89.5 | .291 | .096 | .097 | 95.0 | -2.36 | .305 | .318 | 93.1 | .461 | .500 | .521 | 96.9 |
| **300** | **1.1** | **40** | -1.12 | .053 | .056 | 91.3 | .280 | .098 | .103 | 92.7 | -2.34 | .281 | .283 | 90.0 | .430 | .472 | .521 | 96.1 |
| **500** | **0.0** | **20** | -1.13 | .060 | .064 | 88.9 | .285 | .112 | .108 | 94.3 | -2.45 | .390 | .421 | 93.0 | .460 | .660 | .653 | 97.0 |
| **500** | **0.0** | **30** | -1.12 | .061 | .062 | 93.3 | .284 | .111 | .109 | 95.4 | -2.45 | .360 | .381 | 92.5 | .422 | .627 | .651 | 95.9 |
| **500** | **0.0** | **40** | -1.12 | .062 | .057 | 94.6 | .285 | .114 | .106 | 95.8 | -2.47 | .333 | .345 | 87.2 | .396 | .594 | .631 | 94.3 |
| **500** | **0.7** | **20** | -1.13 | .046 | .045 | 88.8 | .285 | .085 | .083 | 94.4 | -2.36 | .292 | .310 | 90.5 | .472 | .475 | .500 | 96.3 |
| **500** | **0.7** | **30** | -1.13 | .046 | .047 | 90.6 | .287 | .086 | .092 | 92.9 | -2.37 | .268 | .282 | 86.7 | .443 | .450 | .500 | 95.1 |
| **500** | **0.7** | **40** | -1.12 | .048 | .048 | 91.8 | .282 | .088 | .087 | 94.5 | -2.36 | .245 | .239 | 84.2 | .438 | .416 | .413 | 96.0 |
| **500** | **1.1** | **20** | -1.13 | .039 | .040 | 86.9 | .283 | .073 | .076 | 92.7 | -2.32 | .251 | .247 | 91.6 | .476 | .396 | .397 | 97.4 |
| **500** | **1.1** | **30** | -1.13 | .040 | .041 | 90.0 | .284 | .074 | .075 | 93.2 | -2.35 | .234 | .248 | 86.8 | .476 | .378 | .397 | 96.0 |
| **500** | **1.1** | **40** | -1.12 | .041 | .040 | 92.2 | .285 | .076 | .074 | 95.1 | -2.33 | .213 | .217 | 84.2 | .445 | .354 | .378 | 95.6 |

[1] Est: Average of the parameter estimates over 500 simulations

[2] SE: Average of estimated standard errors

[3] ESD: Empirical standard deviation of parameter estimates

[4] CP: Coverage probability of the proportion of simulations that the 95% confidence interval contains the true parameter values

**Table 3.4:** Simulation results for the parameters associated with the measurement error and conditional cumulative hazard from a gamma bridge survival model with no measurement error fit to marker data simulated from a gamma bridge process with no measurement error.

| | | | $\log(\gamma)$ | | | | $\beta_0$ | | | | $\beta_1$ | | | |
|---|---|---|---|---|---|---|---|---|---|---|---|---|---|---|
| **n** | $\log(\gamma)$ | **%Cens** | Est[1] | SE[2] | ESD[3] | CP[4] | Est | SE | ESD | CP | Est | SE | ESD | CP |
| **200** | **0.0** | **20** | -.016 | .107 | .104 | 94.6 | -3.569 | .137 | .137 | 93.4 | .616 | .250 | .242 | 95.8 |
| **200** | **0.0** | **30** | -.017 | .108 | .111 | 92.8 | -3.574 | .142 | .149 | 92.3 | .635 | .254 | .260 | 95.9 |
| **200** | **0.0** | **40** | -.020 | .112 | .106 | 96.1 | -3.58 | .153 | .157 | 93.3 | .614 | .268 | .254 | 96.3 |
| **200** | **0.7** | **20** | .665 | .135 | .137 | 93.2 | -3.576 | .120 | .121 | 94.3 | .629 | .214 | .217 | 94.5 |
| **200** | **0.7** | **30** | .652 | .138 | .141 | 92.4 | -3.577 | .126 | .125 | 95.0 | .625 | .223 | .216 | 95.6 |
| **200** | **0.7** | **40** | .646 | .142 | .156 | 91.0 | -3.589 | .138 | .136 | 94.7 | .628 | .237 | .230 | 95.4 |
| **200** | **1.1** | **20** | 1.06 | .164 | .165 | 94.5 | -3.574 | .113 | .117 | 92.6 | .630 | .200 | .211 | 93.2 |
| **200** | **1.1** | **30** | 1.04 | .165 | .173 | 91.0 | -3.576 | .120 | .123 | 93.8 | .632 | .210 | .211 | 94.0 |
| **200** | **1.1** | **40** | 1.03 | .171 | .187 | 88.9 | -3.594 | .132 | .132 | 96.1 | .634 | .225 | .230 | 95.3 |
| **300** | **0.0** | **20** | -.018 | .086 | .087 | 94.4 | -3.582 | .111 | .103 | 95.3 | .619 | .203 | .198 | 96.0 |
| **300** | **0.0** | **30** | -.031 | .088 | .083 | 94.6 | -3.587 | .117 | .118 | 96.4 | .618 | .211 | .213 | 94.3 |
| **300** | **0.0** | **40** | -.035 | .090 | .091 | 91.7 | -3.599 | .125 | .126 | 94.6 | .628 | .218 | .225 | 94.4 |
| **300** | **0.7** | **20** | .653 | .109 | .107 | 92.9 | -3.582 | .098 | .089 | 95.9 | .619 | .175 | .173 | 94.8 |
| **300** | **0.7** | **30** | .635 | .111 | .112 | 89.8 | -3.581 | .103 | .106 | 93.4 | .605 | .182 | .181 | 95.5 |
| **300** | **0.7** | **40** | .640 | .115 | .115 | 90.2 | -3.595 | .113 | .115 | 95.4 | .627 | .194 | .200 | 93.8 |
| **300** | **1.1** | **20** | 1.04 | .130 | .125 | 91.1 | -3.582 | .093 | .090 | 95.1 | .617 | .165 | .171 | 95.8 |
| **300** | **1.1** | **30** | 1.03 | .133 | .131 | 91.2 | -3.578 | .098 | .101 | 93.7 | .606 | .172 | .172 | 95.8 |
| **300** | **1.1** | **40** | 1.03 | .138 | .137 | 89.4 | -3.596 | .108 | .111 | 93.2 | .628 | .184 | .188 | 94.6 |
| **500** | **0.0** | **20** | -.028 | .066 | .067 | 92.1 | -3.583 | .087 | .092 | 92.5 | .615 | .159 | .154 | 95.7 |
| **500** | **0.0** | **30** | -.033 | .068 | .067 | 91.8 | -3.585 | .090 | .093 | 93.3 | .613 | .161 | .170 | 94.7 |
| **500** | **0.0** | **40** | -.039 | .069 | .067 | 91.9 | -3.587 | .096 | .092 | 96.7 | .612 | .168 | .156 | 96.7 |
| **500** | **0.7** | **20** | .649 | .084 | .086 | 89.2 | -3.579 | .076 | .078 | 92.7 | .615 | .136 | .137 | 95.3 |
| **500** | **0.7** | **30** | .639 | .086 | .086 | 90.3 | -3.578 | .080 | .082 | 94.2 | .613 | .141 | .151 | 92.7 |
| **500** | **0.7** | **40** | .625 | .088 | .089 | 85.7 | -3.584 | .087 | .088 | 94.9 | .620 | .150 | .137 | 96.0 |
| **500** | **1.1** | **20** | 1.04 | .100 | .095 | 90.6 | -3.582 | .072 | .075 | 92.5 | .619 | .128 | .124 | 95.3 |
| **500** | **1.1** | **30** | 1.02 | .101 | .104 | 84.5 | -3.58 | .076 | .078 | 93.4 | .617 | .133 | .139 | 94.5 |
| **500** | **1.1** | **40** | 1.01 | .105 | .105 | 84.8 | -3.583 | .084 | .083 | 95.1 | .617 | .142 | .132 | 96.4 |

[1] Est: Average of the parameter estimates over 500 simulations
[2] SE: Average of estimated standard errors
[3] ESD: Empirical standard deviation of parameter estimates
[4] CP: Coverage probability of the proportion of simulations that the 95% confidence interval contains the true parameter values

ical difficulties in estimation for the measurement-error model in R software, where an approximation of the special Bessel function $K$ is used.

Overall, there is good agreement between the asymptotic standard errors and the empirical standard deviation in all simulation settings, indicating that we are correctly estimating the variability of the parameter estimates. The coverage probability for the conditional hazard parameters is at the 95% nominal level, indicating that the application of the marker process multiplicatively to the conditional hazard has not affected its estimation. The measurement-error model has high bias for the variance parameters and greater variability in its estimates than the model without measurement error. When the measurement-error model is fit to data without error, the $\gamma$ parameter is large and the results are similar to the model without error, indicating that it performs well when fitting a misspecified model. Similarly, the misspecified model without measurement error has low bias and standard errors when fit to data generated with error.

## 3.5 PCPT data analysis

The Prostate Cancer Prevention Trial (PCPT) was designed to study whether the drug finasteride prevented prostate cancer in men aged 55 and older (Thompson et al., 2003, 2013). The study enrolled 18,882 men who showed no evidence of prostate cancer and randomized half of them to receive finasteride and the other half to placebo. PCPT participants were required to visit the study site twice a year to monitor their health. They received a yearly physical exam which included a digital rectal examination (DRE) and PSA blood test. If their PSA values were elevated or their DRE was abnormal, they had a prostate biopsy to check for cancer. At the end of seven years in the study, all participants who had not been diagnosed with prostate cancer received an end-of-study prostate biopsy. This involved using a needle to remove at least six small pieces of prostate tissue.

We restrict our analysis to placebo patients who received at least one biopsy with a

PSA measurement within 3 months of the final biopsy, and censored those who received an end-of-study biopsy without cause. We selected only patients with race coded as white or black, resulting in 4932 subjects being included in the analysis, of which 153 (3%) are black. The data was structured as one biopsy measurement per person (choosing the last biopsy available), the time from registration to the last biopsy, the baseline log-transformed PSA measurement, and the final log-transformed PSA measurement. The marker of interest is the difference in log-transformed PSA from baseline. For the 20% of patients with a decreasing PSA value, their change in PSA was set to 0.

From Figure 3.2, the Kaplan-Meier curves for the model exhibit a large drop in the survival curve at years 1, 2, etc., which is a result of biopsies being conducted every year since baseline. Thus, we specify the conditional cumulative hazard of our model as a mixture of normal distributions to capture this step effect. From Figure 3.2, we see that the survival curves for each race may not be best described by proportional hazards. Thus, we fit the model to each race separately, and then perform a test for common conditional cumualtive hazards across the two groups.

To account for the study participants not having zero risk at study entry (i.e., non-zero PSA), we model the change in log(PSA+1) from baseline as a gamma process with mean $\mu t$ and variance $\sigma^2 t$, where $\mu = \exp\{\mu_r\}, r \in \{W = \text{white}, B = \text{black}\}$ and $\sigma^2 = \exp\{\eta_r\}, r \in \{W, B\}$ and apply its effect multiplicatively to this baseline hazard. We also include the effect of the baseline log(PSA+1) and baseline age in the mean and variance functions (i.e., $\mu_r = \mu_{r0} + \mu_{r1}\log(\text{PSA}_0 + 1) + \mu_{r2}(\text{Age}_0/20)$, $\eta_r = \eta_{r0} + \eta_{r1}\log(\text{PSA}_0 + 1) + \eta_{r2}(\text{Age}_0/20)$). The distributions of these covariates by race are shown in Figure 3.1, where we see good overlap between the two groups.

We fit a measurement-error model, where we model the marker value $v$ as being observed as a random gamma variable with mean $v$ and variance $v^2/\exp\{\gamma_r\}, r \in \{W, B\}$. A higher estimated value for $\gamma_r$ would indicate that the measurement-error model is not required (i.e., the variance of the marker measured with error goes to 0).

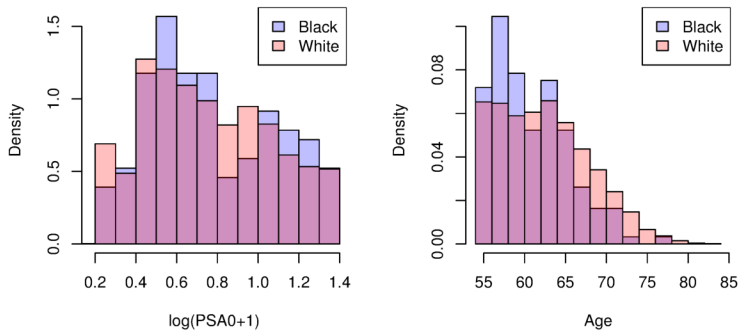


**Figure 3.1:** Distribution of baseline covariates log(PSA+1) (left) and Age (right) by race for PCPT data.

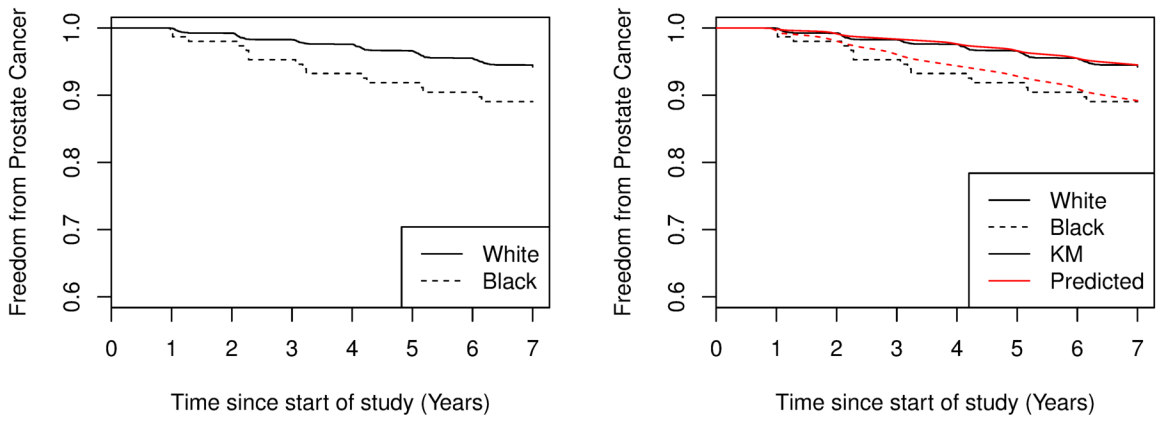


**Figure 3.2:** Kaplan Meier curves (left) and predicted survival probabilities (with $\text{Age}_0 = 60$ and $\text{PSA}_0 = 2.1$ (median values)) from proposed model (right) for Freedom from prostate cancer by race.

Using a likelihood ratio test, we find that the model with conditional cumulative hazard stratified by race is a better fit to the data than a model with common conditional cumulative hazards across the two groups. For black men, the baseline age covariate was not found to be significant in the mean or the variance of the process and these parameters were therefore dropped from the model. The estimate for the measurement error parameters $\gamma$ were large ($\log(\hat{\gamma_B}) = 4.89$, $\log(\hat{\gamma_W}) = 4.88$), and by comparing AIC we find that the model without the gamma measurement error provided a better fit to the data. The coefficient estimates for the mean and variance parameters were similar across both models, resulting in almost identical predictions. Thus, we present the coefficient

estimates and standard errors from the simpler model without measurement error in Table 3.5.

**Table 3.5:** Estimates and standard errors for parameters of the gamma bridge process for difference in log PSA from the gamma bridge survival model with no measurement error applied to PCPT data.

| Parameter | Estimate | SE |
|---|---|---|
| $\mu_{W0}$ | -5.060 | 0.274 |
| $\mu_{W1}$ | 1.081 | 0.080 |
| $\mu_{W2}$ | 0.264 | 0.088 |
| $\eta_{W0}$ | -7.657 | 0.584 |
| $\eta_{W1}$ | 2.059 | 0.173 |
| $\eta_{W2}$ | 0.667 | 0.187 |
| $\mu_{B0}$ | -3.890 | 0.313 |
| $\mu_{B1}$ | 1.118 | 0.360 |
| $\eta_{B0}$ | -4.900 | 0.707 |
| $\eta_{B1}$ | 1.489 | 0.817 |

Since we apply the marker process multiplicatively to the conditional cumulative hazard, we can interpret the effect of the coefficient estimates for the mean of the process directly on survival probabilities. The coefficient estimate for baseline PSA in the mean of the marker process is positive for both white and black men indicating that those that start with a high PSA have a greater increase in PSA and higher probability of developing prostate cancer. The mean coefficient estimate for baseline age is positive for white men, indicating that those who are older at the start of the study have a greater change in PSA and a higher probability of prostate cancer. We show the predicted survival curves from this model (with baseline age and PSA set at their median values) in Figure 3.2 and demonstrate that they align well with the Kaplan-Meier curves. The predicted survival curve for black men falls at the top of the steps for the Kaplan-Meier curve but does not capture the annual step effect as well as the predicted curve for white men does. This is possibly a result of having less data for black men. With a likelihood ratio test we reject the null hypothesis that there is no significant difference in the mean for the gamma process between white and black men. Thus, we conclude that the behavior of the PSA

processes varies between the two races.

### 3.5.1 Marker and Survival Prediction

In Figure 3.3, we show the dynamic predicted values for the survival probability and the average marker prediction for three patients in the data set who were censored. Each individual is censored at $\tau$, indicated by the vertical dotted line, at which time they are measured to have marker value $V_\tau = v$. We use the marginal survival function $S(t)$ given in Eq.(3.3) to predict their survival up to time $\tau$, and then use $S(\tau + t|V_\tau = v)$ in Eq.(3.8) to compute their conditional survival for $t \geq \tau$. To compute the predicted marker, we use Eq.(3.13) to compute the average marker value $\mathbb{E}[W_t|T > t]$ up to time $\tau$ and then use Eq.(3.10) for the prediction of the marker value conditioning on the observation at $\tau$, $\mathbb{E}[W_t|T > t, V_\tau = v]$, for $t \geq \tau$. For demonstration purposes we show the predicted curves for both races.

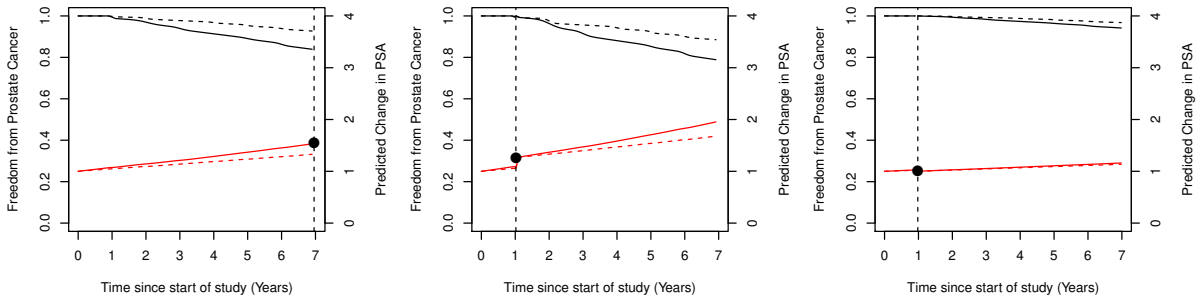


**Figure 3.3:** Dynamic prediction of survival and marker for three individuals in the data set with censored survival times. Individual A (left) is a black male, age 60 at baseline, has $\text{PSA}_0 = 2.1$. Individual B (middle) is a black male, age 65 at baseline, with $\text{PSA}_0 = 3.0$. Individual C (right) is a white male with, age 72 at baseline, with $\text{PSA}_0 = 0.5$. The color of the curves distinguishes the whether the line is for the marker (red) or the survival (black). The line type indicates the prediction for a white (dashed) or a black (solid) man. The black dot indicates the individual's observed marker value at his censoring time.

The predicted survival curves for black men are lower than those for white men and the predicted marker trajectory is higher. Individual A is young but with a high baseline PSA and has a steadily increasing marker process, matched by an increasing probability of prostate cancer diagnosis. Individual B is slightly older with a higher PSA and at time

$\tau$ we see that his observed marker value is higher than the expected value. Individual C is older with very low baseline PSA; we see that his observed marker value is close to predicted, and that they have very slow marker growth, matched by lower risk of prostate cancer. These marker predictions can be useful for comparing the behavior of the marker process for different groups, and the dynamically predicted survival can be used in the context of the previous chapters for informing about a patient's future prognosis.

## 3.6 Discussion

Using a stochastic marker process framework, we have developed a joint model for the incorporation of a partially observed covariate on a time-to-event outcome. We consider the situation of marked data, where a time-dependent marker is observed only at the survival time. We suppose that the marker represents a risk process that accumulates over time leading to the occurrence of a failure event, and model it flexibly using an increasing Lévy bridge process. By using a stochastic process framework, we do not restrict the pattern of the individual marker trajectories based on a functional form, instead allowing for biological variability through individual fluctuations. Thus, this model can be applied to a variety of marker and disease settings. This flexible formulation also allows us to overcome the difficulties of joint modeling with a sparse marked survival data structure.

In this work, we extend the theory of gamma bridge processes to a survival framework. Thus, a limitation of our model is that the behavior of the marker and the survival is dependent on the properties of this particular process. However, we could consider a wide class of non-decreasing Lévy process models in this framework. For example, the compound Poisson process, for which a closed-form characteristic function is defined for its bridge (Hoyle, 2010), or limits of the compound Poisson process. We can also consider alternative methods for incorporating measurement error into the modeling framework, such as a piece-wise exponential function for $Z_\tau|V_\tau$ where we define the cutpoints based on quantiles of the observed marker distribution and estimate a separate measurement

error parameter for each interval. So far, we have considered a fully parametric approach for both the marker and survival components of the joint model. Introducing a semiparametric conditional cumulative hazard $H(t)$ into the current modeling framework is straightforward; however, a semiparametric representation of the marker process will pose difficulties for derivation and estimation.

As outlined in Section 3.3.5, we can extend the survival model formulation to incorporate the effect of multiple marker measurements from longitudinal marker data. Further derivations are required to specify the form for the marginal survival and cumulative hazard functions, which should follow straightforwardly from similar arguments to those presented in Appendix B.1. This will allow us to extend our model to the situation described in Yashin and Manton (1997) when dealing with a marker that is partially observed at multiple time points; however, the gamma framework provides a more analytically tractable form and we expect estimation to be simpler. We may also be interested in using longitudinally measured biomarkers to make dynamic survival predictions, as was the focus in the previous chapters. While with a shared random effects model and our copula method we have to specify a functional form for the marker process, in this framework we use the flexibility of a stochastic process to describe the marker behavior in intervals when it is unobserved.

We can also consider an extension of our proposed model to the multivariate setting using the same arguments as presented in a shared frailty approach (Hougaard, 2012),

$$S(t_1, t_2|W_t) = S_1(t_1)^{-W_t} S_2(t_2)^{-W_t} = e^{-W_t(H_1(t_1)+H_2(t_2))}$$

where we assume that individuals in a pair share the same marker process effect, and that conditional on the marker their lifetimes are independent. This presents a simpler approach to modeling multivariate data than explored in Putter and Van Houwelingen (2015). They use the Lévy process $W_t$ in the hazard rather than the cumulative haz-

ard, which does not produce a tractable representation for large cluster sizes resulting in infeasible estimation when the data has a large number of events. Future work will extend the modeling framework presented in this chapter to address more complicated data structures.

# CONCLUSION

With this dissertation we aim to provide a useful contribution to the literature for modeling survival using longitudinal marker information. Incorporating this time-dependent information is essential for obtaining accurate inference and up-to-date survival predictions. The methods presented in the dissertation can be applied to a variety of medical research problems. As interest in long-term follow-up studies and electronic health systems grows, the availability of longitudinal information is increasing. Thus, developing methods for incorporating their time-varying effects, such as those presented in this dissertation, is essential.

In the first two chapters, we explored the use of longitudinal marker data to make dynamic predictions of survival for a patient at time points beyond baseline. These predictions can be used by clinicians to tailor a patient's treatment strategy. In Chapter I we compared two methods of dynamic prediction, landmarking and joint modeling, with a binary marker. We assessed whether introducing additional flexibility to an approximate approach can improve performance to be on par with a joint model. In this work, we concluded that with a binary marker, the performance of landmarking approaches that of joint modeling when we consider more flexible forms for modeling the relationship of the marker effect on the conditional hazard. Thus, when faced with settings where it might be difficult to fit a joint model, such as with sparsely collected longitudinal information, using an approximate approach such as landmarking can be a sufficient substitute. Future work can consider the comparisons of these methods under more complicated situations, to identify when one method should be selected over the other. For example, when there are multiple markers that are sparsely and irregularly measured, or when dealing with

dependent censoring or competing risks.

In Chapter II, we propose an alternative approximate approach to dynamic prediction. Our aim is to address the limitations posed by joint modeling and landmarking that make them less desirable to use in certain situations. In comparison with landmarking, the proposed copula model uses a longitudinal data set for estimation and does not require us to implement specific data structuring based on prespecifying prediction times and a prediction window of interest. This also allows us to avoid imputing the value of the process at prediction times at which it is not observed, proving our method to be useful for irregular measurement times and unbalanced data. Compared to joint modeling, we do not have to specify the distribution of the marker trajectories, but instead describe the marker distribution as a population-averaged model. We use a pseudo-likelihood based approach that allows for straightforward estimation, and the tractable nature of the Gaussian copula provides a closed-form expression from which we can easily compute the dynamic predictions.

The limitations of this method include its reliance on the correct specification of the marginal distributions. Thus, the bias can be large at later time points at which there is less longitudinal information available for certain groups. As well, the model can produce large standard errors for the parameters in the association function. This is a result of using a two-stage approach, where calculating the variance of parameters in the second stage also takes into account the estimation uncertainty of the parameters the first stage. However, we find that with a sufficiently flexible representation, the performance of the model is robust to the choice of the association function.

In the current copula and landmarking formulation, predictive performance was evaluated by computing the dynamic prediction $[T > \tau + s|T > \tau, Z(\tau)]$, where we compute the survival probability conditional on the individual's last available marker measurement at time $\tau$. To achieve a more accurate prediction, it might be of interest to incorporate an individual's longitudinal marker history $[T > \tau + s|T > \tau, \bar{Z}(\tau)]$, where $\bar{Z}(\tau)$ represents

the individual's history of the longitudinal marker values up to time $\tau$. Joint modeling handles this naturally. Rizopoulos et al. (2013) extended the landmark model specification to consider parameterizations that incorporate the marker relationship with survival in various way, such as the slope of the marker trajectory, $Z_i'(\tau)$, or the area under the longitudinal trajectory up to time $\tau$, $\int_0^\tau Z_i(t)\,\mathrm{d}t$. The copula model can also be extended to incorporate a summary of the marker history up to time $\tau$, by modeling a different aspect of the marginal marker distribution instead of the marginal marker mean described in this dissertation. For example, we could have instead considered a marginal model for the change in the marker value from baseline, $Z(\tau) - Z(0)|T > \tau$. We can also consider more complicated summary measures, such as the area under longitudinal trajectory, or even modeling the behaviour of individual trajectories using a mixed effect model if dictated by the data. Thus, the survival depends on the history of the marker and not just on the distribution of the patient's marker at time $\tau$. The ability to model the marginals and their distributions separately allows for more complicated, better fitting, models to be considered for the marginals, but still maintains simple estimation using the two-stage method.

There are several other extensions that we could consider within the copula framework. The most interesting of these would be to use the tractability of the Gaussian copula to include the effects of multiple time-varying markers. The association structure can provide insight into the relationship between the markers and survival, but can also identify interesting dependencies between the markers themselves. With an increased number of markers, the number of association function parameters will also grow. This means that care should be taken to perform covariate selection even at the second stage of estimation to achieve a more parsimonious model. Future work will explore the predictive performance as well as the interpretations that can be obtained from dealing with other, more complex forms of survival-longitudinal data.

One such data structure often arising in cancer research is that of marked data, where

we assume the marker process to be an underlying latent stochastic process that is observed only at the survival time. The data available for each patient is then a current status observation and an associated cross-sectional surrogate, or "mark", of the stochastic process. This provides us with very sparse longitudinal data. Thus, it is difficult to employ a method that relies on establishing the distribution of the marker over time, as with our proposed copula approach and joint modeling. Landmarking in this situation can introduce bias due to its reliance on imputing marker values at times at which they are not observed. Thus, in Chapter III we consider a new class of survival models that avoids specifying a functional form for the marker, instead letting its behaviour for periods during which it is not observed be modeled as a flexible, increasing stochastic process.

A particular limitation of this method is that it relies heavily on the properties of the chosen process. For our formulations, we specifically consider a gamma process due to its tractable nature. Extensions to this work could explore other processes in the wide family of Lévy processes. Although the Lévy process is known for its analytical tractability, the difficulty comes from our use of a Lévy bridge to extend current stochastic process model formulations to the situation where the marker is partially observed. There is a closed-form representation of the characteristic function for a compound Poisson process bridge from financial applications that could be considered (Hoyle, 2010), along with limits of the process.

We also specify a measurement-error model where we assume that we observe only a surrogate of the marker. To specify the distribution of the surrogate conditional on the true marker value we are restricted to compound distributions. We impose the additional restriction that the mean of the distribution be the true marker value. In the gamma measurement-error model, this specifies the variance of the surrogate marker to be large when the true marker value itself is large, which may not be a reasonable assumption. Thus, future work shall explore additional forms for the measurement-error model distribution, such as the Normal (for which we develop the theory but have not yet been able

to achieve estimation due to numerical difficulties) and a piece-wise exponential, which can be easily adapted from the gamma error model.

Finally, we frame our model using a fully parametric approach for both the marker and survival behaviour. Using a semi-parametric model for the conditional cumulative hazard is likely a straightforward extension; however, a semiparametric marker process will prevent us from taking advantage of the tractability of the gamma process to derive the survival functions, likely rendering such an approach difficult for both derivation and estimation.

We adapt this model from the field of mathematical finance, where the increasing risk process represents aggregate insurance claims data (Brody et al., 2008), to a survival framework. Thus, there are several extensions that can be considered to apply it to more complex forms of survival and longitudinal data. For example, we can consider a multivariate setting, and adapt a shared frailty model where we replace the frailty with our Lévy bridge process. We also begin describing the dynamic predictions that can be obtained from this model. Future work will require describing the estimation and derivation of the survival functions for multiple measurement times. By conditioning on multiple markers, we could compute dynamic predictions that incorporate an individual's entire marker history to make a more accurate survival prediction.

We hope that this work provides readers with an appreciation of the importance of dynamic methods in survival analysis. In this dissertation, we explore existing and new methods for the statistical task of dynamic prediction and inference of survival with longitudinal biomarkers. By considering unique approaches, such as the Gaussian copula and the Lévy-based bridge in a dynamic survival framework, we aim to advance statistical research in this area.

# APPENDICES

# APPENDIX A

# A Gaussian Copula Approach for Dynamic Prediction of Survival with a Longitudinally Measured Marker

## A.1 Two-stage parametric variance estimation

Let $\boldsymbol{\alpha}$, $\boldsymbol{\beta}$ be the parameter vectors for the margins for $T_\tau$ and $Z_\tau$, respectively. Let $\ell_T(\boldsymbol{\alpha})$ and $\ell_Z(\boldsymbol{\beta})$ be the marginal log-likelihoods. Let $\boldsymbol{\theta}$ be the parameter vector of the association parameters. Let $\ell(\boldsymbol{\alpha}, \boldsymbol{\beta}, \boldsymbol{\theta}) = \sum_{i=1}^{N} \sum_{l=1}^{n_i} \ell_{il}(\boldsymbol{\alpha}, \boldsymbol{\beta}, \boldsymbol{\theta})$ be the pseudo-log-likelihood that considers repeated measurements on the same subject to be uncorrelated.

In the first stage, we estimate $\boldsymbol{\alpha}$ and $\boldsymbol{\beta}$ by $\hat{\boldsymbol{\alpha}}$ and $\hat{\boldsymbol{\beta}}$ by solving the score equations

$$\mathbf{U}_1(\boldsymbol{\alpha}) = \sum_{i=1}^{N} \frac{\partial \ell_{i,T}(\boldsymbol{\alpha})}{\partial \boldsymbol{\alpha}} = \mathbf{0} \qquad \mathbf{U}_2(\boldsymbol{\beta}) = \sum_{i=1}^{N} \sum_{l=1}^{n_i} \frac{\partial \ell_{il,Z}(\boldsymbol{\beta})}{\partial \boldsymbol{\beta}} = \mathbf{0}$$

Under regularity conditions, $\sqrt{N}(\hat{\boldsymbol{\alpha}} - \boldsymbol{\alpha})$ converges to a multivariate normal distribution with mean vector $\mathbf{0}$ and variance-covariance matrix $(\mathbf{I}_{\boldsymbol{\alpha}\boldsymbol{\alpha}})^{-1}$, where $\mathbf{I}_{\boldsymbol{\alpha}\boldsymbol{\alpha}} = -\mathbb{E}\left[\frac{\partial^2 \ell_T}{\partial \boldsymbol{\alpha} \partial \boldsymbol{\alpha}'}\right]$ is the Fisher information of $\mathbf{U}_1(\boldsymbol{\alpha})$.

Under regularity conditions, $\sqrt{N}(\hat{\boldsymbol{\beta}} - \boldsymbol{\beta})$ converges to a multivariate normal distribution with mean vector $\mathbf{0}$ and variance-covariance matrix $(\mathbf{I}_{\boldsymbol{\beta}\boldsymbol{\beta}})^{-1}\mathbf{V}(\mathbf{I}_{\boldsymbol{\beta}\boldsymbol{\beta}})^{-1}$, where

$\mathbf{V} = \mathbb{E}\left[\left(\frac{\partial \ell_Z}{\partial \boldsymbol{\beta}}\right)\left(\frac{\partial \ell_Z}{\partial \boldsymbol{\beta}}\right)'\right]$ is the variance-covariance matrix of the score equations $\mathbf{U}_2(\boldsymbol{\beta})$ and $\mathbf{I}_{\boldsymbol{\beta}\boldsymbol{\beta}} = -\mathbb{E}\left[\frac{\partial^2 \ell_Z}{\partial \boldsymbol{\beta}\partial \boldsymbol{\beta}'}\right]$ is the Fisher information of $\mathbf{U}_2(\boldsymbol{\beta})$. The use of a sandwich estimator is necessary since $(\mathbf{I}_{\boldsymbol{\beta}\boldsymbol{\beta}})^{-1}$ is not a consistent estimator of the asymptotic variance-covariance matrix due to the correlation between repeated measurements on the same subject.

In the second stage, the association parameter vector $\boldsymbol{\theta}$ is estimated by plugging in the estimates from the marginal models into the pseudo-log-likelihood, and then maximizing it with respect to $\boldsymbol{\theta}$. Thus, we obtain the estimate $\hat{\boldsymbol{\theta}}$ as the solution to

$$\mathbf{U}_3(\hat{\boldsymbol{\alpha}}, \hat{\boldsymbol{\beta}}, \boldsymbol{\theta}) = \sum_{i=1}^{N}\sum_{l=1}^{n_i} \frac{\partial \ell_{il}(\hat{\boldsymbol{\alpha}}, \hat{\boldsymbol{\beta}}, \boldsymbol{\theta})}{\partial \boldsymbol{\theta}} = \mathbf{0}$$

which is the first derivative of the pseudo-log-likelihood. We now explore the asymptotic variance of $\boldsymbol{\theta}$.

Let $\boldsymbol{\alpha}_0$ and $\boldsymbol{\beta}_0$ denote the true parameter vectors of the margins. Expanding the score functions $\mathbf{U}_1$ and $\mathbf{U}_2$ using a Taylor series around the true values and evaluating it at the true values $\boldsymbol{\alpha} = \boldsymbol{\alpha}_0$ and $\boldsymbol{\beta} = \boldsymbol{\beta}_0$, under the regularity conditions of maximum likelihood theory we get

$$\begin{aligned}
\mathbf{U}_1(\hat{\boldsymbol{\alpha}}) = 0 &= \mathbf{U}_1(\boldsymbol{\alpha}_0) + \left.\frac{\partial \mathbf{U}_1}{\partial \boldsymbol{\alpha}}\right|_{\boldsymbol{\alpha}=\boldsymbol{\alpha}_0} (\hat{\boldsymbol{\alpha}} - \boldsymbol{\alpha}_0) + o_p(\sqrt{N}) \\
\mathbf{U}_2(\hat{\boldsymbol{\beta}}) = 0 &= \mathbf{U}_2(\boldsymbol{\beta}_0) + \left.\frac{\partial \mathbf{U}_2}{\partial \boldsymbol{\beta}}\right|_{\boldsymbol{\beta}=\boldsymbol{\beta}_0} (\hat{\boldsymbol{\beta}} - \boldsymbol{\beta}_0) + o_p(\sqrt{N})
\end{aligned}$$

Similarly,

$$\begin{aligned}
\mathbf{U}_3(\hat{\boldsymbol{\alpha}}, \hat{\boldsymbol{\beta}}, \hat{\boldsymbol{\theta}}) = 0 =& \mathbf{U}_3(\boldsymbol{\alpha}_0, \boldsymbol{\beta}_0, \boldsymbol{\theta}_0) \\
&+ \left.\frac{\partial \mathbf{U}_3}{\partial \boldsymbol{\alpha}}\right|_{(\boldsymbol{\alpha},\boldsymbol{\beta},\boldsymbol{\theta})=(\boldsymbol{\alpha}_0,\boldsymbol{\beta}_0,\boldsymbol{\theta}_0)} (\hat{\boldsymbol{\alpha}} - \boldsymbol{\alpha}_0) + \left.\frac{\partial \mathbf{U}_3}{\partial \boldsymbol{\beta}}\right|_{(\boldsymbol{\alpha},\boldsymbol{\beta},\boldsymbol{\theta})=(\boldsymbol{\alpha}_0,\boldsymbol{\beta}_0,\boldsymbol{\theta}_0)} (\hat{\boldsymbol{\beta}} - \boldsymbol{\beta}_0) \\
&+ \left.\frac{\partial \mathbf{U}_3}{\partial \boldsymbol{\theta}}\right|_{(\boldsymbol{\alpha},\boldsymbol{\beta},\boldsymbol{\theta})=(\boldsymbol{\alpha}_0,\boldsymbol{\beta}_0,\boldsymbol{\theta}_0)} (\hat{\boldsymbol{\theta}} - \boldsymbol{\theta}_0) + o_p(\sqrt{N})
\end{aligned}$$

By the law of large numbers, as $N \to \infty$,

$$
\begin{aligned}
-\frac{1}{N}\frac{\partial \mathbf{U}_1}{\partial \boldsymbol{\alpha}}\bigg|_{\boldsymbol{\alpha}=\boldsymbol{\alpha}_0} &= \frac{1}{N}\sum_{i=1}^{N} -\frac{\partial}{\partial \boldsymbol{\alpha}}\mathbf{U}_{i,1}(\boldsymbol{\alpha}_0) \to \mathbf{I}_{\boldsymbol{\alpha}\boldsymbol{\alpha}} = \mathbb{E}\left[-\frac{\partial}{\partial \boldsymbol{\alpha}}\mathbf{U}_1(\boldsymbol{\alpha}_0)\right] \\
-\frac{1}{N}\frac{\partial \mathbf{U}_2}{\partial \boldsymbol{\beta}}\bigg|_{\boldsymbol{\beta}=\boldsymbol{\beta}_0} &= \frac{1}{N}\sum_{i=1}^{N} -\frac{\partial}{\partial \boldsymbol{\beta}}\mathbf{U}_{i,2}(\boldsymbol{\beta}_0) \to \mathbf{I}_{\boldsymbol{\beta}\boldsymbol{\beta}} = \mathbb{E}\left[-\frac{\partial}{\partial \boldsymbol{\beta}}\mathbf{U}_2(\boldsymbol{\beta}_0)\right] \\
-\frac{1}{N}\frac{\partial \mathbf{U}_3}{\partial \boldsymbol{\theta}}\bigg|_{(\boldsymbol{\alpha},\boldsymbol{\beta},\boldsymbol{\theta})=(\boldsymbol{\alpha}_0,\boldsymbol{\beta}_0,\boldsymbol{\theta}_0)} &= \frac{1}{N}\sum_{i=1}^{N} -\frac{\partial}{\partial \boldsymbol{\theta}}\mathbf{U}_{i,3}(\boldsymbol{\alpha}_0,\boldsymbol{\beta}_0,\boldsymbol{\theta}_0) \to \mathbf{I}_{\boldsymbol{\theta}\boldsymbol{\theta}} = \mathbb{E}\left[-\frac{\partial}{\partial \boldsymbol{\theta}}\mathbf{U}_3(\boldsymbol{\alpha}_0,\boldsymbol{\beta}_0,\boldsymbol{\theta}_0)\right] \\
-\frac{1}{N}\frac{\partial \mathbf{U}_3}{\partial \boldsymbol{\alpha}}\bigg|_{(\boldsymbol{\alpha},\boldsymbol{\beta},\boldsymbol{\theta})=(\boldsymbol{\alpha}_0,\boldsymbol{\beta}_0,\boldsymbol{\theta}_0)} &= \frac{1}{N}\sum_{i=1}^{N} -\frac{\partial}{\partial \boldsymbol{\alpha}}\mathbf{U}_{i,3}(\boldsymbol{\alpha}_0,\boldsymbol{\beta}_0,\boldsymbol{\theta}_0) \to \mathbf{I}_{\boldsymbol{\theta}\boldsymbol{\alpha}} = \mathbb{E}\left[-\frac{\partial}{\partial \boldsymbol{\alpha}}\mathbf{U}_3(\boldsymbol{\alpha}_0,\boldsymbol{\beta}_0,\boldsymbol{\theta}_0)\right] \\
-\frac{1}{N}\frac{\partial \mathbf{U}_3}{\partial \boldsymbol{\beta}}\bigg|_{(\boldsymbol{\alpha},\boldsymbol{\beta},\boldsymbol{\theta})=(\boldsymbol{\alpha}_0,\boldsymbol{\beta}_0,\boldsymbol{\theta}_0)} &= \frac{1}{N}\sum_{i=1}^{N} -\frac{\partial}{\partial \boldsymbol{\beta}}\mathbf{U}_{i,3}(\boldsymbol{\alpha}_0,\boldsymbol{\beta}_0,\boldsymbol{\theta}_0) \to \mathbf{I}_{\boldsymbol{\theta}\boldsymbol{\beta}} = \mathbb{E}\left[-\frac{\partial}{\partial \boldsymbol{\beta}}\mathbf{U}_3(\boldsymbol{\alpha}_0,\boldsymbol{\beta}_0,\boldsymbol{\theta}_0)\right]
\end{aligned}
$$

Thus,

$$
\frac{1}{\sqrt{N}}\begin{pmatrix} \mathbf{U}_1(\boldsymbol{\alpha}_0) \\ \mathbf{U}_2(\boldsymbol{\beta}_0) \\ \mathbf{U}_3(\boldsymbol{\alpha}_0,\boldsymbol{\beta}_0,\boldsymbol{\theta}_0) \end{pmatrix} \to \sqrt{N}\begin{pmatrix} \mathbf{I}_{\boldsymbol{\alpha}\boldsymbol{\alpha}} & 0 & 0 \\ 0 & \mathbf{I}_{\boldsymbol{\beta}\boldsymbol{\beta}} & 0 \\ \mathbf{I}_{\boldsymbol{\theta}\boldsymbol{\alpha}} & \mathbf{I}_{\boldsymbol{\theta}\boldsymbol{\beta}} & \mathbf{I}_{\boldsymbol{\theta}\boldsymbol{\theta}} \end{pmatrix}\begin{pmatrix} \hat{\boldsymbol{\alpha}}-\boldsymbol{\alpha}_0 \\ \hat{\boldsymbol{\beta}}-\boldsymbol{\beta}_0 \\ \hat{\boldsymbol{\theta}}-\boldsymbol{\theta}_0 \end{pmatrix} \tag{A.1}
$$

By the central limit theorem, (A.1) converges to multivariate normal with mean $\mathbf{0}$ and variance-covariance matrix

$$
\begin{pmatrix} \mathbf{I}_{\boldsymbol{\alpha}\boldsymbol{\alpha}} & \mathbf{I}_{\boldsymbol{\alpha}\boldsymbol{\beta}} & \mathbf{I}_{\boldsymbol{\alpha}\boldsymbol{\theta}} \\ \mathbf{I}_{\boldsymbol{\beta}\boldsymbol{\alpha}} & \mathbf{V} & \mathbf{I}_{\boldsymbol{\beta}\boldsymbol{\theta}} \\ \mathbf{I}_{\boldsymbol{\theta}\boldsymbol{\alpha}} & \mathbf{I}_{\boldsymbol{\theta}\boldsymbol{\beta}} & \mathbf{I}_{\boldsymbol{\theta}\boldsymbol{\theta}} \end{pmatrix}
$$

where

$$
\begin{aligned}
&\mathbf{I}_{\boldsymbol{\alpha}\boldsymbol{\beta}} = \mathbb{E}[\mathbf{U}_{1,1}(\boldsymbol{\alpha}_0)\mathbf{U}_{1,2}(\boldsymbol{\beta}_0)^T] && \mathbf{I}_{\boldsymbol{\beta}\boldsymbol{\alpha}} = \mathbb{E}[\mathbf{U}_{1,2}(\boldsymbol{\beta}_0)\mathbf{U}_{1,1}(\boldsymbol{\alpha}_0)^T] \\
&\mathbf{I}_{\boldsymbol{\alpha}\boldsymbol{\theta}} = \mathbb{E}[\mathbf{U}_{1,1}(\boldsymbol{\alpha}_0)\mathbf{U}_{1,3}(\boldsymbol{\alpha}_0,\boldsymbol{\beta}_0,\boldsymbol{\theta}_0)^T] && \mathbf{I}_{\boldsymbol{\theta}\boldsymbol{\alpha}} = \mathbb{E}[\mathbf{U}_{1,3}(\boldsymbol{\alpha}_0,\boldsymbol{\beta}_0,\boldsymbol{\theta}_0)\mathbf{U}_{1,1}(\boldsymbol{\alpha}_0)^T] \\
&\mathbf{I}_{\boldsymbol{\beta}\boldsymbol{\theta}} = \mathbb{E}[\mathbf{U}_{1,2}(\boldsymbol{\beta}_0)\mathbf{U}_{1,3}(\boldsymbol{\alpha}_0,\boldsymbol{\beta}_0,\boldsymbol{\theta}_0)^T] && \mathbf{I}_{\boldsymbol{\theta}\boldsymbol{\beta}} = \mathbb{E}[\mathbf{U}_{1,3}(\boldsymbol{\alpha}_0,\boldsymbol{\beta}_0,\boldsymbol{\theta}_0)\mathbf{U}_{1,2}(\boldsymbol{\beta}_0)^T] \\
&\mathbf{V} = \mathrm{Var}(\mathbf{U}_{1,2}(\boldsymbol{\beta}_0)) = \mathbb{E}[\mathbf{U}_{1,2}(\boldsymbol{\beta}_0)\mathbf{U}_{1,2}(\boldsymbol{\beta}_0)^T]
\end{aligned}
$$

By proof given in Joe and Xu (1996), $\mathbf{I}_{\boldsymbol{\alpha}\boldsymbol{\theta}} = \mathbf{I}_{\boldsymbol{\theta}\boldsymbol{\alpha}} = \mathbf{I}_{\boldsymbol{\beta}\boldsymbol{\theta}} = \mathbf{I}_{\boldsymbol{\theta}\boldsymbol{\beta}} = 0$. Thus,

using theory of inference margins (Joe and Xu, 1996), $\sqrt{N}\begin{pmatrix}\hat{\boldsymbol{\alpha}}-\boldsymbol{\alpha}_0\\ \hat{\boldsymbol{\beta}}-\boldsymbol{\beta}_0\\ \hat{\boldsymbol{\theta}}-\boldsymbol{\theta}_0\end{pmatrix}$ converges to a multivariate normal with mean $\mathbf{0}$ and variance-covariance matrix

$$\begin{pmatrix}\mathbf{I}_{\boldsymbol{\alpha\alpha}} & 0 & 0\\ 0 & \mathbf{I}_{\boldsymbol{\beta\beta}} & 0\\ \mathbf{I}_{\boldsymbol{\theta\alpha}} & \mathbf{I}_{\boldsymbol{\theta\beta}} & \mathbf{I}_{\boldsymbol{\theta\theta}}\end{pmatrix}^{-1}\begin{pmatrix}\mathbf{I}_{\boldsymbol{\alpha\alpha}} & \mathbf{I}_{\boldsymbol{\alpha\beta}} & 0\\ \mathbf{I}_{\boldsymbol{\beta\alpha}} & \mathbf{V} & 0\\ 0 & 0 & \mathbf{I}_{\boldsymbol{\theta\theta}}\end{pmatrix}\begin{pmatrix}\mathbf{I}_{\boldsymbol{\alpha\alpha}} & 0 & 0\\ 0 & \mathbf{I}_{\boldsymbol{\beta\beta}} & 0\\ \mathbf{I}_{\boldsymbol{\theta\alpha}} & \mathbf{I}_{\boldsymbol{\theta\beta}} & \mathbf{I}_{\boldsymbol{\theta\theta}}\end{pmatrix}^{-1^T}$$

$$=\begin{pmatrix}\mathbf{I}_{\boldsymbol{\alpha\alpha}} & \mathbf{I}^{-1}_{\boldsymbol{\alpha\alpha}}\mathbf{I}_{\boldsymbol{\alpha\beta}}\mathbf{I}^{-1}_{\boldsymbol{\beta\beta}} & \mathbf{I}^{-1}_{\boldsymbol{\alpha\alpha}}(\mathbf{I}_{\boldsymbol{\alpha\alpha}}a_1^T+\mathbf{I}_{\boldsymbol{\alpha\beta}}a_2^T)\\ \mathbf{I}^{-1}_{\boldsymbol{\beta\beta}}\mathbf{I}_{\boldsymbol{\beta\alpha}}\mathbf{I}^{-1}_{\boldsymbol{\alpha\alpha}} & \mathbf{I}^{-1}_{\boldsymbol{\beta\beta}}\mathbf{V}\mathbf{I}^{-1}_{\boldsymbol{\beta\beta}} & \mathbf{I}^{-1}_{\boldsymbol{\beta\beta}}(\mathbf{I}_{\boldsymbol{\beta\alpha}}a_1^T+\mathbf{V}a_2^T)\\ (a_1\mathbf{I}_{\boldsymbol{\alpha\alpha}}+a_2\mathbf{I}_{\boldsymbol{\beta\alpha}})\mathbf{I}^{-1}_{\boldsymbol{\alpha\alpha}} & (a_1\mathbf{I}_{\boldsymbol{\alpha\beta}}+a_2\mathbf{V})\mathbf{I}^{-1}_{\boldsymbol{\beta\beta}} & (a_1\mathbf{I}_{\boldsymbol{\alpha\alpha}}+a_2\mathbf{I}_{\boldsymbol{\beta\alpha}})a_1^T+(a_1\mathbf{I}_{\boldsymbol{\alpha\beta}}+a_2\mathbf{V})a_2^T+\mathbf{I}^{-1}_{\boldsymbol{\theta\theta}}\end{pmatrix}$$

where $a_1=-\mathbf{I}_{\boldsymbol{\theta\theta}}\mathbf{I}_{\boldsymbol{\theta\alpha}}\mathbf{I}^{-1}_{\boldsymbol{\alpha\alpha}}$ and $a_2=-\mathbf{I}^{-1}_{\boldsymbol{\theta\theta}}\mathbf{I}_{\boldsymbol{\theta\beta}}\mathbf{I}^{-1}_{\boldsymbol{\beta\beta}}$.

The lower-right element of the covariance matrix is the asymptotic variance of $\sqrt{N}(\hat{\boldsymbol{\theta}}-\boldsymbol{\theta}_0)$ and is given by

$$\mathbf{I}^{-1}_{\boldsymbol{\theta\theta}}(\mathbf{I}_{\boldsymbol{\theta\alpha}}\mathbf{I}^{-1}_{\boldsymbol{\alpha\alpha}}\mathbf{I}_{\boldsymbol{\alpha\theta}}+\mathbf{I}_{\boldsymbol{\theta\beta}}\mathbf{I}^{-1}_{\boldsymbol{\beta\beta}}\mathbf{V}\mathbf{I}^{-1}_{\boldsymbol{\beta\beta}}\mathbf{I}_{\boldsymbol{\beta\theta}}+\mathbf{I}_{\boldsymbol{\theta\beta}}\mathbf{I}^{-1}_{\boldsymbol{\beta\beta}}\mathbf{I}_{\boldsymbol{\beta\alpha}}\mathbf{I}^{-1}_{\boldsymbol{\alpha\alpha}}\mathbf{I}_{\boldsymbol{\alpha\theta}}+\mathbf{I}_{\boldsymbol{\theta\alpha}}\mathbf{I}^{-1}_{\boldsymbol{\alpha\alpha}}\mathbf{I}_{\boldsymbol{\alpha\beta}}\mathbf{I}^{-1}_{\boldsymbol{\beta\beta}}\mathbf{I}_{\boldsymbol{\beta\theta}})\mathbf{I}^{-1}_{\boldsymbol{\theta\theta}}+\mathbf{I}^{-1}_{\boldsymbol{\theta\theta}}$$

## A.2 Derivation under alternative copulas

### A.2.1 Bivariate Student's t copula

Suppose that the joint distribution $F_{T_\tau,Z_\tau}$ is defined by a bivariate Student's t copula as

$$F_{T_\tau,Z_\tau}(r,z) = \boldsymbol{t}_{\nu,\rho}(t_\nu^{-1}(F_{T_\tau}(r)), t_\nu^{-1}(F_{Z_\tau}(z)); \rho_\tau)$$

where $t_\nu$ is a univariate t distribution with $\nu$ degrees of freedom and $\boldsymbol{t}_\nu(\cdot,\rho)$ is the multivariate Student's t distribution with correlation $\rho$ and $\nu$ degrees of freedom, where $\nu$ is fixed and not estimated.

The joint density is then given by

$$\begin{aligned} f_{T_\tau,Z_\tau}(r,z) &= \Pr(T_\tau = r, Z_\tau = z) = \frac{\partial^2}{\partial r \partial z} F_{T_\tau,Z_\tau}(r,z) \\ &= f_{T_\tau}(r) f_{Z_\tau}(z) \frac{\Gamma(\frac{\nu+2}{2})/\Gamma(\frac{\nu}{2})}{\nu\pi dt(x_1(r),\nu) dt(x_2(z),\nu)\sqrt{1-\rho_\tau^2}} \left\{ 1 + \frac{x_1(r)^2 + x_2(z)^2 - 2\rho_\tau x_1(r) x_2(z)}{\nu(1-\rho_\tau^2)} \right\}^{-\frac{\nu+1}{2}} \end{aligned}$$

where $x_1(r) = t_\nu^{-1}(F_{T_\tau}(r))$ and $x_2(z) = t_\nu^{-1}(F_{Z_\tau}(z))$, and $dt(\cdot,\nu)$ and $t_\nu^{-1}(\cdot)$ are the probability density function and quantile functions, respectively, for the standard univariate Student's t-distribution with $\nu$ degrees of freedom, expectation 0, and variance $\nu/(\nu-2)$.

For individuals who are alive at time $\tau$, but are censored at time $t$, the joint density is given by

$$\begin{aligned} \Pr(T_\tau > r, Z_\tau = z) &= \frac{\partial}{\partial z}[F_{Z_\tau}(z) - F_{T_\tau,Z_\tau}(r,z)] \\ &= f_{Z_\tau}(z) - t_{\nu+1}\left\{ \frac{x_1(r) - \rho x_2(z)}{\sqrt{\frac{(\nu + x_2(z)^2)(1-\rho^2)}{\nu+1}}} \right\} f_{Z_\tau}(z) \\ &= t_{\nu+1}\left\{ -\frac{x_1(r) - \rho x_2(z)}{\sqrt{\frac{(\nu + x_2(z)^2)(1-\rho^2)}{\nu+1}}} \right\} f_{Z_\tau}(z) \end{aligned}$$

We can obtain the dynamic prediction of interest as,

$$\begin{aligned}\Pr(T \geq \tau + s | T \geq \tau, Z(\tau) = z; \hat{\boldsymbol{\theta}}) &= \frac{\Pr(T_\tau > \tau + s, Z_\tau = z; \hat{\boldsymbol{\theta}})}{f_{Z_\tau}(z; \hat{\boldsymbol{\theta}})} \\ &= t_{\hat{\nu}+1}\left\{ -\frac{\hat{x}_1(r) - \hat{\rho}_\tau \hat{x}_2(z)}{\sqrt{\frac{(\hat{\nu} + \hat{x}_2(z)^2)(1-\hat{\rho}_\tau^2)}{\hat{\nu}+1}}} \right\}\end{aligned}$$

where $\hat{x}_1(\tau + s) = t_{\hat{\nu}}^{-1}(F_{T_\tau}(\tau + s; \hat{\boldsymbol{\theta}}))$, $\hat{x}_2(z) = t_{\hat{\nu}}^{-1}(F_{Z_\tau}(z; \hat{\boldsymbol{\theta}}))$, and $\hat{\rho}_\tau = \rho(\tau; \hat{\boldsymbol{\theta}})$.

### A.2.2 Bivariate Clayton's copula

The Clayton copula is lower-tail dependent, but not upper. Suppose that the joint distribution $F_{T_\tau, Z_\tau}$ is defined by a bivariate Clayton copula as

$$F_{T_\tau, Z_\tau}(t, z) = \left(F_{T_\tau}(t)^{-\theta} + F_{Z_\tau}(z)^{-\theta} - 1\right)^{-\frac{1}{\theta}} = A(F_{T_\tau}(t), F_{Z_\tau}(z), \theta)^{-\frac{1}{\theta}}$$

where $A(u_1, u_2, \theta) = u_1^{-\theta} + u_2^{-\theta} - 1$.

The joint density is then given by

$$\begin{aligned}f_{T_\tau, Z_\tau}(t, z) = \Pr(T_\tau = t, Z_\tau = z) &= \frac{\partial^2}{\partial t \partial z} F_{T_\tau, Z_\tau}(t, z) \\ &= f_{T_\tau}(t) f_{Z_\tau}(z) \frac{(1+\theta)(F_{T_\tau}(t) \cdot F_{Z_\tau}(z))^{-1-\theta}}{A(F_{T_\tau}(t), F_{Z_\tau}(z), \theta)^{\frac{1}{\theta}+2}}\end{aligned}$$

where $0 < \theta < \infty$ controls the degree of dependence.

For individuals who are alive at time $\tau$, but are censored at time $t$, the joint density is given by

$$\begin{aligned}\Pr(T_\tau > r, Z_\tau = z) &= \frac{\partial}{\partial z}[F_{Z_\tau}(z) - F_{T_\tau, Z_\tau}(r, z)] \\ &= f_{Z_\tau}(z) - \left[F_{Z_\tau}(z)^{-\theta-1} \cdot A(F_{T_\tau}(t), F_{Z_\tau}(z), \theta)^{-1-\frac{1}{\theta}}\right] f_{Z_\tau}(z) \\ &= f_{Z_\tau}(z)\left[1 - F_{Z_\tau}(z)^{-\theta-1} \cdot A(F_{T_\tau}(t), F_{Z_\tau}(z), \theta)^{-1-\frac{1}{\theta}}\right]\end{aligned}$$

We obtain the dynamic prediction of interest as,

$$\begin{aligned}\Pr(T \geq \tau + s | T \geq \tau, Z(\tau) = z; \hat{\boldsymbol{\theta}}) &= \frac{\Pr(T_\tau > \tau + s, Z_\tau = z; \hat{\boldsymbol{\theta}})}{f_{Z_\tau}(z; \hat{\boldsymbol{\theta}})} \\ &= 1 - F_{Z_\tau}(z; \hat{\boldsymbol{\theta}})^{-\hat{\theta}-1} \cdot A(F_{T_\tau}(t; \hat{\boldsymbol{\theta}}), F_{Z_\tau}(z; \hat{\boldsymbol{\theta}}), \hat{\theta})^{-1-\frac{1}{\hat{\theta}}}\end{aligned}$$

### A.2.3 Bivariate Gumbel copula

The Gumbel copula is upper-tail dependent, but not lower. The Gumbel copula is also an asymmetric copula, but it exhibits greater dependence in the positive tail than the negative. Suppose that the joint distribution $F_{T_\tau, Z_\tau}$ is defined by a bivariate Gumbel copula as

$$F_{T_\tau, Z_\tau}(t, z) = \exp\left[-\{(-\log(F_{T_\tau}(t)))^\theta + (-\log(F_{Z_\tau}(z)))^\theta\}\right] = \exp[-(x_1(t) + x_2(z))^{\frac{1}{\theta}}]$$

where $x_1(t) = (-\log(F_{T_\tau}(t)))^\theta$, $x_2(z) = (-\log(F_{Z_\tau}(z)))^\theta$, and $\theta \geq 1$. The joint density is then given by

$$\begin{aligned}f_{T_\tau, Z_\tau}(t, z) =& \Pr(T_\tau = t, Z_\tau = z) = \frac{\partial^2}{\partial t \partial z} F_{T_\tau, Z_\tau}(t, z) \\ =& f_{T_\tau}(t) f_{Z_\tau}(z) F_{T_\tau, Z_\tau}(t, z; \theta) \frac{1}{F_{T_\tau}(t) F_{Z_\tau}(z)} (x_1(t) + x_2(z))^{-2+\frac{2}{\theta}} \\ & \cdot \left[(\log(F_{T_\tau}(t)) \log(F_{Z_\tau}(z)))^{\theta-1} \{1 + (\theta - 1)(x_1(t) + x_2(z))^{-\frac{1}{\theta}}\}\right]\end{aligned}$$

For individuals who are alive at time $\tau$, but are censored at time $t$, the joint density is

$$\begin{aligned}\Pr(T_\tau > r, Z_\tau = z) &= \frac{\partial}{\partial z}[F_{Z_\tau}(z) - F_{T_\tau, Z_\tau}(r, z)] \\ &= f_{Z_\tau}(z) - \left[-\frac{\exp\{-(x_1(t) + x_2(z))^{\frac{1}{\theta}}\}(x_1(t) + x_2(z))^{\frac{1}{\theta}-1} x_2(z)}{F_{Z_\tau}(z) \log(F_{Z_\tau}(z))}\right] f_{Z_\tau}(z) \\ &= f_{Z_\tau}(z) \left[1 + \frac{\exp\{-(x_1(t) + x_2(z))^{\frac{1}{\theta}}\}(x_1(t) + x_2(z))^{\frac{1}{\theta}-1} x_2(z)}{F_{Z_\tau}(z) \log(F_{Z_\tau}(z))}\right]\end{aligned}$$

We obtain the dynamic prediction of interest as,

$$\Pr(T \geq \tau + s | T \geq \tau, Z(\tau) = z; \hat{\boldsymbol{\theta}}) = \frac{\Pr(T_\tau > \tau + s, Z_\tau = z; \hat{\boldsymbol{\theta}})}{f_{Z_\tau}(z; \hat{\boldsymbol{\theta}})}$$
$$= 1 + \frac{\exp\{-(x_1(t; \hat{\boldsymbol{\theta}}) + x_2(z; \hat{\boldsymbol{\theta}}))^{\frac{1}{\delta}}\}(x_1(t; \hat{\boldsymbol{\theta}}) + x_2(z; \hat{\boldsymbol{\theta}}))^{\frac{1}{\delta}-1} x_2(z; \hat{\boldsymbol{\theta}})}{F_{Z_\tau}(z; \hat{\boldsymbol{\theta}}) \log(F_{Z_\tau}(z; \hat{\boldsymbol{\theta}}))}$$

## A.3 Sample of Results from Simulations

Here, we present sample results from the simulation settings used for evaluating the performance of the copula method.

### A.3.1 Continuous marker setting

#### A.3.1.1 Data Summary

**Table A.1:** Proportion of patients ($n = 1000$) with particular number of inspection times within 15 years for the continuous marker simulation setting.

| No. insp times | 1 | 2 | 3 | 4 | 5 | 6 | 7 | 8 | 9 | 10 | 11 | 12 | 13 | ≥14 |
|---|---|---|---|---|---|---|---|---|---|---|---|---|---|---|
| Insp rate 0.5 | 21% | 20% | 21% | 13% | 9% | 5% | 3% | 3% | 2% | 1% | 0.2% | 0.6% | 0.2% | 0% |
| Insp rate 1 | 10% | 10% | 12% | 12% | 11% | 10% | 9% | 6% | 5% | 3% | 3% | 1% | 3% | 6% |
| Every 1 year | 6% | 10% | 19% | 19% | 10% | 9% | 7% | 5% | 4% | 2% | 2% | 2% | 3% | 2% |

#### A.3.1.2 Modeling Failure Time data

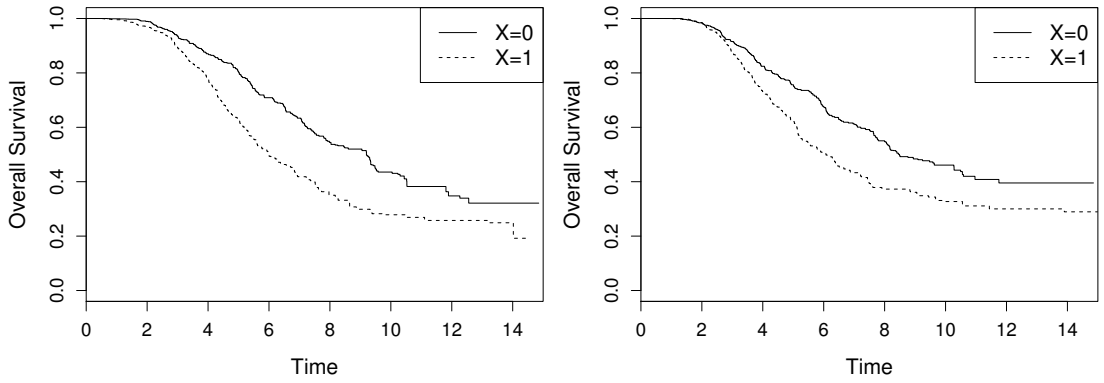


Association ($\phi$): 0.5 Association ($\phi$): 1.5

**Figure A.1:** Overall Kaplan-Meier curves by baseline covariate $X$ for the continuous marker simulation setting.

**Testing proportional hazards assumption:** From the Schoenfeld residuals we find that there is no significant evidence against the assumption of proportional hazards for the baseline covariate $X$ (p=0.89) (Figure A.2).

**Checking influential observations:** We check for outliers by examining the deviance residuals (normalized transform of martingale residuals) and find that they are symmetrically distributed about 0 (Figure A.2).

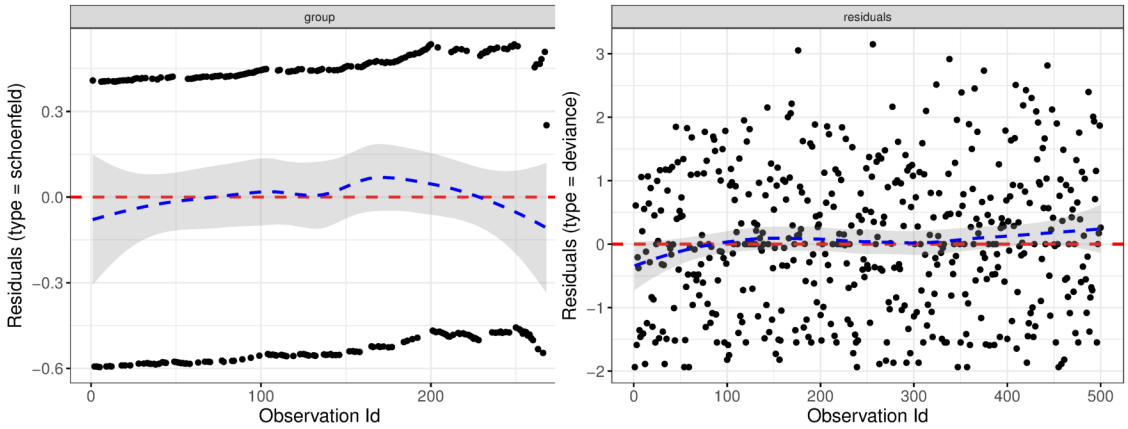


Schoenfeld Residuals Deviance Residuals

**Figure A.2:** Cox model diagnostics for the continuous marker simulation setting.

### A.3.1.3 Modeling Continuous marker data

To identify the functional form for the mean and variance of the model for the marker process, we fit a loess curve to the longitudinal measurements as shown in Figure A.3. The relationship appears to be quadratic with respect to time, thus we consider high order terms for landmark time in the model. Also, there appears to be an interaction effect between time and the baseline covariate. In Figure A.4, we plot the absolute residuals for the marker measurement and loess curve to identify the functional form of the standard deviation in the model. Fitting a loess curve to these residuals, we see an increasing, and possibly quadratic relationship. There does not appear to be an interaction effect between the baseline covariate and time.

### A.3.1.4 Evaluating predictions

We choose a simple form for the association function since more flexible forms did not result in improved predictive performance. Figure A.5 depicts the predicted vs. actual

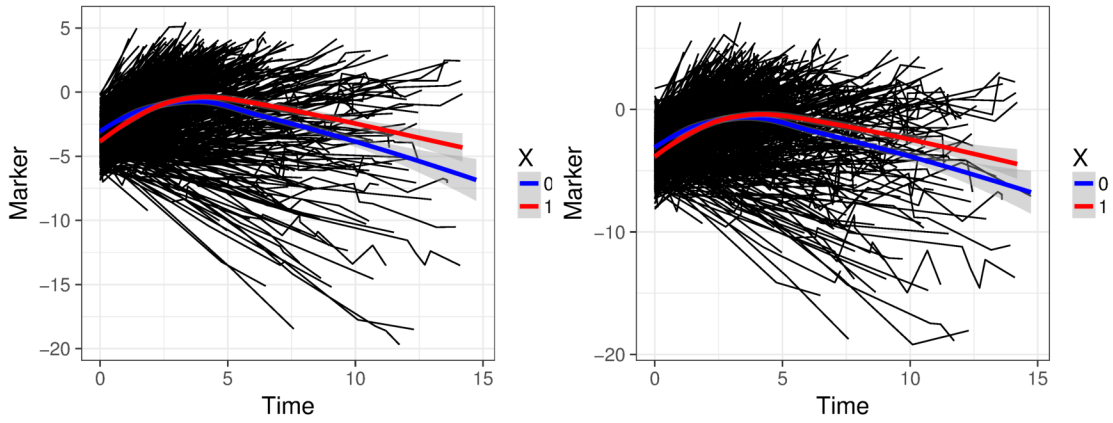


Measurement error ($\sigma_\epsilon$): 0.6 Measurement error ($\sigma_\epsilon$): 1.2

**Figure A.3:** Marker trajectories for 1000 individuals with loess curves by baseline covariate $X$ for continuous marker simulation setting.

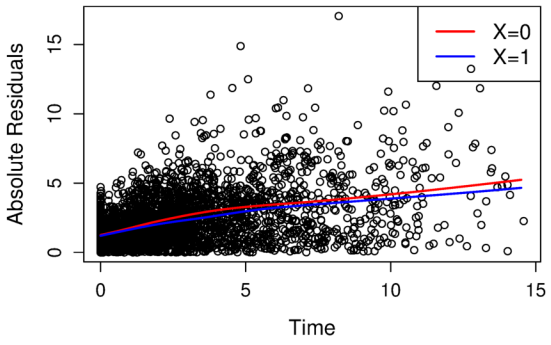


**Figure A.4:** Absolute residuals of marker measurements and predicted mean loess curve for continuous marker simulation setting. Blue and red curves are loess lines fit to absolute residuals by baseline covariate $X$.

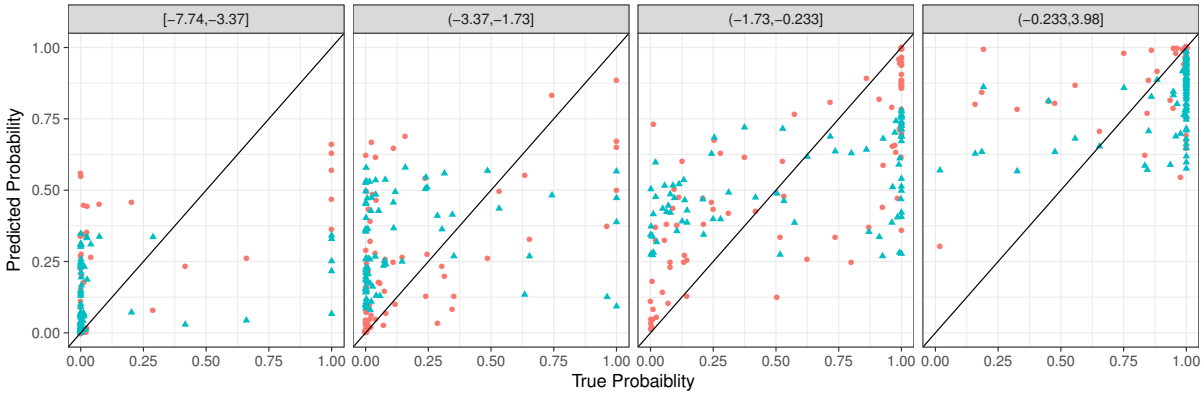


**Figure A.5:** Predicted vs. actual probabilities for patients in the validation data set alive at time 3 by quantiles of the marker measurement at time 3 for continuous marker simulation setting. Red circles indicate predictions produced by the joint model and blue triangles indicate predictions from the copula model.

probabilities of death for patients in the validation data set at landmark time 3. We see overlap between the predictions from both of these models.

### A.3.2 Binary marker setting: Markov

#### A.3.2.1 Data Summary

**Table A.2:** Proportion of patients ($n = 1000$) with particular number of inspection times within 15 years for binary marker Markov simulation setting with one baseline covariate.

| No. insp times | 1 | 2 | 3 | 4 | 5 | 6 | 7 | 8 | 9 | 10 | 11 | 12 | 13 | ≥14 |
|---|---|---|---|---|---|---|---|---|---|---|---|---|---|---|
| Insp rate 0.5 | 26% | 21% | 15% | 11% | 10% | 6% | 4% | 3% | 2% | 1% | 1% | 0% | 0.1% | 0.1% |
| Insp rate 1 | 14% | 14% | 11% | 9% | 9% | 9% | 5% | 7% | 5% | 4% | 3% | 2% | 2% | 6% |

#### A.3.2.2 Modeling Failure Time data

**Testing proportional hazards assumption:** We test the proportional hazards assumption using the Schoenfeld residuals and find that there is no significant evidence against the assumption (p=0.78) (Figure A.7).

**Checking influential observations:** We check for outliers by examining the deviance residuals (normalized transform of martingale residuals) and find that they are symmetrically distributed about 0 (Figure A.7).

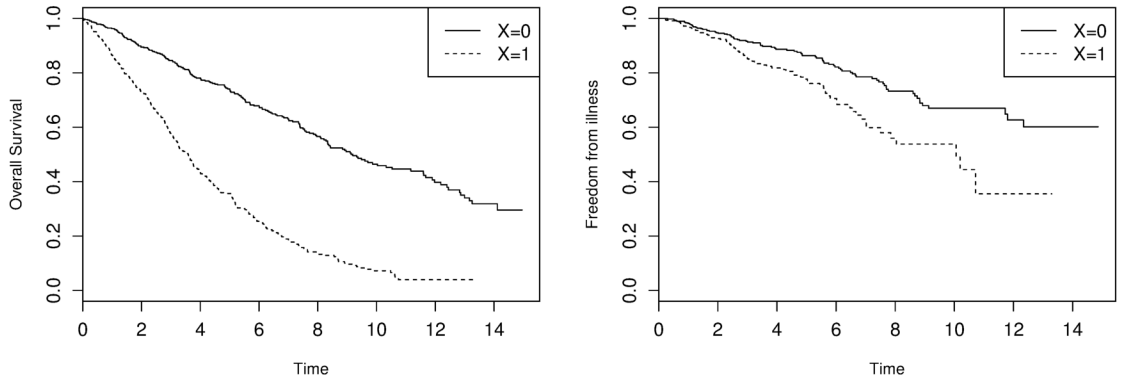


**Figure A.6:** Overall survival (left) and Freedom from illness (right) curves by baseline covariate for binary marker Markov simulation setting with one baseline covariate.

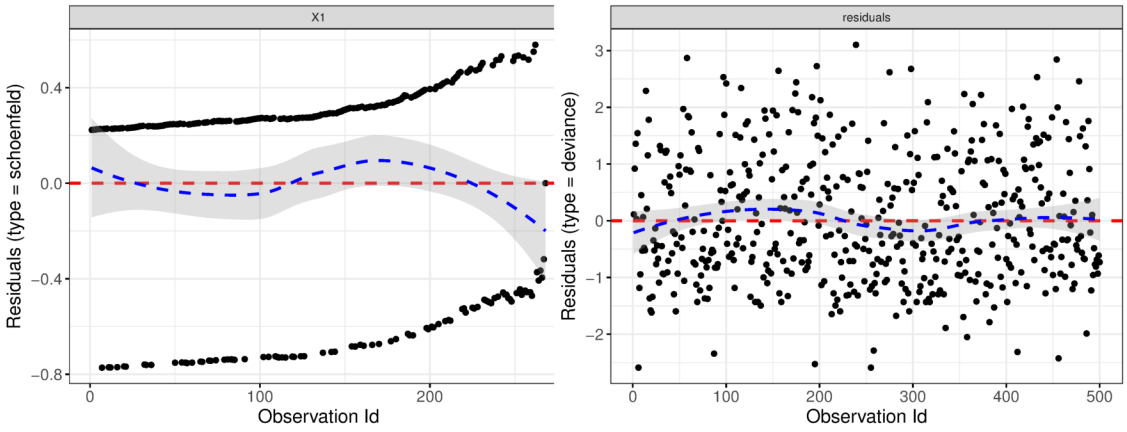


Schoenfeld Residuals Deviance Residuals

**Figure A.7:** Cox model diagnostics for the binary marker Markov simulation setting with one baseline covariate.

#### A.3.2.3 Modeling Binary marker data

We examine the Pearson residuals from the probit model (BC1) fit to the marker data. We see that there is deviation from zero at later landmark times (Figure A.8).

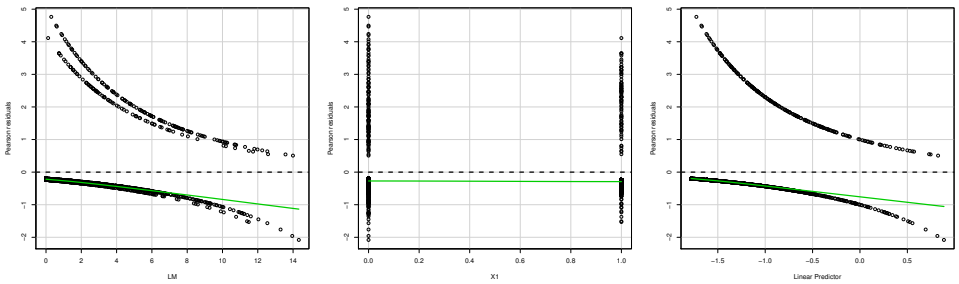


**Figure A.8:** Pearson residuals for probit model (BC1) by landmark time (LM), baseline covariate $X$, and the linear predictor for the binary marker Markov simulation setting with one baseline covariate.

#### A.3.2.4 Evaluating predictions

We compare the predicted vs. actual probabilities for the joint, landmark, and copula models. The predictions for the MM, LMInt3, and BC1 models are similar. However, the predicted probabilities of the LM3 model (landmark model without the interaction) does not have a high enough prediction for those with $X = 1$ and $Z = 1$ (Figure A.9).

### A.3.3 Binary marker setting: Semi-Markov

#### A.3.3.1 Data summary

**Table A.3:** Proportion of patients ($n = 1000$) with particular number of inspection times within 15 years for the binary marker semi-Markov simulation setting with one baseline covariate.

| No. insp times | 1 | 2 | 3 | 4 | 5 | 6 | 7 | 8 | 9 | 10 | 11 | 12 | 13 | ≥14 |
|---|---|---|---|---|---|---|---|---|---|---|---|---|---|---|
| Insp rate 0.5 | 27% | 20% | 14% | 13% | 10% | 6% | 4% | 2% | 1% | 1% | 1% | 1% | 0.3% | 0.4% |
| Insp rate 1 | 14% | 14% | 12% | 10% | 9% | 6% | 7% | 6% | 5% | 4% | 3% | 3% | 2% | 7% |

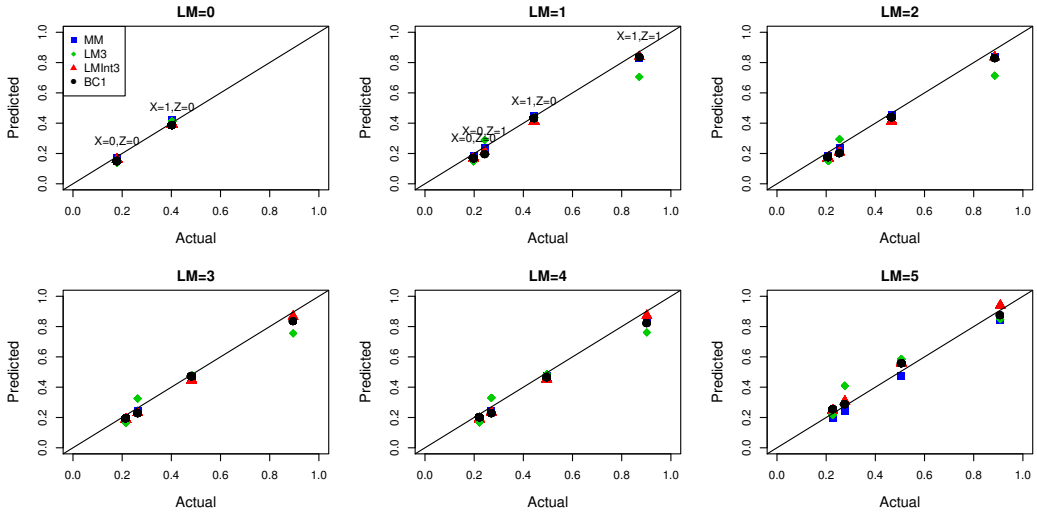


**Figure A.9:** Predicted vs. actual probabilities by landmark time for the binary marker Markov simulation setting with one baseline covariate.

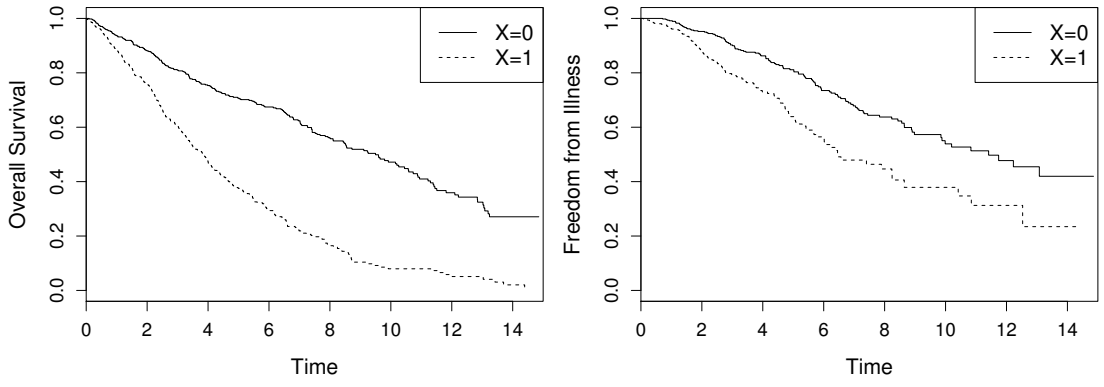


**Figure A.10:** Overall survival (left) and Freedom from illness (right) curves by baseline covariate for the binary marker semi-Markov simulation setting with one baseline covariate.

### A.3.3.2 Modeling Failure Time data

**Testing proportional hazards assumption:** We test the proportional hazards assumption and find that there is possible evidence against the assumption for the baseline covariate $X_1$ (p=0.07). However, looking at the log(-log(Survival)) vs. log(time) we see that the curves are parallel and thus no evidence against the proportional hazards assumption (Figure A.11).

**Checking influential observations:** We check for outliers and find that they are symmetrically distributed about zero (Figure A.11).

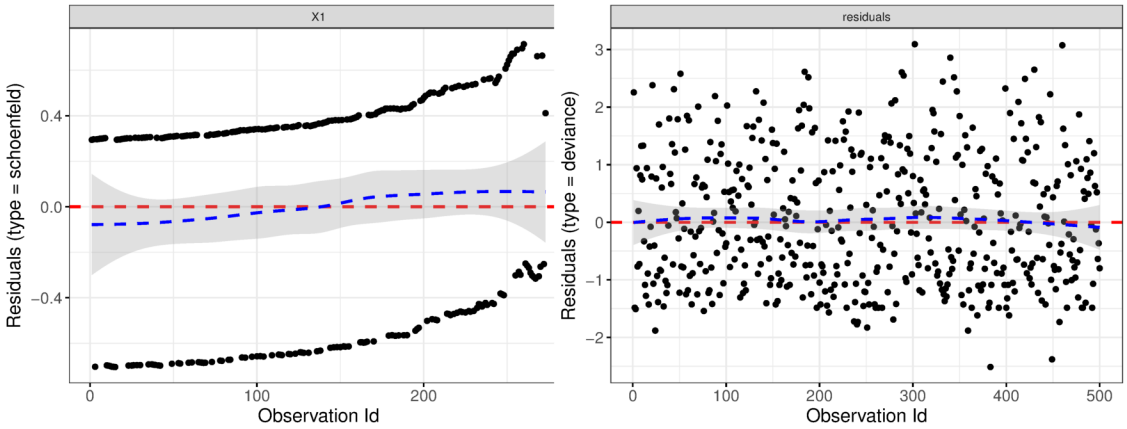


Schoenfeld Residuals | Deviance Residuals

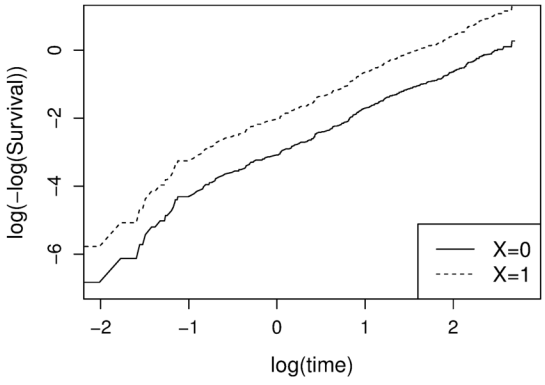


Log(-Log(Survival)) vs. Log(Time)

**Figure A.11:** Cox model diagnostics for the binary marker semi-Markov simulation setting with one baseline covariate.

### A.3.3.3 Modeling Binary marker data

We examine the Pearson residuals from the probit model (BC1) and find that there is deviation from zero at later landmark times (Figure A.12).

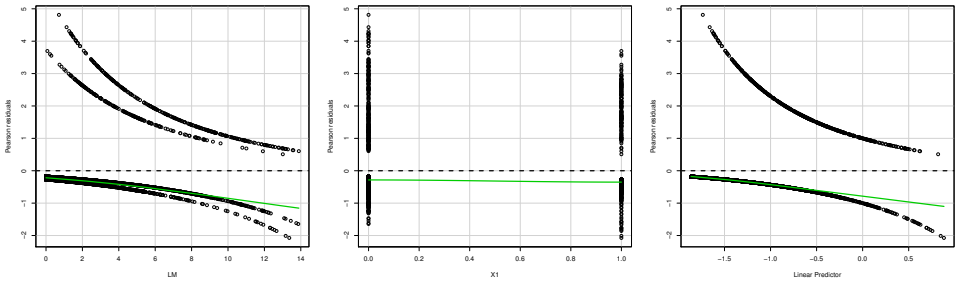


**Figure A.12:** Pearson residuals for probit model (BC1) by landmark time (LM), baseline covariates $X_1$, $X_2$, and the linear predictor for the binary marker semi-Markov simulation setting with one baseline covariate.

### A.3.3.4 Evaluating predictions

We compare the predicted vs. actual probabilities for the joint, landmark, and copula models. The predictions for the landmark model without an interaction (LM3) deviate from the true probabilities for those with $X_1 = 1$ and $Z = 1$ (Figure A.13).

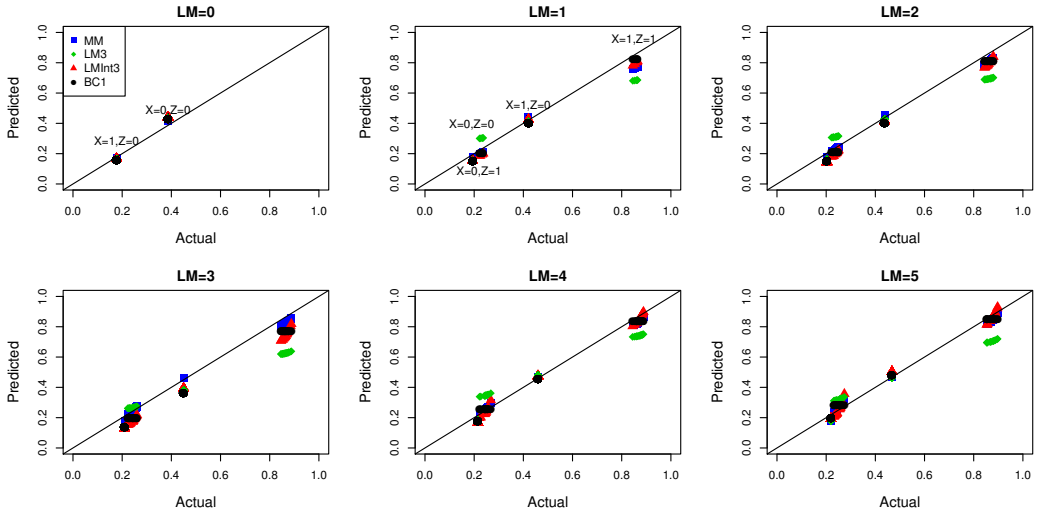


**Figure A.13:** Predicted vs. actual probabilities by landmark time for the binary marker semi-Markov simulation setting with one baseline covariate.

### A.3.4 Binary marker setting: Two baseline covariates

#### A.3.4.1 Data summary

**Table A.4:** Proportion of patients ($n = 1000$) with particular number of inspection times within 15 years for the binary marker Markov simulation setting with two baseline covariates.

| No. insp times | 1 | 2 | 3 | 4 | 5 | 6 | 7 | 8 | 9 | 10 | 11 | 12 | 13 | ≥14 |
|---|---|---|---|---|---|---|---|---|---|---|---|---|---|---|
| Insp rate 0.5 | 27% | 21% | 17% | 11% | 8% | 6% | 4% | 2% | 1% | 1% | 0.5% | 0.6% | 0.1% | 0% |
| Insp rate 1 | 15% | 12% | 12% | 11% | 11% | 8% | 6% | 6% | 4% | 4% | 3% | 2% | 1% | 5% |

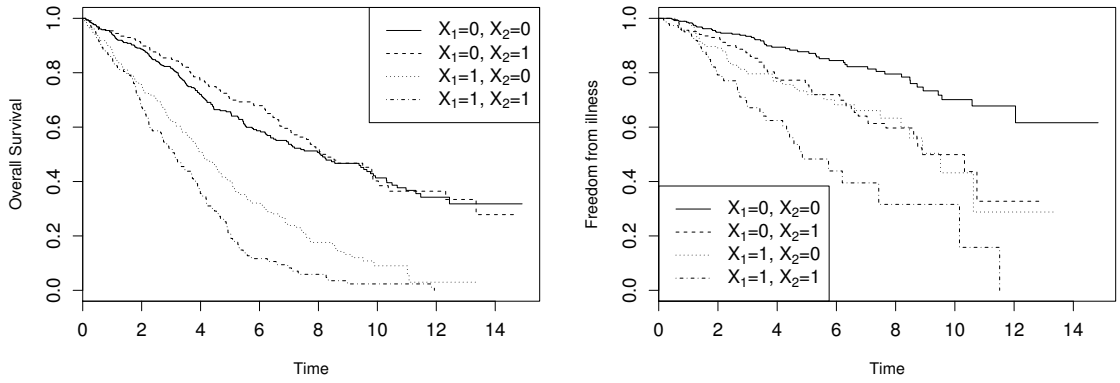


**Figure A.14:** Overall survival (left) and Freedom from illness (right) curves by baseline covariates for the binary marker Markov simulation setting with two baseline covariates.

#### A.3.4.2 Modeling Failure Time data

**Testing proportional hazards assumption:** We test the proportional hazards assumption and find that there is no significant evidence against the assumption for the baseline covariates $X_1$ (p=0.33) and $X_2$ (p=0.15) (Figure A.15).

**Checking influential observations:** We check for outliers and find that they are symmetrically distributed about zero (Figure A.16).

#### A.3.4.3 Modeling Binary marker data

We examine the Pearson residuals from the probit model (BC1) and find that there is deviation from zero at later landmark times (Figure A.17).

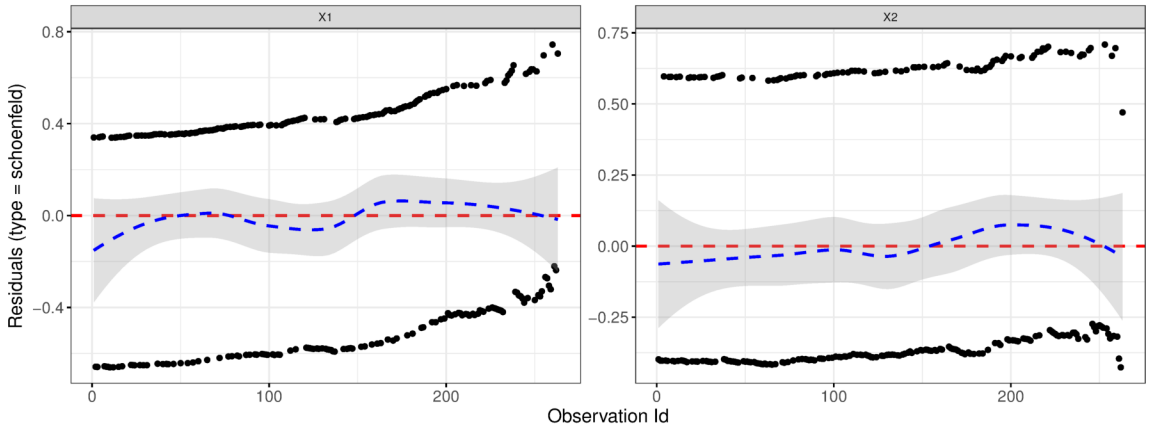


**Figure A.15:** Cox model Schoenfeld residuals for the binary marker Markov simulation setting with two baseline covariates.

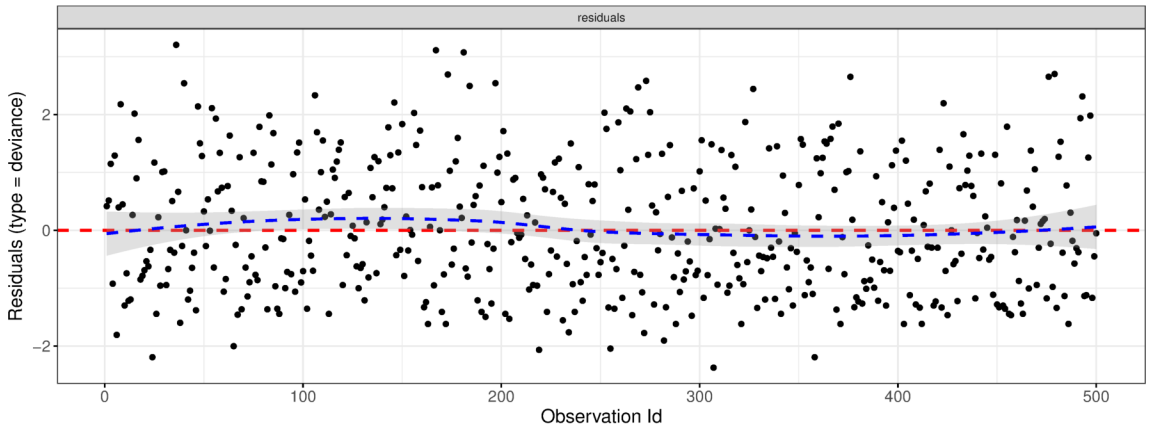


**Figure A.16:** Cox model deviance residuals for the binary marker Markov simulation setting with two baseline covariates.

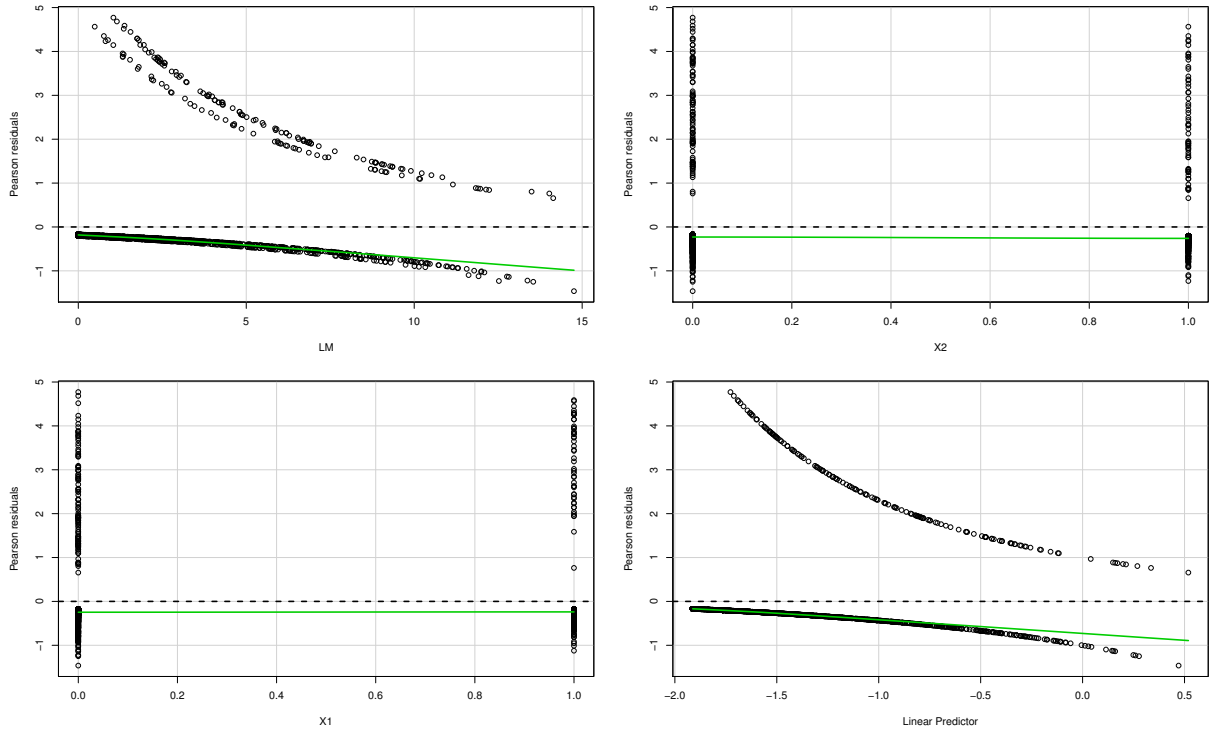


**Figure A.17:** Pearson residuals for probit model (BC1) by landmark time (LM), baseline covariates $X_1$, $X_2$, and the linear predictor for the binary marker Markov simulation setting with two baseline covariates.

### A.3.4.4 Evaluating predictions

We compare the predicted vs. actual probabilities for the joint, landmark, and copula models. The predictions for the landmark model without an interaction (LM3) deviate from the true probabilities for those with $X_1 = 1$ and the intermediate event ($Z = 1$) (Figure A.13).

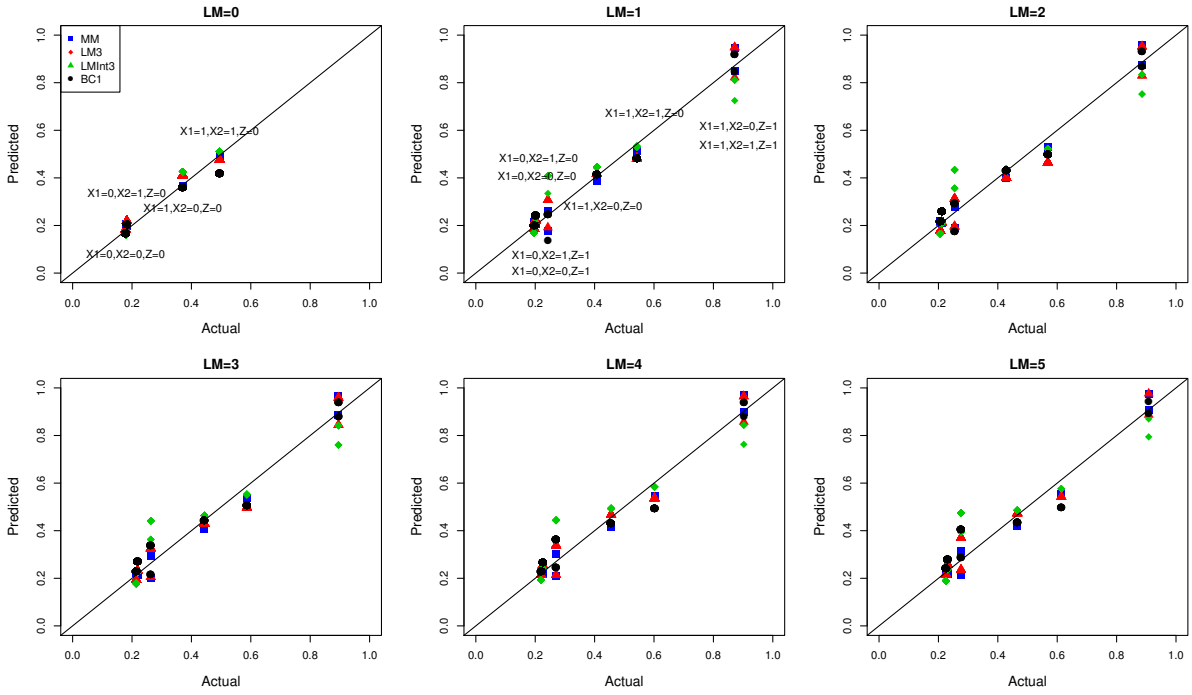


**Figure A.18:** Predicted vs. actual probabilities by landmark time for the binary marker Markov simulation setting with two baseline covariates.

## A.4 Continuous marker simulation results

**Table A.5:** Summary of scenarios for continuous marker process simulations.

| Scenario | $\sigma_\epsilon$ | $\phi$ | Inter-inspection rate |
|---|---|---|---|
| 1a | 0.6 | 1.5 | 0.5 |
| 1b | 0.6 | 1.5 | 1 |
| 1c | 0.6 | 1.5 | Fixed time |
| 2a | 0.6 | 0.5 | 0.5 |
| 2b | 0.6 | 0.5 | 1 |
| 2c | 0.6 | 0.5 | Fixed time |
| 3a | 1.2 | 1.5 | 0.5 |
| 3b | 1.2 | 1.5 | 1 |
| 3c | 1.2 | 1.5 | Fixed time |
| 4a | 1.2 | 0.5 | 0.5 |
| 4b | 1.2 | 0.5 | 1 |
| 4c | 1.2 | 0.5 | Fixed time |

### A.4.1 Continuous marker: Simulation 1a

- Inter-inspection rate: 0.5; Measurement error ($\sigma_\epsilon$): 0.6; Association ($\phi$): 1.5

**Table A.6:** Simulation results for continuous marker Scenario 1a.

**(a)** Mean (and standard deviation) of the root mean squared prediction error in 500 simulations for continuous marker Scenario 1a.

| | $\tau$ | JM | JM2 | LM1 | LMInt1 | LM2 | LMInt2 | CC1 | CW1 | CC2 | CW2 | CC3 | CW3 |
|---|---|---|---|---|---|---|---|---|---|---|---|---|---|
| $X=0$ | 0 | 0.269 (0.019) | 0.270 (0.020) | 0.269 (0.018) | 0.269 (0.018) | 0.324 (0.018) | 0.328 (0.020) | 0.268 (0.020) | 0.268 (0.020) | 0.268 (0.019) | 0.268 (0.019) | 0.271 (0.021) | 0.271 (0.021) |
| | 1 | 0.335 (0.017) | 0.343 (0.020) | 0.344 (0.019) | 0.343 (0.018) | 0.353 (0.015) | 0.354 (0.016) | 0.338 (0.018) | 0.356 (0.018) | 0.341 (0.018) | 0.358 (0.017) | 0.341 (0.019) | 0.360 (0.019) |
| | 2 | 0.324 (0.020) | 0.335 (0.022) | 0.358 (0.015) | 0.358 (0.016) | 0.361 (0.014) | 0.362 (0.014) | 0.335 (0.018) | 0.375 (0.021) | 0.342 (0.018) | 0.379 (0.022) | 0.337 (0.019) | 0.378 (0.022) |
| | 3 | 0.293 (0.024) | 0.299 (0.026) | 0.346 (0.016) | 0.346 (0.015) | 0.351 (0.015) | 0.352 (0.015) | 0.320 (0.017) | 0.359 (0.021) | 0.326 (0.018) | 0.364 (0.022) | 0.321 (0.018) | 0.362 (0.022) |
| | 4 | 0.262 (0.029) | 0.260 (0.030) | 0.322 (0.016) | 0.320 (0.018) | 0.336 (0.015) | 0.336 (0.015) | 0.308 (0.018) | 0.324 (0.024) | 0.312 (0.020) | 0.328 (0.026) | 0.310 (0.019) | 0.326 (0.025) |
| | 5 | 0.235 (0.034) | 0.228 (0.034) | 0.291 (0.017) | 0.288 (0.016) | 0.324 (0.017) | 0.324 (0.017) | 0.299 (0.019) | 0.287 (0.025) | 0.300 (0.022) | 0.288 (0.027) | 0.300 (0.020) | 0.288 (0.026) |
| $X=1$ | 0 | 0.311 (0.018) | 0.331 (0.022) | 0.312 (0.018) | 0.311 (0.019) | 0.327 (0.017) | 0.326 (0.017) | 0.311 (0.022) | 0.310 (0.027) | 0.310 (0.025) | 0.309 (0.030) | 0.313 (0.024) | 0.313 (0.029) |
| | 1 | 0.362 (0.018) | 0.402 (0.022) | 0.376 (0.019) | 0.375 (0.018) | 0.381 (0.018) | 0.382 (0.019) | 0.365 (0.024) | 0.385 (0.029) | 0.368 (0.027) | 0.387 (0.032) | 0.368 (0.025) | 0.388 (0.031) |
| | 2 | 0.334 (0.021) | 0.379 (0.023) | 0.386 (0.024) | 0.385 (0.025) | 0.392 (0.025) | 0.393 (0.023) | 0.346 (0.029) | 0.396 (0.031) | 0.352 (0.032) | 0.404 (0.034) | 0.348 (0.031) | 0.401 (0.033) |
| | 3 | 0.301 (0.024) | 0.332 (0.027) | 0.376 (0.024) | 0.375 (0.023) | 0.378 (0.024) | 0.379 (0.024) | 0.333 (0.033) | 0.386 (0.033) | 0.341 (0.036) | 0.397 (0.036) | 0.336 (0.035) | 0.391 (0.035) |
| | 4 | 0.272 (0.031) | 0.283 (0.032) | 0.354 (0.030) | 0.354 (0.029) | 0.358 (0.037) | 0.357 (0.034) | 0.339 (0.037) | 0.357 (0.033) | 0.347 (0.039) | 0.366 (0.036) | 0.343 (0.039) | 0.362 (0.036) |
| | 5 | 0.248 (0.037) | 0.245 (0.038) | 0.328 (0.032) | 0.328 (0.031) | 0.350 (0.037) | 0.347 (0.036) | 0.351 (0.044) | 0.325 (0.038) | 0.355 (0.046) | 0.329 (0.039) | 0.356 (0.046) | 0.329 (0.040) |

**(b)** Mean (and standard deviation) of the AUC in 500 simulations for continuous marker Scenario 1a.

| $\tau$ | JM | JM2 | LM1 | LMInt1 | LM2 | LMInt2 | CC1 | CW1 | CC2 | CW2 | CC3 | CW3 |
|---|---|---|---|---|---|---|---|---|---|---|---|---|
| 0 | 0.792 (0.030) | 0.783 (0.030) | 0.793 (0.029) | 0.796 (0.028) | 0.788 (0.030) | 0.784 (0.032) | 0.798 (0.028) | 0.797 (0.028) | 0.797 (0.028) | 0.797 (0.028) | 0.797 (0.028) | 0.797 (0.028) |
| 1 | 0.815 (0.024) | 0.805 (0.024) | 0.791 (0.025) | 0.793 (0.024) | 0.785 (0.026) | 0.781 (0.027) | 0.813 (0.023) | 0.813 (0.023) | 0.813 (0.023) | 0.813 (0.023) | 0.813 (0.023) | 0.812 (0.022) |
| 2 | 0.872 (0.021) | 0.861 (0.022) | 0.810 (0.023) | 0.811 (0.023) | 0.805 (0.024) | 0.802 (0.024) | 0.860 (0.019) | 0.860 (0.019) | 0.860 (0.019) | 0.860 (0.019) | 0.860 (0.019) | 0.860 (0.019) |
| 3 | 0.906 (0.024) | 0.899 (0.023) | 0.827 (0.025) | 0.828 (0.024) | 0.824 (0.025) | 0.822 (0.026) | 0.882 (0.020) | 0.882 (0.020) | 0.882 (0.020) | 0.882 (0.020) | 0.882 (0.020) | 0.882 (0.020) |
| 4 | 0.929 (0.026) | 0.925 (0.025) | 0.851 (0.027) | 0.852 (0.026) | 0.850 (0.027) | 0.849 (0.027) | 0.893 (0.023) | 0.893 (0.023) | 0.893 (0.023) | 0.894 (0.023) | 0.893 (0.023) | 0.893 (0.023) |
| 5 | 0.941 (0.026) | 0.941 (0.026) | 0.874 (0.032) | 0.876 (0.029) | 0.869 (0.063) | 0.871 (0.040) | 0.894 (0.028) | 0.895 (0.028) | 0.895 (0.028) | 0.895 (0.027) | 0.893 (0.028) | 0.895 (0.028) |

**(c)** Mean (and standard deviation) of the Brier Score in 500 simulations for continuous marker Scenario 1a.

| $\tau$ | JM | JM2 | LM1 | LMInt1 | LM2 | LMInt2 | CC1 | CW1 | CC2 | CW2 | CC3 | CW3 |
|---|---|---|---|---|---|---|---|---|---|---|---|---|
| 0 | 0.122 (0.011) | 0.129 (0.013) | 0.123 (0.010) | 0.122 (0.010) | 0.144 (0.009) | 0.144 (0.009) | 0.122 (0.011) | 0.122 (0.011) | 0.122 (0.011) | 0.122 (0.010) | 0.123 (0.012) | 0.123 (0.011) |
| 1 | 0.162 (0.012) | 0.180 (0.014) | 0.171 (0.011) | 0.170 (0.011) | 0.176 (0.009) | 0.176 (0.009) | 0.164 (0.012) | 0.178 (0.014) | 0.166 (0.012) | 0.179 (0.015) | 0.166 (0.012) | 0.180 (0.015) |
| 2 | 0.145 (0.013) | 0.165 (0.015) | 0.175 (0.011) | 0.174 (0.011) | 0.179 (0.010) | 0.179 (0.010) | 0.153 (0.011) | 0.186 (0.016) | 0.157 (0.013) | 0.190 (0.017) | 0.154 (0.012) | 0.189 (0.017) |
| 3 | 0.125 (0.016) | 0.136 (0.016) | 0.167 (0.012) | 0.166 (0.013) | 0.169 (0.012) | 0.170 (0.012) | 0.143 (0.013) | 0.175 (0.017) | 0.148 (0.016) | 0.182 (0.020) | 0.145 (0.014) | 0.178 (0.019) |
| 4 | 0.109 (0.018) | 0.111 (0.018) | 0.152 (0.015) | 0.151 (0.015) | 0.158 (0.016) | 0.158 (0.015) | 0.143 (0.019) | 0.154 (0.020) | 0.146 (0.021) | 0.158 (0.022) | 0.144 (0.020) | 0.156 (0.021) |
| 5 | 0.098 (0.020) | 0.095 (0.020) | 0.135 (0.019) | 0.134 (0.018) | 0.153 (0.027) | 0.152 (0.023) | 0.144 (0.025) | 0.133 (0.020) | 0.146 (0.026) | 0.134 (0.022) | 0.146 (0.026) | 0.134 (0.022) |

### A.4.2 Continuous marker: Simulation 1b

- Inter-inspection rate: 1; Measurement error ($\sigma_\epsilon$): 0.6; Association ($\phi$): 1.5

**Table A.7:** Simulation results for continuous marker Scenario 1b.

**(a)** Mean (and standard deviation) of the root mean squared prediction error in 500 simulations for continuous marker Scenario 1b.

| | $\tau$ | JM | JM2 | LM1 | LMInt1 | LM2 | LMInt2 | CC1 | CW1 | CC2 | CW2 | CC3 | CW3 |
|---|---|---|---|---|---|---|---|---|---|---|---|---|---|
| | 0 | 0.268 (0.019) | 0.269 (0.019) | 0.269 (0.017) | 0.268 (0.018) | 0.322 (0.018) | 0.327 (0.020) | 0.270 (0.020) | 0.270 (0.020) | 0.269 (0.020) | 0.269 (0.020) | 0.273 (0.021) | 0.273 (0.021) |
| | 1 | 0.312 (0.017) | 0.318 (0.018) | 0.327 (0.019) | 0.326 (0.018) | 0.340 (0.015) | 0.343 (0.016) | 0.320 (0.019) | 0.344 (0.018) | 0.321 (0.018) | 0.345 (0.017) | 0.321 (0.019) | 0.346 (0.019) |
| | 2 | 0.269 (0.017) | 0.276 (0.019) | 0.317 (0.016) | 0.317 (0.017) | 0.331 (0.014) | 0.333 (0.015) | 0.289 (0.018) | 0.338 (0.022) | 0.290 (0.019) | 0.340 (0.022) | 0.288 (0.019) | 0.340 (0.023) |
| $X = 0$ | 3 | 0.221 (0.019) | 0.223 (0.020) | 0.284 (0.017) | 0.283 (0.016) | 0.311 (0.014) | 0.314 (0.015) | 0.257 (0.018) | 0.302 (0.022) | 0.257 (0.019) | 0.302 (0.022) | 0.256 (0.019) | 0.303 (0.023) |
| | 4 | 0.182 (0.022) | 0.182 (0.023) | 0.252 (0.018) | 0.250 (0.019) | 0.300 (0.015) | 0.303 (0.016) | 0.241 (0.018) | 0.257 (0.024) | 0.239 (0.020) | 0.254 (0.026) | 0.239 (0.019) | 0.256 (0.025) |
| | 5 | 0.152 (0.025) | 0.151 (0.025) | 0.223 (0.019) | 0.222 (0.018) | 0.299 (0.015) | 0.302 (0.015) | 0.234 (0.018) | 0.224 (0.025) | 0.231 (0.020) | 0.221 (0.027) | 0.231 (0.019) | 0.220 (0.027) |
| | 0 | 0.311 (0.017) | 0.328 (0.022) | 0.312 (0.020) | 0.310 (0.021) | 0.323 (0.019) | 0.321 (0.020) | 0.312 (0.020) | 0.311 (0.027) | 0.310 (0.023) | 0.309 (0.030) | 0.315 (0.022) | 0.314 (0.028) |
| | 1 | 0.337 (0.016) | 0.370 (0.020) | 0.360 (0.022) | 0.359 (0.021) | 0.364 (0.018) | 0.364 (0.019) | 0.344 (0.021) | 0.369 (0.029) | 0.345 (0.024) | 0.370 (0.032) | 0.347 (0.023) | 0.373 (0.031) |
| | 2 | 0.277 (0.017) | 0.305 (0.021) | 0.345 (0.024) | 0.344 (0.024) | 0.346 (0.026) | 0.346 (0.026) | 0.296 (0.026) | 0.357 (0.028) | 0.298 (0.029) | 0.362 (0.031) | 0.296 (0.028) | 0.360 (0.030) |
| $X = 1$ | 3 | 0.225 (0.020) | 0.239 (0.022) | 0.310 (0.027) | 0.310 (0.026) | 0.321 (0.027) | 0.319 (0.027) | 0.267 (0.030) | 0.327 (0.030) | 0.268 (0.033) | 0.332 (0.034) | 0.266 (0.032) | 0.329 (0.033) |
| | 4 | 0.190 (0.024) | 0.193 (0.025) | 0.277 (0.027) | 0.278 (0.028) | 0.311 (0.037) | 0.308 (0.038) | 0.266 (0.032) | 0.284 (0.028) | 0.266 (0.034) | 0.285 (0.029) | 0.265 (0.034) | 0.284 (0.030) |
| | 5 | 0.162 (0.027) | 0.162 (0.028) | 0.250 (0.032) | 0.251 (0.030) | 0.320 (0.039) | 0.315 (0.038) | 0.272 (0.041) | 0.250 (0.033) | 0.272 (0.044) | 0.249 (0.035) | 0.274 (0.045) | 0.251 (0.036) |

**(b)** Mean (and standard deviation) of the AUC in 500 simulations for continuous marker Scenario 1b.

| $\tau$ | JM | JM2 | LM1 | LMInt1 | LM2 | LMInt2 | CC1 | CW1 | CC2 | CW2 | CC3 | CW3 |
|---|---|---|---|---|---|---|---|---|---|---|---|---|
| 0 | 0.794 (0.029) | 0.784 (0.029) | 0.793 (0.028) | 0.797 (0.028) | 0.786 (0.030) | 0.780 (0.031) | 0.797 (0.028) | 0.797 (0.028) | 0.797 (0.028) | 0.796 (0.028) | 0.797 (0.028) | 0.797 (0.028) |
| 1 | 0.850 (0.020) | 0.841 (0.020) | 0.818 (0.023) | 0.820 (0.023) | 0.812 (0.024) | 0.808 (0.025) | 0.844 (0.021) | 0.844 (0.021) | 0.844 (0.021) | 0.844 (0.020) | 0.844 (0.021) | 0.843 (0.021) |
| 2 | 0.924 (0.014) | 0.919 (0.014) | 0.865 (0.019) | 0.866 (0.019) | 0.862 (0.019) | 0.861 (0.020) | 0.909 (0.016) | 0.908 (0.016) | 0.909 (0.016) | 0.908 (0.016) | 0.909 (0.016) | 0.909 (0.016) |
| 3 | 0.955 (0.010) | 0.953 (0.011) | 0.902 (0.017) | 0.903 (0.017) | 0.901 (0.018) | 0.900 (0.018) | 0.935 (0.014) | 0.935 (0.014) | 0.935 (0.014) | 0.935 (0.014) | 0.935 (0.014) | 0.935 (0.014) |
| 4 | 0.968 (0.010) | 0.967 (0.010) | 0.926 (0.019) | 0.926 (0.018) | 0.925 (0.019) | 0.925 (0.019) | 0.942 (0.015) | 0.942 (0.015) | 0.942 (0.015) | 0.942 (0.015) | 0.942 (0.016) | 0.942 (0.016) |
| 5 | 0.974 (0.011) | 0.974 (0.012) | 0.939 (0.021) | 0.939 (0.021) | 0.938 (0.021) | 0.938 (0.021) | 0.940 (0.021) | 0.941 (0.021) | 0.940 (0.021) | 0.941 (0.021) | 0.940 (0.021) | 0.941 (0.021) |

**(c)** Mean (and standard deviation) of the Brier Score in 500 simulations for continuous marker Scenario 1b.

| $\tau$ | JM | JM2 | LM1 | LMInt1 | LM2 | LMInt2 | CC1 | CW1 | CC2 | CW2 | CC3 | CW3 |
|---|---|---|---|---|---|---|---|---|---|---|---|---|
| 0 | 0.122 (0.010) | 0.128 (0.012) | 0.123 (0.010) | 0.122 (0.010) | 0.141 (0.009) | 0.143 (0.009) | 0.123 (0.011) | 0.123 (0.011) | 0.122 (0.011) | 0.122 (0.010) | 0.125 (0.012) | 0.124 (0.012) |
| 1 | 0.146 (0.010) | 0.160 (0.013) | 0.159 (0.011) | 0.158 (0.011) | 0.164 (0.009) | 0.165 (0.009) | 0.151 (0.011) | 0.167 (0.014) | 0.151 (0.012) | 0.168 (0.015) | 0.152 (0.012) | 0.170 (0.015) |
| 2 | 0.112 (0.010) | 0.122 (0.011) | 0.146 (0.011) | 0.146 (0.011) | 0.152 (0.009) | 0.152 (0.009) | 0.123 (0.011) | 0.158 (0.015) | 0.124 (0.012) | 0.161 (0.017) | 0.122 (0.011) | 0.160 (0.016) |
| 3 | 0.086 (0.010) | 0.089 (0.011) | 0.124 (0.012) | 0.124 (0.012) | 0.136 (0.012) | 0.136 (0.012) | 0.105 (0.011) | 0.135 (0.016) | 0.105 (0.013) | 0.137 (0.018) | 0.104 (0.012) | 0.136 (0.017) |
| 4 | 0.072 (0.012) | 0.072 (0.012) | 0.107 (0.014) | 0.107 (0.014) | 0.131 (0.018) | 0.131 (0.018) | 0.102 (0.014) | 0.110 (0.015) | 0.101 (0.015) | 0.110 (0.017) | 0.101 (0.015) | 0.110 (0.016) |
| 5 | 0.063 (0.014) | 0.063 (0.014) | 0.095 (0.016) | 0.095 (0.016) | 0.135 (0.026) | 0.135 (0.026) | 0.103 (0.019) | 0.095 (0.017) | 0.103 (0.020) | 0.095 (0.018) | 0.103 (0.021) | 0.095 (0.018) |

### A.4.3 Continuous marker: Simulation 1c

- Fixed inspection time every year; Measurement error ($\sigma_\epsilon$): 0.6; Association ($\phi$): 1.5

**Table A.8:** Simulation results for continuous marker Scenario 1c.

**(a)** Mean (and standard deviation) of the root mean squared prediction error in 500 simulations for continuous marker Scenario 1c.

| | $\tau$ | JM | JM2 | LM1 | LMInt1 | LM2 | LMInt2 | CC1 | CW1 | CC2 | CW2 | CC3 | CW3 |
|---|---|---|---|---|---|---|---|---|---|---|---|---|---|
| | 0 | 0.267 (0.018) | 0.268 (0.017) | 0.270 (0.017) | 0.269 (0.018) | 0.319 (0.017) | 0.324 (0.018) | 0.270 (0.021) | 0.270 (0.021) | 0.269 (0.020) | 0.269 (0.020) | 0.273 (0.022) | 0.274 (0.022) |
| | 1 | 0.233 (0.017) | 0.234 (0.017) | 0.238 (0.020) | 0.237 (0.019) | 0.319 (0.015) | 0.323 (0.016) | 0.241 (0.020) | 0.277 (0.020) | 0.239 (0.018) | 0.276 (0.018) | 0.238 (0.021) | 0.277 (0.021) |
| | 2 | 0.177 (0.017) | 0.177 (0.017) | 0.190 (0.016) | 0.190 (0.017) | 0.309 (0.018) | 0.312 (0.020) | 0.204 (0.016) | 0.237 (0.021) | 0.199 (0.016) | 0.229 (0.021) | 0.200 (0.017) | 0.233 (0.022) |
| $X = 0$ | 3 | 0.144 (0.017) | 0.144 (0.017) | 0.164 (0.016) | 0.164 (0.015) | 0.301 (0.014) | 0.303 (0.015) | 0.190 (0.015) | 0.192 (0.021) | 0.185 (0.015) | 0.178 (0.021) | 0.186 (0.016) | 0.184 (0.023) |
| | 4 | 0.123 (0.018) | 0.124 (0.018) | 0.151 (0.016) | 0.151 (0.017) | 0.304 (0.022) | 0.306 (0.023) | 0.180 (0.015) | 0.167 (0.020) | 0.174 (0.018) | 0.154 (0.021) | 0.175 (0.017) | 0.157 (0.021) |
| | 5 | 0.109 (0.019) | 0.110 (0.020) | 0.144 (0.017) | 0.143 (0.017) | 0.316 (0.021) | 0.318 (0.021) | 0.174 (0.015) | 0.189 (0.021) | 0.168 (0.016) | 0.188 (0.023) | 0.167 (0.016) | 0.187 (0.023) |
| | 0 | 0.310 (0.018) | 0.329 (0.022) | 0.313 (0.017) | 0.311 (0.018) | 0.317 (0.025) | 0.316 (0.026) | 0.313 (0.019) | 0.312 (0.018) | 0.311 (0.023) | 0.310 (0.020) | 0.317 (0.021) | 0.316 (0.019) |
| | 1 | 0.251 (0.016) | 0.258 (0.017) | 0.258 (0.018) | 0.256 (0.017) | 0.301 (0.027) | 0.298 (0.027) | 0.259 (0.018) | 0.298 (0.020) | 0.258 (0.021) | 0.297 (0.022) | 0.257 (0.020) | 0.299 (0.022) |
| | 2 | 0.183 (0.016) | 0.186 (0.018) | 0.197 (0.020) | 0.196 (0.020) | 0.289 (0.029) | 0.285 (0.030) | 0.205 (0.021) | 0.250 (0.015) | 0.199 (0.026) | 0.246 (0.017) | 0.201 (0.025) | 0.249 (0.016) |
| $X = 1$ | 3 | 0.147 (0.017) | 0.147 (0.018) | 0.167 (0.021) | 0.167 (0.020) | 0.294 (0.033) | 0.290 (0.034) | 0.186 (0.021) | 0.200 (0.017) | 0.178 (0.025) | 0.190 (0.019) | 0.181 (0.024) | 0.194 (0.018) |
| | 4 | 0.127 (0.019) | 0.126 (0.019) | 0.154 (0.023) | 0.155 (0.023) | 0.314 (0.037) | 0.310 (0.037) | 0.180 (0.024) | 0.171 (0.028) | 0.172 (0.028) | 0.159 (0.031) | 0.174 (0.029) | 0.162 (0.032) |
| | 5 | 0.114 (0.022) | 0.114 (0.022) | 0.150 (0.025) | 0.151 (0.024) | 0.342 (0.044) | 0.337 (0.045) | 0.181 (0.028) | 0.210 (0.036) | 0.176 (0.031) | 0.209 (0.039) | 0.175 (0.032) | 0.210 (0.041) |

**(b)** Mean (and standard deviation) of the AUC in 500 simulations for continuous marker Scenario 1c.

| $\tau$ | JM | JM2 | LM1 | LMInt1 | LM2 | LMInt2 | CC1 | CW1 | CC2 | CW2 | CC3 | CW3 |
|---|---|---|---|---|---|---|---|---|---|---|---|---|
| 0 | 0.795 (0.028) | 0.784 (0.028) | 0.792 (0.028) | 0.798 (0.027) | 0.784 (0.029) | 0.777 (0.030) | 0.799 (0.027) | 0.798 (0.027) | 0.798 (0.028) | 0.797 (0.028) | 0.798 (0.027) | 0.798 (0.028) |
| 1 | 0.931 (0.012) | 0.930 (0.013) | 0.929 (0.013) | 0.930 (0.013) | 0.928 (0.013) | 0.927 (0.014) | 0.930 (0.013) | 0.930 (0.013) | 0.930 (0.013) | 0.930 (0.013) | 0.930 (0.013) | 0.929 (0.013) |
| 2 | 0.970 (0.008) | 0.969 (0.008) | 0.966 (0.008) | 0.966 (0.008) | 0.966 (0.008) | 0.966 (0.008) | 0.966 (0.008) | 0.966 (0.008) | 0.966 (0.008) | 0.966 (0.008) | 0.966 (0.008) | 0.966 (0.008) |
| 3 | 0.979 (0.007) | 0.979 (0.007) | 0.975 (0.007) | 0.975 (0.007) | 0.975 (0.008) | 0.975 (0.008) | 0.975 (0.008) | 0.975 (0.008) | 0.975 (0.008) | 0.975 (0.008) | 0.975 (0.008) | 0.975 (0.008) |
| 4 | 0.982 (0.007) | 0.982 (0.007) | 0.977 (0.008) | 0.977 (0.008) | 0.977 (0.008) | 0.976 (0.008) | 0.977 (0.008) | 0.977 (0.008) | 0.977 (0.008) | 0.977 (0.008) | 0.977 (0.008) | 0.977 (0.008) |
| 5 | 0.982 (0.009) | 0.981 (0.009) | 0.977 (0.010) | 0.977 (0.010) | 0.974 (0.011) | 0.973 (0.012) | 0.976 (0.011) | 0.975 (0.011) | 0.976 (0.011) | 0.976 (0.011) | 0.976 (0.011) | 0.976 (0.011) |

**(c)** Mean (and standard deviation) of the Brier Score in 500 simulations for continuous marker Scenario 1c.

| $\tau$ | JM | JM2 | LM1 | LMInt1 | LM2 | LMInt2 | CC1 | CW1 | CC2 | CW2 | CC3 | CW3 |
|---|---|---|---|---|---|---|---|---|---|---|---|---|
| 0 | 0.121 (0.010) | 0.127 (0.012) | 0.123 (0.011) | 0.122 (0.011) | 0.139 (0.009) | 0.140 (0.010) | 0.123 (0.012) | 0.123 (0.012) | 0.122 (0.011) | 0.122 (0.011) | 0.125 (0.013) | 0.125 (0.013) |
| 1 | 0.100 (0.010) | 0.102 (0.010) | 0.102 (0.010) | 0.102 (0.010) | 0.137 (0.011) | 0.138 (0.011) | 0.103 (0.009) | 0.123 (0.012) | 0.103 (0.009) | 0.123 (0.012) | 0.102 (0.010) | 0.124 (0.012) |
| 2 | 0.069 (0.009) | 0.071 (0.010) | 0.075 (0.009) | 0.075 (0.009) | 0.127 (0.013) | 0.127 (0.013) | 0.079 (0.009) | 0.097 (0.011) | 0.077 (0.010) | 0.094 (0.011) | 0.077 (0.009) | 0.096 (0.011) |
| 3 | 0.057 (0.010) | 0.057 (0.009) | 0.064 (0.010) | 0.064 (0.010) | 0.125 (0.016) | 0.125 (0.016) | 0.071 (0.010) | 0.075 (0.010) | 0.069 (0.011) | 0.070 (0.011) | 0.070 (0.010) | 0.072 (0.010) |
| 4 | 0.053 (0.011) | 0.053 (0.010) | 0.061 (0.011) | 0.061 (0.011) | 0.133 (0.020) | 0.133 (0.020) | 0.070 (0.011) | 0.066 (0.009) | 0.068 (0.013) | 0.062 (0.010) | 0.068 (0.012) | 0.063 (0.010) |
| 5 | 0.052 (0.013) | 0.053 (0.014) | 0.061 (0.014) | 0.061 (0.013) | 0.147 (0.028) | 0.147 (0.028) | 0.071 (0.013) | 0.079 (0.016) | 0.069 (0.015) | 0.079 (0.017) | 0.069 (0.015) | 0.079 (0.018) |

### A.4.4 Continuous marker: Simulation 2a

- Inter-inspection rate: 0.5; Measurement error ($\sigma_\epsilon$): 0.6; Association ($\phi$): 0.5

**Table A.9:** Simulation results for continuous marker Scenario 2a.

**(a)** Mean (and standard deviation) of the root mean squared prediction error in 500 simulations for continuous marker Scenario 2a.

| | $\tau$ | JM | JM2 | LM1 | LMInt1 | LM2 | LMInt2 | CC1 | CW1 | CC2 | CW2 | CC3 | CW3 |
|---|---|---|---|---|---|---|---|---|---|---|---|---|---|
| | 0 | 0.123 (0.013) | 0.124 (0.014) | 0.126 (0.013) | 0.125 (0.013) | 0.227 (0.022) | 0.234 (0.025) | 0.125 (0.013) | 0.126 (0.012) | 0.123 (0.013) | 0.124 (0.012) | 0.130 (0.014) | 0.131 (0.014) |
| | 1 | 0.207 (0.014) | 0.211 (0.016) | 0.217 (0.014) | 0.216 (0.014) | 0.242 (0.019) | 0.245 (0.019) | 0.210 (0.013) | 0.214 (0.012) | 0.210 (0.014) | 0.214 (0.012) | 0.214 (0.014) | 0.218 (0.014) |
| | 2 | 0.228 (0.014) | 0.234 (0.017) | 0.261 (0.014) | 0.260 (0.014) | 0.271 (0.015) | 0.274 (0.017) | 0.236 (0.014) | 0.258 (0.016) | 0.236 (0.014) | 0.257 (0.016) | 0.237 (0.015) | 0.260 (0.017) |
| $X = 0$ | 3 | 0.214 (0.016) | 0.218 (0.019) | 0.267 (0.015) | 0.266 (0.014) | 0.275 (0.013) | 0.277 (0.013) | 0.229 (0.014) | 0.262 (0.016) | 0.229 (0.014) | 0.262 (0.016) | 0.230 (0.015) | 0.264 (0.017) |
| | 4 | 0.193 (0.018) | 0.191 (0.020) | 0.253 (0.015) | 0.252 (0.016) | 0.267 (0.014) | 0.269 (0.015) | 0.218 (0.015) | 0.246 (0.020) | 0.218 (0.016) | 0.245 (0.020) | 0.218 (0.017) | 0.247 (0.021) |
| | 5 | 0.174 (0.023) | 0.166 (0.023) | 0.230 (0.015) | 0.228 (0.014) | 0.257 (0.015) | 0.259 (0.016) | 0.218 (0.015) | 0.221 (0.021) | 0.217 (0.016) | 0.221 (0.022) | 0.218 (0.016) | 0.221 (0.022) |
| | 0 | 0.169 (0.013) | 0.182 (0.017) | 0.171 (0.017) | 0.171 (0.018) | 0.223 (0.016) | 0.218 (0.016) | 0.171 (0.018) | 0.172 (0.023) | 0.170 (0.019) | 0.171 (0.024) | 0.175 (0.019) | 0.177 (0.024) |
| | 1 | 0.250 (0.013) | 0.281 (0.019) | 0.266 (0.016) | 0.266 (0.015) | 0.273 (0.017) | 0.272 (0.017) | 0.254 (0.018) | 0.261 (0.025) | 0.255 (0.019) | 0.261 (0.027) | 0.257 (0.020) | 0.264 (0.027) |
| | 2 | 0.251 (0.014) | 0.289 (0.019) | 0.300 (0.020) | 0.299 (0.021) | 0.307 (0.020) | 0.307 (0.021) | 0.260 (0.022) | 0.294 (0.025) | 0.260 (0.024) | 0.295 (0.026) | 0.261 (0.024) | 0.297 (0.027) |
| $X = 1$ | 3 | 0.225 (0.016) | 0.257 (0.021) | 0.298 (0.020) | 0.297 (0.019) | 0.302 (0.019) | 0.302 (0.019) | 0.244 (0.026) | 0.293 (0.029) | 0.244 (0.027) | 0.294 (0.031) | 0.245 (0.028) | 0.296 (0.032) |
| | 4 | 0.200 (0.022) | 0.214 (0.024) | 0.280 (0.024) | 0.280 (0.024) | 0.284 (0.029) | 0.283 (0.030) | 0.236 (0.028) | 0.273 (0.028) | 0.237 (0.029) | 0.276 (0.029) | 0.238 (0.030) | 0.277 (0.029) |
| | 5 | 0.181 (0.028) | 0.180 (0.028) | 0.254 (0.026) | 0.256 (0.025) | 0.269 (0.027) | 0.266 (0.026) | 0.247 (0.036) | 0.246 (0.032) | 0.248 (0.037) | 0.248 (0.033) | 0.251 (0.038) | 0.250 (0.035) |

**(b)** Mean (and standard deviation) of the AUC in 500 simulations for continuous marker Scenario 2a.

| $\tau$ | JM | JM2 | LM1 | LMInt1 | LM2 | LMInt2 | CC1 | CW1 | CC2 | CW2 | CC3 | CW3 |
|---|---|---|---|---|---|---|---|---|---|---|---|---|
| 0 | 0.730 (0.035) | 0.722 (0.036) | 0.727 (0.036) | 0.730 (0.036) | 0.724 (0.037) | 0.718 (0.039) | 0.731 (0.035) | 0.731 (0.035) | 0.731 (0.035) | 0.731 (0.035) | 0.729 (0.035) | 0.730 (0.035) |
| 1 | 0.772 (0.026) | 0.762 (0.026) | 0.754 (0.027) | 0.755 (0.027) | 0.748 (0.028) | 0.743 (0.030) | 0.771 (0.026) | 0.771 (0.026) | 0.771 (0.026) | 0.771 (0.026) | 0.770 (0.026) | 0.770 (0.026) |
| 2 | 0.833 (0.023) | 0.820 (0.023) | 0.782 (0.026) | 0.782 (0.026) | 0.776 (0.026) | 0.772 (0.028) | 0.826 (0.023) | 0.826 (0.023) | 0.826 (0.023) | 0.826 (0.023) | 0.826 (0.023) | 0.825 (0.023) |
| 3 | 0.874 (0.021) | 0.864 (0.021) | 0.810 (0.024) | 0.810 (0.024) | 0.806 (0.024) | 0.804 (0.025) | 0.863 (0.021) | 0.862 (0.021) | 0.862 (0.021) | 0.862 (0.021) | 0.862 (0.021) | 0.862 (0.021) |
| 4 | 0.897 (0.022) | 0.891 (0.023) | 0.836 (0.028) | 0.836 (0.028) | 0.834 (0.028) | 0.833 (0.028) | 0.881 (0.024) | 0.880 (0.024) | 0.880 (0.024) | 0.880 (0.024) | 0.880 (0.024) | 0.880 (0.024) |
| 5 | 0.909 (0.022) | 0.907 (0.023) | 0.859 (0.031) | 0.859 (0.031) | 0.859 (0.030) | 0.858 (0.031) | 0.887 (0.026) | 0.887 (0.026) | 0.887 (0.026) | 0.887 (0.026) | 0.886 (0.027) | 0.886 (0.027) |

**(c)** Mean (and standard deviation) of the Brier Score in 500 simulations for continuous marker Scenario 2a.

| $\tau$ | JM | JM2 | LM1 | LMInt1 | LM2 | LMInt2 | CC1 | CW1 | CC2 | CW2 | CC3 | CW3 |
|---|---|---|---|---|---|---|---|---|---|---|---|---|
| 0 | 0.108 (0.011) | 0.110 (0.013) | 0.108 (0.011) | 0.108 (0.011) | 0.136 (0.010) | 0.137 (0.010) | 0.108 (0.011) | 0.108 (0.011) | 0.108 (0.011) | 0.108 (0.010) | 0.110 (0.012) | 0.110 (0.011) |
| 1 | 0.160 (0.010) | 0.169 (0.013) | 0.166 (0.010) | 0.166 (0.010) | 0.174 (0.009) | 0.174 (0.009) | 0.161 (0.011) | 0.164 (0.012) | 0.161 (0.011) | 0.164 (0.012) | 0.163 (0.012) | 0.166 (0.013) |
| 2 | 0.161 (0.011) | 0.173 (0.013) | 0.182 (0.011) | 0.182 (0.011) | 0.187 (0.009) | 0.188 (0.009) | 0.165 (0.011) | 0.180 (0.014) | 0.165 (0.012) | 0.180 (0.015) | 0.166 (0.012) | 0.181 (0.015) |
| 3 | 0.144 (0.012) | 0.153 (0.013) | 0.176 (0.011) | 0.176 (0.011) | 0.180 (0.009) | 0.180 (0.010) | 0.152 (0.012) | 0.173 (0.015) | 0.152 (0.013) | 0.174 (0.016) | 0.152 (0.013) | 0.175 (0.017) |
| 4 | 0.132 (0.015) | 0.134 (0.015) | 0.164 (0.013) | 0.163 (0.013) | 0.169 (0.013) | 0.169 (0.013) | 0.145 (0.015) | 0.161 (0.017) | 0.145 (0.016) | 0.161 (0.018) | 0.145 (0.017) | 0.162 (0.018) |
| 5 | 0.124 (0.016) | 0.122 (0.016) | 0.151 (0.016) | 0.150 (0.016) | 0.162 (0.018) | 0.162 (0.018) | 0.146 (0.019) | 0.147 (0.018) | 0.146 (0.020) | 0.147 (0.019) | 0.147 (0.020) | 0.148 (0.020) |

### A.4.5 Continuous marker: Simulation 2b

- Inter-inspection rate: 1; Measurement error ($\sigma_\epsilon$): 0.6; Association ($\phi$): 0.5

**Table A.10:** Simulation results for continuous marker Scenario 2b.

**(a)** Mean (and standard deviation) of the root mean squared prediction error in 500 simulations for continuous marker Scenario 2b.

| | $\tau$ | JM | JM2 | LM1 | LMInt1 | LM2 | LMInt2 | CC1 | CW1 | CC2 | CW2 | CC3 | CW3 |
|---|---|---|---|---|---|---|---|---|---|---|---|---|---|
| | 0 | 0.123 (0.013) | 0.124 (0.013) | 0.125 (0.013) | 0.124 (0.013) | 0.227 (0.022) | 0.236 (0.025) | 0.125 (0.013) | 0.126 (0.013) | 0.124 (0.014) | 0.124 (0.013) | 0.131 (0.014) | 0.131 (0.014) |
| | 1 | 0.191 (0.013) | 0.193 (0.014) | 0.204 (0.015) | 0.202 (0.014) | 0.236 (0.019) | 0.241 (0.019) | 0.195 (0.014) | 0.202 (0.012) | 0.195 (0.014) | 0.202 (0.012) | 0.198 (0.015) | 0.205 (0.014) |
| | 2 | 0.182 (0.014) | 0.185 (0.016) | 0.223 (0.014) | 0.223 (0.014) | 0.250 (0.015) | 0.253 (0.017) | 0.195 (0.014) | 0.223 (0.016) | 0.194 (0.014) | 0.222 (0.016) | 0.195 (0.015) | 0.224 (0.016) |
| $X = 0$ | 3 | 0.150 (0.014) | 0.150 (0.015) | 0.207 (0.015) | 0.207 (0.014) | 0.242 (0.013) | 0.245 (0.013) | 0.173 (0.014) | 0.211 (0.016) | 0.171 (0.014) | 0.208 (0.016) | 0.172 (0.015) | 0.210 (0.017) |
| | 4 | 0.121 (0.016) | 0.119 (0.017) | 0.184 (0.016) | 0.183 (0.017) | 0.233 (0.015) | 0.237 (0.017) | 0.157 (0.014) | 0.187 (0.018) | 0.153 (0.015) | 0.183 (0.019) | 0.154 (0.015) | 0.184 (0.020) |
| | 5 | 0.099 (0.017) | 0.097 (0.017) | 0.159 (0.016) | 0.157 (0.015) | 0.232 (0.013) | 0.236 (0.013) | 0.155 (0.015) | 0.158 (0.022) | 0.152 (0.015) | 0.155 (0.022) | 0.151 (0.016) | 0.154 (0.023) |
| | 0 | 0.169 (0.013) | 0.181 (0.016) | 0.171 (0.017) | 0.170 (0.018) | 0.219 (0.018) | 0.213 (0.019) | 0.171 (0.015) | 0.173 (0.021) | 0.170 (0.015) | 0.171 (0.022) | 0.177 (0.015) | 0.177 (0.023) |
| | 1 | 0.230 (0.013) | 0.254 (0.018) | 0.252 (0.018) | 0.251 (0.017) | 0.260 (0.015) | 0.259 (0.015) | 0.238 (0.016) | 0.246 (0.025) | 0.238 (0.017) | 0.246 (0.026) | 0.239 (0.017) | 0.249 (0.027) |
| | 2 | 0.200 (0.014) | 0.223 (0.018) | 0.261 (0.020) | 0.261 (0.021) | 0.268 (0.025) | 0.267 (0.026) | 0.216 (0.020) | 0.259 (0.024) | 0.215 (0.020) | 0.258 (0.024) | 0.215 (0.020) | 0.260 (0.025) |
| $X = 1$ | 3 | 0.157 (0.015) | 0.170 (0.018) | 0.235 (0.022) | 0.235 (0.022) | 0.248 (0.023) | 0.245 (0.023) | 0.185 (0.022) | 0.242 (0.026) | 0.183 (0.023) | 0.241 (0.027) | 0.183 (0.023) | 0.242 (0.028) |
| | 4 | 0.127 (0.018) | 0.129 (0.021) | 0.204 (0.022) | 0.206 (0.022) | 0.234 (0.034) | 0.230 (0.035) | 0.173 (0.025) | 0.212 (0.023) | 0.171 (0.025) | 0.212 (0.023) | 0.170 (0.026) | 0.212 (0.024) |
| | 5 | 0.105 (0.020) | 0.103 (0.020) | 0.176 (0.025) | 0.178 (0.024) | 0.234 (0.035) | 0.228 (0.034) | 0.179 (0.030) | 0.177 (0.027) | 0.178 (0.031) | 0.176 (0.027) | 0.177 (0.033) | 0.175 (0.030) |

**(b)** Mean (and standard deviation) of the AUC in 500 simulations for continuous marker Scenario 2b.

| $\tau$ | JM | JM2 | LM1 | LMInt1 | LM2 | LMInt2 | CC1 | CW1 | CC2 | CW2 | CC3 | CW3 |
|---|---|---|---|---|---|---|---|---|---|---|---|---|
| 0 | 0.730 (0.035) | 0.722 (0.035) | 0.727 (0.036) | 0.730 (0.036) | 0.723 (0.037) | 0.715 (0.039) | 0.730 (0.035) | 0.730 (0.035) | 0.730 (0.035) | 0.730 (0.035) | 0.730 (0.035) | 0.730 (0.035) |
| 1 | 0.798 (0.025) | 0.789 (0.026) | 0.773 (0.027) | 0.774 (0.027) | 0.768 (0.029) | 0.762 (0.031) | 0.793 (0.025) | 0.793 (0.025) | 0.793 (0.025) | 0.793 (0.025) | 0.793 (0.026) | 0.793 (0.026) |
| 2 | 0.873 (0.019) | 0.866 (0.020) | 0.825 (0.022) | 0.825 (0.022) | 0.822 (0.023) | 0.819 (0.024) | 0.864 (0.020) | 0.864 (0.020) | 0.864 (0.020) | 0.864 (0.020) | 0.864 (0.020) | 0.863 (0.020) |
| 3 | 0.912 (0.017) | 0.909 (0.016) | 0.872 (0.020) | 0.872 (0.020) | 0.870 (0.021) | 0.869 (0.021) | 0.903 (0.018) | 0.902 (0.018) | 0.902 (0.018) | 0.902 (0.018) | 0.902 (0.018) | 0.902 (0.018) |
| 4 | 0.928 (0.018) | 0.927 (0.018) | 0.897 (0.022) | 0.897 (0.022) | 0.896 (0.022) | 0.896 (0.022) | 0.916 (0.019) | 0.916 (0.019) | 0.916 (0.019) | 0.916 (0.019) | 0.916 (0.019) | 0.916 (0.019) |
| 5 | 0.933 (0.019) | 0.933 (0.019) | 0.912 (0.023) | 0.912 (0.023) | 0.912 (0.022) | 0.912 (0.023) | 0.919 (0.022) | 0.919 (0.022) | 0.920 (0.022) | 0.920 (0.022) | 0.919 (0.021) | 0.919 (0.021) |

**(c)** Mean (and standard deviation) of the Brier Score in 500 simulations for continuous marker Scenario 2b.

| $\tau$ | JM | JM2 | LM1 | LMInt1 | LM2 | LMInt2 | CC1 | CW1 | CC2 | CW2 | CC3 | CW3 |
|---|---|---|---|---|---|---|---|---|---|---|---|---|
| 0 | 0.108 (0.011) | 0.110 (0.012) | 0.108 (0.011) | 0.108 (0.011) | 0.135 (0.010) | 0.136 (0.010) | 0.108 (0.012) | 0.108 (0.011) | 0.108 (0.011) | 0.108 (0.010) | 0.110 (0.012) | 0.110 (0.011) |
| 1 | 0.151 (0.010) | 0.158 (0.012) | 0.159 (0.010) | 0.159 (0.010) | 0.169 (0.008) | 0.170 (0.009) | 0.154 (0.011) | 0.158 (0.012) | 0.154 (0.011) | 0.158 (0.012) | 0.155 (0.012) | 0.159 (0.013) |
| 2 | 0.140 (0.011) | 0.146 (0.012) | 0.163 (0.011) | 0.163 (0.011) | 0.171 (0.009) | 0.172 (0.009) | 0.146 (0.011) | 0.162 (0.014) | 0.146 (0.011) | 0.161 (0.014) | 0.146 (0.012) | 0.163 (0.015) |
| 3 | 0.119 (0.012) | 0.122 (0.012) | 0.145 (0.011) | 0.145 (0.011) | 0.156 (0.011) | 0.156 (0.011) | 0.128 (0.011) | 0.147 (0.014) | 0.127 (0.011) | 0.146 (0.014) | 0.127 (0.012) | 0.147 (0.015) |
| 4 | 0.108 (0.014) | 0.109 (0.014) | 0.130 (0.013) | 0.130 (0.013) | 0.148 (0.015) | 0.148 (0.015) | 0.120 (0.013) | 0.133 (0.015) | 0.119 (0.014) | 0.132 (0.015) | 0.119 (0.014) | 0.133 (0.016) |
| 5 | 0.103 (0.015) | 0.102 (0.015) | 0.119 (0.015) | 0.119 (0.015) | 0.147 (0.021) | 0.147 (0.021) | 0.120 (0.016) | 0.120 (0.016) | 0.119 (0.017) | 0.119 (0.016) | 0.119 (0.017) | 0.119 (0.016) |

### A.4.6 Continuous marker: Simulation 2c

- Fixed inspection time every year; Measurement error ($\sigma_\epsilon$): 0.6; Association ($\phi$): 0.5

**Table A.11:** Simulation results for continuous marker Scenario 2c.

**(a)** Mean (and standard deviation) of the root mean squared prediction error in 500 simulations for continuous marker Scenario 2c.

| | $\tau$ | JM | JM2 | LM1 | LMInt1 | LM2 | LMInt2 | CC1 | CW1 | CC2 | CW2 | CC3 | CW3 |
|---|---|---|---|---|---|---|---|---|---|---|---|---|---|
| | 0 | 0.123 (0.013) | 0.124 (0.013) | 0.128 (0.013) | 0.127 (0.013) | 0.226 (0.020) | 0.234 (0.023) | 0.125 (0.014) | 0.125 (0.012) | 0.124 (0.014) | 0.123 (0.012) | 0.131 (0.014) | 0.130 (0.013) |
| | 1 | 0.129 (0.010) | 0.131 (0.010) | 0.134 (0.014) | 0.133 (0.014) | 0.237 (0.017) | 0.243 (0.018) | 0.136 (0.014) | 0.147 (0.013) | 0.136 (0.014) | 0.148 (0.012) | 0.133 (0.015) | 0.145 (0.014) |
| | 2 | 0.104 (0.009) | 0.104 (0.009) | 0.115 (0.011) | 0.114 (0.011) | 0.239 (0.019) | 0.243 (0.021) | 0.123 (0.011) | 0.145 (0.015) | 0.121 (0.011) | 0.141 (0.015) | 0.120 (0.011) | 0.137 (0.015) |
| $X = 0$ | 3 | 0.082 (0.008) | 0.082 (0.008) | 0.099 (0.011) | 0.098 (0.011) | 0.236 (0.015) | 0.239 (0.016) | 0.119 (0.012) | 0.127 (0.015) | 0.117 (0.012) | 0.120 (0.015) | 0.117 (0.012) | 0.117 (0.016) |
| | 4 | 0.069 (0.008) | 0.069 (0.008) | 0.089 (0.010) | 0.089 (0.010) | 0.237 (0.021) | 0.239 (0.022) | 0.112 (0.011) | 0.107 (0.015) | 0.109 (0.012) | 0.098 (0.015) | 0.108 (0.012) | 0.095 (0.015) |
| | 5 | 0.061 (0.009) | 0.061 (0.009) | 0.085 (0.010) | 0.084 (0.010) | 0.246 (0.019) | 0.248 (0.020) | 0.105 (0.010) | 0.099 (0.019) | 0.101 (0.010) | 0.094 (0.019) | 0.097 (0.010) | 0.089 (0.020) |
| | 0 | 0.169 (0.013) | 0.181 (0.016) | 0.171 (0.010) | 0.170 (0.010) | 0.212 (0.023) | 0.207 (0.024) | 0.171 (0.016) | 0.171 (0.014) | 0.170 (0.017) | 0.169 (0.014) | 0.177 (0.018) | 0.175 (0.014) |
| | 1 | 0.156 (0.010) | 0.160 (0.011) | 0.162 (0.010) | 0.162 (0.011) | 0.223 (0.023) | 0.217 (0.024) | 0.169 (0.015) | 0.185 (0.017) | 0.170 (0.015) | 0.185 (0.018) | 0.165 (0.015) | 0.182 (0.018) |
| | 2 | 0.114 (0.009) | 0.115 (0.010) | 0.125 (0.012) | 0.126 (0.012) | 0.218 (0.028) | 0.213 (0.028) | 0.134 (0.018) | 0.175 (0.012) | 0.131 (0.020) | 0.172 (0.011) | 0.128 (0.021) | 0.169 (0.011) |
| $X = 1$ | 3 | 0.087 (0.008) | 0.087 (0.008) | 0.103 (0.012) | 0.105 (0.012) | 0.217 (0.030) | 0.212 (0.030) | 0.120 (0.017) | 0.147 (0.014) | 0.115 (0.018) | 0.141 (0.014) | 0.115 (0.019) | 0.139 (0.014) |
| | 4 | 0.072 (0.009) | 0.072 (0.009) | 0.092 (0.014) | 0.094 (0.014) | 0.227 (0.034) | 0.222 (0.035) | 0.115 (0.018) | 0.114 (0.013) | 0.110 (0.019) | 0.108 (0.013) | 0.109 (0.021) | 0.104 (0.014) |
| | 5 | 0.064 (0.011) | 0.064 (0.011) | 0.089 (0.015) | 0.091 (0.015) | 0.247 (0.039) | 0.242 (0.039) | 0.114 (0.021) | 0.110 (0.020) | 0.111 (0.022) | 0.107 (0.021) | 0.107 (0.024) | 0.103 (0.022) |

**(b)** Mean (and standard deviation) of the AUC in 500 simulations for continuous marker Scenario 2c.

| $\tau$ | JM | JM2 | LM1 | LMInt1 | LM2 | LMInt2 | CC1 | CW1 | CC2 | CW2 | CC3 | CW3 |
|---|---|---|---|---|---|---|---|---|---|---|---|---|
| 0 | 0.730 (0.036) | 0.723 (0.037) | 0.724 (0.036) | 0.729 (0.036) | 0.721 (0.037) | 0.713 (0.039) | 0.731 (0.035) | 0.731 (0.036) | 0.731 (0.035) | 0.731 (0.036) | 0.730 (0.036) | 0.730 (0.036) |
| 1 | 0.858 (0.020) | 0.857 (0.021) | 0.857 (0.020) | 0.857 (0.020) | 0.856 (0.021) | 0.855 (0.021) | 0.857 (0.021) | 0.857 (0.021) | 0.857 (0.021) | 0.857 (0.021) | 0.857 (0.020) | 0.856 (0.021) |
| 2 | 0.911 (0.015) | 0.911 (0.015) | 0.909 (0.015) | 0.908 (0.015) | 0.908 (0.016) | 0.908 (0.016) | 0.908 (0.015) | 0.908 (0.015) | 0.908 (0.015) | 0.908 (0.015) | 0.908 (0.015) | 0.908 (0.016) |
| 3 | 0.933 (0.015) | 0.934 (0.014) | 0.931 (0.015) | 0.930 (0.015) | 0.931 (0.015) | 0.931 (0.015) | 0.931 (0.015) | 0.930 (0.015) | 0.931 (0.015) | 0.930 (0.015) | 0.931 (0.015) | 0.930 (0.015) |
| 4 | 0.940 (0.015) | 0.941 (0.015) | 0.937 (0.015) | 0.937 (0.015) | 0.937 (0.015) | 0.936 (0.015) | 0.937 (0.015) | 0.937 (0.015) | 0.937 (0.015) | 0.937 (0.015) | 0.937 (0.015) | 0.937 (0.015) |
| 5 | 0.940 (0.018) | 0.940 (0.018) | 0.937 (0.018) | 0.937 (0.018) | 0.937 (0.018) | 0.936 (0.018) | 0.937 (0.018) | 0.937 (0.019) | 0.937 (0.019) | 0.937 (0.019) | 0.937 (0.018) | 0.937 (0.019) |

**(c)** Mean (and standard deviation) of the Brier Score in 500 simulations for continuous marker Scenario 2c.

| $\tau$ | JM | JM2 | LM1 | LMInt1 | LM2 | LMInt2 | CC1 | CW1 | CC2 | CW2 | CC3 | CW3 |
|---|---|---|---|---|---|---|---|---|---|---|---|---|
| 0 | 0.107 (0.011) | 0.109 (0.012) | 0.108 (0.011) | 0.107 (0.011) | 0.133 (0.009) | 0.134 (0.010) | 0.107 (0.012) | 0.107 (0.011) | 0.107 (0.012) | 0.107 (0.011) | 0.109 (0.012) | 0.108 (0.012) |
| 1 | 0.128 (0.010) | 0.129 (0.011) | 0.129 (0.010) | 0.129 (0.010) | 0.160 (0.009) | 0.161 (0.009) | 0.131 (0.010) | 0.135 (0.011) | 0.131 (0.010) | 0.135 (0.011) | 0.130 (0.011) | 0.134 (0.012) |
| 2 | 0.116 (0.011) | 0.116 (0.011) | 0.118 (0.010) | 0.118 (0.010) | 0.157 (0.012) | 0.157 (0.012) | 0.120 (0.009) | 0.130 (0.011) | 0.120 (0.010) | 0.128 (0.012) | 0.119 (0.010) | 0.127 (0.012) |
| 3 | 0.103 (0.012) | 0.102 (0.012) | 0.106 (0.011) | 0.106 (0.011) | 0.148 (0.014) | 0.147 (0.014) | 0.110 (0.011) | 0.114 (0.012) | 0.109 (0.012) | 0.113 (0.012) | 0.109 (0.012) | 0.112 (0.012) |
| 4 | 0.097 (0.013) | 0.097 (0.013) | 0.101 (0.012) | 0.101 (0.012) | 0.147 (0.017) | 0.147 (0.017) | 0.106 (0.012) | 0.105 (0.012) | 0.105 (0.013) | 0.103 (0.012) | 0.105 (0.013) | 0.102 (0.012) |
| 5 | 0.096 (0.015) | 0.096 (0.015) | 0.100 (0.015) | 0.100 (0.015) | 0.155 (0.024) | 0.154 (0.023) | 0.104 (0.014) | 0.103 (0.014) | 0.104 (0.015) | 0.102 (0.014) | 0.103 (0.016) | 0.102 (0.015) |

### A.4.7 Continuous marker: Simulation 3a

- Inter-inspection rate: 0.5; Measurement error ($\sigma_\epsilon$): 1.2; Association ($\phi$): 1.5

**Table A.12:** Simulation results for continuous marker Scenario 3a.

**(a)** Mean (and standard deviation) of the root mean squared prediction error in 500 simulations for continuous marker Scenario 3a.

| | $\tau$ | JM | JM2 | LM1 | LMInt1 | LM2 | LMInt2 | CC1 | CW1 | CC2 | CW2 | CC3 | CW3 |
|---|---|---|---|---|---|---|---|---|---|---|---|---|---|
| $X=0$ | 0 | 0.288 (0.020) | 0.293 (0.022) | 0.287 (0.018) | 0.288 (0.019) | 0.339 (0.017) | 0.342 (0.018) | 0.288 (0.019) | 0.287 (0.020) | 0.287 (0.019) | 0.286 (0.019) | 0.291 (0.020) | 0.290 (0.020) |
| | 1 | 0.366 (0.017) | 0.380 (0.019) | 0.370 (0.018) | 0.370 (0.018) | 0.382 (0.015) | 0.384 (0.016) | 0.371 (0.018) | 0.382 (0.018) | 0.374 (0.018) | 0.383 (0.017) | 0.374 (0.019) | 0.385 (0.018) |
| | 2 | 0.365 (0.018) | 0.381 (0.021) | 0.382 (0.015) | 0.382 (0.016) | 0.388 (0.014) | 0.389 (0.014) | 0.378 (0.017) | 0.406 (0.020) | 0.385 (0.017) | 0.410 (0.020) | 0.380 (0.018) | 0.409 (0.021) |
| | 3 | 0.341 (0.021) | 0.348 (0.024) | 0.369 (0.014) | 0.369 (0.014) | 0.376 (0.012) | 0.377 (0.013) | 0.362 (0.016) | 0.390 (0.019) | 0.369 (0.017) | 0.396 (0.020) | 0.364 (0.017) | 0.393 (0.020) |
| | 4 | 0.315 (0.025) | 0.312 (0.027) | 0.346 (0.015) | 0.345 (0.016) | 0.359 (0.014) | 0.360 (0.014) | 0.346 (0.017) | 0.357 (0.022) | 0.350 (0.019) | 0.361 (0.023) | 0.348 (0.018) | 0.359 (0.023) |
| | 5 | 0.292 (0.031) | 0.283 (0.031) | 0.318 (0.015) | 0.316 (0.015) | 0.344 (0.014) | 0.344 (0.015) | 0.328 (0.018) | 0.320 (0.022) | 0.330 (0.021) | 0.322 (0.024) | 0.330 (0.019) | 0.322 (0.023) |
| $X=1$ | 0 | 0.335 (0.018) | 0.359 (0.023) | 0.334 (0.017) | 0.334 (0.018) | 0.355 (0.016) | 0.354 (0.016) | 0.335 (0.021) | 0.335 (0.025) | 0.333 (0.024) | 0.333 (0.027) | 0.338 (0.022) | 0.338 (0.026) |
| | 1 | 0.396 (0.016) | 0.448 (0.022) | 0.402 (0.018) | 0.402 (0.017) | 0.403 (0.016) | 0.403 (0.017) | 0.402 (0.021) | 0.415 (0.026) | 0.405 (0.024) | 0.417 (0.028) | 0.404 (0.022) | 0.418 (0.027) |
| | 2 | 0.377 (0.017) | 0.432 (0.021) | 0.404 (0.022) | 0.404 (0.023) | 0.405 (0.022) | 0.406 (0.021) | 0.390 (0.027) | 0.428 (0.028) | 0.397 (0.029) | 0.435 (0.031) | 0.392 (0.028) | 0.431 (0.030) |
| | 3 | 0.349 (0.020) | 0.383 (0.023) | 0.392 (0.023) | 0.392 (0.022) | 0.393 (0.022) | 0.393 (0.022) | 0.375 (0.029) | 0.413 (0.030) | 0.383 (0.032) | 0.422 (0.033) | 0.377 (0.031) | 0.417 (0.032) |
| | 4 | 0.329 (0.028) | 0.338 (0.028) | 0.372 (0.028) | 0.372 (0.027) | 0.376 (0.031) | 0.375 (0.029) | 0.371 (0.034) | 0.383 (0.031) | 0.378 (0.035) | 0.391 (0.033) | 0.374 (0.035) | 0.387 (0.033) |
| | 5 | 0.310 (0.034) | 0.304 (0.033) | 0.350 (0.029) | 0.350 (0.028) | 0.364 (0.031) | 0.362 (0.030) | 0.370 (0.040) | 0.352 (0.035) | 0.374 (0.042) | 0.355 (0.036) | 0.375 (0.042) | 0.356 (0.037) |

**(b)** Mean (and standard deviation) of the AUC in 500 simulations for continuous marker Scenario 3a.

| $\tau$ | JM | JM2 | LM1 | LMInt1 | LM2 | LMInt2 | CC1 | CW1 | CC2 | CW2 | CC3 | CW3 |
|---|---|---|---|---|---|---|---|---|---|---|---|---|
| 0 | 0.717 (0.033) | 0.697 (0.036) | 0.723 (0.033) | 0.724 (0.033) | 0.718 (0.034) | 0.715 (0.035) | 0.725 (0.033) | 0.725 (0.033) | 0.724 (0.033) | 0.724 (0.033) | 0.724 (0.033) | 0.724 (0.033) |
| 1 | 0.749 (0.027) | 0.731 (0.027) | 0.734 (0.027) | 0.735 (0.027) | 0.728 (0.027) | 0.725 (0.028) | 0.744 (0.026) | 0.744 (0.026) | 0.744 (0.026) | 0.744 (0.026) | 0.744 (0.026) | 0.744 (0.026) |
| 2 | 0.813 (0.025) | 0.797 (0.026) | 0.771 (0.025) | 0.772 (0.025) | 0.766 (0.025) | 0.764 (0.026) | 0.798 (0.023) | 0.798 (0.023) | 0.798 (0.023) | 0.797 (0.023) | 0.798 (0.023) | 0.797 (0.023) |
| 3 | 0.854 (0.028) | 0.845 (0.028) | 0.798 (0.027) | 0.798 (0.027) | 0.794 (0.028) | 0.793 (0.028) | 0.828 (0.025) | 0.828 (0.025) | 0.828 (0.025) | 0.828 (0.025) | 0.828 (0.025) | 0.828 (0.025) |
| 4 | 0.881 (0.031) | 0.878 (0.030) | 0.825 (0.029) | 0.826 (0.029) | 0.824 (0.029) | 0.822 (0.029) | 0.848 (0.027) | 0.848 (0.027) | 0.848 (0.027) | 0.848 (0.027) | 0.848 (0.027) | 0.848 (0.027) |
| 5 | 0.899 (0.033) | 0.900 (0.031) | 0.849 (0.032) | 0.849 (0.031) | 0.847 (0.041) | 0.848 (0.032) | 0.858 (0.031) | 0.858 (0.031) | 0.858 (0.031) | 0.859 (0.031) | 0.858 (0.031) | 0.858 (0.031) |

**(c)** Mean (and standard deviation) of the Brier Score in 500 simulations for continuous marker Scenario 3a.

| $\tau$ | JM | JM2 | LM1 | LMInt1 | LM2 | LMInt2 | CC1 | CW1 | CC2 | CW2 | CC3 | CW3 |
|---|---|---|---|---|---|---|---|---|---|---|---|---|
| 0 | 0.136 (0.011) | 0.146 (0.014) | 0.135 (0.011) | 0.135 (0.011) | 0.158 (0.010) | 0.159 (0.010) | 0.135 (0.011) | 0.135 (0.011) | 0.134 (0.011) | 0.134 (0.011) | 0.137 (0.012) | 0.137 (0.012) |
| 1 | 0.186 (0.011) | 0.213 (0.015) | 0.190 (0.010) | 0.190 (0.010) | 0.195 (0.009) | 0.195 (0.009) | 0.190 (0.011) | 0.199 (0.014) | 0.192 (0.012) | 0.201 (0.014) | 0.192 (0.012) | 0.202 (0.015) |
| 2 | 0.175 (0.012) | 0.203 (0.014) | 0.191 (0.010) | 0.191 (0.010) | 0.194 (0.009) | 0.195 (0.009) | 0.184 (0.012) | 0.211 (0.015) | 0.190 (0.014) | 0.216 (0.017) | 0.186 (0.013) | 0.213 (0.016) |
| 3 | 0.156 (0.015) | 0.170 (0.016) | 0.181 (0.012) | 0.181 (0.012) | 0.184 (0.011) | 0.184 (0.011) | 0.172 (0.014) | 0.198 (0.017) | 0.178 (0.016) | 0.204 (0.019) | 0.174 (0.015) | 0.201 (0.018) |
| 4 | 0.141 (0.018) | 0.143 (0.017) | 0.166 (0.015) | 0.166 (0.015) | 0.173 (0.015) | 0.173 (0.015) | 0.166 (0.019) | 0.174 (0.019) | 0.170 (0.021) | 0.179 (0.021) | 0.168 (0.020) | 0.177 (0.021) |
| 5 | 0.130 (0.021) | 0.124 (0.021) | 0.150 (0.018) | 0.150 (0.017) | 0.164 (0.022) | 0.163 (0.020) | 0.161 (0.024) | 0.152 (0.020) | 0.163 (0.025) | 0.154 (0.021) | 0.163 (0.025) | 0.154 (0.021) |

### A.4.8 Continuous marker: Simulation 3b

- Inter-inspection rate: 1; Measurement error ($\sigma_\epsilon$): 1.2; Association ($\phi$): 1.5

**Table A.13:** Simulation results for continuous marker Scenario 3b.

**(a)** Mean (and standard deviation) of the root mean squared prediction error in 500 simulations for continuous marker Scenario 3b.

| | $\tau$ | JM | JM2 | LM1 | LMInt1 | LM2 | LMInt2 | CC1 | CW1 | CC2 | CW2 | CC3 | CW3 |
|---|---|---|---|---|---|---|---|---|---|---|---|---|---|
| $X=0$ | 0 | 0.288 (0.020) | 0.292 (0.021) | 0.287 (0.018) | 0.287 (0.019) | 0.338 (0.017) | 0.343 (0.018) | 0.289 (0.019) | 0.288 (0.019) | 0.287 (0.019) | 0.286 (0.019) | 0.292 (0.021) | 0.292 (0.021) |
| | 1 | 0.348 (0.016) | 0.359 (0.019) | 0.358 (0.018) | 0.358 (0.018) | 0.374 (0.015) | 0.376 (0.016) | 0.358 (0.018) | 0.371 (0.018) | 0.359 (0.017) | 0.372 (0.017) | 0.361 (0.019) | 0.375 (0.019) |
| | 2 | 0.322 (0.016) | 0.333 (0.019) | 0.351 (0.015) | 0.350 (0.016) | 0.366 (0.014) | 0.368 (0.015) | 0.341 (0.017) | 0.376 (0.020) | 0.343 (0.017) | 0.377 (0.020) | 0.342 (0.018) | 0.378 (0.021) |
| | 3 | 0.283 (0.019) | 0.288 (0.021) | 0.323 (0.016) | 0.323 (0.015) | 0.347 (0.013) | 0.349 (0.014) | 0.313 (0.017) | 0.346 (0.020) | 0.315 (0.018) | 0.347 (0.020) | 0.313 (0.018) | 0.348 (0.021) |
| | 4 | 0.248 (0.022) | 0.249 (0.024) | 0.295 (0.016) | 0.295 (0.017) | 0.331 (0.015) | 0.334 (0.015) | 0.293 (0.017) | 0.305 (0.022) | 0.293 (0.019) | 0.304 (0.023) | 0.293 (0.018) | 0.305 (0.023) |
| | 5 | 0.219 (0.027) | 0.217 (0.027) | 0.272 (0.017) | 0.271 (0.016) | 0.324 (0.013) | 0.326 (0.014) | 0.279 (0.017) | 0.271 (0.022) | 0.278 (0.019) | 0.270 (0.023) | 0.279 (0.018) | 0.271 (0.023) |
| $X=1$ | 0 | 0.335 (0.018) | 0.359 (0.023) | 0.334 (0.019) | 0.333 (0.019) | 0.352 (0.018) | 0.350 (0.018) | 0.336 (0.020) | 0.336 (0.025) | 0.333 (0.022) | 0.332 (0.027) | 0.340 (0.021) | 0.340 (0.026) |
| | 1 | 0.378 (0.015) | 0.424 (0.022) | 0.390 (0.021) | 0.390 (0.020) | 0.391 (0.018) | 0.391 (0.018) | 0.387 (0.020) | 0.403 (0.026) | 0.388 (0.023) | 0.404 (0.028) | 0.390 (0.022) | 0.406 (0.027) |
| | 2 | 0.331 (0.016) | 0.372 (0.021) | 0.372 (0.023) | 0.371 (0.023) | 0.374 (0.023) | 0.373 (0.024) | 0.351 (0.025) | 0.395 (0.027) | 0.353 (0.027) | 0.398 (0.029) | 0.352 (0.026) | 0.398 (0.028) |
| | 3 | 0.288 (0.019) | 0.309 (0.022) | 0.342 (0.024) | 0.342 (0.024) | 0.351 (0.024) | 0.350 (0.024) | 0.323 (0.026) | 0.366 (0.028) | 0.326 (0.029) | 0.370 (0.030) | 0.323 (0.028) | 0.368 (0.029) |
| | 4 | 0.257 (0.024) | 0.263 (0.025) | 0.315 (0.026) | 0.316 (0.027) | 0.339 (0.032) | 0.336 (0.032) | 0.313 (0.031) | 0.326 (0.028) | 0.315 (0.032) | 0.328 (0.029) | 0.314 (0.032) | 0.327 (0.029) |
| | 5 | 0.234 (0.029) | 0.233 (0.030) | 0.295 (0.030) | 0.296 (0.029) | 0.337 (0.032) | 0.334 (0.032) | 0.311 (0.038) | 0.296 (0.032) | 0.312 (0.040) | 0.296 (0.033) | 0.312 (0.040) | 0.296 (0.034) |

**(b)** Mean (and standard deviation) of the AUC in 500 simulations for continuous marker Scenario 3b.

| $\tau$ | JM | JM2 | LM1 | LMInt1 | LM2 | LMInt2 | CC1 | CW1 | CC2 | CW2 | CC3 | CW3 |
|---|---|---|---|---|---|---|---|---|---|---|---|---|
| 0 | 0.718 (0.033) | 0.697 (0.034) | 0.723 (0.032) | 0.724 (0.032) | 0.717 (0.034) | 0.712 (0.035) | 0.724 (0.032) | 0.724 (0.032) | 0.724 (0.032) | 0.724 (0.032) | 0.724 (0.033) | 0.724 (0.033) |
| 1 | 0.788 (0.024) | 0.772 (0.024) | 0.762 (0.025) | 0.763 (0.025) | 0.757 (0.026) | 0.753 (0.027) | 0.774 (0.024) | 0.774 (0.024) | 0.774 (0.024) | 0.774 (0.024) | 0.774 (0.024) | 0.774 (0.024) |
| 2 | 0.874 (0.018) | 0.865 (0.019) | 0.827 (0.022) | 0.827 (0.022) | 0.824 (0.022) | 0.822 (0.023) | 0.852 (0.021) | 0.852 (0.021) | 0.852 (0.021) | 0.852 (0.021) | 0.851 (0.021) | 0.851 (0.021) |
| 3 | 0.916 (0.016) | 0.912 (0.016) | 0.868 (0.020) | 0.868 (0.020) | 0.868 (0.021) | 0.867 (0.021) | 0.888 (0.019) | 0.888 (0.019) | 0.888 (0.019) | 0.888 (0.019) | 0.888 (0.019) | 0.888 (0.019) |
| 4 | 0.937 (0.016) | 0.936 (0.016) | 0.894 (0.023) | 0.894 (0.023) | 0.894 (0.023) | 0.894 (0.023) | 0.904 (0.021) | 0.904 (0.021) | 0.904 (0.021) | 0.904 (0.021) | 0.904 (0.021) | 0.904 (0.021) |
| 5 | 0.948 (0.018) | 0.948 (0.018) | 0.909 (0.026) | 0.909 (0.026) | 0.909 (0.026) | 0.908 (0.026) | 0.907 (0.027) | 0.908 (0.027) | 0.907 (0.026) | 0.908 (0.026) | 0.908 (0.027) | 0.908 (0.026) |

**(c)** Mean (and standard deviation) of the Brier Score in 500 simulations for continuous marker Scenario 3b.

| $\tau$ | JM | JM2 | LM1 | LMInt1 | LM2 | LMInt2 | CC1 | CW1 | CC2 | CW2 | CC3 | CW3 |
|---|---|---|---|---|---|---|---|---|---|---|---|---|
| 0 | 0.135 (0.011) | 0.145 (0.014) | 0.135 (0.011) | 0.135 (0.011) | 0.157 (0.010) | 0.158 (0.010) | 0.136 (0.011) | 0.136 (0.011) | 0.134 (0.011) | 0.134 (0.011) | 0.138 (0.012) | 0.138 (0.012) |
| 1 | 0.172 (0.010) | 0.195 (0.014) | 0.181 (0.010) | 0.180 (0.011) | 0.187 (0.009) | 0.187 (0.009) | 0.179 (0.011) | 0.190 (0.014) | 0.180 (0.012) | 0.191 (0.014) | 0.181 (0.012) | 0.193 (0.015) |
| 2 | 0.144 (0.011) | 0.162 (0.012) | 0.167 (0.011) | 0.167 (0.011) | 0.174 (0.009) | 0.175 (0.009) | 0.157 (0.011) | 0.186 (0.015) | 0.158 (0.013) | 0.187 (0.016) | 0.157 (0.012) | 0.188 (0.016) |
| 3 | 0.118 (0.012) | 0.125 (0.013) | 0.147 (0.012) | 0.147 (0.012) | 0.158 (0.012) | 0.158 (0.011) | 0.138 (0.012) | 0.163 (0.016) | 0.139 (0.014) | 0.165 (0.018) | 0.138 (0.013) | 0.164 (0.017) |
| 4 | 0.101 (0.014) | 0.103 (0.014) | 0.130 (0.014) | 0.130 (0.014) | 0.150 (0.017) | 0.150 (0.017) | 0.129 (0.015) | 0.137 (0.016) | 0.130 (0.016) | 0.137 (0.017) | 0.129 (0.016) | 0.137 (0.017) |
| 5 | 0.090 (0.016) | 0.089 (0.016) | 0.119 (0.017) | 0.119 (0.017) | 0.148 (0.022) | 0.148 (0.022) | 0.126 (0.020) | 0.119 (0.018) | 0.126 (0.021) | 0.119 (0.018) | 0.126 (0.021) | 0.119 (0.019) |

### A.4.9 Continuous marker: Simulation 3c

- Fixed inspection time every year; Measurement error ($\sigma_\epsilon$): 1.2; Association ($\phi$): 1.5

**Table A.14:** Simulation results for continuous marker Scenario 3c.

**(a)** Mean (and standard deviation) of the root mean squared prediction error in 500 simulations for continuous marker Scenario 3c.

| | $\tau$ | JM | JM2 | LM1 | LMInt1 | LM2 | LMInt2 | CC1 | CW1 | CC2 | CW2 | CC3 | CW3 |
|---|---|---|---|---|---|---|---|---|---|---|---|---|---|
| | 0 | 0.287 (0.019) | 0.293 (0.021) | 0.289 (0.018) | 0.288 (0.019) | 0.337 (0.016) | 0.341 (0.017) | 0.288 (0.020) | 0.288 (0.020) | 0.286 (0.019) | 0.285 (0.020) | 0.292 (0.021) | 0.292 (0.021) |
| | 1 | 0.299 (0.017) | 0.302 (0.017) | 0.301 (0.019) | 0.300 (0.019) | 0.355 (0.016) | 0.358 (0.016) | 0.301 (0.019) | 0.323 (0.019) | 0.301 (0.018) | 0.323 (0.017) | 0.300 (0.020) | 0.324 (0.020) |
| | 2 | 0.253 (0.018) | 0.256 (0.018) | 0.268 (0.016) | 0.268 (0.016) | 0.343 (0.016) | 0.346 (0.017) | 0.272 (0.016) | 0.302 (0.020) | 0.269 (0.016) | 0.297 (0.020) | 0.270 (0.017) | 0.301 (0.021) |
| $X = 0$ | 3 | 0.217 (0.020) | 0.221 (0.019) | 0.244 (0.015) | 0.244 (0.015) | 0.331 (0.013) | 0.333 (0.014) | 0.251 (0.015) | 0.265 (0.019) | 0.248 (0.015) | 0.257 (0.019) | 0.249 (0.015) | 0.261 (0.020) |
| | 4 | 0.193 (0.021) | 0.195 (0.021) | 0.230 (0.017) | 0.230 (0.018) | 0.328 (0.019) | 0.330 (0.020) | 0.237 (0.015) | 0.235 (0.019) | 0.233 (0.017) | 0.229 (0.021) | 0.234 (0.017) | 0.230 (0.021) |
| | 5 | 0.176 (0.024) | 0.176 (0.025) | 0.224 (0.017) | 0.223 (0.017) | 0.332 (0.018) | 0.334 (0.019) | 0.229 (0.015) | 0.236 (0.020) | 0.227 (0.017) | 0.234 (0.021) | 0.226 (0.017) | 0.234 (0.021) |
| | 0 | 0.335 (0.018) | 0.365 (0.023) | 0.335 (0.019) | 0.335 (0.020) | 0.348 (0.022) | 0.346 (0.022) | 0.337 (0.017) | 0.337 (0.020) | 0.333 (0.020) | 0.333 (0.021) | 0.341 (0.018) | 0.341 (0.021) |
| | 1 | 0.322 (0.015) | 0.343 (0.017) | 0.325 (0.019) | 0.325 (0.019) | 0.352 (0.024) | 0.349 (0.025) | 0.325 (0.018) | 0.349 (0.020) | 0.325 (0.020) | 0.349 (0.022) | 0.324 (0.019) | 0.350 (0.022) |
| | 2 | 0.258 (0.018) | 0.271 (0.020) | 0.274 (0.021) | 0.274 (0.021) | 0.329 (0.026) | 0.326 (0.026) | 0.277 (0.019) | 0.313 (0.018) | 0.273 (0.021) | 0.310 (0.020) | 0.275 (0.021) | 0.312 (0.019) |
| $X = 1$ | 3 | 0.219 (0.020) | 0.227 (0.020) | 0.247 (0.024) | 0.248 (0.023) | 0.324 (0.029) | 0.321 (0.030) | 0.254 (0.021) | 0.271 (0.020) | 0.249 (0.023) | 0.265 (0.022) | 0.252 (0.023) | 0.268 (0.022) |
| | 4 | 0.199 (0.023) | 0.201 (0.022) | 0.237 (0.025) | 0.238 (0.026) | 0.333 (0.033) | 0.329 (0.033) | 0.245 (0.024) | 0.243 (0.025) | 0.240 (0.025) | 0.237 (0.027) | 0.241 (0.026) | 0.239 (0.027) |
| | 5 | 0.184 (0.026) | 0.185 (0.025) | 0.233 (0.027) | 0.234 (0.027) | 0.349 (0.039) | 0.345 (0.039) | 0.242 (0.025) | 0.256 (0.030) | 0.239 (0.027) | 0.254 (0.032) | 0.239 (0.028) | 0.254 (0.033) |

**(b)** Mean (and standard deviation) of the AUC in 500 simulations for continuous marker Scenario 3c.

| $\tau$ | JM | JM2 | LM1 | LMInt1 | LM2 | LMInt2 | CC1 | CW1 | CC2 | CW2 | CC3 | CW3 |
|---|---|---|---|---|---|---|---|---|---|---|---|---|
| 0 | 0.719 (0.033) | 0.695 (0.034) | 0.723 (0.032) | 0.726 (0.032) | 0.717 (0.032) | 0.712 (0.033) | 0.727 (0.032) | 0.727 (0.032) | 0.727 (0.032) | 0.726 (0.032) | 0.726 (0.032) | 0.726 (0.032) |
| 1 | 0.869 (0.019) | 0.864 (0.018) | 0.869 (0.018) | 0.869 (0.018) | 0.867 (0.018) | 0.866 (0.019) | 0.869 (0.018) | 0.869 (0.018) | 0.869 (0.018) | 0.869 (0.018) | 0.869 (0.018) | 0.868 (0.018) |
| 2 | 0.935 (0.013) | 0.933 (0.014) | 0.926 (0.014) | 0.926 (0.014) | 0.926 (0.014) | 0.926 (0.013) | 0.926 (0.014) | 0.926 (0.014) | 0.926 (0.014) | 0.926 (0.014) | 0.926 (0.014) | 0.926 (0.014) |
| 3 | 0.956 (0.011) | 0.955 (0.010) | 0.944 (0.013) | 0.944 (0.013) | 0.944 (0.013) | 0.944 (0.013) | 0.944 (0.013) | 0.944 (0.013) | 0.944 (0.013) | 0.944 (0.013) | 0.944 (0.013) | 0.944 (0.013) |
| 4 | 0.963 (0.011) | 0.962 (0.011) | 0.949 (0.014) | 0.949 (0.014) | 0.948 (0.014) | 0.948 (0.014) | 0.948 (0.014) | 0.948 (0.014) | 0.948 (0.014) | 0.948 (0.014) | 0.948 (0.014) | 0.948 (0.014) |
| 5 | 0.966 (0.013) | 0.965 (0.013) | 0.948 (0.017) | 0.948 (0.017) | 0.947 (0.018) | 0.946 (0.018) | 0.947 (0.018) | 0.947 (0.018) | 0.948 (0.018) | 0.947 (0.018) | 0.947 (0.018) | 0.947 (0.018) |

**(c)** Mean (and standard deviation) of the Brier Score in 500 simulations for continuous marker Scenario 3c.

| $\tau$ | JM | JM2 | LM1 | LMInt1 | LM2 | LMInt2 | CC1 | CW1 | CC2 | CW2 | CC3 | CW3 |
|---|---|---|---|---|---|---|---|---|---|---|---|---|
| 0 | 0.135 (0.011) | 0.147 (0.014) | 0.136 (0.011) | 0.135 (0.011) | 0.155 (0.010) | 0.156 (0.010) | 0.136 (0.012) | 0.136 (0.012) | 0.134 (0.011) | 0.134 (0.011) | 0.139 (0.012) | 0.138 (0.012) |
| 1 | 0.137 (0.011) | 0.146 (0.011) | 0.139 (0.010) | 0.139 (0.010) | 0.166 (0.010) | 0.166 (0.010) | 0.139 (0.010) | 0.154 (0.012) | 0.139 (0.010) | 0.154 (0.012) | 0.139 (0.010) | 0.155 (0.012) |
| 2 | 0.103 (0.011) | 0.107 (0.012) | 0.111 (0.010) | 0.111 (0.010) | 0.150 (0.013) | 0.150 (0.012) | 0.113 (0.009) | 0.132 (0.011) | 0.111 (0.010) | 0.129 (0.012) | 0.112 (0.010) | 0.131 (0.012) |
| 3 | 0.084 (0.011) | 0.086 (0.011) | 0.097 (0.011) | 0.097 (0.011) | 0.144 (0.016) | 0.144 (0.015) | 0.100 (0.010) | 0.108 (0.011) | 0.098 (0.012) | 0.105 (0.012) | 0.099 (0.011) | 0.107 (0.012) |
| 4 | 0.076 (0.012) | 0.078 (0.012) | 0.093 (0.012) | 0.093 (0.012) | 0.147 (0.018) | 0.147 (0.018) | 0.096 (0.012) | 0.095 (0.011) | 0.094 (0.013) | 0.092 (0.012) | 0.094 (0.013) | 0.093 (0.012) |
| 5 | 0.072 (0.015) | 0.073 (0.015) | 0.091 (0.015) | 0.091 (0.015) | 0.155 (0.025) | 0.155 (0.025) | 0.095 (0.015) | 0.099 (0.016) | 0.094 (0.015) | 0.099 (0.017) | 0.093 (0.016) | 0.099 (0.018) |

### A.4.10 Continuous marker: Simulation 4a

- Inter-inspection rate: 0.5; Measurement error ($\sigma_\epsilon$): 1.2; Association ($\phi$): 0.5

**Table A.15:** Simulation results for continuous marker Scenario 4a.

**(a)** Mean (and standard deviation) of the root mean squared prediction error in 500 simulations for continuous marker Scenario 4a.

| | $\tau$ | JM | JM2 | LM1 | LMInt1 | LM2 | LMInt2 | CC1 | CW1 | CC2 | CW2 | CC3 | CW3 |
|---|---|---|---|---|---|---|---|---|---|---|---|---|---|
| | 0 | 0.135 (0.014) | 0.138 (0.016) | 0.136 (0.014) | 0.136 (0.014) | 0.232 (0.022) | 0.238 (0.024) | 0.138 (0.014) | 0.141 (0.013) | 0.136 (0.014) | 0.138 (0.013) | 0.145 (0.015) | 0.148 (0.015) |
| | 1 | 0.231 (0.014) | 0.239 (0.017) | 0.237 (0.015) | 0.236 (0.014) | 0.265 (0.019) | 0.268 (0.019) | 0.238 (0.014) | 0.238 (0.013) | 0.238 (0.014) | 0.239 (0.013) | 0.242 (0.015) | 0.243 (0.014) |
| | 2 | 0.264 (0.014) | 0.275 (0.017) | 0.282 (0.014) | 0.281 (0.014) | 0.294 (0.016) | 0.296 (0.017) | 0.275 (0.014) | 0.290 (0.016) | 0.278 (0.014) | 0.292 (0.016) | 0.277 (0.015) | 0.293 (0.016) |
| $X = 0$ | 3 | 0.255 (0.015) | 0.261 (0.018) | 0.286 (0.014) | 0.285 (0.014) | 0.296 (0.013) | 0.298 (0.013) | 0.271 (0.014) | 0.297 (0.016) | 0.274 (0.015) | 0.298 (0.016) | 0.273 (0.015) | 0.299 (0.017) |
| | 4 | 0.236 (0.017) | 0.234 (0.020) | 0.272 (0.014) | 0.271 (0.015) | 0.286 (0.014) | 0.287 (0.015) | 0.257 (0.015) | 0.279 (0.019) | 0.259 (0.016) | 0.280 (0.019) | 0.259 (0.016) | 0.281 (0.019) |
| | 5 | 0.219 (0.022) | 0.209 (0.021) | 0.250 (0.014) | 0.249 (0.014) | 0.273 (0.013) | 0.275 (0.014) | 0.250 (0.015) | 0.252 (0.020) | 0.250 (0.016) | 0.252 (0.021) | 0.251 (0.016) | 0.254 (0.021) |
| | 0 | 0.187 (0.014) | 0.205 (0.019) | 0.188 (0.016) | 0.188 (0.017) | 0.243 (0.016) | 0.239 (0.016) | 0.189 (0.017) | 0.193 (0.022) | 0.187 (0.019) | 0.190 (0.023) | 0.195 (0.018) | 0.198 (0.023) |
| | 1 | 0.281 (0.013) | 0.321 (0.020) | 0.289 (0.015) | 0.289 (0.015) | 0.293 (0.015) | 0.292 (0.015) | 0.287 (0.017) | 0.292 (0.024) | 0.288 (0.019) | 0.292 (0.025) | 0.291 (0.019) | 0.296 (0.025) |
| | 2 | 0.290 (0.013) | 0.338 (0.019) | 0.317 (0.019) | 0.317 (0.020) | 0.320 (0.020) | 0.320 (0.020) | 0.302 (0.021) | 0.329 (0.024) | 0.305 (0.023) | 0.331 (0.025) | 0.304 (0.023) | 0.332 (0.025) |
| $X = 1$ | 3 | 0.267 (0.015) | 0.303 (0.020) | 0.312 (0.020) | 0.312 (0.019) | 0.314 (0.018) | 0.315 (0.019) | 0.286 (0.024) | 0.324 (0.027) | 0.289 (0.026) | 0.328 (0.029) | 0.288 (0.026) | 0.328 (0.029) |
| | 4 | 0.245 (0.021) | 0.259 (0.023) | 0.295 (0.022) | 0.296 (0.023) | 0.298 (0.027) | 0.297 (0.027) | 0.273 (0.026) | 0.301 (0.027) | 0.276 (0.027) | 0.305 (0.028) | 0.276 (0.028) | 0.305 (0.028) |
| | 5 | 0.229 (0.027) | 0.224 (0.026) | 0.273 (0.025) | 0.273 (0.024) | 0.281 (0.025) | 0.280 (0.025) | 0.273 (0.033) | 0.272 (0.031) | 0.274 (0.033) | 0.273 (0.032) | 0.277 (0.035) | 0.275 (0.033) |

**(b)** Mean (and standard deviation) of the AUC in 500 simulations for continuous marker Scenario 4a.

| $\tau$ | JM | JM2 | LM1 | LMInt1 | LM2 | LMInt2 | CC1 | CW1 | CC2 | CW2 | CC3 | CW3 |
|---|---|---|---|---|---|---|---|---|---|---|---|---|
| 0 | 0.677 (0.038) | 0.664 (0.037) | 0.677 (0.038) | 0.678 (0.038) | 0.673 (0.039) | 0.668 (0.041) | 0.678 (0.038) | 0.679 (0.038) | 0.679 (0.038) | 0.679 (0.038) | 0.676 (0.038) | 0.677 (0.038) |
| 1 | 0.721 (0.028) | 0.706 (0.028) | 0.708 (0.029) | 0.709 (0.029) | 0.702 (0.030) | 0.697 (0.031) | 0.715 (0.028) | 0.715 (0.028) | 0.715 (0.028) | 0.715 (0.028) | 0.715 (0.028) | 0.715 (0.028) |
| 2 | 0.788 (0.025) | 0.772 (0.025) | 0.750 (0.027) | 0.751 (0.027) | 0.744 (0.028) | 0.741 (0.029) | 0.775 (0.026) | 0.775 (0.025) | 0.775 (0.026) | 0.775 (0.026) | 0.775 (0.026) | 0.774 (0.026) |
| 3 | 0.837 (0.024) | 0.825 (0.024) | 0.787 (0.026) | 0.788 (0.026) | 0.783 (0.026) | 0.780 (0.027) | 0.820 (0.025) | 0.820 (0.025) | 0.819 (0.025) | 0.819 (0.025) | 0.819 (0.025) | 0.819 (0.025) |
| 4 | 0.866 (0.026) | 0.860 (0.026) | 0.817 (0.029) | 0.817 (0.029) | 0.814 (0.030) | 0.813 (0.030) | 0.845 (0.027) | 0.845 (0.027) | 0.845 (0.027) | 0.845 (0.027) | 0.845 (0.027) | 0.845 (0.027) |
| 5 | 0.882 (0.026) | 0.881 (0.026) | 0.841 (0.032) | 0.841 (0.032) | 0.840 (0.032) | 0.839 (0.032) | 0.857 (0.030) | 0.858 (0.030) | 0.858 (0.030) | 0.858 (0.030) | 0.857 (0.030) | 0.857 (0.030) |

**(c)** Mean (and standard deviation) of the Brier Score in 500 simulations for continuous marker Scenario 4a.

| $\tau$ | JM | JM2 | LM1 | LMInt1 | LM2 | LMInt2 | CC1 | CW1 | CC2 | CW2 | CC3 | CW3 |
|---|---|---|---|---|---|---|---|---|---|---|---|---|
| 0 | 0.113 (0.012) | 0.117 (0.014) | 0.113 (0.012) | 0.113 (0.012) | 0.142 (0.010) | 0.143 (0.010) | 0.113 (0.012) | 0.114 (0.011) | 0.113 (0.012) | 0.113 (0.011) | 0.115 (0.012) | 0.116 (0.011) |
| 1 | 0.174 (0.010) | 0.188 (0.014) | 0.177 (0.011) | 0.177 (0.011) | 0.185 (0.008) | 0.186 (0.009) | 0.177 (0.011) | 0.178 (0.013) | 0.177 (0.011) | 0.179 (0.013) | 0.179 (0.012) | 0.180 (0.013) |
| 2 | 0.180 (0.010) | 0.198 (0.014) | 0.193 (0.010) | 0.193 (0.010) | 0.198 (0.009) | 0.199 (0.009) | 0.187 (0.011) | 0.200 (0.014) | 0.188 (0.012) | 0.201 (0.015) | 0.188 (0.012) | 0.201 (0.015) |
| 3 | 0.164 (0.012) | 0.176 (0.013) | 0.186 (0.011) | 0.185 (0.011) | 0.190 (0.009) | 0.190 (0.010) | 0.174 (0.012) | 0.193 (0.016) | 0.175 (0.014) | 0.194 (0.017) | 0.175 (0.014) | 0.195 (0.017) |
| 4 | 0.151 (0.015) | 0.154 (0.015) | 0.173 (0.013) | 0.173 (0.013) | 0.178 (0.013) | 0.179 (0.013) | 0.163 (0.015) | 0.177 (0.017) | 0.164 (0.017) | 0.179 (0.018) | 0.164 (0.017) | 0.179 (0.018) |
| 5 | 0.142 (0.017) | 0.139 (0.016) | 0.160 (0.016) | 0.160 (0.016) | 0.169 (0.018) | 0.170 (0.018) | 0.160 (0.019) | 0.161 (0.019) | 0.161 (0.020) | 0.161 (0.020) | 0.161 (0.020) | 0.162 (0.020) |

### A.4.11 Continuous marker: Simulation 4b

- Inter-inspection rate: 1; Measurement error ($\sigma_\epsilon$): 1.2; Association ($\phi$): 0.5

**Table A.16:** Simulation results for continuous marker Scenario 4b.

**(a)** Mean (and standard deviation) of the root mean squared prediction error in 500 simulations for continuous marker Scenario 4b.

| | $\tau$ | JM | JM2 | LM1 | LMInt1 | LM2 | LMInt2 | CC1 | CW1 | CC2 | CW2 | CC3 | CW3 |
|---|---|---|---|---|---|---|---|---|---|---|---|---|---|
| | 0 | 0.135 (0.014) | 0.137 (0.016) | 0.136 (0.014) | 0.136 (0.014) | 0.234 (0.021) | 0.241 (0.024) | 0.139 (0.014) | 0.142 (0.014) | 0.136 (0.014) | 0.138 (0.013) | 0.146 (0.015) | 0.149 (0.015) |
| | 1 | 0.218 (0.014) | 0.224 (0.016) | 0.227 (0.015) | 0.227 (0.014) | 0.261 (0.020) | 0.266 (0.019) | 0.227 (0.014) | 0.229 (0.013) | 0.227 (0.014) | 0.229 (0.013) | 0.232 (0.015) | 0.234 (0.015) |
| | 2 | 0.226 (0.013) | 0.232 (0.016) | 0.252 (0.014) | 0.251 (0.014) | 0.278 (0.016) | 0.281 (0.017) | 0.242 (0.014) | 0.262 (0.015) | 0.242 (0.014) | 0.262 (0.015) | 0.243 (0.015) | 0.264 (0.016) |
| $X = 0$ | 3 | 0.199 (0.014) | 0.201 (0.016) | 0.239 (0.015) | 0.238 (0.014) | 0.270 (0.013) | 0.273 (0.013) | 0.223 (0.015) | 0.254 (0.016) | 0.223 (0.015) | 0.252 (0.016) | 0.223 (0.015) | 0.254 (0.017) |
| | 4 | 0.169 (0.016) | 0.169 (0.017) | 0.216 (0.015) | 0.215 (0.015) | 0.258 (0.015) | 0.260 (0.016) | 0.204 (0.015) | 0.228 (0.018) | 0.202 (0.015) | 0.225 (0.018) | 0.203 (0.016) | 0.227 (0.019) |
| | 5 | 0.147 (0.019) | 0.144 (0.019) | 0.195 (0.015) | 0.194 (0.014) | 0.251 (0.012) | 0.254 (0.013) | 0.195 (0.014) | 0.197 (0.020) | 0.193 (0.015) | 0.196 (0.020) | 0.194 (0.016) | 0.195 (0.021) |
| | 0 | 0.187 (0.014) | 0.206 (0.018) | 0.188 (0.016) | 0.188 (0.017) | 0.241 (0.017) | 0.236 (0.018) | 0.190 (0.015) | 0.194 (0.020) | 0.187 (0.016) | 0.190 (0.021) | 0.196 (0.016) | 0.200 (0.022) |
| | 1 | 0.265 (0.013) | 0.301 (0.019) | 0.278 (0.016) | 0.278 (0.016) | 0.284 (0.015) | 0.282 (0.015) | 0.275 (0.015) | 0.281 (0.022) | 0.275 (0.016) | 0.281 (0.024) | 0.278 (0.017) | 0.284 (0.024) |
| | 2 | 0.248 (0.014) | 0.282 (0.019) | 0.286 (0.019) | 0.286 (0.020) | 0.292 (0.023) | 0.291 (0.024) | 0.267 (0.019) | 0.299 (0.023) | 0.267 (0.020) | 0.299 (0.023) | 0.267 (0.020) | 0.301 (0.024) |
| $X = 1$ | 3 | 0.208 (0.015) | 0.227 (0.018) | 0.262 (0.021) | 0.263 (0.021) | 0.272 (0.021) | 0.270 (0.021) | 0.237 (0.020) | 0.280 (0.024) | 0.236 (0.021) | 0.280 (0.026) | 0.236 (0.022) | 0.281 (0.026) |
| | 4 | 0.178 (0.018) | 0.183 (0.020) | 0.235 (0.021) | 0.235 (0.022) | 0.256 (0.030) | 0.253 (0.031) | 0.219 (0.024) | 0.248 (0.023) | 0.218 (0.024) | 0.248 (0.023) | 0.218 (0.025) | 0.248 (0.024) |
| | 5 | 0.156 (0.022) | 0.153 (0.021) | 0.211 (0.023) | 0.212 (0.022) | 0.249 (0.030) | 0.245 (0.029) | 0.214 (0.027) | 0.213 (0.025) | 0.214 (0.028) | 0.212 (0.026) | 0.214 (0.029) | 0.212 (0.027) |

**(b)** Mean (and standard deviation) of the AUC in 500 simulations for continuous marker Scenario 4b.

| $\tau$ | JM | JM2 | LM1 | LMInt1 | LM2 | LMInt2 | CC1 | CW1 | CC2 | CW2 | CC3 | CW3 |
|---|---|---|---|---|---|---|---|---|---|---|---|---|
| 0 | 0.677 (0.038) | 0.663 (0.039) | 0.677 (0.039) | 0.678 (0.039) | 0.672 (0.039) | 0.665 (0.041) | 0.678 (0.038) | 0.679 (0.038) | 0.679 (0.038) | 0.679 (0.038) | 0.677 (0.038) | 0.678 (0.038) |
| 1 | 0.751 (0.028) | 0.738 (0.028) | 0.729 (0.029) | 0.730 (0.029) | 0.724 (0.031) | 0.719 (0.032) | 0.738 (0.028) | 0.738 (0.028) | 0.738 (0.028) | 0.738 (0.028) | 0.738 (0.028) | 0.738 (0.028) |
| 2 | 0.835 (0.022) | 0.826 (0.022) | 0.794 (0.024) | 0.794 (0.024) | 0.791 (0.025) | 0.789 (0.026) | 0.818 (0.023) | 0.818 (0.023) | 0.818 (0.023) | 0.818 (0.023) | 0.818 (0.023) | 0.818 (0.023) |
| 3 | 0.886 (0.019) | 0.881 (0.019) | 0.848 (0.022) | 0.848 (0.022) | 0.846 (0.023) | 0.845 (0.023) | 0.868 (0.021) | 0.868 (0.021) | 0.868 (0.021) | 0.868 (0.021) | 0.868 (0.021) | 0.867 (0.021) |
| 4 | 0.908 (0.020) | 0.906 (0.020) | 0.876 (0.023) | 0.876 (0.023) | 0.875 (0.024) | 0.875 (0.024) | 0.889 (0.021) | 0.889 (0.021) | 0.889 (0.021) | 0.889 (0.021) | 0.889 (0.021) | 0.888 (0.021) |
| 5 | 0.918 (0.021) | 0.918 (0.021) | 0.893 (0.025) | 0.893 (0.025) | 0.893 (0.025) | 0.893 (0.025) | 0.897 (0.025) | 0.897 (0.024) | 0.897 (0.024) | 0.897 (0.024) | 0.897 (0.024) | 0.897 (0.024) |

**(c)** Mean (and standard deviation) of the Brier Score in 500 simulations for continuous marker Scenario 4b.

| $\tau$ | JM | JM2 | LM1 | LMInt1 | LM2 | LMInt2 | CC1 | CW1 | CC2 | CW2 | CC3 | CW3 |
|---|---|---|---|---|---|---|---|---|---|---|---|---|
| 0 | 0.113 (0.012) | 0.117 (0.014) | 0.113 (0.012) | 0.113 (0.012) | 0.142 (0.010) | 0.143 (0.010) | 0.114 (0.012) | 0.115 (0.011) | 0.113 (0.012) | 0.113 (0.011) | 0.116 (0.012) | 0.117 (0.011) |
| 1 | 0.166 (0.010) | 0.177 (0.013) | 0.172 (0.010) | 0.171 (0.010) | 0.182 (0.009) | 0.182 (0.009) | 0.171 (0.011) | 0.173 (0.012) | 0.171 (0.011) | 0.173 (0.012) | 0.173 (0.012) | 0.175 (0.013) |
| 2 | 0.160 (0.011) | 0.170 (0.013) | 0.177 (0.010) | 0.177 (0.010) | 0.185 (0.009) | 0.186 (0.009) | 0.169 (0.011) | 0.183 (0.014) | 0.169 (0.012) | 0.182 (0.014) | 0.169 (0.012) | 0.184 (0.015) |
| 3 | 0.137 (0.012) | 0.142 (0.013) | 0.158 (0.011) | 0.158 (0.011) | 0.170 (0.011) | 0.170 (0.011) | 0.149 (0.011) | 0.167 (0.014) | 0.148 (0.012) | 0.167 (0.015) | 0.148 (0.012) | 0.168 (0.015) |
| 4 | 0.123 (0.014) | 0.124 (0.014) | 0.143 (0.013) | 0.143 (0.013) | 0.159 (0.015) | 0.159 (0.015) | 0.138 (0.013) | 0.150 (0.015) | 0.137 (0.014) | 0.149 (0.015) | 0.137 (0.014) | 0.150 (0.016) |
| 5 | 0.115 (0.016) | 0.114 (0.015) | 0.133 (0.015) | 0.132 (0.015) | 0.155 (0.020) | 0.155 (0.020) | 0.134 (0.016) | 0.134 (0.016) | 0.133 (0.017) | 0.134 (0.016) | 0.133 (0.017) | 0.133 (0.017) |

### A.4.12 Continuous marker: Simulation 4c

- Fixed inspection time every year; Measurement error ($\sigma_\epsilon$): 1.2; Association ($\phi$): 0.5

**Table A.17:** Simulation results for continuous marker Scenario 4c.

**(a)** Mean (and standard deviation) of the root mean squared prediction error in 500 simulations for continuous marker Scenario 4c.

| | $\tau$ | JM | JM2 | LM1 | LMInt1 | LM2 | LMInt2 | CC1 | CW1 | CC2 | CW2 | CC3 | CW3 |
|---|---|---|---|---|---|---|---|---|---|---|---|---|---|
| | 0 | 0.135 (0.014) | 0.137 (0.016) | 0.139 (0.013) | 0.138 (0.014) | 0.234 (0.019) | 0.241 (0.021) | 0.140 (0.014) | 0.142 (0.013) | 0.136 (0.014) | 0.138 (0.013) | 0.146 (0.015) | 0.149 (0.014) |
| | 1 | 0.179 (0.013) | 0.182 (0.013) | 0.183 (0.015) | 0.182 (0.014) | 0.260 (0.018) | 0.264 (0.019) | 0.182 (0.014) | 0.189 (0.014) | 0.182 (0.014) | 0.189 (0.013) | 0.182 (0.015) | 0.189 (0.015) |
| | 2 | 0.162 (0.012) | 0.164 (0.013) | 0.176 (0.012) | 0.175 (0.013) | 0.266 (0.017) | 0.269 (0.019) | 0.179 (0.013) | 0.200 (0.015) | 0.177 (0.013) | 0.196 (0.015) | 0.176 (0.014) | 0.196 (0.016) |
| $X = 0$ | 3 | 0.137 (0.011) | 0.137 (0.012) | 0.160 (0.012) | 0.159 (0.011) | 0.260 (0.014) | 0.263 (0.015) | 0.169 (0.012) | 0.184 (0.014) | 0.166 (0.012) | 0.177 (0.014) | 0.166 (0.013) | 0.178 (0.015) |
| | 4 | 0.117 (0.011) | 0.118 (0.011) | 0.148 (0.011) | 0.147 (0.012) | 0.256 (0.019) | 0.258 (0.020) | 0.157 (0.011) | 0.159 (0.016) | 0.154 (0.012) | 0.153 (0.015) | 0.154 (0.012) | 0.153 (0.016) |
| | 5 | 0.103 (0.012) | 0.104 (0.012) | 0.141 (0.012) | 0.141 (0.012) | 0.260 (0.016) | 0.261 (0.017) | 0.149 (0.011) | 0.145 (0.018) | 0.146 (0.011) | 0.142 (0.019) | 0.145 (0.012) | 0.140 (0.019) |
| | 0 | 0.187 (0.014) | 0.207 (0.018) | 0.188 (0.013) | 0.188 (0.013) | 0.235 (0.021) | 0.231 (0.022) | 0.190 (0.013) | 0.194 (0.015) | 0.187 (0.014) | 0.189 (0.015) | 0.197 (0.014) | 0.200 (0.016) |
| | 1 | 0.217 (0.011) | 0.231 (0.014) | 0.220 (0.013) | 0.220 (0.013) | 0.260 (0.021) | 0.256 (0.022) | 0.223 (0.014) | 0.233 (0.017) | 0.223 (0.014) | 0.233 (0.017) | 0.222 (0.014) | 0.233 (0.018) |
| | 2 | 0.177 (0.012) | 0.185 (0.014) | 0.192 (0.014) | 0.193 (0.014) | 0.252 (0.026) | 0.248 (0.026) | 0.197 (0.015) | 0.230 (0.014) | 0.194 (0.016) | 0.226 (0.014) | 0.194 (0.017) | 0.226 (0.014) |
| $X = 1$ | 3 | 0.143 (0.012) | 0.147 (0.013) | 0.167 (0.015) | 0.168 (0.015) | 0.244 (0.027) | 0.240 (0.027) | 0.177 (0.015) | 0.200 (0.015) | 0.172 (0.016) | 0.195 (0.016) | 0.173 (0.017) | 0.196 (0.016) |
| | 4 | 0.122 (0.012) | 0.124 (0.013) | 0.153 (0.016) | 0.153 (0.016) | 0.245 (0.032) | 0.241 (0.032) | 0.164 (0.016) | 0.167 (0.014) | 0.160 (0.017) | 0.162 (0.014) | 0.161 (0.018) | 0.161 (0.015) |
| | 5 | 0.109 (0.014) | 0.109 (0.015) | 0.147 (0.018) | 0.148 (0.018) | 0.256 (0.035) | 0.252 (0.035) | 0.159 (0.019) | 0.157 (0.018) | 0.157 (0.019) | 0.154 (0.019) | 0.155 (0.021) | 0.153 (0.020) |

**(b)** Mean (and standard deviation) of the AUC in 500 simulations for continuous marker Scenario 4c.

| $\tau$ | JM | JM2 | LM1 | LMInt1 | LM2 | LMInt2 | CC1 | CW1 | CC2 | CW2 | CC3 | CW3 |
|---|---|---|---|---|---|---|---|---|---|---|---|---|
| 0 | 0.679 (0.037) | 0.665 (0.037) | 0.676 (0.037) | 0.679 (0.037) | 0.672 (0.038) | 0.666 (0.040) | 0.680 (0.037) | 0.681 (0.037) | 0.681 (0.037) | 0.681 (0.037) | 0.679 (0.037) | 0.680 (0.037) |
| 1 | 0.813 (0.023) | 0.808 (0.024) | 0.812 (0.023) | 0.812 (0.023) | 0.810 (0.023) | 0.809 (0.024) | 0.812 (0.023) | 0.811 (0.023) | 0.812 (0.023) | 0.811 (0.023) | 0.811 (0.023) | 0.810 (0.023) |
| 2 | 0.885 (0.017) | 0.884 (0.018) | 0.879 (0.018) | 0.878 (0.018) | 0.878 (0.018) | 0.878 (0.018) | 0.878 (0.018) | 0.878 (0.018) | 0.878 (0.018) | 0.878 (0.018) | 0.878 (0.018) | 0.878 (0.018) |
| 3 | 0.918 (0.017) | 0.918 (0.017) | 0.909 (0.018) | 0.909 (0.017) | 0.909 (0.018) | 0.909 (0.018) | 0.909 (0.018) | 0.909 (0.018) | 0.909 (0.018) | 0.909 (0.018) | 0.909 (0.018) | 0.909 (0.018) |
| 4 | 0.929 (0.017) | 0.930 (0.016) | 0.920 (0.017) | 0.919 (0.017) | 0.919 (0.017) | 0.919 (0.017) | 0.919 (0.017) | 0.919 (0.017) | 0.919 (0.017) | 0.919 (0.017) | 0.919 (0.017) | 0.919 (0.017) |
| 5 | 0.932 (0.019) | 0.932 (0.020) | 0.922 (0.021) | 0.922 (0.021) | 0.922 (0.021) | 0.921 (0.021) | 0.921 (0.021) | 0.921 (0.021) | 0.921 (0.021) | 0.921 (0.021) | 0.921 (0.021) | 0.921 (0.021) |

**(c)** Mean (and standard deviation) of the Brier Score in 500 simulations for continuous marker Scenario 4c.

| $\tau$ | JM | JM2 | LM1 | LMInt1 | LM2 | LMInt2 | CC1 | CW1 | CC2 | CW2 | CC3 | CW3 |
|---|---|---|---|---|---|---|---|---|---|---|---|---|
| 0 | 0.111 (0.011) | 0.116 (0.013) | 0.112 (0.012) | 0.112 (0.012) | 0.140 (0.010) | 0.141 (0.010) | 0.113 (0.012) | 0.114 (0.011) | 0.112 (0.012) | 0.112 (0.011) | 0.115 (0.012) | 0.116 (0.012) |
| 1 | 0.147 (0.011) | 0.151 (0.011) | 0.148 (0.010) | 0.148 (0.010) | 0.175 (0.009) | 0.175 (0.009) | 0.149 (0.010) | 0.152 (0.011) | 0.149 (0.010) | 0.152 (0.011) | 0.148 (0.011) | 0.152 (0.012) |
| 2 | 0.133 (0.011) | 0.135 (0.012) | 0.138 (0.010) | 0.138 (0.010) | 0.171 (0.011) | 0.171 (0.011) | 0.139 (0.010) | 0.150 (0.012) | 0.138 (0.010) | 0.149 (0.012) | 0.138 (0.010) | 0.149 (0.013) |
| 3 | 0.115 (0.012) | 0.115 (0.012) | 0.122 (0.012) | 0.122 (0.012) | 0.160 (0.014) | 0.160 (0.014) | 0.125 (0.011) | 0.132 (0.012) | 0.124 (0.012) | 0.130 (0.013) | 0.124 (0.012) | 0.130 (0.013) |
| 4 | 0.107 (0.013) | 0.106 (0.013) | 0.115 (0.013) | 0.115 (0.013) | 0.156 (0.016) | 0.156 (0.016) | 0.118 (0.012) | 0.119 (0.012) | 0.117 (0.013) | 0.117 (0.012) | 0.117 (0.013) | 0.117 (0.013) |
| 5 | 0.103 (0.016) | 0.103 (0.016) | 0.113 (0.016) | 0.113 (0.016) | 0.160 (0.023) | 0.160 (0.023) | 0.116 (0.015) | 0.115 (0.014) | 0.115 (0.015) | 0.114 (0.015) | 0.115 (0.016) | 0.114 (0.016) |

## A.5 Binary marker simulation results

**Table A.18:** Summary of scenarios for binary marker process simulations.

| Scenario | Model | Baseline covariates | Inter-inspection rate |
|---|---|---|---|
| 1a | Markov | $X$ | 0.5 |
| 1b | Markov | $X$ | 1 |
| 1c | Markov | $X$ | Continuously observed |
| 2a | Semi-Markov | $X$ | 0.5 |
| 2b | Semi-Markov | $X$ | 1 |
| 2c | Semi-Markov | $X$ | Continuously observed |
| 3a | Markov | $X_1, X_2$ | 0.5 |
| 3b | Markov | $X_1, X_2$ | 1 |
| 3c | Markov | $X_1, X_2$ | Continuously observed |

### A.5.1 Binary marker: Simulation 1a

- Markov model; Marker observed at random inspection times (rate=0.5); Single baseline covariate $X$

**Table A.19:** Simulation results for binary marker Scenario 1a.

**(a)** Mean (and standard deviation) of the root mean squared prediction error in 500 simulations for binary marker Scenario 1a.

| | $\tau$ | MM | MMCox | LM3 | LMInt3 | LM4 | LMInt4 | BC1 | BW1 | BC2 | BW2 | BC3 | Bw3 |
|---|---|---|---|---|---|---|---|---|---|---|---|---|---|
| | 0 | 0.015 (0.011) | 0.017 (0.012) | 0.023 (0.016) | 0.019 (0.014) | 0.023 (0.016) | 0.019 (0.014) | 0.020 (0.013) | 0.019 (0.013) | 0.020 (0.013) | 0.019 (0.013) | 0.020 (0.013) | 0.019 (0.013) |
| | 1 | 0.016 (0.010) | 0.020 (0.013) | 0.027 (0.015) | 0.024 (0.015) | 0.032 (0.016) | 0.025 (0.016) | 0.020 (0.013) | 0.017 (0.010) | 0.020 (0.013) | 0.017 (0.010) | 0.021 (0.013) | 0.017 (0.010) |
| | 2 | 0.019 (0.011) | 0.025 (0.015) | 0.037 (0.016) | 0.028 (0.017) | 0.043 (0.017) | 0.030 (0.018) | 0.026 (0.016) | 0.021 (0.012) | 0.026 (0.016) | 0.021 (0.012) | 0.027 (0.016) | 0.022 (0.012) |
| $X = 0$ | 3 | 0.022 (0.012) | 0.030 (0.019) | 0.047 (0.019) | 0.034 (0.020) | 0.052 (0.019) | 0.035 (0.021) | 0.033 (0.020) | 0.026 (0.015) | 0.033 (0.020) | 0.026 (0.015) | 0.033 (0.020) | 0.026 (0.015) |
| | 4 | 0.024 (0.014) | 0.035 (0.020) | 0.057 (0.022) | 0.039 (0.022) | 0.059 (0.023) | 0.041 (0.023) | 0.038 (0.022) | 0.030 (0.017) | 0.038 (0.022) | 0.030 (0.017) | 0.038 (0.022) | 0.030 (0.017) |
| | 5 | 0.026 (0.015) | 0.040 (0.023) | 0.066 (0.025) | 0.044 (0.026) | 0.063 (0.028) | 0.047 (0.026) | 0.041 (0.024) | 0.034 (0.019) | 0.041 (0.024) | 0.034 (0.019) | 0.041 (0.024) | 0.035 (0.019) |
| | 0 | 0.021 (0.017) | 0.023 (0.018) | 0.028 (0.021) | 0.026 (0.020) | 0.027 (0.021) | 0.026 (0.019) | 0.024 (0.019) | 0.020 (0.016) | 0.024 (0.019) | 0.021 (0.016) | 0.024 (0.018) | 0.020 (0.016) |
| | 1 | 0.021 (0.015) | 0.036 (0.022) | 0.043 (0.024) | 0.035 (0.024) | 0.039 (0.025) | 0.037 (0.024) | 0.030 (0.021) | 0.023 (0.015) | 0.030 (0.021) | 0.024 (0.016) | 0.030 (0.020) | 0.024 (0.015) |
| | 2 | 0.024 (0.016) | 0.046 (0.025) | 0.054 (0.028) | 0.042 (0.028) | 0.048 (0.029) | 0.043 (0.028) | 0.036 (0.023) | 0.028 (0.017) | 0.036 (0.023) | 0.028 (0.018) | 0.036 (0.023) | 0.028 (0.017) |
| $X = 1$ | 3 | 0.027 (0.018) | 0.054 (0.030) | 0.061 (0.032) | 0.046 (0.032) | 0.056 (0.033) | 0.047 (0.033) | 0.041 (0.026) | 0.031 (0.018) | 0.041 (0.026) | 0.031 (0.018) | 0.041 (0.026) | 0.031 (0.018) |
| | 4 | 0.030 (0.020) | 0.060 (0.035) | 0.068 (0.034) | 0.053 (0.034) | 0.069 (0.035) | 0.055 (0.035) | 0.045 (0.029) | 0.034 (0.019) | 0.044 (0.029) | 0.033 (0.019) | 0.045 (0.029) | 0.034 (0.019) |
| | 5 | 0.033 (0.021) | 0.063 (0.040) | 0.076 (0.041) | 0.061 (0.043) | 0.082 (0.042) | 0.064 (0.044) | 0.054 (0.032) | 0.038 (0.020) | 0.054 (0.032) | 0.038 (0.020) | 0.054 (0.033) | 0.039 (0.021) |

**(b)** Mean (and standard deviation) of the AUC in 500 simulations for binary marker Scenario 1a.

| $\tau$ | MM | MMCox | LM3 | LMInt3 | LM4 | LMInt4 | BC1 | BW1 | BC2 | BW2 | BC3 | Bw3 |
|---|---|---|---|---|---|---|---|---|---|---|---|---|
| 0 | 0.638 (0.024) | 0.638 (0.024) | 0.638 (0.024) | 0.638 (0.024) | 0.638 (0.024) | 0.638 (0.024) | 0.638 (0.024) | 0.638 (0.024) | 0.638 (0.024) | 0.638 (0.024) | 0.638 (0.024) | 0.638 (0.024) |
| 1 | 0.665 (0.027) | 0.665 (0.027) | 0.665 (0.027) | 0.665 (0.027) | 0.664 (0.027) | 0.665 (0.027) | 0.665 (0.027) | 0.665 (0.027) | 0.665 (0.027) | 0.665 (0.027) | 0.665 (0.027) | 0.665 (0.027) |
| 2 | 0.682 (0.029) | 0.682 (0.029) | 0.682 (0.029) | 0.682 (0.029) | 0.680 (0.029) | 0.682 (0.029) | 0.682 (0.029) | 0.682 (0.029) | 0.682 (0.029) | 0.682 (0.029) | 0.682 (0.029) | 0.682 (0.029) |
| 3 | 0.690 (0.035) | 0.689 (0.035) | 0.689 (0.035) | 0.690 (0.035) | 0.687 (0.036) | 0.689 (0.035) | 0.689 (0.035) | 0.689 (0.035) | 0.690 (0.035) | 0.690 (0.035) | 0.689 (0.035) | 0.689 (0.035) |
| 4 | 0.691 (0.038) | 0.690 (0.038) | 0.690 (0.039) | 0.690 (0.038) | 0.688 (0.040) | 0.689 (0.038) | 0.690 (0.038) | 0.691 (0.038) | 0.691 (0.038) | 0.691 (0.038) | 0.690 (0.038) | 0.691 (0.038) |
| 5 | 0.688 (0.045) | 0.687 (0.045) | 0.685 (0.047) | 0.687 (0.045) | 0.685 (0.047) | 0.685 (0.045) | 0.687 (0.046) | 0.686 (0.046) | 0.686 (0.045) | 0.686 (0.045) | 0.686 (0.045) | 0.686 (0.045) |

**(c)** Mean (and standard deviation) of the Brier Score in 500 simulations for binary marker Scenario 1a.

| $\tau$ | MM | MMCox | LM3 | LMInt3 | LM4 | LMInt4 | BC1 | BW1 | BC2 | BW2 | BC3 | Bw3 |
|---|---|---|---|---|---|---|---|---|---|---|---|---|
| 0 | 0.195 (0.009) | 0.195 (0.009) | 0.195 (0.009) | 0.195 (0.009) | 0.195 (0.009) | 0.195 (0.009) | 0.195 (0.009) | 0.195 (0.009) | 0.195 (0.009) | 0.195 (0.009) | 0.195 (0.009) | 0.195 (0.009) |
| 1 | 0.203 (0.010) | 0.203 (0.010) | 0.204 (0.010) | 0.204 (0.010) | 0.204 (0.010) | 0.204 (0.010) | 0.203 (0.010) | 0.203 (0.010) | 0.203 (0.010) | 0.203 (0.010) | 0.203 (0.010) | 0.203 (0.010) |
| 2 | 0.203 (0.010) | 0.203 (0.010) | 0.204 (0.011) | 0.205 (0.011) | 0.205 (0.011) | 0.205 (0.011) | 0.203 (0.010) | 0.203 (0.010) | 0.203 (0.010) | 0.203 (0.010) | 0.203 (0.010) | 0.203 (0.010) |
| 3 | 0.202 (0.013) | 0.201 (0.012) | 0.203 (0.013) | 0.203 (0.013) | 0.204 (0.013) | 0.203 (0.013) | 0.202 (0.012) | 0.201 (0.012) | 0.201 (0.012) | 0.201 (0.012) | 0.202 (0.012) | 0.201 (0.012) |
| 4 | 0.200 (0.014) | 0.200 (0.014) | 0.203 (0.015) | 0.203 (0.015) | 0.204 (0.015) | 0.203 (0.015) | 0.201 (0.013) | 0.200 (0.013) | 0.200 (0.013) | 0.200 (0.013) | 0.201 (0.013) | 0.200 (0.013) |
| 5 | 0.199 (0.016) | 0.199 (0.016) | 0.204 (0.017) | 0.202 (0.017) | 0.203 (0.017) | 0.202 (0.017) | 0.200 (0.015) | 0.199 (0.015) | 0.199 (0.015) | 0.199 (0.015) | 0.200 (0.015) | 0.199 (0.015) |

### A.5.2 Binary marker: Simulation 1b

- Markov model; Marker observed at random inspection times (rate=1); Single baseline covariate $X$

**Table A.20:** Simulation results for binary marker Scenario 1b.

**(a)** Mean (and standard deviation) of the root mean squared prediction error in 500 simulations for binary marker Scenario 1b.

| | $\tau$ | MM | MMCox | LM3 | LMInt3 | LM4 | LMInt4 | BC1 | BW1 | BC2 | BW2 | BC3 | Bw3 |
|---|---|---|---|---|---|---|---|---|---|---|---|---|---|
| | 0 | 0.015 (0.011) | 0.016 (0.012) | 0.024 (0.015) | 0.018 (0.014) | 0.024 (0.015) | 0.018 (0.014) | 0.020 (0.013) | 0.019 (0.013) | 0.020 (0.013) | 0.019 (0.013) | 0.020 (0.014) | 0.019 (0.013) |
| | 1 | 0.016 (0.010) | 0.020 (0.013) | 0.028 (0.014) | 0.021 (0.014) | 0.035 (0.015) | 0.023 (0.014) | 0.021 (0.013) | 0.018 (0.010) | 0.021 (0.013) | 0.018 (0.010) | 0.022 (0.013) | 0.019 (0.010) |
| | 2 | 0.019 (0.011) | 0.025 (0.015) | 0.039 (0.014) | 0.026 (0.016) | 0.048 (0.015) | 0.028 (0.016) | 0.027 (0.016) | 0.022 (0.012) | 0.027 (0.016) | 0.022 (0.012) | 0.028 (0.017) | 0.023 (0.013) |
| $X = 0$ | 3 | 0.022 (0.012) | 0.029 (0.017) | 0.050 (0.017) | 0.032 (0.018) | 0.057 (0.018) | 0.034 (0.019) | 0.033 (0.020) | 0.026 (0.015) | 0.033 (0.020) | 0.026 (0.015) | 0.034 (0.020) | 0.027 (0.016) |
| | 4 | 0.024 (0.014) | 0.035 (0.019) | 0.060 (0.020) | 0.037 (0.021) | 0.062 (0.022) | 0.039 (0.021) | 0.038 (0.022) | 0.030 (0.017) | 0.038 (0.022) | 0.030 (0.017) | 0.038 (0.022) | 0.031 (0.017) |
| | 5 | 0.027 (0.015) | 0.040 (0.021) | 0.067 (0.023) | 0.041 (0.023) | 0.063 (0.026) | 0.043 (0.024) | 0.041 (0.024) | 0.034 (0.019) | 0.041 (0.024) | 0.034 (0.019) | 0.042 (0.024) | 0.034 (0.019) |
| | 0 | 0.021 (0.016) | 0.023 (0.018) | 0.029 (0.022) | 0.026 (0.020) | 0.029 (0.021) | 0.026 (0.020) | 0.025 (0.019) | 0.021 (0.017) | 0.026 (0.020) | 0.022 (0.017) | 0.025 (0.019) | 0.021 (0.016) |
| | 1 | 0.021 (0.014) | 0.033 (0.022) | 0.045 (0.021) | 0.031 (0.021) | 0.037 (0.023) | 0.033 (0.022) | 0.029 (0.020) | 0.022 (0.015) | 0.029 (0.020) | 0.022 (0.015) | 0.029 (0.019) | 0.023 (0.014) |
| | 2 | 0.023 (0.015) | 0.040 (0.024) | 0.055 (0.024) | 0.037 (0.024) | 0.046 (0.025) | 0.038 (0.025) | 0.034 (0.022) | 0.026 (0.016) | 0.034 (0.022) | 0.026 (0.016) | 0.035 (0.022) | 0.027 (0.016) |
| $X = 1$ | 3 | 0.026 (0.017) | 0.047 (0.027) | 0.062 (0.026) | 0.041 (0.027) | 0.055 (0.028) | 0.043 (0.028) | 0.039 (0.025) | 0.030 (0.017) | 0.039 (0.025) | 0.030 (0.017) | 0.039 (0.025) | 0.030 (0.017) |
| | 4 | 0.029 (0.018) | 0.052 (0.032) | 0.067 (0.030) | 0.047 (0.030) | 0.066 (0.031) | 0.049 (0.031) | 0.044 (0.028) | 0.034 (0.018) | 0.044 (0.028) | 0.033 (0.018) | 0.044 (0.029) | 0.034 (0.018) |
| | 5 | 0.032 (0.020) | 0.057 (0.037) | 0.073 (0.033) | 0.054 (0.034) | 0.079 (0.036) | 0.058 (0.035) | 0.054 (0.032) | 0.039 (0.020) | 0.053 (0.031) | 0.038 (0.019) | 0.054 (0.033) | 0.039 (0.020) |

**(b)** Mean (and standard deviation) of the AUC in 500 simulations for binary marker Scenario 1b.

| $\tau$ | MM | MMCox | LM3 | LMInt3 | LM4 | LMInt4 | BC1 | BW1 | BC2 | BW2 | BC3 | Bw3 |
|---|---|---|---|---|---|---|---|---|---|---|---|---|
| 0 | 0.638 (0.024) | 0.638 (0.024) | 0.638 (0.024) | 0.638 (0.024) | 0.638 (0.024) | 0.638 (0.024) | 0.638 (0.024) | 0.638 (0.024) | 0.638 (0.024) | 0.638 (0.024) | 0.638 (0.024) | 0.638 (0.024) |
| 1 | 0.668 (0.027) | 0.668 (0.027) | 0.668 (0.027) | 0.667 (0.027) | 0.666 (0.027) | 0.668 (0.027) | 0.667 (0.027) | 0.667 (0.027) | 0.667 (0.027) | 0.667 (0.027) | 0.667 (0.027) | 0.667 (0.027) |
| 2 | 0.687 (0.030) | 0.687 (0.029) | 0.687 (0.030) | 0.687 (0.030) | 0.685 (0.030) | 0.687 (0.030) | 0.687 (0.030) | 0.687 (0.030) | 0.687 (0.030) | 0.687 (0.030) | 0.687 (0.030) | 0.687 (0.030) |
| 3 | 0.695 (0.035) | 0.695 (0.035) | 0.695 (0.035) | 0.695 (0.035) | 0.693 (0.036) | 0.695 (0.036) | 0.695 (0.035) | 0.695 (0.035) | 0.695 (0.035) | 0.695 (0.035) | 0.694 (0.035) | 0.695 (0.035) |
| 4 | 0.696 (0.038) | 0.695 (0.039) | 0.695 (0.038) | 0.695 (0.038) | 0.694 (0.039) | 0.695 (0.038) | 0.695 (0.038) | 0.695 (0.038) | 0.695 (0.038) | 0.695 (0.038) | 0.695 (0.038) | 0.695 (0.038) |
| 5 | 0.691 (0.046) | 0.691 (0.046) | 0.690 (0.048) | 0.691 (0.046) | 0.690 (0.047) | 0.690 (0.047) | 0.691 (0.046) | 0.691 (0.046) | 0.691 (0.045) | 0.691 (0.045) | 0.691 (0.046) | 0.691 (0.046) |

**(c)** Mean (and standard deviation) of the Brier Score in 500 simulations for binary marker Scenario 1b.

| $\tau$ | MM | MMCox | LM3 | LMInt3 | LM4 | LMInt4 | BC1 | BW1 | BC2 | BW2 | BC3 | Bw3 |
|---|---|---|---|---|---|---|---|---|---|---|---|---|
| 0 | 0.195 (0.009) | 0.195 (0.009) | 0.195 (0.009) | 0.195 (0.009) | 0.195 (0.009) | 0.195 (0.009) | 0.195 (0.009) | 0.195 (0.009) | 0.195 (0.009) | 0.195 (0.009) | 0.195 (0.009) | 0.195 (0.009) |
| 1 | 0.202 (0.010) | 0.202 (0.010) | 0.202 (0.010) | 0.203 (0.010) | 0.203 (0.010) | 0.203 (0.010) | 0.202 (0.010) | 0.202 (0.010) | 0.202 (0.010) | 0.202 (0.010) | 0.202 (0.010) | 0.202 (0.010) |
| 2 | 0.201 (0.011) | 0.201 (0.011) | 0.202 (0.011) | 0.202 (0.011) | 0.202 (0.011) | 0.202 (0.011) | 0.201 (0.011) | 0.201 (0.011) | 0.201 (0.011) | 0.201 (0.011) | 0.201 (0.011) | 0.201 (0.011) |
| 3 | 0.199 (0.013) | 0.199 (0.012) | 0.201 (0.013) | 0.200 (0.013) | 0.201 (0.013) | 0.200 (0.013) | 0.199 (0.012) | 0.199 (0.012) | 0.199 (0.012) | 0.199 (0.012) | 0.199 (0.012) | 0.199 (0.012) |
| 4 | 0.198 (0.014) | 0.198 (0.014) | 0.201 (0.014) | 0.199 (0.014) | 0.201 (0.014) | 0.200 (0.014) | 0.199 (0.013) | 0.198 (0.013) | 0.198 (0.013) | 0.198 (0.013) | 0.199 (0.013) | 0.198 (0.013) |
| 5 | 0.196 (0.016) | 0.197 (0.016) | 0.201 (0.017) | 0.198 (0.017) | 0.201 (0.017) | 0.199 (0.017) | 0.198 (0.015) | 0.197 (0.015) | 0.197 (0.015) | 0.197 (0.015) | 0.198 (0.015) | 0.197 (0.015) |

### A.5.3 Binary marker: Simulation 1c

- Markov model; Marker observed continuously; Single baseline covariate $X$

**Table A.21:** Simulation results for binary marker Scenario 1c.

**(a)** Mean (and standard deviation) of the root mean squared prediction error in 500 simulations for binary marker Scenario 1c.

| | $\tau$ | MM | MMCox | LM3 | LMInt3 | LM4 | LMInt4 | BC1 | BW1 | BC2 | BW2 | BC3 | Bw3 |
|---|---|---|---|---|---|---|---|---|---|---|---|---|---|
| | 0 | 0.015 (0.011) | 0.016 (0.013) | 0.023 (0.014) | 0.016 (0.012) | 0.023 (0.014) | 0.016 (0.012) | 0.020 (0.013) | 0.019 (0.013) | 0.020 (0.013) | 0.018 (0.013) | 0.020 (0.013) | 0.019 (0.013) |
| | 1 | 0.017 (0.010) | 0.022 (0.013) | 0.037 (0.011) | 0.022 (0.013) | 0.047 (0.015) | 0.024 (0.014) | 0.024 (0.013) | 0.021 (0.011) | 0.024 (0.013) | 0.021 (0.011) | 0.025 (0.014) | 0.022 (0.012) |
| | 2 | 0.020 (0.011) | 0.026 (0.014) | 0.049 (0.014) | 0.026 (0.015) | 0.058 (0.015) | 0.028 (0.016) | 0.029 (0.017) | 0.024 (0.013) | 0.029 (0.017) | 0.024 (0.014) | 0.030 (0.017) | 0.025 (0.014) |
| $X = 0$ | 3 | 0.022 (0.012) | 0.030 (0.017) | 0.060 (0.018) | 0.030 (0.018) | 0.064 (0.019) | 0.032 (0.018) | 0.034 (0.021) | 0.027 (0.016) | 0.034 (0.021) | 0.028 (0.016) | 0.034 (0.021) | 0.028 (0.016) |
| | 4 | 0.024 (0.014) | 0.035 (0.018) | 0.069 (0.021) | 0.035 (0.020) | 0.067 (0.023) | 0.037 (0.020) | 0.038 (0.023) | 0.031 (0.018) | 0.038 (0.023) | 0.031 (0.018) | 0.039 (0.023) | 0.031 (0.018) |
| | 5 | 0.026 (0.015) | 0.039 (0.022) | 0.076 (0.024) | 0.039 (0.022) | 0.066 (0.027) | 0.040 (0.022) | 0.042 (0.024) | 0.034 (0.019) | 0.041 (0.024) | 0.034 (0.020) | 0.043 (0.024) | 0.035 (0.020) |
| | 0 | 0.020 (0.016) | 0.023 (0.018) | 0.027 (0.020) | 0.023 (0.018) | 0.027 (0.020) | 0.024 (0.018) | 0.025 (0.019) | 0.020 (0.016) | 0.025 (0.019) | 0.021 (0.016) | 0.024 (0.019) | 0.020 (0.016) |
| | 1 | 0.021 (0.014) | 0.029 (0.018) | 0.050 (0.018) | 0.030 (0.018) | 0.038 (0.021) | 0.032 (0.019) | 0.030 (0.019) | 0.023 (0.014) | 0.029 (0.019) | 0.023 (0.014) | 0.030 (0.019) | 0.024 (0.014) |
| | 2 | 0.023 (0.014) | 0.031 (0.019) | 0.056 (0.021) | 0.033 (0.020) | 0.046 (0.022) | 0.033 (0.020) | 0.033 (0.020) | 0.026 (0.015) | 0.033 (0.020) | 0.026 (0.015) | 0.033 (0.020) | 0.026 (0.015) |
| $X = 1$ | 3 | 0.025 (0.015) | 0.036 (0.022) | 0.061 (0.023) | 0.037 (0.022) | 0.057 (0.025) | 0.038 (0.023) | 0.038 (0.023) | 0.031 (0.016) | 0.038 (0.023) | 0.030 (0.016) | 0.038 (0.023) | 0.031 (0.016) |
| | 4 | 0.027 (0.017) | 0.042 (0.026) | 0.064 (0.026) | 0.041 (0.026) | 0.069 (0.029) | 0.043 (0.026) | 0.046 (0.027) | 0.039 (0.019) | 0.044 (0.027) | 0.037 (0.019) | 0.046 (0.028) | 0.039 (0.019) |
| | 5 | 0.029 (0.018) | 0.050 (0.031) | 0.071 (0.029) | 0.048 (0.030) | 0.084 (0.033) | 0.052 (0.030) | 0.063 (0.036) | 0.051 (0.024) | 0.060 (0.035) | 0.047 (0.024) | 0.064 (0.036) | 0.051 (0.025) |

**(b)** Mean (and standard deviation) of the AUC in 500 simulations for binary marker Scenario 1c.

| $\tau$ | MM | MMCox | LM3 | LMInt3 | LM4 | LMInt4 | BC1 | BW1 | BC2 | BW2 | BC3 | Bw3 |
|---|---|---|---|---|---|---|---|---|---|---|---|---|
| 0 | 0.638 (0.024) | 0.638 (0.024) | 0.638 (0.024) | 0.638 (0.024) | 0.638 (0.024) | 0.638 (0.024) | 0.638 (0.024) | 0.638 (0.024) | 0.638 (0.024) | 0.638 (0.024) | 0.638 (0.024) | 0.638 (0.024) |
| 1 | 0.681 (0.028) | 0.681 (0.028) | 0.681 (0.028) | 0.681 (0.028) | 0.679 (0.028) | 0.681 (0.028) | 0.681 (0.028) | 0.681 (0.028) | 0.681 (0.028) | 0.681 (0.028) | 0.681 (0.028) | 0.681 (0.028) |
| 2 | 0.702 (0.030) | 0.701 (0.030) | 0.701 (0.031) | 0.701 (0.030) | 0.699 (0.031) | 0.701 (0.030) | 0.701 (0.030) | 0.701 (0.030) | 0.701 (0.030) | 0.701 (0.030) | 0.701 (0.030) | 0.701 (0.030) |
| 3 | 0.707 (0.036) | 0.707 (0.035) | 0.706 (0.036) | 0.706 (0.035) | 0.705 (0.036) | 0.706 (0.035) | 0.707 (0.036) | 0.707 (0.036) | 0.707 (0.036) | 0.707 (0.036) | 0.706 (0.035) | 0.707 (0.035) |
| 4 | 0.705 (0.038) | 0.705 (0.039) | 0.705 (0.039) | 0.704 (0.039) | 0.705 (0.040) | 0.704 (0.039) | 0.704 (0.038) | 0.705 (0.038) | 0.705 (0.038) | 0.705 (0.038) | 0.704 (0.038) | 0.704 (0.038) |
| 5 | 0.700 (0.046) | 0.700 (0.046) | 0.698 (0.048) | 0.699 (0.047) | 0.700 (0.048) | 0.699 (0.047) | 0.700 (0.047) | 0.700 (0.047) | 0.700 (0.047) | 0.700 (0.047) | 0.699 (0.047) | 0.699 (0.047) |

**(c)** Mean (and standard deviation) of the Brier Score in 500 simulations for binary marker Scenario 1c.

| $\tau$ | MM | MMCox | LM3 | LMInt3 | LM4 | LMInt4 | BC1 | BW1 | BC2 | BW2 | BC3 | Bw3 |
|---|---|---|---|---|---|---|---|---|---|---|---|---|
| 0 | 0.195 (0.009) | 0.195 (0.009) | 0.195 (0.009) | 0.195 (0.009) | 0.195 (0.009) | 0.195 (0.009) | 0.195 (0.009) | 0.195 (0.009) | 0.195 (0.009) | 0.195 (0.009) | 0.195 (0.009) | 0.195 (0.009) |
| 1 | 0.196 (0.010) | 0.196 (0.010) | 0.198 (0.010) | 0.196 (0.010) | 0.198 (0.011) | 0.197 (0.010) | 0.196 (0.010) | 0.196 (0.010) | 0.196 (0.010) | 0.196 (0.010) | 0.196 (0.010) | 0.196 (0.010) |
| 2 | 0.194 (0.011) | 0.195 (0.011) | 0.197 (0.011) | 0.195 (0.011) | 0.197 (0.011) | 0.195 (0.011) | 0.195 (0.011) | 0.194 (0.011) | 0.194 (0.011) | 0.194 (0.011) | 0.195 (0.011) | 0.194 (0.011) |
| 3 | 0.193 (0.013) | 0.193 (0.013) | 0.196 (0.013) | 0.193 (0.013) | 0.196 (0.013) | 0.193 (0.013) | 0.194 (0.012) | 0.193 (0.012) | 0.193 (0.012) | 0.193 (0.012) | 0.194 (0.012) | 0.193 (0.012) |
| 4 | 0.192 (0.014) | 0.193 (0.015) | 0.197 (0.014) | 0.193 (0.015) | 0.197 (0.014) | 0.193 (0.015) | 0.194 (0.014) | 0.193 (0.014) | 0.193 (0.014) | 0.193 (0.014) | 0.194 (0.014) | 0.193 (0.014) |
| 5 | 0.191 (0.017) | 0.193 (0.017) | 0.197 (0.017) | 0.192 (0.017) | 0.196 (0.016) | 0.193 (0.017) | 0.193 (0.016) | 0.192 (0.015) | 0.192 (0.015) | 0.192 (0.015) | 0.193 (0.016) | 0.192 (0.015) |

### A.5.4 Binary marker: Simulation 2a

- Semi-Markov model; Marker observed at random inspection times (rate=0.5); Single baseline covariate $X$

**Table A.22:** Simulation results for binary marker Scenario 2a.

**(a)** Mean (and standard deviation) of the root mean squared prediction error in 500 simulations for binary marker Scenario 2a.

| | $\tau$ | MSM | MSMCox | SMM | LSM3 | LSM4 | BC1 | BW1 | BC2 | BW2 | BC3 | BW3 |
|---|---|---|---|---|---|---|---|---|---|---|---|---|
| $X=0$ | 0 | 0.013 (0.010) | 0.016 (0.012) | 0.014 (0.011) | 0.023 (0.015) | 0.022 (0.015) | 0.021 (0.014) | 0.020 (0.013) | 0.021 (0.014) | 0.020 (0.013) | 0.021 (0.014) | 0.020 (0.013) |
| | 1 | 0.014 (0.009) | 0.019 (0.012) | 0.015 (0.010) | 0.031 (0.016) | 0.033 (0.016) | 0.020 (0.012) | 0.017 (0.010) | 0.020 (0.012) | 0.017 (0.010) | 0.021 (0.012) | 0.018 (0.010) |
| | 2 | 0.016 (0.010) | 0.025 (0.015) | 0.018 (0.011) | 0.043 (0.017) | 0.046 (0.017) | 0.026 (0.015) | 0.021 (0.012) | 0.026 (0.015) | 0.021 (0.012) | 0.027 (0.015) | 0.022 (0.012) |
| | 3 | 0.019 (0.011) | 0.030 (0.017) | 0.022 (0.012) | 0.054 (0.020) | 0.055 (0.020) | 0.032 (0.018) | 0.026 (0.014) | 0.032 (0.018) | 0.026 (0.014) | 0.033 (0.018) | 0.027 (0.014) |
| | 4 | 0.021 (0.011) | 0.037 (0.020) | 0.025 (0.013) | 0.064 (0.022) | 0.062 (0.024) | 0.038 (0.021) | 0.031 (0.016) | 0.038 (0.021) | 0.031 (0.016) | 0.038 (0.021) | 0.031 (0.016) |
| | 5 | 0.025 (0.013) | 0.043 (0.024) | 0.028 (0.014) | 0.072 (0.026) | 0.068 (0.029) | 0.043 (0.026) | 0.035 (0.018) | 0.043 (0.026) | 0.035 (0.018) | 0.043 (0.026) | 0.036 (0.018) |
| $X=1$ | 0 | 0.021 (0.016) | 0.022 (0.017) | 0.021 (0.015) | 0.027 (0.020) | 0.027 (0.020) | 0.023 (0.018) | 0.021 (0.016) | 0.023 (0.017) | 0.021 (0.016) | 0.023 (0.018) | 0.021 (0.016) |
| | 1 | 0.023 (0.015) | 0.040 (0.026) | 0.022 (0.015) | 0.043 (0.025) | 0.041 (0.024) | 0.034 (0.023) | 0.026 (0.017) | 0.034 (0.024) | 0.026 (0.018) | 0.034 (0.023) | 0.026 (0.017) |
| | 2 | 0.026 (0.017) | 0.052 (0.031) | 0.026 (0.016) | 0.052 (0.029) | 0.048 (0.027) | 0.041 (0.027) | 0.032 (0.020) | 0.041 (0.027) | 0.032 (0.020) | 0.041 (0.027) | 0.031 (0.020) |
| | 3 | 0.029 (0.018) | 0.060 (0.032) | 0.029 (0.017) | 0.058 (0.030) | 0.058 (0.030) | 0.044 (0.027) | 0.035 (0.021) | 0.044 (0.027) | 0.035 (0.021) | 0.044 (0.027) | 0.035 (0.021) |
| | 4 | 0.032 (0.020) | 0.067 (0.035) | 0.032 (0.018) | 0.068 (0.031) | 0.073 (0.033) | 0.046 (0.028) | 0.038 (0.021) | 0.046 (0.027) | 0.038 (0.020) | 0.047 (0.028) | 0.038 (0.021) |
| | 5 | 0.036 (0.021) | 0.074 (0.041) | 0.034 (0.019) | 0.078 (0.036) | 0.087 (0.039) | 0.054 (0.031) | 0.042 (0.020) | 0.054 (0.031) | 0.043 (0.020) | 0.056 (0.031) | 0.043 (0.021) |

**(b)** Mean (and standard deviation) of the AUC in 500 simulations for binary marker Scenario 2a.

| $\tau$ | MSM | MSMCox | SMM | LSM3 | LSM4 | BC1 | BW1 | BC2 | BW2 | BC3 | BW3 |
|---|---|---|---|---|---|---|---|---|---|---|---|
| 0 | 0.629 (0.026) | 0.629 (0.026) | 0.629 (0.026) | 0.629 (0.026) | 0.629 (0.026) | 0.629 (0.026) | 0.629 (0.026) | 0.629 (0.026) | 0.629 (0.026) | 0.629 (0.026) | 0.629 (0.026) |
| 1 | 0.657 (0.027) | 0.657 (0.027) | 0.657 (0.027) | 0.656 (0.027) | 0.656 (0.027) | 0.657 (0.027) | 0.657 (0.027) | 0.657 (0.027) | 0.657 (0.027) | 0.657 (0.027) | 0.657 (0.027) |
| 2 | 0.677 (0.028) | 0.677 (0.028) | 0.677 (0.028) | 0.676 (0.028) | 0.675 (0.029) | 0.677 (0.028) | 0.677 (0.028) | 0.677 (0.028) | 0.677 (0.028) | 0.677 (0.028) | 0.677 (0.028) |
| 3 | 0.690 (0.032) | 0.690 (0.032) | 0.690 (0.032) | 0.687 (0.033) | 0.687 (0.033) | 0.690 (0.032) | 0.690 (0.031) | 0.690 (0.032) | 0.690 (0.032) | 0.690 (0.032) | 0.690 (0.032) |
| 4 | 0.694 (0.037) | 0.693 (0.037) | 0.693 (0.038) | 0.690 (0.038) | 0.690 (0.039) | 0.693 (0.037) | 0.693 (0.037) | 0.693 (0.037) | 0.693 (0.037) | 0.693 (0.037) | 0.693 (0.037) |
| 5 | 0.691 (0.042) | 0.690 (0.043) | 0.691 (0.043) | 0.687 (0.044) | 0.687 (0.045) | 0.691 (0.043) | 0.691 (0.043) | 0.691 (0.043) | 0.691 (0.043) | 0.691 (0.043) | 0.691 (0.043) |

**(c)** Mean (and standard deviation) of the Brier Score in 500 simulations for binary marker Scenario 2a.

| $\tau$ | MSM | MSMCox | SMM | LSM3 | LSM4 | BC1 | BW1 | BC2 | BW2 | BC3 | BW3 |
|---|---|---|---|---|---|---|---|---|---|---|---|
| 0 | 0.192 (0.009) | 0.192 (0.010) | 0.192 (0.009) | 0.193 (0.010) | 0.193 (0.010) | 0.193 (0.010) | 0.192 (0.010) | 0.193 (0.010) | 0.193 (0.010) | 0.193 (0.010) | 0.193 (0.010) |
| 1 | 0.201 (0.010) | 0.201 (0.010) | 0.201 (0.010) | 0.202 (0.010) | 0.202 (0.010) | 0.201 (0.010) | 0.201 (0.010) | 0.201 (0.010) | 0.201 (0.010) | 0.201 (0.010) | 0.201 (0.010) |
| 2 | 0.201 (0.010) | 0.201 (0.010) | 0.202 (0.010) | 0.203 (0.011) | 0.203 (0.011) | 0.202 (0.010) | 0.201 (0.010) | 0.202 (0.010) | 0.202 (0.010) | 0.202 (0.010) | 0.201 (0.010) |
| 3 | 0.200 (0.012) | 0.199 (0.012) | 0.200 (0.013) | 0.202 (0.013) | 0.202 (0.013) | 0.200 (0.012) | 0.199 (0.012) | 0.200 (0.012) | 0.200 (0.012) | 0.200 (0.012) | 0.199 (0.012) |
| 4 | 0.198 (0.014) | 0.198 (0.014) | 0.198 (0.015) | 0.201 (0.015) | 0.201 (0.015) | 0.199 (0.014) | 0.198 (0.014) | 0.199 (0.014) | 0.199 (0.014) | 0.199 (0.014) | 0.198 (0.014) |
| 5 | 0.196 (0.016) | 0.196 (0.016) | 0.196 (0.016) | 0.200 (0.017) | 0.201 (0.017) | 0.198 (0.015) | 0.196 (0.015) | 0.198 (0.015) | 0.198 (0.015) | 0.198 (0.015) | 0.196 (0.015) |

### A.5.5 Binary marker: Simulation 2b

- Semi-Markov model; Marker observed at random inspection times (rate=1); Single baseline covariate $X$

**Table A.23:** Simulation results for binary marker Scenario 2b.

**(a)** Mean (and standard deviation) of the root mean squared prediction error in 500 simulations for binary marker Scenario 2b.

| | $\tau$ | MSM | MSMCox | SMM | LSM3 | LSM4 | BC1 | BW1 | BC2 | BW2 | BC3 | BW3 |
|---|---|---|---|---|---|---|---|---|---|---|---|---|
| $X=0$ | 0 | 0.013 (0.011) | 0.015 (0.012) | 0.014 (0.011) | 0.024 (0.016) | 0.023 (0.016) | 0.021 (0.014) | 0.020 (0.013) | 0.021 (0.014) | 0.020 (0.013) | 0.021 (0.014) | 0.020 (0.014) |
| | 1 | 0.014 (0.010) | 0.020 (0.013) | 0.016 (0.010) | 0.034 (0.015) | 0.038 (0.015) | 0.021 (0.013) | 0.018 (0.010) | 0.021 (0.013) | 0.018 (0.011) | 0.022 (0.013) | 0.019 (0.011) |
| | 2 | 0.017 (0.010) | 0.025 (0.015) | 0.019 (0.011) | 0.047 (0.016) | 0.051 (0.016) | 0.027 (0.016) | 0.022 (0.012) | 0.027 (0.016) | 0.022 (0.012) | 0.028 (0.016) | 0.023 (0.013) |
| | 3 | 0.019 (0.011) | 0.030 (0.016) | 0.022 (0.012) | 0.058 (0.019) | 0.060 (0.019) | 0.033 (0.018) | 0.026 (0.015) | 0.033 (0.018) | 0.027 (0.015) | 0.033 (0.018) | 0.027 (0.015) |
| | 4 | 0.022 (0.012) | 0.035 (0.020) | 0.025 (0.013) | 0.067 (0.023) | 0.065 (0.024) | 0.038 (0.021) | 0.031 (0.017) | 0.038 (0.021) | 0.031 (0.017) | 0.038 (0.021) | 0.031 (0.017) |
| | 5 | 0.025 (0.013) | 0.041 (0.022) | 0.028 (0.014) | 0.075 (0.026) | 0.069 (0.029) | 0.042 (0.025) | 0.035 (0.018) | 0.042 (0.025) | 0.035 (0.018) | 0.043 (0.025) | 0.036 (0.018) |
| $X=1$ | 0 | 0.021 (0.016) | 0.022 (0.016) | 0.020 (0.015) | 0.028 (0.020) | 0.028 (0.020) | 0.024 (0.018) | 0.022 (0.017) | 0.024 (0.018) | 0.022 (0.017) | 0.024 (0.018) | 0.022 (0.016) |
| | 1 | 0.023 (0.015) | 0.037 (0.025) | 0.022 (0.015) | 0.044 (0.024) | 0.039 (0.023) | 0.032 (0.022) | 0.024 (0.015) | 0.032 (0.022) | 0.024 (0.016) | 0.032 (0.022) | 0.024 (0.015) |
| | 2 | 0.026 (0.016) | 0.045 (0.028) | 0.025 (0.016) | 0.054 (0.026) | 0.048 (0.024) | 0.039 (0.024) | 0.029 (0.017) | 0.039 (0.025) | 0.029 (0.017) | 0.039 (0.025) | 0.029 (0.017) |
| | 3 | 0.028 (0.017) | 0.051 (0.029) | 0.029 (0.016) | 0.061 (0.027) | 0.060 (0.027) | 0.042 (0.024) | 0.033 (0.018) | 0.042 (0.024) | 0.033 (0.018) | 0.042 (0.024) | 0.032 (0.018) |
| | 4 | 0.031 (0.018) | 0.056 (0.032) | 0.031 (0.017) | 0.067 (0.029) | 0.072 (0.031) | 0.045 (0.027) | 0.036 (0.019) | 0.045 (0.026) | 0.036 (0.018) | 0.045 (0.027) | 0.036 (0.019) |
| | 5 | 0.033 (0.019) | 0.063 (0.036) | 0.033 (0.018) | 0.078 (0.033) | 0.087 (0.037) | 0.053 (0.030) | 0.041 (0.019) | 0.053 (0.030) | 0.041 (0.019) | 0.054 (0.031) | 0.042 (0.020) |

**(b)** Mean (and standard deviation) of the AUC in 500 simulations for binary marker Scenario 2b.

| $\tau$ | MSM | MSMCox | SMM | LSM3 | LSM4 | BC1 | BW1 | BC2 | BW2 | BC3 | BW3 |
|---|---|---|---|---|---|---|---|---|---|---|---|
| 0 | 0.630 (0.026) | 0.630 (0.026) | 0.630 (0.026) | 0.630 (0.026) | 0.630 (0.026) | 0.630 (0.026) | 0.630 (0.026) | 0.630 (0.026) | 0.630 (0.026) | 0.630 (0.026) | 0.630 (0.026) |
| 1 | 0.660 (0.027) | 0.660 (0.027) | 0.660 (0.027) | 0.659 (0.027) | 0.659 (0.027) | 0.660 (0.027) | 0.660 (0.027) | 0.660 (0.027) | 0.660 (0.027) | 0.660 (0.027) | 0.660 (0.027) |
| 2 | 0.683 (0.028) | 0.683 (0.029) | 0.683 (0.029) | 0.681 (0.028) | 0.680 (0.029) | 0.683 (0.028) | 0.683 (0.029) | 0.683 (0.028) | 0.683 (0.028) | 0.683 (0.028) | 0.683 (0.028) |
| 3 | 0.696 (0.031) | 0.696 (0.032) | 0.696 (0.031) | 0.694 (0.033) | 0.693 (0.033) | 0.696 (0.032) | 0.695 (0.032) | 0.696 (0.032) | 0.696 (0.032) | 0.696 (0.032) | 0.696 (0.032) |
| 4 | 0.699 (0.038) | 0.698 (0.037) | 0.698 (0.038) | 0.697 (0.039) | 0.696 (0.040) | 0.698 (0.038) | 0.699 (0.038) | 0.699 (0.038) | 0.699 (0.038) | 0.699 (0.038) | 0.699 (0.038) |
| 5 | 0.696 (0.045) | 0.695 (0.044) | 0.696 (0.045) | 0.694 (0.043) | 0.694 (0.043) | 0.696 (0.045) | 0.696 (0.045) | 0.696 (0.045) | 0.696 (0.045) | 0.696 (0.045) | 0.696 (0.045) |

**(c)** Mean (and standard deviation) of the Brier Score in 500 simulations for binary marker Scenario 2b.

| $\tau$ | MSM | MSMCox | SMM | LSM3 | LSM4 | BC1 | BW1 | BC2 | BW2 | BC3 | BW3 |
|---|---|---|---|---|---|---|---|---|---|---|---|
| 0 | 0.192 (0.009) | 0.192 (0.009) | 0.192 (0.009) | 0.193 (0.010) | 0.193 (0.010) | 0.193 (0.010) | 0.192 (0.010) | 0.193 (0.010) | 0.193 (0.010) | 0.193 (0.010) | 0.192 (0.010) |
| 1 | 0.200 (0.010) | 0.200 (0.010) | 0.200 (0.010) | 0.201 (0.010) | 0.201 (0.010) | 0.200 (0.010) | 0.200 (0.010) | 0.200 (0.010) | 0.200 (0.010) | 0.200 (0.010) | 0.200 (0.010) |
| 2 | 0.199 (0.011) | 0.199 (0.010) | 0.199 (0.011) | 0.201 (0.011) | 0.201 (0.011) | 0.199 (0.010) | 0.199 (0.010) | 0.199 (0.010) | 0.199 (0.010) | 0.199 (0.010) | 0.199 (0.010) |
| 3 | 0.196 (0.012) | 0.197 (0.012) | 0.197 (0.012) | 0.199 (0.012) | 0.199 (0.012) | 0.197 (0.012) | 0.196 (0.012) | 0.197 (0.012) | 0.197 (0.012) | 0.197 (0.012) | 0.196 (0.012) |
| 4 | 0.195 (0.015) | 0.196 (0.014) | 0.195 (0.015) | 0.198 (0.015) | 0.199 (0.015) | 0.196 (0.014) | 0.195 (0.014) | 0.196 (0.014) | 0.196 (0.014) | 0.196 (0.014) | 0.195 (0.014) |
| 5 | 0.193 (0.017) | 0.194 (0.017) | 0.193 (0.017) | 0.198 (0.016) | 0.198 (0.016) | 0.195 (0.016) | 0.194 (0.016) | 0.195 (0.016) | 0.195 (0.016) | 0.195 (0.016) | 0.194 (0.016) |

### A.5.6 Binary marker: Simulation 2c

- Semi-Markov model; Marker observed continuously; Single baseline covariate $X$

**Table A.24:** Simulation results for binary marker Scenario 2c.

**(a)** Mean (and standard deviation) of the root mean squared prediction error in 500 simulations for binary marker Scenario 2c.

| | $\tau$ | MSM | MSMCox | SMM | LSM3 | LSM4 | BC1 | BW1 | BC2 | BW2 | BC3 | BW3 |
|---|---|---|---|---|---|---|---|---|---|---|---|---|
| $X=0$ | 0 | 0.015 (0.011) | 0.016 (0.013) | 0.010 (0.008) | 0.023 (0.014) | 0.023 (0.014) | 0.021 (0.013) | 0.020 (0.013) | 0.021 (0.014) | 0.020 (0.013) | 0.021 (0.013) | 0.019 (0.013) |
| | 1 | 0.017 (0.010) | 0.022 (0.013) | 0.012 (0.007) | 0.041 (0.013) | 0.048 (0.015) | 0.025 (0.014) | 0.022 (0.012) | 0.025 (0.014) | 0.022 (0.011) | 0.026 (0.014) | 0.023 (0.012) |
| | 2 | 0.020 (0.011) | 0.026 (0.014) | 0.014 (0.007) | 0.055 (0.016) | 0.061 (0.015) | 0.030 (0.017) | 0.025 (0.014) | 0.030 (0.017) | 0.025 (0.014) | 0.030 (0.018) | 0.025 (0.015) |
| | 3 | 0.023 (0.013) | 0.031 (0.016) | 0.016 (0.008) | 0.066 (0.018) | 0.068 (0.019) | 0.035 (0.021) | 0.028 (0.016) | 0.035 (0.021) | 0.028 (0.016) | 0.035 (0.021) | 0.028 (0.016) |
| | 4 | 0.026 (0.015) | 0.036 (0.018) | 0.017 (0.009) | 0.074 (0.021) | 0.071 (0.023) | 0.040 (0.022) | 0.032 (0.018) | 0.040 (0.022) | 0.032 (0.018) | 0.040 (0.022) | 0.032 (0.018) |
| | 5 | 0.029 (0.016) | 0.042 (0.021) | 0.019 (0.010) | 0.080 (0.024) | 0.072 (0.027) | 0.043 (0.024) | 0.036 (0.020) | 0.043 (0.024) | 0.036 (0.020) | 0.045 (0.025) | 0.038 (0.021) |
| $X=1$ | 0 | 0.021 (0.016) | 0.023 (0.018) | 0.015 (0.012) | 0.027 (0.020) | 0.027 (0.020) | 0.025 (0.019) | 0.021 (0.016) | 0.025 (0.019) | 0.021 (0.016) | 0.025 (0.019) | 0.021 (0.016) |
| | 1 | 0.024 (0.014) | 0.030 (0.018) | 0.016 (0.010) | 0.048 (0.021) | 0.040 (0.021) | 0.031 (0.019) | 0.024 (0.014) | 0.031 (0.019) | 0.025 (0.014) | 0.033 (0.018) | 0.026 (0.014) |
| | 2 | 0.026 (0.015) | 0.033 (0.019) | 0.018 (0.010) | 0.055 (0.022) | 0.048 (0.021) | 0.034 (0.020) | 0.026 (0.015) | 0.034 (0.020) | 0.027 (0.015) | 0.034 (0.020) | 0.026 (0.015) |
| | 3 | 0.029 (0.015) | 0.038 (0.021) | 0.019 (0.010) | 0.062 (0.024) | 0.061 (0.025) | 0.037 (0.022) | 0.029 (0.016) | 0.037 (0.022) | 0.029 (0.016) | 0.036 (0.022) | 0.029 (0.016) |
| | 4 | 0.031 (0.017) | 0.046 (0.026) | 0.020 (0.011) | 0.070 (0.027) | 0.074 (0.030) | 0.044 (0.026) | 0.037 (0.019) | 0.044 (0.026) | 0.037 (0.019) | 0.046 (0.026) | 0.039 (0.019) |
| | 5 | 0.034 (0.018) | 0.053 (0.030) | 0.021 (0.011) | 0.082 (0.032) | 0.090 (0.034) | 0.063 (0.035) | 0.051 (0.025) | 0.062 (0.034) | 0.050 (0.025) | 0.067 (0.034) | 0.055 (0.025) |

**(b)** Mean (and standard deviation) of the AUC in 500 simulations for binary marker Scenario 2c.

| $\tau$ | MSM | MSMCox | SMM | LSM3 | LSM4 | BC1 | BW1 | BC2 | BW2 | BC3 | BW3 |
|---|---|---|---|---|---|---|---|---|---|---|---|
| 0 | 0.630 (0.027) | 0.631 (0.025) | 0.631 (0.025) | 0.631 (0.025) | 0.631 (0.025) | 0.631 (0.025) | 0.631 (0.025) | 0.631 (0.025) | 0.631 (0.025) | 0.631 (0.025) | 0.631 (0.025) |
| 1 | 0.676 (0.028) | 0.676 (0.028) | 0.677 (0.028) | 0.675 (0.029) | 0.673 (0.029) | 0.676 (0.028) | 0.676 (0.028) | 0.676 (0.028) | 0.675 (0.028) | 0.675 (0.028) | 0.675 (0.028) |
| 2 | 0.698 (0.031) | 0.698 (0.031) | 0.699 (0.031) | 0.696 (0.031) | 0.694 (0.031) | 0.698 (0.031) | 0.698 (0.031) | 0.698 (0.031) | 0.697 (0.031) | 0.697 (0.031) | 0.697 (0.031) |
| 3 | 0.705 (0.036) | 0.705 (0.037) | 0.707 (0.036) | 0.703 (0.037) | 0.702 (0.037) | 0.705 (0.036) | 0.705 (0.036) | 0.705 (0.036) | 0.704 (0.036) | 0.704 (0.036) | 0.704 (0.036) |
| 4 | 0.707 (0.039) | 0.705 (0.039) | 0.709 (0.038) | 0.704 (0.040) | 0.704 (0.040) | 0.705 (0.039) | 0.705 (0.039) | 0.705 (0.039) | 0.705 (0.039) | 0.705 (0.039) | 0.705 (0.039) |
| 5 | 0.702 (0.047) | 0.701 (0.047) | 0.706 (0.046) | 0.699 (0.047) | 0.700 (0.047) | 0.700 (0.046) | 0.701 (0.046) | 0.700 (0.046) | 0.701 (0.047) | 0.701 (0.047) | 0.701 (0.047) |

**(c)** Mean (and standard deviation) of the Brier Score in 500 simulations for binary marker Scenario 2c.

| $\tau$ | MSM | MSMCox | SMM | LSM3 | LSM4 | BC1 | BW1 | BC2 | BW2 | BC3 | BW3 |
|---|---|---|---|---|---|---|---|---|---|---|---|
| 0 | 0.192 (0.009) | 0.192 (0.009) | 0.191 (0.009) | 0.193 (0.009) | 0.193 (0.009) | 0.192 (0.010) | 0.192 (0.010) | 0.193 (0.010) | 0.192 (0.010) | 0.192 (0.010) | 0.192 (0.010) |
| 1 | 0.194 (0.010) | 0.194 (0.010) | 0.193 (0.010) | 0.195 (0.011) | 0.195 (0.011) | 0.194 (0.010) | 0.194 (0.010) | 0.194 (0.010) | 0.194 (0.010) | 0.194 (0.010) | 0.194 (0.010) |
| 2 | 0.192 (0.011) | 0.192 (0.011) | 0.191 (0.011) | 0.195 (0.011) | 0.195 (0.011) | 0.192 (0.011) | 0.192 (0.011) | 0.192 (0.011) | 0.192 (0.011) | 0.192 (0.011) | 0.192 (0.011) |
| 3 | 0.191 (0.013) | 0.191 (0.014) | 0.189 (0.013) | 0.194 (0.013) | 0.195 (0.013) | 0.191 (0.013) | 0.191 (0.013) | 0.191 (0.013) | 0.191 (0.013) | 0.191 (0.013) | 0.191 (0.013) |
| 4 | 0.190 (0.015) | 0.191 (0.015) | 0.188 (0.015) | 0.194 (0.015) | 0.194 (0.014) | 0.191 (0.014) | 0.190 (0.014) | 0.191 (0.014) | 0.191 (0.014) | 0.191 (0.014) | 0.190 (0.014) |
| 5 | 0.188 (0.017) | 0.190 (0.018) | 0.187 (0.017) | 0.195 (0.017) | 0.194 (0.017) | 0.190 (0.017) | 0.189 (0.016) | 0.190 (0.017) | 0.191 (0.017) | 0.191 (0.017) | 0.190 (0.016) |

### A.5.7 Binary marker: Simulation 3a

- Markov model; Marker observed at random inspection times (rate=0.5); Two baseline covariates $X_1, X_2$

**Table A.25:** Simulation results for binary marker Scenario 3a.

**(a)** Mean (and standard deviation) of the root mean squared prediction error in 500 simulations for binary marker Scenario 3a.

| | $\tau$ | MM | MMCox | LM3 | LMInt3 | LM4 | LMInt4 | BC1 | BW1 | BC2 | BW2 | BC3 | BW3 |
|---|---|---|---|---|---|---|---|---|---|---|---|---|---|
| | 0 | 0.018 (0.013) | 0.022 (0.014) | 0.027 (0.018) | 0.022 (0.016) | 0.027 (0.018) | 0.022 (0.016) | 0.028 (0.017) | 0.029 (0.016) | 0.029 (0.017) | 0.029 (0.016) | 0.029 (0.017) | 0.029 (0.016) |
| | 1 | 0.018 (0.012) | 0.022 (0.014) | 0.029 (0.017) | 0.026 (0.017) | 0.033 (0.018) | 0.027 (0.017) | 0.024 (0.015) | 0.023 (0.014) | 0.024 (0.015) | 0.024 (0.014) | 0.025 (0.015) | 0.024 (0.014) |
| $X_1 = 0$ | 2 | 0.021 (0.012) | 0.025 (0.015) | 0.034 (0.018) | 0.031 (0.019) | 0.039 (0.018) | 0.032 (0.019) | 0.027 (0.015) | 0.024 (0.013) | 0.027 (0.015) | 0.024 (0.013) | 0.028 (0.015) | 0.025 (0.013) |
| $X_2 = 0$ | 3 | 0.024 (0.013) | 0.030 (0.016) | 0.040 (0.019) | 0.035 (0.021) | 0.044 (0.020) | 0.036 (0.021) | 0.031 (0.017) | 0.026 (0.014) | 0.031 (0.017) | 0.026 (0.014) | 0.031 (0.017) | 0.026 (0.014) |
| | 4 | 0.026 (0.014) | 0.032 (0.018) | 0.046 (0.020) | 0.040 (0.022) | 0.047 (0.021) | 0.041 (0.022) | 0.033 (0.018) | 0.028 (0.015) | 0.033 (0.018) | 0.028 (0.015) | 0.033 (0.018) | 0.028 (0.015) |
| | 5 | 0.029 (0.016) | 0.037 (0.020) | 0.050 (0.022) | 0.043 (0.024) | 0.049 (0.024) | 0.045 (0.025) | 0.036 (0.019) | 0.030 (0.016) | 0.037 (0.019) | 0.030 (0.016) | 0.037 (0.019) | 0.031 (0.017) |
| | 0 | 0.027 (0.020) | 0.030 (0.024) | 0.048 (0.034) | 0.036 (0.027) | 0.046 (0.034) | 0.036 (0.027) | 0.031 (0.024) | 0.029 (0.023) | 0.031 (0.024) | 0.028 (0.022) | 0.032 (0.024) | 0.029 (0.023) |
| | 1 | 0.028 (0.021) | 0.045 (0.032) | 0.062 (0.036) | 0.040 (0.030) | 0.055 (0.036) | 0.041 (0.030) | 0.046 (0.033) | 0.039 (0.026) | 0.044 (0.032) | 0.037 (0.026) | 0.047 (0.033) | 0.040 (0.027) |
| $X_1 = 1$ | 2 | 0.030 (0.021) | 0.057 (0.034) | 0.073 (0.035) | 0.046 (0.031) | 0.064 (0.035) | 0.047 (0.031) | 0.056 (0.034) | 0.046 (0.029) | 0.054 (0.034) | 0.043 (0.028) | 0.056 (0.035) | 0.046 (0.029) |
| $X_2 = 0$ | 3 | 0.033 (0.023) | 0.063 (0.037) | 0.078 (0.035) | 0.051 (0.033) | 0.072 (0.036) | 0.051 (0.034) | 0.058 (0.036) | 0.048 (0.030) | 0.055 (0.035) | 0.046 (0.029) | 0.058 (0.036) | 0.048 (0.030) |
| | 4 | 0.035 (0.024) | 0.067 (0.041) | 0.085 (0.037) | 0.056 (0.038) | 0.085 (0.038) | 0.059 (0.039) | 0.057 (0.036) | 0.049 (0.030) | 0.055 (0.036) | 0.047 (0.029) | 0.056 (0.037) | 0.048 (0.030) |
| | 5 | 0.037 (0.026) | 0.068 (0.044) | 0.085 (0.040) | 0.058 (0.042) | 0.092 (0.043) | 0.062 (0.043) | 0.056 (0.036) | 0.048 (0.029) | 0.055 (0.035) | 0.047 (0.028) | 0.057 (0.037) | 0.048 (0.031) |
| | 0 | 0.021 (0.016) | 0.022 (0.017) | 0.021 (0.016) | 0.028 (0.022) | 0.021 (0.016) | 0.028 (0.022) | 0.020 (0.016) | 0.019 (0.014) | 0.020 (0.016) | 0.019 (0.014) | 0.020 (0.016) | 0.019 (0.015) |
| | 1 | 0.023 (0.016) | 0.032 (0.021) | 0.030 (0.018) | 0.033 (0.024) | 0.035 (0.019) | 0.034 (0.024) | 0.033 (0.022) | 0.029 (0.018) | 0.034 (0.022) | 0.029 (0.018) | 0.034 (0.022) | 0.029 (0.019) |
| $X_1 = 0$ | 2 | 0.027 (0.016) | 0.039 (0.024) | 0.044 (0.021) | 0.039 (0.026) | 0.052 (0.022) | 0.041 (0.026) | 0.045 (0.026) | 0.039 (0.021) | 0.046 (0.026) | 0.040 (0.021) | 0.046 (0.026) | 0.039 (0.021) |
| $X_2 = 1$ | 3 | 0.030 (0.017) | 0.045 (0.024) | 0.056 (0.024) | 0.045 (0.026) | 0.062 (0.025) | 0.046 (0.026) | 0.053 (0.028) | 0.047 (0.023) | 0.053 (0.028) | 0.047 (0.023) | 0.053 (0.028) | 0.046 (0.023) |
| | 4 | 0.032 (0.017) | 0.050 (0.026) | 0.066 (0.029) | 0.051 (0.029) | 0.069 (0.030) | 0.052 (0.030) | 0.058 (0.030) | 0.053 (0.025) | 0.058 (0.031) | 0.052 (0.025) | 0.058 (0.031) | 0.053 (0.025) |
| | 5 | 0.035 (0.019) | 0.054 (0.029) | 0.073 (0.032) | 0.054 (0.031) | 0.071 (0.035) | 0.056 (0.033) | 0.061 (0.033) | 0.058 (0.027) | 0.060 (0.033) | 0.057 (0.028) | 0.063 (0.034) | 0.060 (0.029) |
| | 0 | 0.036 (0.027) | 0.042 (0.029) | 0.047 (0.034) | 0.054 (0.038) | 0.048 (0.034) | 0.053 (0.038) | 0.056 (0.037) | 0.053 (0.038) | 0.050 (0.035) | 0.046 (0.031) | 0.056 (0.037) | 0.052 (0.033) |
| | 1 | 0.036 (0.026) | 0.041 (0.027) | 0.059 (0.034) | 0.066 (0.040) | 0.060 (0.037) | 0.067 (0.040) | 0.053 (0.033) | 0.067 (0.040) | 0.049 (0.030) | 0.047 (0.029) | 0.053 (0.032) | 0.052 (0.030) |
| $X_1 = 1$ | 2 | 0.040 (0.028) | 0.047 (0.029) | 0.070 (0.039) | 0.073 (0.044) | 0.068 (0.042) | 0.074 (0.044) | 0.053 (0.036) | 0.074 (0.044) | 0.051 (0.034) | 0.052 (0.031) | 0.054 (0.035) | 0.056 (0.032) |
| $X_2 = 1$ | 3 | 0.044 (0.029) | 0.053 (0.032) | 0.079 (0.042) | 0.079 (0.046) | 0.078 (0.044) | 0.079 (0.047) | 0.063 (0.039) | 0.079 (0.047) | 0.062 (0.039) | 0.064 (0.035) | 0.063 (0.040) | 0.064 (0.035) |
| | 4 | 0.047 (0.031) | 0.058 (0.035) | 0.090 (0.051) | 0.084 (0.052) | 0.092 (0.052) | 0.087 (0.053) | 0.078 (0.047) | 0.087 (0.053) | 0.083 (0.049) | 0.080 (0.041) | 0.079 (0.049) | 0.076 (0.040) |
| | 5 | 0.050 (0.034) | 0.065 (0.040) | 0.101 (0.059) | 0.089 (0.057) | 0.106 (0.059) | 0.093 (0.058) | 0.102 (0.060) | 0.093 (0.058) | 0.116 (0.064) | 0.104 (0.050) | 0.106 (0.063) | 0.094 (0.048) |

**(b)** Mean (and standard deviation) of the AUC in 500 simulations simulations for binary marker Scenario 3a.

| $\tau$ | MM | MMCox | LM3 | LMInt3 | LM4 | LMInt4 | BC1 | BW1 | BC2 | BW2 | BC3 | BW3 |
|---|---|---|---|---|---|---|---|---|---|---|---|---|
| 0 | 0.655 (0.030) | 0.656 (0.030) | 0.653 (0.031) | 0.654 (0.031) | 0.653 (0.031) | 0.654 (0.031) | 0.655 (0.030) | 0.655 (0.030) | 0.656 (0.030) | 0.656 (0.030) | 0.655 (0.030) | 0.655 (0.030) |
| 1 | 0.679 (0.030) | 0.681 (0.029) | 0.678 (0.030) | 0.679 (0.030) | 0.678 (0.030) | 0.679 (0.030) | 0.679 (0.029) | 0.679 (0.029) | 0.680 (0.029) | 0.680 (0.029) | 0.679 (0.029) | 0.679 (0.029) |
| 2 | 0.690 (0.034) | 0.691 (0.033) | 0.689 (0.033) | 0.690 (0.033) | 0.689 (0.033) | 0.690 (0.033) | 0.689 (0.032) | 0.689 (0.032) | 0.690 (0.032) | 0.690 (0.032) | 0.689 (0.033) | 0.690 (0.032) |
| 3 | 0.689 (0.038) | 0.689 (0.037) | 0.690 (0.038) | 0.689 (0.037) | 0.688 (0.038) | 0.689 (0.037) | 0.689 (0.037) | 0.688 (0.037) | 0.689 (0.037) | 0.689 (0.037) | 0.688 (0.037) | 0.688 (0.037) |
| 4 | 0.678 (0.042) | 0.676 (0.041) | 0.679 (0.042) | 0.677 (0.042) | 0.678 (0.042) | 0.677 (0.042) | 0.676 (0.042) | 0.677 (0.041) | 0.676 (0.041) | 0.676 (0.041) | 0.676 (0.042) | 0.676 (0.042) |
| 5 | 0.662 (0.047) | 0.660 (0.047) | 0.664 (0.046) | 0.661 (0.048) | 0.664 (0.047) | 0.661 (0.047) | 0.661 (0.047) | 0.662 (0.047) | 0.661 (0.047) | 0.661 (0.047) | 0.660 (0.047) | 0.661 (0.046) |

**(c)** Mean (and standard deviation) of the Brier Score in 500 simulations simulations for binary marker Scenario 3a.

| $\tau$ | MM | MMCox | LM3 | LMInt3 | LM4 | LMInt4 | BC1 | BW1 | BC2 | BW2 | BC3 | BW3 |
|---|---|---|---|---|---|---|---|---|---|---|---|---|
| 0 | 0.186 (0.010) | 0.186 (0.010) | 0.186 (0.010) | 0.186 (0.010) | 0.186 (0.010) | 0.186 (0.010) | 0.186 (0.010) | 0.186 (0.010) | 0.186 (0.010) | 0.186 (0.010) | 0.186 (0.010) | 0.186 (0.010) |
| 1 | 0.193 (0.010) | 0.193 (0.010) | 0.195 (0.010) | 0.195 (0.010) | 0.195 (0.010) | 0.195 (0.010) | 0.194 (0.010) | 0.194 (0.010) | 0.194 (0.010) | 0.194 (0.010) | 0.194 (0.010) | 0.194 (0.010) |
| 2 | 0.194 (0.011) | 0.194 (0.011) | 0.196 (0.011) | 0.196 (0.011) | 0.196 (0.011) | 0.196 (0.011) | 0.195 (0.011) | 0.195 (0.011) | 0.194 (0.011) | 0.194 (0.011) | 0.195 (0.011) | 0.195 (0.011) |
| 3 | 0.192 (0.013) | 0.193 (0.013) | 0.195 (0.013) | 0.195 (0.013) | 0.196 (0.013) | 0.195 (0.013) | 0.194 (0.012) | 0.194 (0.012) | 0.194 (0.012) | 0.194 (0.012) | 0.194 (0.012) | 0.194 (0.012) |
| 4 | 0.193 (0.014) | 0.194 (0.013) | 0.197 (0.014) | 0.196 (0.014) | 0.197 (0.014) | 0.197 (0.014) | 0.195 (0.013) | 0.195 (0.013) | 0.195 (0.013) | 0.195 (0.013) | 0.195 (0.013) | 0.195 (0.013) |
| 5 | 0.194 (0.017) | 0.195 (0.017) | 0.198 (0.018) | 0.197 (0.018) | 0.198 (0.018) | 0.197 (0.018) | 0.197 (0.016) | 0.196 (0.016) | 0.196 (0.016) | 0.196 (0.016) | 0.197 (0.017) | 0.196 (0.016) |

### A.5.8 Binary marker: Simulation 3b

- Markov model; Marker observed at random inspection times (rate=1); Two baseline covariate $X_1, X_2$

**Table A.26:** Simulation results for binary marker Scenario 3b.

**(a)** Mean (and standard deviation) of the root mean squared prediction error in 500 simulations for binary marker Scenario 3b.

| | $\tau$ | MM | MMCox | LM3 | LMInt3 | LM4 | LMInt4 | BC1 | BW1 | BC2 | BW2 | BC3 | BW3 |
|---|---|---|---|---|---|---|---|---|---|---|---|---|---|
| | 0 | 0.017 (0.013) | 0.020 (0.013) | 0.027 (0.017) | 0.021 (0.014) | 0.027 (0.017) | 0.021 (0.014) | 0.029 (0.017) | 0.029 (0.016) | 0.029 (0.017) | 0.029 (0.016) | 0.029 (0.017) | 0.029 (0.016) |
| | 1 | 0.018 (0.012) | 0.022 (0.014) | 0.029 (0.016) | 0.024 (0.015) | 0.033 (0.016) | 0.025 (0.016) | 0.025 (0.014) | 0.024 (0.014) | 0.025 (0.015) | 0.024 (0.014) | 0.026 (0.015) | 0.025 (0.014) |
| $X_1 = 0$ | 2 | 0.021 (0.012) | 0.026 (0.015) | 0.034 (0.016) | 0.029 (0.016) | 0.040 (0.016) | 0.030 (0.017) | 0.028 (0.015) | 0.025 (0.013) | 0.028 (0.015) | 0.025 (0.013) | 0.029 (0.015) | 0.025 (0.013) |
| $X_2 = 0$ | 3 | 0.023 (0.012) | 0.030 (0.016) | 0.040 (0.017) | 0.033 (0.017) | 0.044 (0.017) | 0.034 (0.018) | 0.031 (0.017) | 0.026 (0.014) | 0.031 (0.017) | 0.026 (0.014) | 0.032 (0.017) | 0.027 (0.014) |
| | 4 | 0.026 (0.013) | 0.033 (0.017) | 0.044 (0.018) | 0.036 (0.019) | 0.045 (0.019) | 0.037 (0.020) | 0.033 (0.018) | 0.028 (0.015) | 0.033 (0.018) | 0.028 (0.015) | 0.033 (0.018) | 0.028 (0.015) |
| | 5 | 0.028 (0.014) | 0.037 (0.019) | 0.049 (0.020) | 0.041 (0.022) | 0.047 (0.022) | 0.043 (0.022) | 0.037 (0.019) | 0.031 (0.016) | 0.037 (0.020) | 0.031 (0.017) | 0.038 (0.020) | 0.031 (0.017) |
| | 0 | 0.026 (0.020) | 0.030 (0.023) | 0.051 (0.034) | 0.035 (0.027) | 0.049 (0.033) | 0.035 (0.027) | 0.031 (0.024) | 0.027 (0.022) | 0.030 (0.023) | 0.027 (0.021) | 0.031 (0.024) | 0.028 (0.022) |
| | 1 | 0.028 (0.020) | 0.041 (0.029) | 0.068 (0.033) | 0.039 (0.028) | 0.058 (0.033) | 0.040 (0.028) | 0.045 (0.031) | 0.037 (0.025) | 0.042 (0.030) | 0.035 (0.024) | 0.046 (0.031) | 0.038 (0.025) |
| $X_1 = 1$ | 2 | 0.030 (0.020) | 0.049 (0.030) | 0.080 (0.032) | 0.044 (0.029) | 0.068 (0.031) | 0.045 (0.029) | 0.054 (0.033) | 0.043 (0.027) | 0.051 (0.032) | 0.041 (0.026) | 0.054 (0.033) | 0.044 (0.027) |
| $X_2 = 0$ | 3 | 0.032 (0.021) | 0.053 (0.033) | 0.085 (0.032) | 0.047 (0.029) | 0.077 (0.032) | 0.048 (0.029) | 0.055 (0.034) | 0.046 (0.028) | 0.053 (0.034) | 0.044 (0.027) | 0.055 (0.034) | 0.046 (0.028) |
| | 4 | 0.034 (0.022) | 0.057 (0.035) | 0.089 (0.034) | 0.051 (0.033) | 0.088 (0.035) | 0.053 (0.033) | 0.055 (0.034) | 0.047 (0.028) | 0.054 (0.033) | 0.046 (0.027) | 0.055 (0.034) | 0.047 (0.028) |
| | 5 | 0.036 (0.023) | 0.058 (0.038) | 0.091 (0.036) | 0.056 (0.037) | 0.097 (0.040) | 0.058 (0.038) | 0.057 (0.034) | 0.048 (0.027) | 0.055 (0.034) | 0.047 (0.027) | 0.056 (0.035) | 0.048 (0.028) |
| | 0 | 0.020 (0.016) | 0.021 (0.017) | 0.021 (0.016) | 0.028 (0.022) | 0.021 (0.016) | 0.028 (0.022) | 0.020 (0.016) | 0.019 (0.014) | 0.020 (0.016) | 0.019 (0.014) | 0.020 (0.017) | 0.019 (0.015) |
| | 1 | 0.023 (0.015) | 0.029 (0.020) | 0.032 (0.016) | 0.033 (0.024) | 0.040 (0.018) | 0.035 (0.024) | 0.033 (0.022) | 0.029 (0.018) | 0.034 (0.022) | 0.029 (0.018) | 0.034 (0.021) | 0.030 (0.018) |
| $X_1 = 0$ | 2 | 0.026 (0.016) | 0.035 (0.021) | 0.046 (0.020) | 0.038 (0.024) | 0.057 (0.021) | 0.039 (0.024) | 0.045 (0.025) | 0.038 (0.021) | 0.045 (0.025) | 0.039 (0.021) | 0.045 (0.025) | 0.039 (0.021) |
| $X_2 = 1$ | 3 | 0.029 (0.016) | 0.039 (0.022) | 0.058 (0.024) | 0.043 (0.025) | 0.067 (0.024) | 0.043 (0.025) | 0.052 (0.028) | 0.045 (0.023) | 0.052 (0.028) | 0.045 (0.023) | 0.052 (0.028) | 0.045 (0.023) |
| | 4 | 0.032 (0.017) | 0.044 (0.024) | 0.068 (0.029) | 0.047 (0.028) | 0.071 (0.031) | 0.048 (0.029) | 0.056 (0.030) | 0.051 (0.025) | 0.056 (0.030) | 0.050 (0.025) | 0.057 (0.030) | 0.051 (0.026) |
| | 5 | 0.034 (0.019) | 0.049 (0.027) | 0.076 (0.034) | 0.053 (0.030) | 0.073 (0.037) | 0.055 (0.031) | 0.059 (0.033) | 0.055 (0.027) | 0.058 (0.033) | 0.055 (0.027) | 0.061 (0.034) | 0.057 (0.028) |
| | 0 | 0.035 (0.026) | 0.043 (0.029) | 0.046 (0.033) | 0.055 (0.038) | 0.047 (0.033) | 0.055 (0.038) | 0.063 (0.039) | 0.055 (0.038) | 0.056 (0.037) | 0.052 (0.033) | 0.062 (0.039) | 0.058 (0.036) |
| | 1 | 0.036 (0.026) | 0.041 (0.027) | 0.059 (0.031) | 0.065 (0.038) | 0.056 (0.033) | 0.066 (0.037) | 0.058 (0.034) | 0.066 (0.037) | 0.053 (0.032) | 0.052 (0.031) | 0.058 (0.034) | 0.058 (0.032) |
| $X_1 = 1$ | 2 | 0.038 (0.026) | 0.045 (0.028) | 0.071 (0.036) | 0.069 (0.041) | 0.064 (0.037) | 0.070 (0.041) | 0.058 (0.036) | 0.070 (0.041) | 0.054 (0.035) | 0.057 (0.032) | 0.058 (0.036) | 0.061 (0.033) |
| $X_2 = 1$ | 3 | 0.041 (0.027) | 0.051 (0.031) | 0.079 (0.040) | 0.072 (0.043) | 0.075 (0.041) | 0.073 (0.043) | 0.066 (0.040) | 0.073 (0.043) | 0.065 (0.040) | 0.067 (0.035) | 0.066 (0.041) | 0.068 (0.036) |
| | 4 | 0.044 (0.028) | 0.055 (0.034) | 0.086 (0.044) | 0.076 (0.043) | 0.088 (0.046) | 0.078 (0.045) | 0.080 (0.048) | 0.078 (0.045) | 0.083 (0.049) | 0.081 (0.040) | 0.081 (0.048) | 0.079 (0.040) |
| | 5 | 0.046 (0.030) | 0.062 (0.039) | 0.098 (0.055) | 0.081 (0.050) | 0.104 (0.056) | 0.084 (0.051) | 0.102 (0.059) | 0.084 (0.051) | 0.111 (0.061) | 0.100 (0.048) | 0.106 (0.059) | 0.094 (0.046) |

**(b)** Mean (and standard deviation) of the AUC in 500 simulations for binary marker Scenario 3b.

| $\tau$ | MM | MMCox | LM3 | LMInt3 | LM4 | LMInt4 | BC1 | BW1 | BC2 | BW2 | BC3 | BW3 |
|---|---|---|---|---|---|---|---|---|---|---|---|---|
| 0 | 0.655 (0.030) | 0.656 (0.030) | 0.651 (0.031) | 0.654 (0.031) | 0.651 (0.031) | 0.654 (0.031) | 0.654 (0.030) | 0.654 (0.030) | 0.656 (0.030) | 0.656 (0.030) | 0.654 (0.030) | 0.654 (0.030) |
| 1 | 0.681 (0.030) | 0.682 (0.030) | 0.678 (0.030) | 0.680 (0.030) | 0.677 (0.030) | 0.680 (0.030) | 0.680 (0.029) | 0.680 (0.029) | 0.681 (0.030) | 0.681 (0.030) | 0.680 (0.029) | 0.680 (0.029) |
| 2 | 0.694 (0.034) | 0.694 (0.033) | 0.692 (0.033) | 0.692 (0.033) | 0.691 (0.033) | 0.692 (0.033) | 0.692 (0.033) | 0.692 (0.033) | 0.693 (0.032) | 0.693 (0.032) | 0.692 (0.033) | 0.692 (0.033) |
| 3 | 0.692 (0.038) | 0.692 (0.037) | 0.693 (0.037) | 0.691 (0.037) | 0.692 (0.038) | 0.692 (0.037) | 0.690 (0.037) | 0.691 (0.037) | 0.691 (0.037) | 0.691 (0.037) | 0.691 (0.037) | 0.691 (0.037) |
| 4 | 0.681 (0.042) | 0.680 (0.042) | 0.682 (0.043) | 0.679 (0.042) | 0.682 (0.043) | 0.679 (0.043) | 0.678 (0.042) | 0.678 (0.043) | 0.678 (0.042) | 0.678 (0.042) | 0.679 (0.043) | 0.678 (0.042) |
| 5 | 0.664 (0.049) | 0.662 (0.047) | 0.666 (0.048) | 0.663 (0.048) | 0.666 (0.048) | 0.663 (0.048) | 0.663 (0.047) | 0.662 (0.047) | 0.662 (0.047) | 0.662 (0.047) | 0.662 (0.048) | 0.662 (0.048) |

**(c)** Mean (and standard deviation) of the Brier Score in 500 simulations for binary marker Scenario 3b.

| $\tau$ | MM | MMCox | LM3 | LMInt3 | LM4 | LMInt4 | BC1 | BW1 | BC2 | BW2 | BC3 | BW3 |
|---|---|---|---|---|---|---|---|---|---|---|---|---|
| 0 | 0.185 (0.010) | 0.186 (0.010) | 0.187 (0.010) | 0.186 (0.010) | 0.186 (0.010) | 0.186 (0.010) | 0.186 (0.010) | 0.186 (0.010) | 0.186 (0.010) | 0.186 (0.010) | 0.186 (0.010) | 0.186 (0.010) |
| 1 | 0.192 (0.010) | 0.192 (0.010) | 0.194 (0.010) | 0.194 (0.010) | 0.194 (0.010) | 0.194 (0.010) | 0.193 (0.010) | 0.193 (0.010) | 0.193 (0.010) | 0.193 (0.010) | 0.194 (0.010) | 0.193 (0.010) |
| 2 | 0.192 (0.012) | 0.192 (0.011) | 0.194 (0.011) | 0.194 (0.011) | 0.194 (0.011) | 0.194 (0.011) | 0.193 (0.011) | 0.193 (0.011) | 0.193 (0.011) | 0.193 (0.011) | 0.193 (0.011) | 0.193 (0.011) |
| 3 | 0.191 (0.013) | 0.191 (0.013) | 0.193 (0.013) | 0.192 (0.013) | 0.194 (0.013) | 0.193 (0.013) | 0.192 (0.012) | 0.192 (0.012) | 0.192 (0.013) | 0.192 (0.013) | 0.192 (0.012) | 0.192 (0.012) |
| 4 | 0.191 (0.014) | 0.192 (0.014) | 0.195 (0.014) | 0.193 (0.014) | 0.195 (0.014) | 0.193 (0.014) | 0.193 (0.013) | 0.193 (0.013) | 0.193 (0.013) | 0.193 (0.013) | 0.193 (0.013) | 0.193 (0.013) |
| 5 | 0.192 (0.017) | 0.194 (0.017) | 0.197 (0.017) | 0.195 (0.017) | 0.197 (0.017) | 0.195 (0.017) | 0.195 (0.016) | 0.194 (0.016) | 0.194 (0.016) | 0.194 (0.016) | 0.195 (0.017) | 0.194 (0.016) |

### A.5.9 Binary marker: Simulation 3c

- Markov model; Marker observed continuously; Two baseline covariate $X_1, X_2$

**Table A.27:** Simulation results for binary marker Scenario 3c.

**(a)** Mean (and standard deviation) of the root mean squared prediction error in 500 simulations for binary marker Scenario 3c.

| | $\tau$ | MM | MMCox | LM3 | LMInt3 | LM4 | LMInt4 | BC1 | BW1 | BC2 | BW2 | BC3 | BW3 |
|---|---|---|---|---|---|---|---|---|---|---|---|---|---|
| | 0 | 0.016 (0.013) | 0.018 (0.014) | 0.027 (0.017) | 0.020 (0.014) | 0.027 (0.017) | 0.020 (0.014) | 0.028 (0.016) | 0.028 (0.016) | 0.029 (0.017) | 0.029 (0.016) | 0.028 (0.017) | 0.028 (0.016) |
| | 1 | 0.019 (0.011) | 0.024 (0.015) | 0.033 (0.014) | 0.025 (0.014) | 0.039 (0.014) | 0.027 (0.014) | 0.028 (0.015) | 0.027 (0.014) | 0.028 (0.015) | 0.027 (0.014) | 0.030 (0.014) | 0.028 (0.014) |
| $X_1 = 0$ | 2 | 0.021 (0.011) | 0.028 (0.016) | 0.039 (0.014) | 0.029 (0.015) | 0.045 (0.014) | 0.030 (0.015) | 0.030 (0.016) | 0.027 (0.014) | 0.030 (0.016) | 0.027 (0.014) | 0.032 (0.016) | 0.028 (0.014) |
| $X_2 = 0$ | 3 | 0.023 (0.012) | 0.032 (0.018) | 0.044 (0.016) | 0.032 (0.017) | 0.046 (0.016) | 0.033 (0.018) | 0.033 (0.018) | 0.028 (0.015) | 0.033 (0.018) | 0.028 (0.015) | 0.033 (0.018) | 0.028 (0.015) |
| | 4 | 0.025 (0.013) | 0.035 (0.019) | 0.048 (0.016) | 0.034 (0.018) | 0.046 (0.018) | 0.036 (0.019) | 0.034 (0.019) | 0.029 (0.016) | 0.034 (0.019) | 0.029 (0.016) | 0.034 (0.019) | 0.030 (0.016) |
| | 5 | 0.027 (0.014) | 0.039 (0.021) | 0.052 (0.017) | 0.038 (0.020) | 0.046 (0.019) | 0.039 (0.021) | 0.037 (0.020) | 0.031 (0.017) | 0.038 (0.020) | 0.031 (0.017) | 0.039 (0.020) | 0.033 (0.018) |
| | 0 | 0.026 (0.020) | 0.029 (0.022) | 0.050 (0.032) | 0.032 (0.025) | 0.048 (0.032) | 0.032 (0.025) | 0.031 (0.024) | 0.028 (0.022) | 0.030 (0.023) | 0.027 (0.021) | 0.031 (0.024) | 0.028 (0.022) |
| | 1 | 0.027 (0.019) | 0.035 (0.022) | 0.075 (0.026) | 0.038 (0.025) | 0.062 (0.030) | 0.040 (0.025) | 0.046 (0.030) | 0.038 (0.024) | 0.043 (0.029) | 0.036 (0.023) | 0.047 (0.030) | 0.040 (0.025) |
| $X_1 = 1$ | 2 | 0.029 (0.019) | 0.037 (0.024) | 0.084 (0.026) | 0.041 (0.025) | 0.073 (0.026) | 0.042 (0.025) | 0.051 (0.031) | 0.042 (0.025) | 0.049 (0.030) | 0.040 (0.025) | 0.052 (0.031) | 0.043 (0.026) |
| $X_2 = 0$ | 3 | 0.030 (0.020) | 0.040 (0.027) | 0.087 (0.027) | 0.043 (0.027) | 0.083 (0.028) | 0.044 (0.027) | 0.051 (0.030) | 0.043 (0.025) | 0.050 (0.030) | 0.041 (0.025) | 0.051 (0.030) | 0.043 (0.025) |
| | 4 | 0.032 (0.021) | 0.044 (0.028) | 0.090 (0.028) | 0.045 (0.028) | 0.094 (0.032) | 0.048 (0.029) | 0.052 (0.029) | 0.044 (0.024) | 0.051 (0.030) | 0.043 (0.025) | 0.052 (0.029) | 0.044 (0.025) |
| | 5 | 0.033 (0.022) | 0.050 (0.032) | 0.091 (0.031) | 0.048 (0.031) | 0.104 (0.035) | 0.051 (0.032) | 0.061 (0.033) | 0.049 (0.025) | 0.057 (0.032) | 0.047 (0.026) | 0.061 (0.034) | 0.050 (0.027) |
| | 0 | 0.018 (0.014) | 0.019 (0.015) | 0.019 (0.014) | 0.027 (0.021) | 0.019 (0.015) | 0.027 (0.021) | 0.020 (0.016) | 0.018 (0.014) | 0.020 (0.016) | 0.019 (0.014) | 0.020 (0.015) | 0.018 (0.014) |
| | 1 | 0.022 (0.013) | 0.025 (0.015) | 0.042 (0.016) | 0.034 (0.021) | 0.056 (0.020) | 0.036 (0.021) | 0.036 (0.021) | 0.032 (0.018) | 0.037 (0.021) | 0.033 (0.018) | 0.038 (0.022) | 0.033 (0.019) |
| $X_1 = 0$ | 2 | 0.025 (0.014) | 0.030 (0.017) | 0.059 (0.022) | 0.038 (0.022) | 0.070 (0.024) | 0.039 (0.022) | 0.046 (0.026) | 0.040 (0.021) | 0.047 (0.026) | 0.040 (0.022) | 0.047 (0.026) | 0.040 (0.022) |
| $X_2 = 1$ | 3 | 0.027 (0.016) | 0.034 (0.019) | 0.071 (0.027) | 0.042 (0.023) | 0.076 (0.029) | 0.044 (0.024) | 0.052 (0.028) | 0.045 (0.024) | 0.052 (0.028) | 0.046 (0.023) | 0.052 (0.028) | 0.046 (0.024) |
| | 4 | 0.029 (0.017) | 0.038 (0.021) | 0.080 (0.030) | 0.045 (0.025) | 0.077 (0.033) | 0.047 (0.025) | 0.055 (0.030) | 0.050 (0.025) | 0.055 (0.030) | 0.049 (0.025) | 0.056 (0.030) | 0.051 (0.026) |
| | 5 | 0.031 (0.019) | 0.043 (0.024) | 0.085 (0.033) | 0.048 (0.028) | 0.074 (0.035) | 0.050 (0.029) | 0.057 (0.033) | 0.053 (0.027) | 0.056 (0.032) | 0.052 (0.027) | 0.060 (0.034) | 0.056 (0.029) |
| | 0 | 0.033 (0.025) | 0.038 (0.027) | 0.042 (0.031) | 0.051 (0.035) | 0.042 (0.031) | 0.051 (0.036) | 0.058 (0.037) | 0.051 (0.036) | 0.054 (0.036) | 0.050 (0.032) | 0.058 (0.037) | 0.054 (0.033) |
| | 1 | 0.034 (0.023) | 0.041 (0.026) | 0.065 (0.030) | 0.060 (0.032) | 0.056 (0.031) | 0.062 (0.033) | 0.056 (0.030) | 0.062 (0.033) | 0.053 (0.029) | 0.052 (0.028) | 0.058 (0.031) | 0.057 (0.029) |
| $X_1 = 1$ | 2 | 0.035 (0.023) | 0.043 (0.028) | 0.072 (0.036) | 0.062 (0.034) | 0.062 (0.035) | 0.062 (0.034) | 0.057 (0.033) | 0.062 (0.034) | 0.055 (0.032) | 0.058 (0.030) | 0.058 (0.033) | 0.061 (0.031) |
| $X_2 = 1$ | 3 | 0.036 (0.023) | 0.047 (0.030) | 0.077 (0.038) | 0.063 (0.034) | 0.075 (0.038) | 0.065 (0.034) | 0.069 (0.039) | 0.065 (0.034) | 0.069 (0.039) | 0.072 (0.035) | 0.069 (0.039) | 0.072 (0.035) |
| | 4 | 0.038 (0.024) | 0.050 (0.030) | 0.083 (0.041) | 0.065 (0.035) | 0.089 (0.043) | 0.069 (0.036) | 0.090 (0.048) | 0.069 (0.036) | 0.093 (0.049) | 0.093 (0.041) | 0.092 (0.048) | 0.090 (0.040) |
| | 5 | 0.040 (0.025) | 0.058 (0.037) | 0.093 (0.050) | 0.069 (0.041) | 0.107 (0.052) | 0.074 (0.042) | 0.121 (0.060) | 0.074 (0.042) | 0.129 (0.062) | 0.119 (0.048) | 0.125 (0.060) | 0.114 (0.046) |

**(b)** Mean (and standard deviation) of the AUC in 500 simulations for binary marker Scenario 3c.

| $\tau$ | MM | MMCox | LM3 | LMInt3 | LM4 | LMInt4 | BC1 | BW1 | BC2 | BW2 | BC3 | BW3 |
|---|---|---|---|---|---|---|---|---|---|---|---|---|
| 0 | 0.655 (0.030) | 0.655 (0.030) | 0.654 (0.031) | 0.655 (0.031) | 0.654 (0.031) | 0.655 (0.031) | 0.655 (0.030) | 0.655 (0.030) | 0.656 (0.030) | 0.656 (0.030) | 0.655 (0.030) | 0.655 (0.030) |
| 1 | 0.687 (0.030) | 0.688 (0.030) | 0.687 (0.030) | 0.687 (0.030) | 0.685 (0.030) | 0.687 (0.030) | 0.687 (0.029) | 0.687 (0.029) | 0.688 (0.030) | 0.688 (0.030) | 0.687 (0.030) | 0.687 (0.029) |
| 2 | 0.701 (0.034) | 0.701 (0.034) | 0.701 (0.033) | 0.700 (0.032) | 0.700 (0.033) | 0.700 (0.032) | 0.700 (0.032) | 0.700 (0.033) | 0.700 (0.033) | 0.700 (0.033) | 0.700 (0.033) | 0.700 (0.033) |
| 3 | 0.700 (0.038) | 0.699 (0.038) | 0.701 (0.037) | 0.698 (0.037) | 0.700 (0.037) | 0.698 (0.037) | 0.698 (0.037) | 0.698 (0.037) | 0.698 (0.037) | 0.698 (0.037) | 0.697 (0.037) | 0.698 (0.037) |
| 4 | 0.687 (0.041) | 0.685 (0.042) | 0.688 (0.041) | 0.686 (0.042) | 0.687 (0.041) | 0.685 (0.042) | 0.684 (0.041) | 0.684 (0.041) | 0.684 (0.041) | 0.684 (0.041) | 0.684 (0.041) | 0.684 (0.042) |
| 5 | 0.670 (0.049) | 0.667 (0.049) | 0.672 (0.047) | 0.667 (0.047) | 0.671 (0.047) | 0.667 (0.047) | 0.666 (0.047) | 0.666 (0.047) | 0.666 (0.047) | 0.666 (0.047) | 0.666 (0.048) | 0.665 (0.048) |

**(c)** Mean (and standard deviation) of the Brier Score in 500 simulations.

| $\tau$ | MM | MMCox | LM3 | LMInt3 | LM4 | LMInt4 | BC1 | BW1 | BC2 | BW2 | BC3 | BW3 |
|---|---|---|---|---|---|---|---|---|---|---|---|---|
| 0 | 0.185 (0.010) | 0.186 (0.010) | 0.186 (0.010) | 0.186 (0.010) | 0.186 (0.010) | 0.186 (0.010) | 0.186 (0.010) | 0.186 (0.010) | 0.186 (0.010) | 0.186 (0.010) | 0.186 (0.010) | 0.186 (0.010) |
| 1 | 0.188 (0.010) | 0.188 (0.010) | 0.190 (0.010) | 0.189 (0.010) | 0.191 (0.010) | 0.189 (0.010) | 0.189 (0.010) | 0.189 (0.010) | 0.189 (0.010) | 0.189 (0.010) | 0.189 (0.010) | 0.189 (0.010) |
| 2 | 0.187 (0.012) | 0.187 (0.012) | 0.190 (0.011) | 0.188 (0.012) | 0.190 (0.012) | 0.188 (0.012) | 0.188 (0.011) | 0.188 (0.011) | 0.188 (0.011) | 0.188 (0.011) | 0.188 (0.011) | 0.188 (0.011) |
| 3 | 0.186 (0.013) | 0.187 (0.013) | 0.190 (0.013) | 0.187 (0.013) | 0.190 (0.013) | 0.187 (0.013) | 0.188 (0.012) | 0.187 (0.012) | 0.187 (0.012) | 0.187 (0.012) | 0.188 (0.012) | 0.187 (0.012) |
| 4 | 0.188 (0.014) | 0.189 (0.014) | 0.192 (0.014) | 0.189 (0.014) | 0.192 (0.013) | 0.189 (0.014) | 0.190 (0.013) | 0.189 (0.013) | 0.189 (0.013) | 0.189 (0.013) | 0.190 (0.013) | 0.189 (0.013) |
| 5 | 0.189 (0.017) | 0.191 (0.018) | 0.194 (0.017) | 0.191 (0.018) | 0.194 (0.017) | 0.191 (0.018) | 0.192 (0.017) | 0.191 (0.016) | 0.191 (0.016) | 0.191 (0.016) | 0.193 (0.017) | 0.192 (0.016) |

# APPENDIX B

# Dynamic Risk Modelling with a Partially Observed Covariate using Lévy-based Bridge Processes

## B.1 Derivation of conditional and marginal survival functions

### B.1.1 Gamma bridge process

If $U_t$ is gamma process with mean and variance $\mu t$, then the gamma bridge from 0 to 1 over the interval $[0, \tau]$ is distributed $U_{t\tau} \sim \text{Beta}(\mu t, \mu(\tau - t))$, for $0 \leq t \leq \tau$. The Laplace function of the bridge is then given by

$$\mathbb{E}[\exp\{-sU_{t\tau}\}] = 1 + \sum_{k=1}^{\infty} \left[ \prod_{r=1}^{k} \frac{\alpha + r - 1}{\alpha + \beta + r - 1} \right] \frac{(-1)^k}{k!} s^k := M(\alpha, \alpha + \beta, -s) \qquad \text{(B.1)}$$

where $\alpha = \mu t$ and $\beta = \mu(\tau - t)$, and $M$ is Kummer's confluent hypergeometric function.

If $U_t$ is a scaled gamma process with mean $\mu t$ and variance $\sigma^2 t$, then the gamma bridge is distributed $U_{t\tau} \sim \text{Beta}(mt, m(\tau - t))$, where $m = \mu^2/\sigma^2$ represents a standardized growth rate. The Laplace function of the bridge, is then given as in Eq.(B.1), where $\alpha = mt$ and $\beta = m(\tau - t)$.

The survival function conditional on the value of the marker at time $\tau$, $V_\tau = v$, is then

given by

$$S(t|v) = \mathbb{E}_U[\exp\{-H(t)U_{t\tau}v\}] = 1 + \sum_{k=1}^{\infty}\prod_{r=1}^{k}\frac{\alpha+r-1}{\alpha+\beta+r-1}\frac{(-1)^k v^k H^k(t)}{k!}$$
$$= M(\alpha, \alpha+\beta, -vH(t))$$
$$= M(mt, m\tau, -vH(t)) \tag{B.2}$$

The conditional hazard is derived as

$$\begin{aligned}
d\Lambda(t|v) &= \frac{\partial}{\partial t}[-\log S(t|v)] \\
&= -\frac{1}{S(t|v)}\frac{\partial}{\partial t}\left[S(t|v)\right] \\
&= -\frac{1}{S(t|v)}\frac{\partial}{\partial t}M(\alpha, \alpha+\beta, -H(t)v) \\
&= -\frac{1}{S(t|v)}\frac{\partial}{\partial t}\sum_{k=0}^{\infty}\frac{(\alpha)_k}{(\alpha+\beta)_k}\frac{(-1)^k v^k H^k(t)}{k!} \\
&= -\frac{1}{S(t|v)}\frac{\partial}{\partial t}\sum_{k=0}^{\infty}\frac{\Gamma(mt+k)}{\Gamma(mt)}\frac{\Gamma(m\tau)}{\Gamma(m\tau+k)}\frac{(-1)^k v^k H^k(t)}{k!} \\
&= -\frac{1}{S(t|v)}\frac{\partial}{\partial t}\left[1+\sum_{k=1}^{\infty}\frac{1}{B(mt,k)}\frac{\Gamma(m\tau)}{\Gamma(m\tau+k)}\frac{(-1)^k v^k H^k(t)}{k}\right] \\
&= -\frac{1}{S(t|v)}\sum_{k=1}^{\infty}\frac{\Gamma(m\tau)}{\Gamma(m\tau+k)}\frac{(-1)^k v^k}{k}\frac{\partial}{\partial t}\left[\frac{H^k(t)}{B(mt,k)}\right] \\
&= -\frac{1}{S(t|v)}\sum_{k=1}^{\infty}\frac{\Gamma(m\tau)}{\Gamma(m\tau+k)}\frac{(-1)^k v^k}{k}\left[\frac{mH^k(t)}{B(mt,k)}[\psi_0(mt+k)-\psi_0(mt)] + \frac{kH^{k-1}(t)h(t)}{B(mt,k)}\right] \\
&= -\frac{1}{S(t|v)}\sum_{k=1}^{\infty}\frac{1}{B(mt,k)}\frac{\Gamma(m\tau)}{\Gamma(m\tau+k)}\frac{(-1)^k v^k H^k(t)}{k}\left[m[\psi_0(mt+k)-\psi_0(mt)] + \frac{kh(t)}{H(t)}\right]
\end{aligned} \tag{B.3}$$

where $(x)_n = \Gamma(x+n)/\Gamma(x)$ is the Pochhammer symbol and $\psi_0(\cdot)$ is the digamma function.

#### B.1.1.1 $V_\tau$ and $U_t$ are based on a common $W_t$

The marginal survival function is obtained by integrating the conditional survival in Eq.(B.2) over the distribution of $V_\tau$,

$$S(t) = \mathbb{E}_{V_\tau}[\mathbb{E}_U[\exp\{-H(t)U_{t\tau}V_\tau\}]] = 1 + \sum_{k=1}^{\infty}\prod_{r=1}^{k}\frac{\alpha+r-1}{\alpha+\beta+r-1}\frac{(-1)^k p_k H^k(t)}{k!}$$

where $p_k$ is the $k$th moment of $V_\tau$, $\mathbb{E}[V_\tau^k]$.

Although various models can be considered for the value of the observed marker, for the purposes of our formulation we suppose that $V_\tau$ and $U_t$ are based on the common gamma process $W_t$ with mean $\mu t$ and variance $\sigma^2 t$. Thus, $V_\tau \sim \text{Gamma}(\text{shape} = m\tau, \text{scale} = \kappa)$ and the $k$th moment of $V_\tau$ is $p_k = \kappa^k(m\tau + k - 1)!/(m\tau - 1)!$. Thus, the survival function in Eq.(3.5) is given by

$$\begin{aligned}
S(t) &= 1 + \sum_{k=1}^{\infty} \left[ \prod_{r=1}^{k} \frac{\alpha + r - 1}{\alpha + \beta + r - 1} \right] \frac{(-1)^k p_k H^k(t)}{k!} \\
&= 1 + \sum_{k=1}^{\infty} \left[ \prod_{r=1}^{k} \frac{mt + r - 1}{mt + m(\tau - t) + r - 1} \right] \frac{(-1)^k H^k(t)}{k!} \frac{\kappa^k (m\tau + k - 1)!}{(m\tau - 1)!} \\
&= 1 + \sum_{k=1}^{\infty} \left[ \frac{(mt + k - 1)!}{(mt - 1)!} \frac{(m\tau - 1)!}{(m\tau + k - 1)!} \right] \frac{(-1)^k H^k(t)}{k!} \frac{\kappa^k (m\tau + k - 1)!}{(m\tau - 1)!} \\
&= 1 + \sum_{k=1}^{\infty} \frac{\Gamma(mt + k)}{\Gamma(mt)} \frac{(-1)^k \kappa^k H^k(t)}{k!} \\
&= \sum_{k=0}^{\infty} \binom{mt + k - 1}{k} [-\kappa H(t)]^k \\
&= (1 + \kappa H(t))^{-mt}
\end{aligned}$$

which is the Laplace transform of a gamma random variable with shape $mt$ and scale $\kappa$, i.e., $\mathcal{L}(s) = (1 - \kappa s)^{-mt}$ with $s = -H(t)$.

The cumulative hazard is then $\Lambda(t) = -\log S(t)$ and the hazard is given by

$$\begin{aligned}
d\Lambda(t) &= \partial/\partial t[-\log S(t)] \\
&= m \log(1 + \kappa H(t)) + \frac{\kappa m t}{1 + \kappa H(t)} h(t)
\end{aligned}$$

We perform estimation of the model parameters by maximizing the log-likelihood

$$l = \sum_{i=1}^{n} \{\delta_i \log(d\Lambda(T_i|v_{T_i}) S(T_i|v_{T_i}) f(v_{T_i})) + (1 - \delta_i) \log[S(T_i|v_{T_i}) g(v_{T_i})]\}$$

where $\delta_i$ is an indicator of whether the patient had the event of interest, and $v_{T_i}$ is the observed value of $V_\tau$ at the event time $T$ for subject $i$.

### B.1.2 Incorporating measurement error with $Z_\tau \sim V_\tau$

We suppose that $V_\tau$ is gamma distributed with mean $\mu\tau$ and variance $\sigma^2\tau$ (shape=$m\tau$, scale=$\kappa$). Then the probability density function of $V_\tau$ is given as

$$g(v) = \frac{1}{\Gamma(m\tau)\kappa^{m\tau}} v^{m\tau-1} e^{-v/\kappa}$$

We now extend to the situation where we write $Z_\tau$ as a regression on $V_\tau$, $Z_\tau \sim V_\tau$. We then write the conditional survival function $G(t|Z_\tau)$ as an average of $S(t|V_\tau)$ over the regression $Z_\tau \sim V_\tau$, where $z$ is the observed value of $Z_\tau$. We use the assumption that given $V_\tau$, $T \perp Z_\tau$. Let $f(z|v)$ be the probability density function of $Z_\tau|V_\tau$ and $g(v)$ be the probability density function of $V_\tau$.

$$\begin{aligned}
G(t|Z_\tau = z) &= \frac{\Pr(T > t, Z_\tau = z)}{\Pr(Z_\tau = z)} \\
&= \frac{\int \Pr(T > t, Z_\tau = z|V_\tau) g(V_\tau)\, \mathrm{d}V_\tau}{\int \Pr(Z_\tau = z|V_\tau) g(V_\tau)\, \mathrm{d}V_\tau} \\
&= \frac{\int \Pr(T > t|V_\tau) \Pr(Z_\tau = z|V_\tau) g(V_\tau)\, \mathrm{d}V_\tau}{\int \Pr(Z_\tau = z|V_\tau) g(V_\tau)\, \mathrm{d}V_\tau} \\
&= \frac{\int S(t|V_\tau) f(z|V_\tau) g(V_\tau)\, \mathrm{d}V_\tau}{\int f(z|V_\tau) g(V_\tau)\, \mathrm{d}V_\tau} \\
&= \frac{\mathbb{E}_{V_\tau}[S(t|V_\tau) \times f(z|V_\tau)]}{\mathbb{E}_{V_\tau}[f(z|V_\tau)]}
\end{aligned}$$

The denominator is given by

$$\mathbb{E}_{V_\tau}[f(z|V_\tau)] = f(z) = \int f(z|v) g(v)\, \mathrm{d}v \tag{B.4}$$

The numerator is given by

$$\begin{aligned}\mathbb{E}_{V_\tau}[S(t|V_\tau) \times f(z|V_\tau)] &= \int S(t|v) f(z|v) g(v)\,\mathrm{d}v \\ &= \int \left(1 + \sum_{k=1}^{\infty} \prod_{r=1}^{k} \frac{\alpha + r - 1}{\alpha + \beta + r - 1} \frac{(-1)^k v^k H^k(t)}{k!}\right) f(z|v) g(v)\,\mathrm{d}v \\ &= \sum_{k=0}^{\infty} \frac{\Gamma(\alpha + k)}{\Gamma(\alpha)} \frac{\Gamma(\alpha + \beta)}{\Gamma(\alpha + \beta + k)} \frac{(-1)^k H^k(t)}{k!} \int v^k f(z|v) g(v)\,\mathrm{d}v\end{aligned}$$

The survival function of $[T|Z_\tau]$ is then derived as

$$G(t|Z_\tau = z) = \frac{\displaystyle\sum_{k=0}^{\infty} \frac{\Gamma(\alpha + k)}{\Gamma(\alpha)} \frac{\Gamma(\alpha + \beta)}{\Gamma(\alpha + \beta + k)} \frac{(-1)^k H^k(t)}{k!} \int v^k f(z|v) g(v)\,\mathrm{d}v}{\int f(z|v) g(v)\,\mathrm{d}v} \tag{B.5}$$

Let $\Phi(t)$ denote the cumulative hazard of the survival model $G(t)$. To get the conditional hazard $d\Phi(t|Z_T)$ we take the derivative of the negative log of the conditional survival function,

$$\begin{aligned}d\Phi(t|z) &= \frac{\partial}{\partial t}\left[-\log G(t|z)\right] \\ &= -\frac{1}{G(t|z)} \frac{\partial}{\partial t} G(t|z)\end{aligned} \tag{B.6}$$

and derive the derivative of $G(t|z)$ with respect to $t$.

The marginal survival function, $S(t)$, is given as above by

$$S(t) = (1 + \kappa H(t))^{-mt}$$

where $\kappa = 1$ and $m = \mu$ if the process is a standard gamma process with mean and variance $\mu t$.

The hazard is given by

$$d\Lambda(t) = \partial/\partial t[-\log G(t)] = m \log(1 + \kappa H(t)) + \frac{\kappa m t}{1 + \kappa H(t)} h(t)$$

We perform estimation of the model parameters by maximizing the log-likelihood

$$l = \sum_{i=1}^{n} \delta_i \log(d\Phi(T_i|z_{T_i})G(T_i|z_{T_i})f(z_{T_i})) + (1-\delta_i)\log[G(T_i|z_{T_i})f(z_{T_i})]$$

The following subsections derive the conditional and unconditional survival functions for various distributions of $Z_\tau|V_\tau$.

#### B.1.2.1 Compound Gamma-Gamma distribution

We assume that $Z_\tau|V_\tau = v$ is **Gamma distributed** with shape $\gamma$ and scale $v/\gamma$ (i.e., mean $v$ and variance $v^2/\gamma$). Thus, the probability distribution function of $Z_\tau|V_\tau$ is given by

$$f(z|v) = \frac{\gamma^\gamma}{\Gamma(\gamma)v^\gamma} z^{\gamma-1} e^{-z\gamma/v}$$

The denominator of the conditional survival $[T|Z_\tau]$ is then given by

$$\begin{aligned} f_{Z_\tau}(z) = \mathbb{E}_{V_\tau}[f(z|V_\tau)] &= \int f(z|v)g(v)\,\mathrm{d}v \\ &= \int_0^\infty \frac{1}{\Gamma(\gamma)}\frac{\gamma^\gamma}{v^\gamma} z^{\gamma-1} e^{-z\gamma/v} \frac{1}{\Gamma(m\tau)\kappa^{m\tau}} v^{m\tau-1} e^{-v/\kappa}\,\mathrm{d}v \\ &= \frac{2}{\Gamma(\gamma)\Gamma(m\tau)z}\left(\frac{\gamma z}{\kappa}\right)^{\frac{\gamma+m\tau}{2}} K_{m\tau-\gamma}(2\sqrt{\gamma z/\kappa}) \quad \{\mathrm{Re}[\gamma z/\kappa] > 0\} \end{aligned}$$

where $K_\alpha(n)$ is the modified Bessel function of the second kind. The mean and variance of $Z_\tau$ are then given by

$$\mathbb{E}(Z_\tau) = \mu\tau = m\kappa\tau \quad \mathrm{Var}(Z) = \sigma^2\tau\frac{(m\tau+\gamma+1)}{\gamma} = m\kappa^2\tau\frac{(m\tau+\gamma+1)}{\gamma}$$

The numerator is given by

$$\begin{aligned}
&\mathbb{E}_{V_\tau}[S(t|V_\tau) \times f(z|V_\tau)] = \int S(t|v) f(z|v) g(v)\,\mathrm{d}v \\
&= \sum_{k=0}^{\infty} \frac{\Gamma(\alpha+k)}{\Gamma(\alpha)} \frac{\Gamma(\alpha+\beta)}{\Gamma(\alpha+\beta+k)} \frac{(-1)^k H^k(t)}{k!} \int_0^{\infty} v^k \frac{1}{\Gamma(\gamma)} \frac{\gamma^\gamma}{v^\gamma} z^{\gamma-1} e^{-z\gamma/v} \frac{1}{\Gamma(m\tau)\kappa^{m\tau}} v^{m\tau-1} e^{-v/\kappa}\,\mathrm{d}v \\
&= \sum_{k=0}^{\infty} \frac{\Gamma(mt+k)}{\Gamma(mt)} \frac{\Gamma(m\tau)}{\Gamma(m\tau+k)} \frac{(-1)^k H^k(t)}{k!} \frac{2}{\Gamma(\gamma)\Gamma(m\tau)z} \left(\frac{\gamma z}{\kappa}\right)^{\frac{\gamma+m\tau}{2}} (\gamma\kappa z)^{\frac{k}{2}} K_{m\tau-\gamma+k}(2\sqrt{\gamma z/\kappa}) \\
&\{\mathrm{Re}[\gamma z/\kappa] > 0\}
\end{aligned}$$

The survival function is then

$$G(t|z) = 1 + \sum_{k=1}^{\infty} \frac{1}{k} \frac{1}{B(mt,k)} \frac{\Gamma(m\tau)}{\Gamma(m\tau+k)} \left((-1)H(t)\sqrt{\gamma\kappa z}\right)^k \frac{K_{m\tau-\gamma+k}(2\sqrt{\gamma z/\kappa})}{K_{m\tau-\gamma}(2\sqrt{\gamma z/\kappa})}$$

where $B(\cdot,\cdot)$ is the Beta function.
To get the conditional hazard, the derivative of $G(t|z)$ is given by

$$\begin{aligned}
\frac{\partial}{\partial t} G(t|Z_\tau) &= \frac{\partial}{\partial t}\left[1 + \sum_{k=1}^{\infty} \frac{1}{k} \frac{1}{B(mt,k)} \frac{\Gamma(m\tau)}{\Gamma(m\tau+k)} \left((-1)H(t)\sqrt{\gamma\kappa z}\right)^k \frac{K_{m\tau-\gamma+k}(2\sqrt{\gamma z/\kappa})}{K_{m\tau-\gamma}(2\sqrt{\gamma z/\kappa})}\right] \\
&= \sum_{k=1}^{\infty} \frac{1}{k} \frac{\Gamma(m\tau)}{\Gamma(m\tau+k)} \left((-1)\sqrt{\gamma\kappa z}\right)^k \frac{K_{m\tau-\gamma+k}(2\sqrt{\gamma z/\kappa})}{K_{m\tau-\gamma}(2\sqrt{\gamma z/\kappa})} \frac{\partial}{\partial t}\left[\frac{H^k(t)}{B(mt,k)}\right] \\
&= \sum_{k=1}^{\infty} \frac{1}{k} \frac{\Gamma(m\tau)}{\Gamma(m\tau+k)} \left((-1)\sqrt{\gamma\kappa z}\right)^k \frac{K_{m\tau-\gamma+k}(2\sqrt{\gamma\kappa z})}{K_{m\tau-\gamma}(2\sqrt{\gamma z/\kappa})} \left(\frac{mH^k(t)}{B(mt,k)}(\psi_0(mt+k) - \psi_0(mt)) + \frac{kH^{k-1}(t)h(t)}{B(mt,k)}\right) \\
&= \sum_{k=1}^{\infty} \frac{1}{k} \frac{1}{B(mt,k)} \frac{\Gamma(m\tau)}{\Gamma(m\tau+k)} \left((-1)H(t)\sqrt{\gamma\kappa z}\right)^k \frac{K_{m\tau-\gamma+k}(2\sqrt{\gamma z/\kappa})}{K_{m\tau-\gamma}(2\sqrt{\gamma z/\kappa})} \left(m(\psi_0(mt+k) - \psi_0(mt)) + \frac{kh(t)}{H(t)}\right)
\end{aligned}$$

where $\psi_0(\cdot)$ is the digamma function.

#### B.1.2.2 Compound Normal-Gamma distribution

We assume that $Z_\tau|V_\tau = v$ is **Normal distributed** with mean $v$ and variance $\tau^2 = 1/\gamma^2$. Thus, the probability distribution function of $Z_\tau|V_\tau$ is given by

$$f(z|v) = \frac{1}{\sqrt{2\pi}\tau} e^{-\frac{1}{2\tau^2}(z-v)^2}$$

The denominator of the conditional survival $[T|Z_\tau]$ is then given by

$$
\begin{aligned}
\mathbb{E}_{V_\tau}[f(z|V_\tau)] &= \int f(z|v)g(v)\,\mathrm{d}v \\
&= \int_0^\infty \frac{1}{\sqrt{2\pi}\tau} e^{-\frac{1}{2\tau^2}(z-v)^2} \frac{1}{\Gamma(m\tau)\kappa^{m\tau}} v^{m\tau-1} e^{-v/\kappa}\,\mathrm{d}v \\
&= \frac{1}{\sqrt{2\pi}\tau}\frac{1}{\Gamma(m\tau)\kappa^{m\tau}} e^{-\frac{1}{2\tau^2}z^2} \int_0^\infty e^{\frac{1}{\tau^2}zv} e^{-\frac{1}{2\tau^2}v^2} e^{-v/\kappa} v^{m\tau-1}\,\mathrm{d}v \\
&= \frac{1}{\sqrt{2\pi}\tau}\frac{1}{\Gamma(m\tau)\kappa^{m\tau}} e^{-\frac{1}{2\tau^2}z^2} \int_0^\infty e^{-1/(2\tau^2)v^2-(1/\kappa-z/\tau^2)v} v^{m\tau-1}\,\mathrm{d}v \\
&= \frac{1}{\sqrt{2\pi}\tau}\frac{1}{\Gamma(m\tau)\kappa^{m\tau}} e^{-\frac{1}{2\tau^2}z^2} \int_0^\infty e^{-\beta v^2-\gamma v} v^{\alpha-1}\,\mathrm{d}v \qquad \left\{\alpha = m\tau; \beta = \frac{1}{2\tau^2}; \gamma = \frac{\tau^2-\kappa z}{\kappa\tau^2}\right\} \\
&= \frac{1}{\sqrt{2\pi}\tau}\frac{1}{\Gamma(m\tau)\kappa^{m\tau}} e^{-\frac{1}{2\tau^2}z^2} \left((2\beta)^{-\alpha/2}\Gamma(\alpha)e^{\gamma^2/(8\beta)} D_{-\alpha}\left(\frac{\gamma}{\sqrt{2\beta}}\right)\right) \qquad \{\mathrm{Re}[\alpha,\beta] > 0\} \\
&= \frac{1}{\sqrt{2\pi}\tau}\frac{1}{\Gamma(m\tau)\kappa^{m\tau}} e^{-\frac{1}{2\tau^2}z^2} \left(\frac{1}{\tau^2}\right)^{-\frac{m\tau}{2}} \Gamma(m\tau)\exp\left\{\frac{(\tau^2-\kappa z)^2}{4\kappa^2\tau^2}\right\} D_{-m\tau}\left(\frac{\tau^2-\kappa z}{\kappa\tau}\right) \\
&= \frac{1}{\sqrt{2\pi}\tau}\frac{1}{\kappa^{m\tau}} \left(\frac{1}{\tau^2}\right)^{-\frac{m\tau}{2}} \exp\left\{-\frac{1}{2\tau^2}z^2 + \frac{(\tau^2-\kappa z)^2}{4\kappa^2\tau^2}\right\} D_{-m\tau}\left(\frac{\tau^2-\kappa z}{\kappa\tau}\right)
\end{aligned}
$$

where $D_n$ is the parabolic cylinder function and can be written in terms of the Whittaker function $W_{k,m}(z)$ as

$$
D_\nu(z) = 2^{\nu/2+1/4} z^{-1/2} W_{\nu/2+1/4,-1/4}\left(\frac{1}{2}z^2\right)
$$

The numerator is given by

$$
\begin{aligned}
&\mathbb{E}_{V_\tau}[S(t|V_\tau) \times f(z|V_\tau)] \\
&= \int S(t|v) f(z|v) g(v)\, \mathrm{d}v \\
&= \sum_{k=0}^{\infty} \frac{\Gamma(\alpha+k)}{\Gamma(\alpha)} \frac{\Gamma(\alpha+\beta)}{\Gamma(\alpha+\beta+k)} \frac{(-1)^k H^k(t)}{k!} \int_0^{\infty} v^k \frac{1}{\sqrt{2\pi}\tau} e^{-\frac{1}{2\tau^2}(z-v)^2} \frac{1}{\Gamma(m\tau)\kappa^{m\tau}} v^{m\tau-1} e^{-v/\kappa}\, \mathrm{d}v \\
&= \sum_{k=0}^{\infty} \frac{\Gamma(mt+k)}{\Gamma(mt)} \frac{\Gamma(m\tau)}{\Gamma(m\tau+k)} \frac{(-1)^k H^k(t)}{k!} \frac{1}{\sqrt{2\pi}\tau} \frac{1}{\Gamma(m\tau)\kappa^{m\tau}} e^{-\frac{1}{2\tau^2}z^2} \int_0^{\infty} e^{-1/(2\tau^2)v^2 - (1/\kappa - z/\tau^2)v} v^{m\tau+k-1}\, \mathrm{d}v \\
&= \sum_{k=0}^{\infty} \frac{\Gamma(mt+k)}{\Gamma(mt)} \frac{\Gamma(m\tau)}{\Gamma(m\tau+k)} \frac{(-1)^k H^k(t)}{k!} \frac{1}{\sqrt{2\pi}\tau} \frac{e^{-\frac{1}{2\tau^2}z^2}}{\Gamma(m\tau)\kappa^{m\tau}} \int_0^{\infty} e^{-\beta v^2 - \gamma v} v^{\alpha-1}\, \mathrm{d}v \quad \left\{\alpha = m\tau + k; \beta = \frac{1}{2\tau^2}; \gamma = \frac{\tau^2 - \kappa z}{\kappa\tau^2}\right\} \\
&= \sum_{k=0}^{\infty} \frac{\Gamma(mt+k)}{\Gamma(mt)} \frac{\Gamma(m\tau)}{\Gamma(m\tau+k)} \frac{(-1)^k H^k(t)}{k!} \frac{1}{\sqrt{2\pi}\tau} \frac{1}{\Gamma(m\tau)\kappa^{m\tau}} e^{-\frac{1}{2\tau^2}z^2} \left[(2\beta)^{-\alpha/2}\Gamma(\alpha) e^{\gamma^2/(8\beta)} D_{-\alpha}\left(\frac{\gamma}{\sqrt{2\beta}}\right)\right] \\
&= \sum_{k=0}^{\infty} \frac{\Gamma(mt+k)}{\Gamma(mt)} \frac{\Gamma(m\tau)}{\Gamma(m\tau+k)} \frac{(-1)^k H^k(t)}{k!} \frac{1}{\sqrt{2\pi}\tau} \frac{e^{-\frac{1}{2\tau^2}z^2}}{\Gamma(m\tau)\kappa^{m\tau}} \left(\frac{1}{\tau^2}\right)^{-\frac{m\tau+k}{2}} \Gamma(m\tau+k) e^{\frac{(\tau^2-\kappa z)^2}{4\kappa^2\tau^2}} D_{-m\tau-k}\left(\frac{\tau^2-\kappa z}{\kappa\tau}\right) \\
&= \sum_{k=0}^{\infty} \frac{\Gamma(mt+k)}{\Gamma(mt)} \frac{(-1)^k H^k(t)}{k!} \frac{1}{\sqrt{2\pi}\tau} \frac{1}{\kappa^{m\tau}} \left(\frac{1}{\tau^2}\right)^{-\frac{m\tau+k}{2}} \exp\left\{-\frac{1}{2\tau^2}z^2 + \frac{(\tau^2-\kappa z)^2}{4\kappa^2\tau^2}\right\} D_{-m\tau-k}\left(\frac{\tau^2-\kappa z}{\kappa\tau}\right) \\
&= \frac{1}{\sqrt{2\pi}\tau} \frac{1}{\kappa^{m\tau}} \left(\frac{1}{\tau^2}\right)^{-\frac{m\tau}{2}} \exp\left\{-\frac{1}{2\tau^2}z^2 + \frac{(\tau^2-\kappa z)^2}{4\kappa^2\tau^2}\right\} D_{-m\tau}\left(\frac{\tau^2-\kappa z}{\kappa\tau}\right) \\
&+ \sum_{k=1}^{\infty} \frac{1}{k} \frac{1}{B(mt,k)} (-1)^k H^k(t) \frac{1}{\sqrt{2\pi}\tau} \frac{1}{\kappa^{m\tau}} \left(\frac{1}{\tau^2}\right)^{-\frac{m\tau+k}{2}} \exp\left\{-\frac{1}{2\tau^2}z^2 + \frac{(\tau^2-\kappa z)^2}{4\kappa^2\tau^2}\right\} D_{-m\tau-k}\left(\frac{\tau^2-\kappa z}{\kappa\tau}\right)
\end{aligned}
$$

The survival function is then

$$
G(t|z) = 1 + \frac{1}{D_{-m\tau}\left(\frac{\tau^2-\kappa z}{\kappa\tau}\right)} \sum_{k=1}^{\infty} \frac{1}{k} \frac{1}{B(mt,k)} \left((-1)H(t)\tau\right)^k D_{-m\tau-k}\left(\frac{\tau^2-\kappa z}{\kappa\tau}\right)
$$

To get the conditional hazard, the derivative of $G(t|z)$ is given by

$$
\begin{aligned}
\frac{\partial}{\partial t} G(t|Z_\tau) &= \frac{\partial}{\partial t}\left[1 + \frac{1}{D_{-m\tau}\left(\frac{\tau^2-\kappa z}{\kappa\tau}\right)} \sum_{k=1}^{\infty} \frac{1}{k} \frac{1}{B(mt,k)} \left((-1)H(t)\tau\right)^k D_{-m\tau-k}\left(\frac{\tau^2-\kappa z}{\kappa\tau}\right)\right] \\
&= \frac{1}{D_{-m\tau}\left(\frac{\tau}{\kappa} - \frac{z}{\tau}\right)} \sum_{k=1}^{\infty} \frac{1}{k} (-1)^k \tau^k D_{-m\tau-k}\left(\frac{\tau}{\kappa} - \frac{z}{\tau}\right) \frac{\partial}{\partial t}\left[\frac{H^k(t)}{B(mt,k)}\right] \\
&= \frac{1}{D_{-m\tau}\left(\frac{\tau}{\kappa} - \frac{z}{\tau}\right)} \sum_{k=1}^{\infty} \frac{1}{k} (-1)^k \tau^k D_{-m\tau-k}\left(\frac{\tau}{\kappa} - \frac{z}{\tau}\right) \left(\frac{mH^k(t)}{B(mt,k)}(\psi_0(mt+k) - \psi_0(mt)) + \frac{kH^{k-1}(t)h(t)}{B(mt,k)}\right) \\
&= \frac{1}{D_{-m\tau}\left(\frac{\tau}{\kappa} - \frac{z}{\tau}\right)} \sum_{k=1}^{\infty} \frac{1}{k} \frac{1}{B(mt,k)} \left((-1)H(t)\tau\right)^k D_{-m\tau-k}\left(\frac{\tau}{\kappa} - \frac{z}{\tau}\right) \left(m(\psi_0(mt+k) - \psi_0(mt)) + \frac{kh(t)}{H(t)}\right)
\end{aligned}
$$

where $\psi_0(\cdot)$ is the digamma function.

### B.1.3 Alternate method of derivation

Alternatively, we could have specified the likelihood in the following form, where we specify the distributions conditional on $V_\tau$ and then take the expectation with respect to the unobserved random variable. As a check, we find that the resulting likelihood contributions are the same as with the previous specification.

$$l = \sum_{i=1}^{n} \delta_i \log\left(\mathbb{E}_V[d\Lambda(T_i|v_i)S(T_i|v_i)f(z_{T_i}|v_i)]\right) - (1-\delta_i)\Lambda(T_i)$$

where

$$\begin{aligned}
&\mathbb{E}_V[d\Lambda(t|V)S(t|V)f(z|V)] \\
&\quad = \int d\Lambda(t|v)S(t|v)f(z|v)g(v)\,\mathrm{d}v \\
&\quad = \int -\frac{1}{S(t|v)}\left[\frac{\partial}{\partial t}S(t|v)\right]S(t|v)f(z|v)g(v)\,\mathrm{d}v \\
&\quad = \int -\left[\frac{\partial}{\partial t}S(t|v)\right]f(z|v)g(v)\,\mathrm{d}v \\
&\quad = -\int \sum_{k=1}^{\infty} \frac{1}{B(mt,k)}\frac{\Gamma(m\tau)}{\Gamma(m\tau+k)}\frac{(-1)^k v^k H^k(t)}{k}\left[m[\psi_0(mt+k)-\psi_0(mt)]+\frac{kh(t)}{H(t)}\right]f(z|v)g(v)\,\mathrm{d}v \\
&\quad = -\sum_{k=1}^{\infty} \frac{1}{B(mt,k)}\frac{\Gamma(m\tau)}{\Gamma(m\tau+k)}\frac{(-1)^k H^k(t)}{k}\left[m[\psi_0(mt+k)-\psi_0(mt)]+\frac{kh(t)}{H(t)}\right]\int v^k f(z|v)g(v)\,\mathrm{d}v \\
&\quad = -\sum_{k=1}^{\infty} C_k \int v^k f(z|v)g(v)\,\mathrm{d}v
\end{aligned}$$

where $C_k = \dfrac{1}{B(mt,k)}\dfrac{\Gamma(m\tau)}{\Gamma(m\tau+k)}\dfrac{(-1)^k H^k(t)}{k}\left[m[\psi_0(mt+k)-\psi_0(mt)]+\dfrac{kh(t)}{H(t)}\right]$

#### B.1.3.1 Compound Gamma-Gamma distribution

Assume that $Z_\tau|V_\tau = v$ is **Gamma distributed** with shape $\gamma$ and scale $v/\gamma$ (i.e., mean $v$ and variance $v^2/\gamma$). The probability distribution function of $Z_\tau|V_\tau$ is given by

$$f(z|v) = \frac{\gamma^\gamma}{\Gamma(\gamma)v^\gamma} z^{\gamma-1} e^{-z\gamma/v}$$

Then,

$$
\begin{aligned}
&\mathbb{E}_V[d\Lambda(t|V)S(t|V)f(z|V)] \\
&= -\sum_{k=1}^{\infty} C_k \int_0^{\infty} v^k \frac{1}{\Gamma(\gamma)} \frac{\gamma^\gamma}{v^\gamma} z^{\gamma-1} e^{-z\gamma/v} \frac{1}{\Gamma(m\tau)\kappa^{m\tau}} v^{m\tau-1} e^{-v/\kappa}\, \mathrm{d}v \\
&= -\sum_{k=1}^{\infty} C_k \frac{2}{\Gamma(\gamma)\Gamma(m\tau)z} \left(\frac{\gamma z}{\kappa}\right)^{\frac{\gamma+m\tau}{2}} (\gamma\kappa z)^{\frac{k}{2}} K_{m\tau-\gamma+k}(2\sqrt{\gamma z/\kappa}) \quad \{\mathrm{Re}[\gamma z/\kappa] > 0\}
\end{aligned}
$$

### B.1.3.2 Compound Normal-Gamma distribution

Assume that $Z_\tau|V_\tau = v$ is **Normal distributed** with mean $v$ and variance $\tau^2$. The probability distribution function of $Z_\tau|V_\tau$ is given by

$$
f(z|v) = \frac{1}{\sqrt{2\pi}\tau} e^{-\frac{1}{2\tau^2}(z-v)^2}
$$

Then,

$$
\begin{aligned}
&\mathbb{E}_V[d\Lambda(t|V)S(t|V)f(z|V)] \\
&= -\sum_{k=1}^{\infty} C_k \int_0^{\infty} v^k \frac{1}{\sqrt{2\pi}\tau} e^{-\frac{1}{2\tau^2}(z-v)^2} \frac{1}{\Gamma(m\tau)\kappa^{m\tau}} v^{m\tau-1} e^{-v/\kappa}\, \mathrm{d}v \\
&= -\sum_{k=1}^{\infty} C_k \frac{1}{\sqrt{2\pi}\tau} \frac{1}{\Gamma(m\tau)\kappa^{m\tau}} e^{-\frac{1}{2\tau^2}z^2} \int_0^{\infty} e^{-1/(2\tau^2)v^2-(1/\kappa-z/\tau^2)v} v^{m\tau+k-1}\, \mathrm{d}v \\
&= -\sum_{k=1}^{\infty} C_k \frac{1}{\sqrt{2\pi}\tau} \frac{1}{\Gamma(m\tau)\kappa^{m\tau}} e^{-\frac{1}{2\tau^2}z^2} \int_0^{\infty} e^{-\beta v^2-\gamma v} v^{\alpha-1}\, \mathrm{d}v \qquad \left\{\alpha = m\tau+k; \beta = \frac{1}{2\tau^2}; \gamma = \frac{1}{\kappa} - \frac{z}{\tau^2}\right\} \\
&= -\sum_{k=1}^{\infty} C_k \frac{1}{\sqrt{2\pi}\tau} \frac{1}{\Gamma(m\tau)\kappa^{m\tau}} e^{-\frac{1}{2\tau^2}z^2} \left[(2\beta)^{-\alpha/2}\Gamma(\alpha) e^{\gamma^2/(8\beta)} D_{-\alpha}\left(\frac{\gamma}{\sqrt{2\beta}}\right)\right] \\
&= \sum_{k=1}^{\infty} C_k \frac{1}{\sqrt{2\pi}\tau} \frac{1}{\Gamma(m\tau)\kappa^{m\tau}} e^{-\frac{1}{2\tau^2}z^2} \left(\frac{1}{\tau^2}\right)^{-\frac{m\tau+k}{2}} \Gamma(m\tau+k) \exp\left\{\frac{(\tau^2-\kappa z)^2}{4\kappa^2\tau^2}\right\} D_{-m\tau-k}\left(\frac{\tau^2-\kappa z}{\kappa\tau}\right) \\
&= \sum_{k=1}^{\infty} C_k \frac{1}{\sqrt{2\pi}\tau} \frac{\tau^{m\tau+k}}{\kappa^{m\tau}} \frac{\Gamma(m\tau+k)}{\Gamma(m\tau)} \exp\left\{\frac{(\tau^2-\kappa z)^2}{4\kappa^2\tau^2} - \frac{z^2}{2\tau^2}\right\} D_{-m\tau-k}\left(\frac{\tau^2-\kappa z}{\kappa\tau}\right)
\end{aligned}
$$

where $D_\nu(z)$ is the parabolic cylinder function.

## B.2 Derivations for dynamic prediction

In this section, we repeat the derivations for the conditional survival functions for the measurement error model where only a surrogate $Z_\tau$ for $V_\tau$ is observed. Recall, the conditional survival for $0 \leq t \leq \tau$ is given by

$$G(t|z) = 1 + \sum_{k=1}^{\infty} \frac{1}{k} \frac{1}{B(mt,k)} \frac{\Gamma(m\tau)}{\Gamma(m\tau+k)} \left((-1)H(t)\sqrt{\gamma\kappa z}\right)^k \frac{K_{m\tau-\gamma+k}(2\sqrt{\gamma z/\kappa})}{K_{m\tau-\gamma}(2\sqrt{\gamma z/\kappa})}$$

Suppose that we are interested in making predictions for a person beyond their last observed marker value. Then the future predicted survival for $0 \leq \tau \leq t$ is given by

$$\begin{aligned}
G(t|Z_\tau = z) &= \frac{\int P(T > t|Z_\tau, V_\tau) P(Z_\tau|V_\tau) P(V_\tau)\, \mathrm{d}V_\tau}{f_{Z_\tau}(z)} \\
&= \frac{1}{f_{Z_\tau}(z)} \int_0^\infty S(t|V_\tau = v) f_{Z_\tau|V_\tau}(z|v) g(v)\, \mathrm{d}v \\
&= \frac{1}{f_{Z_\tau}(z)} \int_0^\infty e^{-H(t)v} (1+\kappa H(t))^{-m(t-\tau)} \frac{\gamma^\gamma}{\Gamma(\gamma) v^\gamma} z^{\gamma-1} e^{-z\gamma/v} \frac{1}{\Gamma(m\tau)\kappa^{m\tau}} v^{m\tau-1} e^{-v/\kappa}\, \mathrm{d}v \\
&= (1+\kappa H(t))^{-m(t-\tau)+\frac{1}{2}(\gamma-m\tau)} \frac{K_{m\tau-\gamma}\left(2\sqrt{(H(t)+\frac{1}{\kappa})(\gamma z)}\right)}{K_{m\tau-\gamma}\left(2\sqrt{\frac{1}{\kappa}(\gamma z)}\right)}
\end{aligned}$$

Thus, the dynamic prediction at time $\tau$ for surviving a prediction horizon of $\tau + s$ is given by

$$\begin{aligned}
G(\tau+s|Z_\tau = z, T > \tau) &= \frac{G(\tau+s|Z_\tau = z)}{G(\tau|Z_\tau = z)} \\
&= \frac{(1+\kappa H(\tau+s))^{-ms+\frac{1}{2}(\gamma-m\tau)}}{(1+\kappa H(\tau))^{\frac{1}{2}(\gamma-m\tau)}} \frac{K_{m\tau-\gamma}\left(2\sqrt{(H(\tau+s)+\frac{1}{\kappa})(\gamma z)}\right)}{K_{m\tau-\gamma}\left(2\sqrt{(H(\tau)+\frac{1}{\kappa})(\gamma z)}\right)}
\end{aligned}$$

## B.3 Derivations for marker predictions

- Corresponding to Eq.(3.9). For $0 \leq t \leq \tau \leq T$,

$$\begin{aligned}
\mathbb{E}[W_t|T>\tau, V_\tau] &= \frac{\int P(T>\tau|W_t,V_\tau)q(W_t|V_\tau)g(V_\tau)W_t\,\mathrm{d}W_t}{\int P(T>\tau|W_t,V_\tau)q(W_t|V_\tau)g(V_\tau)\,\mathrm{d}W_t} \\
&= \frac{\int S(\tau|V_\tau)q(W_t|V_\tau)g(V_\tau)W_t\,\mathrm{d}W_t}{\int S(\tau|V_\tau)q(W_t|V_\tau)g(V_\tau)\,\mathrm{d}W_t} \\
&= \frac{\int q(W_t|V_\tau)W_t\,\mathrm{d}W_t}{\int q(W_t|V_\tau)\,\mathrm{d}W_t} \\
&= \frac{\int_0^v \frac{1}{vB(mt,m(\tau-t))}\left(\frac{w}{v}\right)^{mt-1}\left(\frac{v-w}{v}\right)^{m(\tau-t)-1} w\,\mathrm{d}w}{\int_0^v \frac{1}{vB(mt,m(\tau-t))}\left(\frac{w}{v}\right)^{mt-1}\left(\frac{v-w}{v}\right)^{m(\tau-t)-1} \mathrm{d}w} \\
&= \frac{mtv}{mt+m(\tau-t)} \\
&= \frac{tv}{\tau}
\end{aligned}$$

- Corresponding to Eq.(3.10). For $0 \leq \tau \leq t \leq T$,

$$\begin{aligned}
\mathbb{E}[W_t|T>t, V_\tau=v] &= \frac{\int P(T>t|W_t,V_\tau)q(W_t|V_\tau)g(V_\tau)W_t\,\mathrm{d}W_t}{\int P(T>t|W_t,V_\tau)q(W_t|V_\tau)g(V_\tau)\,\mathrm{d}W_t} \\
&= \frac{\int S(t|W_t,V_\tau)q(W_t|V_\tau)g(V_\tau)W_t\,\mathrm{d}W_t}{\int S(t|W_t,V_\tau)q(W_t|V_\tau)g(V_\tau)\,\mathrm{d}W_t} \\
&= \frac{\int_v^\infty e^{-H_t w}\frac{1}{\Gamma(m(t-\tau))\kappa^{m(t-\tau)}}(w-v)^{m(t-\tau)-1}e^{-\frac{(w-v)}{\kappa}}\frac{1}{\Gamma(m\tau)\kappa^{m\tau}}v^{m\tau-1}e^{-v/\kappa}w\,\mathrm{d}w}{\int_v^\infty e^{-H_t w}\frac{1}{\Gamma(m(t-\tau))\kappa^{m(t-\tau)}}(w-v)^{m(t-\tau)-1}e^{-\frac{(w-v)}{\kappa}}\frac{1}{\Gamma(m\tau)\kappa^{m\tau}}v^{m\tau-1}e^{-v/\kappa}\,\mathrm{d}w} \\
&= v + \frac{\kappa m(t-\tau)}{1+\kappa H_t}
\end{aligned}$$

- Corresponding to Eq.(3.11). For $0 \le t \le \tau \le T$,

$$
\begin{aligned}
&\mathbb{E}[W_t | T > \tau, Z_\tau] \\
&= \frac{\int P(T > \tau, W_t, Z_\tau) W_t \, \mathrm{d}W_t}{\int P(T > \tau, W_t, Z_\tau) \, \mathrm{d}W_t} \\
&= \frac{\int_{W_t} \left[ \int_{V_\tau} P(T > \tau, W_t, Z_\tau, V_\tau) \, \mathrm{d}V_\tau \right] W_t \, \mathrm{d}W_t}{\int P(T > \tau, W_t, Z_\tau) \, \mathrm{d}W_t} \\
&= \frac{\int_{W_t} \left[ \int_{V_\tau} P(T > \tau | W_t, Z_\tau, V_\tau) q(W_t | Z_\tau, V_\tau) f(Z_\tau | V_\tau) g(V_\tau) \, \mathrm{d}V_\tau \right] W_t \, \mathrm{d}W_t}{\int_{W_t} \left[ \int_{V_\tau} P(T > \tau | W_t, Z_\tau, V_\tau) q(W_t | Z_\tau, V_\tau) f(Z_\tau | V_\tau) g(V_\tau) \, \mathrm{d}V_\tau \right] \mathrm{d}W_t} \\
&= \frac{\int_{W_t} \left[ \int_{V_\tau} S(\tau | V_\tau) q(W_t | V_\tau) f(Z_\tau | V_\tau) g(V_\tau) \, \mathrm{d}V_\tau \right] W_t \, \mathrm{d}W_t}{\int_{W_t} \left[ \int_{V_\tau} S(\tau | V_\tau) q(W_t | V_\tau) f(Z_\tau | V_\tau) g(V_\tau) \, \mathrm{d}V_\tau \right] \mathrm{d}W_t} \\
&= \frac{\int_0^\infty \left[ \int_0^v S(\tau | v) q(w | v) f(z | v) g(v) w \, \mathrm{d}w \right] \mathrm{d}v}{\int_0^\infty \left[ \int_0^v S(\tau | v) q(w | v) f(z | v) g(v) \, \mathrm{d}w \right] \mathrm{d}v} \\
&= \frac{\int_0^\infty \left[ \int_0^v \frac{1}{vB(mt, m(\tau - t))} \left( \frac{w}{v} \right)^{mt-1} \left( \frac{v - w}{v} \right)^{m(\tau-t)-1} w \, \mathrm{d}w \right] e^{-H_t v} \frac{\gamma^\gamma}{\Gamma(\gamma) v^\gamma} z^{\gamma-1} e^{-z\gamma/v} \frac{v^{m\tau-1}}{\Gamma(m\tau)\kappa^{m\tau}} e^{-v/\kappa} \, \mathrm{d}v}{\int_0^\infty \left[ \int_0^v \frac{1}{vB(mt, m(\tau - t))} \left( \frac{w}{v} \right)^{mt-1} \left( \frac{v - w}{v} \right)^{m(\tau-t)-1} \mathrm{d}w \right] e^{-H_t v} \frac{\gamma^\gamma}{\Gamma(\gamma) v^\gamma} z^{\gamma-1} e^{-z\gamma/v} \frac{v^{m\tau-1}}{\Gamma(m\tau)\kappa^{m\tau}} e^{-v/\kappa} \, \mathrm{d}v} \\
&= \frac{t}{\tau} (\gamma z)^{\frac{1}{2}} \left( H(t) + \frac{1}{\kappa} \right)^{-\frac{1}{2}} \frac{K_{m\tau-\gamma+1} \left( 2\sqrt{\left( H(t) + \frac{1}{\kappa} \right)(\gamma z)} \right)}{K_{m\tau-\gamma} \left( 2\sqrt{\left( H(t) + \frac{1}{\kappa} \right)(\gamma z)} \right)}
\end{aligned}
$$

- Corresponding to Eq.(3.12). For $0 \le \tau \le t \le T$,

$$
\begin{aligned}
&\mathbb{E}[W_t | T > t, Z_\tau] \\
&= \frac{\int P(T > t, W_t, Z_\tau) W_t \, \mathrm{d}W_t}{\int P(T > t, W_t, Z_\tau) \, \mathrm{d}W_t} \\
&= \frac{\int_{W_t} \left[ \int_{V_\tau} S(t | W_t) q(W_t | V_\tau) f(Z_\tau | V_\tau) g(V_\tau) \, \mathrm{d}V_\tau \right] W_t \, \mathrm{d}W_t}{\int_{W_t} \left[ \int_{V_\tau} S(t | W_t) q(W_t | V_\tau) f(Z_\tau | V_\tau) g(V_\tau) \, \mathrm{d}V_\tau \right] \mathrm{d}W_t} \\
&= \frac{\int_0^\infty \left[ \int_0^\infty S(t | w) q(w | v) f(z | v) g(v) w \, \mathrm{d}w \right] \mathrm{d}v}{\int_0^\infty \left[ \int_0^\infty S(t | w) q(w | v) f(z | v) g(v) \, \mathrm{d}w \right] \mathrm{d}v} \\
&= \frac{\int_0^\infty \left[ \int_v^\infty e^{-H_t w} \frac{1}{\Gamma(m(t-\tau))\kappa^{m(t-\tau)}} (w - v)^{m(t-\tau)-1} e^{-\frac{w-v}{\kappa}} w \, \mathrm{d}w \right] \frac{\gamma^\gamma}{\Gamma(\gamma) v^\gamma} z^{\gamma-1} e^{-z\gamma/v} \frac{v^{m\tau-1}}{\Gamma(m\tau)\kappa^{m\tau}} e^{-v/\kappa} \, \mathrm{d}v}{\int_0^\infty \left[ \int_v^\infty e^{-H_t w} \frac{1}{\Gamma(m(t-\tau))\kappa^{m(t-\tau)}} (w - v)^{m(t-\tau)-1} e^{-\frac{w-v}{\kappa}} \, \mathrm{d}w \right] \frac{\gamma^\gamma}{\Gamma(\gamma) v^\gamma} z^{\gamma-1} e^{-z\gamma/v} \frac{v^{m\tau-1}}{\Gamma(m\tau)\kappa^{m\tau}} e^{-v/\kappa} \, \mathrm{d}v} \\
&= (\gamma z)^{\frac{1}{2}} \left( H(t) + \frac{1}{\kappa} \right)^{-\frac{1}{2}} \frac{K_{m\tau-\gamma+1} \left( 2\sqrt{\left( H(t) + \frac{1}{\kappa} \right)(\gamma z)} \right)}{K_{m\tau-\gamma} \left( 2\sqrt{\left( H(t) + \frac{1}{\kappa} \right)(\gamma z)} \right)} + \frac{\kappa m (t - \tau)}{1 + \kappa H(t)}
\end{aligned}
$$

- Corresponding to Eq.(3.13),

$$\begin{aligned}
\mathbb{E}[W_t|T>t] &= \frac{\int P(T>t|W_t)q(W_t)W_t\,\mathrm{d}W_t}{\int P(T>t|W_t)q(W_t)\,\mathrm{d}W_t} \\
&= \frac{\int_0^\infty e^{-H_t w}\dfrac{1}{\Gamma(mt)\kappa^{mt}}w^{mt-1}e^{-w/\kappa}w\,\mathrm{d}w}{\int_0^\infty e^{-H_t w}\dfrac{1}{\Gamma(mt)\kappa^{mt}}w^{mt-1}e^{-w/\kappa}\,\mathrm{d}w} \\
&= \frac{\kappa mt(1+\kappa H_t)^{-mt-1}}{(1+\kappa H_t)^{-mt}} \\
&= \frac{\kappa mt}{(1+\kappa H_t)}
\end{aligned}$$

## B.4 Univariate frailty model for conditional cumulative hazard

We can model the baseline hazard using a frailty. We define the hazard as

$$h(t) = R\lambda_0(t)\exp\{\boldsymbol{\beta}'\mathbf{X}\}$$

where $R$ represents the frailty and $X$ is a vector of baseline covariates. The conditional cumulative hazard is then given by

$$H(t) = R\Lambda_0(t)\exp\{\boldsymbol{\beta}'\mathbf{X}\} = R\Lambda(t)$$

We exclude baseline covariates for brevity. The survival function is then given by

$$\begin{aligned}
S(t) &= \mathbb{E}_R[\mathbb{E}_{V_\tau}[\mathbb{E}_U[e^{-H(t)U_{t\tau}V_\tau}]]] \\
&= \mathbb{E}_R[\mathbb{E}_{V_\tau}[\mathbb{E}_U[e^{-R\Lambda(t)U_{t\tau}V_\tau}]]] \\
&= \mathbb{E}_R\left[1 + \sum_{k=1}^{\infty}\prod_{r=1}^{k}\frac{\alpha+r-1}{\alpha+\beta+r-1}\frac{(-1)^k p_k R^k \Lambda^k(t)}{k!}\right] \\
&= 1 + \sum_{k=1}^{\infty}\prod_{r=1}^{k}\frac{\alpha+r-1}{\alpha+\beta+r-1}\frac{(-1)^k p_k q_k \Lambda^k(t)}{k!}
\end{aligned}$$

where $p_k$ is the $k$th moment of $V_\tau$, $\mathbb{E}[V_\tau^k]$ and $q_k$ is the $k$th moment of $R$, $\mathbb{E}[R^k]$. Taking $V_\tau \sim \text{Gamma}(\text{shape} = m\tau, \text{scale} = \kappa)$, the $k$th moment of $V_\tau$ is $p_k = \kappa^k(m\tau + k - 1)!/(m\tau - 1)!$. If $R \sim \text{Gamma}(\text{shape} = 1/\rho^2, \text{scale} = \rho^2)$. The $k$th moment of $R$ is then

$q_k = (\rho^2)^k(1/\rho^2 + k - 1)!/(1/\rho^2 - 1)!$. Thus, the survival function is then

$$\begin{aligned}
S(t) &= 1 + \sum_{k=1}^{\infty} \left[ \prod_{r=1}^{k} \frac{\alpha + r - 1}{\alpha + \beta + r - 1} \right] \frac{(-1)^k p_k q_k \Lambda^k(t)}{k!} \\
&= 1 + \sum_{k=1}^{\infty} \left[ \prod_{r=1}^{k} \frac{mt + r - 1}{mt + m(\tau - t) + r - 1} \right] \frac{(-1)^k \Lambda^k(t) \kappa^k \rho^{2k}}{k!} \frac{(m\tau + k - 1)!}{(m\tau - 1)!} \frac{(1/\rho^2 + k - 1)!}{(1/\rho^2 - 1)!} \\
&= 1 + \sum_{k=1}^{\infty} \left[ \frac{(mt + k - 1)!}{(mt - 1)!} \frac{(m\tau - 1)!}{(m\tau + k - 1)!} \right] \frac{(-1)^k \Lambda^k(t) \kappa^k \rho^{2k}}{k!} \frac{(m\tau + k - 1)!}{(m\tau - 1)!} \frac{(1/\rho^2 + k - 1)!}{(1/\rho^2 - 1)!} \\
&= 1 + \sum_{k=1}^{\infty} \frac{\Gamma(mt + k)}{\Gamma(mt)} \frac{\Gamma(1/\rho^2 + k)}{\Gamma(1/\rho^2)} \frac{(-1)^k \Lambda^k(t) \kappa^k \rho^{2k}}{k!}
\end{aligned}$$

The conditional survival is given by

$$\begin{aligned}
S(t|V_\tau) &= \mathbb{E}_R[\mathbb{E}_U[\exp\{-H(t)U_{t\tau}V_\tau\}]] \\
&= \mathbb{E}_R[\mathbb{E}_U[\exp\{-R\Lambda(t)U_{t\tau}V_\tau\}]] \\
&= \mathbb{E}_R\left[ 1 + \sum_{k=1}^{\infty} \prod_{r=1}^{k} \frac{\alpha + r - 1}{\alpha + \beta + r - 1} \frac{(-1)^k {V_\tau}^k R^k \Lambda^k(t)}{k!} \right] \\
&= 1 + \sum_{k=1}^{\infty} \prod_{r=1}^{k} \frac{\alpha + r - 1}{\alpha + \beta + r - 1} \frac{(-1)^k {V_\tau}^k q_k \Lambda^k(t)}{k!} \\
&= 1 + \sum_{k=1}^{\infty} \prod_{r=1}^{k} \frac{\alpha + r - 1}{\alpha + \beta + r - 1} \frac{(-1)^k {V_\tau}^k q_k \Lambda^k(t)}{k!} \\
&= 1 + \sum_{k=1}^{\infty} \frac{\Gamma(mt + k)}{\Gamma(mt)} \frac{\Gamma(m\tau)}{\Gamma(m\tau + k)} \frac{\Gamma(1/\rho^2 + k)}{\Gamma(1/\rho^2)} \frac{(-1)^k V_\tau^k \rho^{2k} \Lambda^k(t)}{k!} \\
&= 1 + \sum_{k=1}^{\infty} \frac{1}{B(mt, k)} \frac{\Gamma(m\tau)}{\Gamma(m\tau + k)} \frac{\Gamma(1/\rho^2 + k)}{\Gamma(1/\rho^2)} \frac{(-1)^k V_\tau^k \rho^{2k} \Lambda^k(t)}{k!}
\end{aligned}$$

The conditional hazard is given by $-\frac{1}{S(t|v)} \frac{\partial}{\partial t}[S(t|v)]$, where

$$\begin{aligned}
\frac{\partial}{\partial t} S(t|v) &= \frac{\partial}{\partial t} \left[ \sum_{k=0}^{\infty} \frac{1}{B(mt, k)} \frac{\Gamma(m\tau)}{\Gamma(m\tau + k)} \frac{\Gamma(1/\rho^2 + k)}{\Gamma(1/\rho^2)} \frac{(-1)^k v^k \rho^{2k} \Lambda^k(t)}{k} \right] \\
&= \sum_{k=0}^{\infty} \frac{\Gamma(m\tau)}{\Gamma(m\tau + k)} \frac{\Gamma(1/\rho^2 + k)}{\Gamma(1/\rho^2)} \frac{(-1)^k v^k \rho^{2k}}{k} \frac{\partial}{\partial t} \left[ \frac{\Lambda^k(t)}{B(mt, k)} \right] \\
&= \sum_{k=0}^{\infty} \frac{\Gamma(m\tau)}{\Gamma(m\tau + k)} \frac{\Gamma(1/\rho^2 + k)}{\Gamma(1/\rho^2)} \frac{(-1)^k v^k \rho^{2k} \Lambda^k(t)}{k} \left[ m[\psi_0(mt + k) - \psi_0(mt)] + \frac{k\lambda(t)}{\Lambda(t)} \right]
\end{aligned}$$

## B.5 Simulation setup

For subjects $i = 1, \ldots, n$, we generate data using the following process:

1. Simulate a gamma process $\{W_t\}$ with mean $mt$ and variance $\sigma^2 t$, using the method described in Avramidis et al. (2003)

2. Derive event time, $Y$, using the inverse transform method by generating random variable $A \sim \text{Unif}(0, 1)$ and solving $S(t) = A \Rightarrow e^{-H(t)W_t} - A = 0$ for $t$.

3. Simulate censoring by generating $C \sim \text{Unif}(0, \tau)$ and apply administrative censoring at time $\tau$.

4. Set $T = \min(Y, C)$ to get the observed time. Set $\delta = I(T = Y)$ as an indicator of whether the individual experienced the event of interest.

5. If $\delta = 1$ (i.e., for individuals that experienced the event),

   (a) Obtain $V_\tau = v$ from $\{W_t\}$ at time $\tau = T$.

   (b) Simulate $Z_\tau = z$ from the distribution $Z_\tau | V_\tau$

We perform estimation by maximizing the log-likelihood for the model without measurement error

$$l = \sum_{i=1}^{n} \{\delta_i \log(d\Lambda(T_i|v_{T_i})S(T_i|v_{T_i})g(v_{T_i})) + (1 - \delta_i) \log[S(T_i|v_{T_i})g(v_{T_i})]\}$$

or the log-likelihood for the model with measurement error

$$l = \sum_{i=1}^{n} \{\delta_i \log(d\Phi(T_i|z_{T_i})G(T_i|z_{T_i})f(z_{T_i})) + (1 - \delta_i) \log[G(T_i|z_{T_i})f(z_{T_i})]\}$$

## B.6 Additional simulation results

Here we present additional simulations from the misspecified models fit in the simulation study in Section 3.4.

**Table B.1:** Simulation results for the parameters associated with the stochastic marker process from a gamma bridge survival model with no measurement error fit to marker data simulated from a gamma bridge process with measurement error.

| | | $\mu_0$ | | | | $\mu_1$ | | | | $\eta_0$ | | | | $\eta_1$ | | | |
|---|---|---|---|---|---|---|---|---|---|---|---|---|---|---|---|---|---|
| **n** | **%Cens** | Est[1] | SE[2] | ESD[3] | CP[4] | Est | SE | ESD | CP | Est | SE | ESD | CP | Est | SE | ESD | CP |
| **200** | **20** | -1.13 | .032 | .030 | 84.9 | .290 | .064 | .064 | 93.6 | -2.28 | .194 | .202 | 87.2 | .497 | .287 | .292 | 93.6 |
| **200** | **30** | -1.12 | .033 | .034 | 89.3 | .287 | .067 | .062 | 94.7 | -2.26 | .182 | .181 | 89.5 | .493 | .282 | .295 | 92.4 |
| **200** | **40** | -1.12 | .035 | .035 | 89.6 | .290 | .069 | .070 | 93.0 | -2.27 | .184 | .183 | 87.0 | .488 | .284 | .289 | 93.8 |
| **300** | **20** | -1.13 | .026 | .023 | 82.9 | .291 | .052 | .050 | 94.7 | -2.24 | .149 | .144 | 83.4 | .502 | .226 | .225 | 93.9 |
| **300** | **30** | -1.12 | .027 | .026 | 87.4 | .286 | .054 | .052 | 94.8 | -2.26 | .148 | .150 | 81.2 | .492 | .227 | .237 | 93.2 |
| **300** | **40** | -1.12 | .029 | .028 | 89.1 | .284 | .057 | .058 | 91.8 | -2.25 | .147 | .142 | 87.8 | .478 | .232 | .228 | 95.5 |
| **500** | **20** | -1.13 | .020 | .019 | 74.0 | .286 | .040 | .041 | 91.1 | -2.24 | .115 | .110 | 78.8 | .496 | .173 | .178 | 90.3 |
| **500** | **30** | -1.13 | .022 | .022 | 77.8 | .289 | .043 | .040 | 95.5 | -2.24 | .116 | .113 | 78.1 | .513 | .183 | .180 | 93.2 |
| **500** | **40** | -1.12 | .022 | .022 | 85.8 | .284 | .044 | .042 | 94.9 | -2.24 | .113 | .115 | 74.6 | .486 | .176 | .175 | 94.6 |

[1] Est: Average of the parameter estimates over 500 simulations
[2] SE: Average of estimated standard errors
[3] ESD: Empirical standard deviation of parameter estimates
[4] CP: Coverage probability of the proportion of simulations that the 95% confidence interval contains the true parameter values

**Table B.2:** Simulation results for the parameters associated with the conditional cumulative hazard from a gamma bridge survival model with no measurement error fit to marker data simulated from a gamma bridge process with measurement error.

| | | $\log(\gamma)$ | | | | $\beta_0$ | | | | $\beta_1$ | | | |
|---|---|---|---|---|---|---|---|---|---|---|---|---|---|
| **n** | **%Cens** | Est[1] | SE[2] | ESD[3] | CP[4] | Est | SE | ESD | CP | Est | SE | ESD | CP |
| **200** | **20** | 4.35 | 1.04 | .692 | - | -3.58 | .096 | .096 | 93.9 | .624 | .170 | .173 | 94.8 |
| **200** | **30** | 4.32 | 1.05 | .683 | - | -3.58 | .104 | .105 | 94.1 | .628 | .182 | .175 | 94.1 |
| **200** | **40** | 4.21 | 1.07 | .726 | - | -3.59 | .119 | .122 | 93.7 | .623 | .199 | .204 | 93.3 |
| **300** | **20** | 4.45 | .843 | .596 | - | -3.58 | .078 | .077 | 94.7 | .618 | .138 | .146 | 93.5 |
| **300** | **30** | 4.30 | .857 | .649 | - | -3.58 | .085 | .087 | 92.5 | .614 | .148 | .146 | 95.0 |
| **300** | **40** | 4.24 | .909 | .683 | - | -3.60 | .097 | .096 | 95.7 | .624 | .162 | .166 | 94.6 |
| **500** | **20** | 4.44 | .702 | .525 | - | -3.58 | .060 | .063 | 91.8 | .615 | .108 | .110 | 93.4 |
| **500** | **30** | 4.40 | .716 | .565 | - | -3.58 | .065 | .067 | 93.2 | .613 | .114 | .119 | 93.3 |
| **500** | **40** | 4.25 | .726 | .603 | - | -3.58 | .075 | .071 | 96.2 | .621 | .125 | .120 | 95.8 |

[1] Est: Average of the parameter estimates over 500 simulations
[2] SE: Average of estimated standard errors
[3] ESD: Empirical standard deviation of parameter estimates
[4] CP: Coverage probability of the proportion of simulations that the 95% confidence interval contains the true parameter values

**Table B.3:** Simulation results for the parameters associated with the stochastic marker process from a gamma bridge survival model with no measurement error fit to marker data simulated from a gamma bridge process with measurement error.

| | | | $\mu_0$ | | | | $\mu_1$ | | | | $\eta_0$ | | | | $\eta_1$ | | | |
|---|---|---|---|---|---|---|---|---|---|---|---|---|---|---|---|---|---|---|
| **n** | log($\gamma$) | **%Cens** | Est[1] | SE[2] | ESD[3] | CP[4] | Est | SE | ESD | CP | Est | SE | ESD | CP | Est | SE | ESD | CP |
| **200** | **0.0** | **20** | -1.13 | .031 | .030 | 84.5 | .290 | .062 | .064 | 93.6 | -2.17 | .131 | .134 | 91.0 | .447 | .244 | .251 | 94.2 |
| **200** | **0.0** | **30** | -1.12 | .032 | .033 | 88.4 | .286 | .064 | .061 | 95.1 | -2.16 | .132 | .136 | 92.7 | .448 | .246 | .257 | 92.3 |
| **200** | **0.0** | **40** | -1.12 | .034 | .034 | 89.4 | .290 | .067 | .069 | 92.6 | -2.15 | .133 | .133 | 93.2 | .450 | .248 | .255 | 93.6 |
| **200** | **0.7** | **20** | -1.13 | .031 | .030 | 84.6 | .290 | .062 | .064 | 93.6 | -2.17 | .131 | .135 | 91.0 | .448 | .244 | .251 | 94.2 |
| **200** | **0.7** | **30** | -1.12 | .032 | .033 | 88.4 | .287 | .064 | .062 | 95.0 | -2.16 | .132 | .136 | 92.8 | .449 | .246 | .257 | 92.4 |
| **200** | **0.7** | **40** | -1.12 | .034 | .034 | 89.4 | .290 | .067 | .069 | 92.6 | -2.15 | .133 | .133 | 93.2 | .451 | .248 | .255 | 93.8 |
| **200** | **1.1** | **20** | -1.13 | .031 | .030 | 84.6 | .290 | .062 | .064 | 93.6 | -2.17 | .131 | .134 | 91.0 | .447 | .244 | .251 | 94.2 |
| **200** | **1.1** | **30** | -1.12 | .032 | .033 | 88.2 | .287 | .064 | .062 | 95.0 | -2.16 | .132 | .136 | 92.6 | .449 | .246 | .257 | 92.4 |
| **200** | **1.1** | **40** | -1.12 | .034 | .034 | 89.4 | .290 | .067 | .069 | 92.6 | -2.15 | .133 | .133 | 93.2 | .451 | .248 | .255 | 93.6 |
| **300** | **0.0** | **20** | -1.13 | .025 | .022 | 83.4 | .291 | .050 | .049 | 94.6 | -2.17 | .107 | .108 | 90.4 | .458 | .199 | .200 | 94.0 |
| **300** | **0.0** | **30** | -1.12 | .026 | .025 | 88.2 | .285 | .052 | .051 | 94.6 | -2.16 | .107 | .115 | 89.4 | .449 | .200 | .212 | 92.6 |
| **300** | **0.0** | **40** | -1.12 | .028 | .028 | 88.6 | .284 | .055 | .058 | 91.4 | -2.15 | .109 | .110 | 92.8 | .448 | .202 | .202 | 93.8 |
| **300** | **0.7** | **20** | -1.13 | .025 | .022 | 83.4 | .291 | .050 | .049 | 94.6 | -2.17 | .107 | .108 | 90.4 | .458 | .199 | .200 | 94.0 |
| **300** | **0.7** | **30** | -1.12 | .026 | .025 | 88.2 | .285 | .052 | .051 | 94.6 | -2.16 | .107 | .115 | 89.4 | .450 | .200 | .212 | 92.6 |
| **300** | **0.7** | **40** | -1.12 | .028 | .028 | 88.6 | .284 | .055 | .058 | 91.4 | -2.15 | .109 | .110 | 92.8 | .447 | .202 | .202 | 93.8 |
| **300** | **1.1** | **20** | -1.13 | .025 | .022 | 83.4 | .291 | .050 | .049 | 94.6 | -2.17 | .107 | .108 | 90.4 | .458 | .199 | .200 | 94.0 |
| **300** | **1.1** | **30** | -1.12 | .026 | .025 | 88.2 | .285 | .052 | .051 | 94.6 | -2.16 | .107 | .115 | 89.4 | .450 | .200 | .212 | 92.6 |
| **300** | **1.1** | **40** | -1.12 | .028 | .028 | 88.6 | .284 | .055 | .058 | 91.4 | -2.15 | .109 | .110 | 92.8 | .448 | .202 | .202 | 93.8 |
| **500** | **0.0** | **20** | -1.13 | .019 | .019 | 73.0 | .286 | .039 | .040 | 92.0 | -2.16 | .083 | .082 | 89.4 | .455 | .154 | .153 | 92.8 |
| **500** | **0.0** | **30** | -1.13 | .020 | .021 | 77.2 | .289 | .041 | .039 | 95.0 | -2.16 | .083 | .084 | 88.0 | .470 | .155 | .161 | 93.4 |
| **500** | **0.0** | **40** | -1.12 | .022 | .022 | 83.8 | .284 | .043 | .042 | 94.0 | -2.15 | .084 | .085 | 89.4 | .451 | .156 | .157 | 93.8 |
| **500** | **0.7** | **20** | -1.13 | .019 | .019 | 73.0 | .286 | .039 | .040 | 92.0 | -2.16 | .083 | .082 | 89.4 | .455 | .154 | .153 | 92.8 |
| **500** | **0.7** | **30** | -1.13 | .020 | .021 | 77.2 | .289 | .041 | .039 | 95.0 | -2.16 | .083 | .084 | 88.0 | .470 | .155 | .161 | 93.4 |
| **500** | **0.7** | **40** | -1.12 | .022 | .022 | 83.8 | .284 | .043 | .042 | 94.0 | -2.15 | .084 | .085 | 89.4 | .451 | .156 | .157 | 93.8 |
| **500** | **1.1** | **20** | -1.13 | .019 | .019 | 73.0 | .286 | .039 | .040 | 92.0 | -2.16 | .083 | .082 | 89.4 | .455 | .154 | .153 | 92.8 |
| **500** | **1.1** | **30** | -1.13 | .020 | .021 | 77.2 | .289 | .041 | .039 | 95.0 | -2.16 | .083 | .084 | 88.0 | .470 | .155 | .161 | 93.4 |
| **500** | **1.1** | **40** | -1.12 | .022 | .022 | 83.8 | .284 | .043 | .042 | 94.0 | -2.15 | .084 | .085 | 89.4 | .451 | .156 | .157 | 93.8 |

[1] Est: Average of the parameter estimates over 500 simulations

[2] SE: Average of estimated standard errors

[3] ESD: Empirical standard deviation of parameter estimates

[4] CP: Coverage probability of the proportion of simulations that the 95% confidence interval contains the true parameter values

**Table B.4:** Simulation results for the parameters associated with the conditional cumulative hazard from a gamma bridge survival model with no measurement error fit to marker data simulated from a gamma bridge process with measurement error.

| | | | $\beta_0$ | | | | $\beta_1$ | | | |
|---|---|---|---|---|---|---|---|---|---|---|
| **n** | log($\gamma$) | **%Cens** | Est[1] | SE[2] | ESD[3] | CP[4] | Est | SE | ESD | CP |
| **200** | **0.0** | **20** | -3.60 | .090 | .090 | 95.0 | .610 | .170 | .170 | 95.6 |
| **200** | **0.0** | **30** | -3.60 | .100 | .100 | 94.9 | .610 | .180 | .170 | 95.7 |
| **200** | **0.0** | **40** | -3.61 | .120 | .120 | 94.4 | .610 | .200 | .200 | 94.0 |
| **200** | **0.7** | **20** | -3.60 | .090 | .090 | 95.0 | .610 | .170 | .170 | 95.6 |
| **200** | **0.7** | **30** | -3.60 | .100 | .100 | 94.8 | .610 | .180 | .170 | 95.8 |
| **200** | **0.7** | **40** | -3.61 | .120 | .120 | 94.4 | .610 | .200 | .200 | 94.0 |
| **200** | **1.1** | **20** | -3.60 | .090 | .090 | 95.2 | .610 | .170 | .170 | 95.6 |
| **200** | **1.1** | **30** | -3.60 | .100 | .100 | 94.8 | .610 | .180 | .170 | 95.8 |
| **200** | **1.1** | **40** | -3.61 | .120 | .120 | 94.4 | .610 | .200 | .200 | 94.0 |
| **300** | **0.0** | **20** | -3.60 | .080 | .080 | 96.0 | .600 | .140 | .140 | 94.6 |
| **300** | **0.0** | **30** | -3.60 | .080 | .080 | 94.0 | .600 | .150 | .140 | 95.2 |
| **300** | **0.0** | **40** | -3.61 | .100 | .090 | 95.8 | .610 | .160 | .160 | 94.0 |
| **300** | **0.7** | **20** | -3.60 | .080 | .080 | 96.0 | .600 | .140 | .140 | 94.6 |
| **300** | **0.7** | **30** | -3.60 | .080 | .080 | 94.0 | .600 | .150 | .140 | 95.2 |
| **300** | **0.7** | **40** | -3.61 | .100 | .090 | 95.8 | .610 | .160 | .160 | 94.0 |
| **300** | **1.1** | **20** | -3.60 | .080 | .080 | 96.0 | .600 | .140 | .140 | 94.6 |
| **300** | **1.1** | **30** | -3.60 | .080 | .080 | 94.0 | .600 | .150 | .140 | 95.2 |
| **300** | **1.1** | **40** | -3.61 | .100 | .090 | 95.8 | .610 | .160 | .160 | 94.0 |
| **500** | **0.0** | **20** | -3.60 | .060 | .060 | 95.2 | .600 | .110 | .110 | 94.8 |
| **500** | **0.0** | **30** | -3.59 | .060 | .070 | 95.2 | .600 | .110 | .120 | 95.8 |
| **500** | **0.0** | **40** | -3.60 | .070 | .070 | 95.8 | .610 | .120 | .120 | 96.8 |
| **500** | **0.7** | **20** | -3.60 | .060 | .060 | 95.2 | .600 | .110 | .110 | 94.8 |
| **500** | **0.7** | **30** | -3.59 | .060 | .070 | 95.2 | .600 | .110 | .120 | 95.8 |
| **500** | **0.7** | **40** | -3.60 | .070 | .070 | 95.8 | .610 | .120 | .120 | 96.8 |
| **500** | **1.1** | **20** | -3.60 | .060 | .060 | 95.2 | .600 | .110 | .110 | 94.8 |
| **500** | **1.1** | **30** | -3.59 | .060 | .070 | 95.2 | .600 | .110 | .120 | 95.8 |
| **500** | **1.1** | **40** | -3.60 | .070 | .070 | 95.8 | .610 | .120 | .120 | 96.8 |

[1] Est: Average of the parameter estimates over 500 simulations
[2] SE: Average of estimated standard errors
[3] ESD: Empirical standard deviation of parameter estimates
[4] CP: Coverage probability of the proportion of simulations that the 95% confidence interval contains the true parameter values

# BIBLIOGRAPHY

# BIBLIOGRAPHY


Aalen, O. O. (1992), Modelling heterogeneity in survival analysis by the compound Poisson distribution, *The Annals of Applied Probability*, pp. 951–972.

Andersen, P. K., and R. D. Gill (1982), Cox's regression model for counting processes: a large sample study, *The Annals of Statistics*, pp. 1100–1120.

Anderson, J. R., K. C. Cain, and R. D. Gelber (1983), Analysis of survival by tumor response., *Journal of Clinical Oncology*, *1*(11), 710–719.

Andrinopoulou, E.-R., and D. Rizopoulos (2016), Bayesian shrinkage approach for a joint model of longitudinal and survival outcomes assuming different association structures, *Statistics in Medicine*, *35*(26), 4813–4823.

Andrinopoulou, E.-R., D. Rizopoulos, J. J. Takkenberg, and E. Lesaffre (2015), Combined dynamic predictions using joint models of two longitudinal outcomes and competing risk data, *Statistical Methods in Medical Research*, *26*(4), 1787–1801.

Arnold, B. C., and D. Strauss (1991), Pseudolikelihood estimation: Some examples, *Sankhyā: The Indian Journal of Statistics, Series B*, pp. 233–243.

Avramidis, A. N., P. L'ecuyer, and P.-A. Tremblay (2003), Efficient simulation of gamma and variance-gamma processes, in *Proceedings of the 2003 Winter Simulation Conference*, vol. 1, pp. 319–326.

Bertoin, J. (1998), *Lévy processes*, vol. 121 of Cambridge Tracts in Mathematics, Cambridge University Press, Cambridge.

Blanche, P., C. Proust-Lima, L. Loubère, C. Berr, J.-F. Dartigues, and H. Jacqmin-Gadda (2015), Quantifying and comparing dynamic predictive accuracy of joint models for longitudinal marker and time-to-event in presence of censoring and competing risks, *Biometrics*, *71*(1), 102–113.

Brody, D. C., L. P. Hughston, and A. Macrina (2008), Dam rain and cumulative gain, *Proceedings of the Royal Society of London A: Mathematical, Physical and Engineering Sciences*, *464*(2095), 1801–1822.

Bycott, P., and J. Taylor (1998), A comparison of smoothing techniques for cd4 data measured with error in a time-dependent Cox proportional hazards model, *Statistics in Medicine*, *17*(18), 2061–2077.

Commenges, D. (2002), Inference for multi-state models from interval-censored data, *Statistical Methods in Medical Research*, *11*(2), 167–182.

Cortese, G., T. A. Gerds, and P. K. Andersen (2013), Comparing predictions among competing risks models with time-dependent covariates, *Statistics in Medicine*, *32*(18), 3089–3101.

Dartigues, J.-F., M. Gagnon, P. Barberger-Gateau, L. Letenneur, D. Commenges, C. Sauvel, P. Michel, and R. Salamon (1992), The Paquid epidemiological program on brain ageing, *Neuroepidemiology*, *11*(Suppl. 1), 14–18.

de Leon, A. R., and B. Wu (2011), Copula-based regression models for a bivariate mixed discrete and continuous outcome, *Statistics in Medicine*, *30*(2), 175–185.

de Wreede, L. C., M. Fiocco, H. Putter, et al. (2011), mstate: An R package for the analysis of competing risks and multi-state models, *Journal of Statistical Software*, *38*(7), 1–30.

Efron, B., and R. J. Tibshirani (1994), *An introduction to the bootstrap*, CRC press.

Emura, T., M. Nakatochi, S. Matsui, H. Michimae, and V. Rondeau (2018), Personalized dynamic prediction of death according to tumour progression and high-dimensional genetic factors: Meta-analysis with a joint model, *Statistical Methods in Medical Research*, *27*(9), 2842–2858.

Ferrer, L., H. Putter, and C. Proust-Lima (2017), Individual dynamic predictions using landmarking and joint modelling: Validation of estimators and robustness assessment, arXiv:1707.03706 [stat.AP].

Fitzsimmons, P., J. Pitman, and M. Yor (1993), Markovian bridges: Construction, palm interpretation, and splicing, in *Seminar on Stochastic Processes, 1992*, pp. 101–134, Springer.

Foucher, Y., M. Giral, J. Soulillou, and J. Daures (2010), A flexible semi-Markov model for interval-censored data and goodness-of-fit testing, *Statistical Methods in Medical Research*, *19*(2), 127–145.

Ganjali, M., and T. Baghfalaki (2015), A copula approach to joint modeling of longitudinal measurements and survival times using Monte Carlo expectation-maximization with application to AIDS studies, *Journal of Biopharmaceutical Statistics*, *25*(5), 1077–1099.

Gjessing, H. K., O. O. Aalen, and N. L. Hjort (2003), Frailty models based on Lévy processes, *Advances in Applied Probability*, *35*(2), 532–550.

Gong, Q., and D. E. Schaubel (2013), Partly conditional estimation of the effect of a time-dependent factor in the presence of dependent censoring, *Biometrics*, *69*(2), 338–347.

Henderson, R., P. Diggle, and A. Dobson (2000), Joint modelling of longitudinal measurements and event time data, *Biostatistics*, *1*(4), 465–480.

Hougaard, P. (2012), *Analysis of multivariate survival data*, Springer Science & Business Media.

Hoyle, E. (2010), Information-based models for finance and insurance, Ph.D. thesis, Imperial College London.

Huang, X., F. Yan, J. Ning, Z. Feng, S. Choi, and J. Cortes (2016), A two-stage approach for dynamic prediction of time-to-event distributions, *Statistics in Medicine*, *35*(13), 2167–2182.

Jewell, N. P., and J. Kalbfleisch (1996), Marker processes in survival analysis, *Lifetime Data Analysis*, *2*(1), 15–29.

Jewell, N. P., and J. D. Kalbfleisch (1992), Marker models in survival analysis and applications to issues associated with AIDS, in *AIDS Epidemiology*, pp. 211–230, Springer.

Jewell, N. P., and J. P. Nielsen (1993), A framework for consistent prediction rules based on markers, *Biometrika*, *80*(1), 153–164.

Joe, H., and J. J. Xu (1996), The estimation method of inference functions for margins for multivariate models, *Technical Report*.

Kalbfleisch, J. D., and R. L. Prentice (2011), *The statistical analysis of failure time data*, vol. 360, John Wiley & Sons.

Lawless, J., and M. Crowder (2004), Covariates and random effects in a gamma process model with application to degradation and failure, *Lifetime Data Analysis*, *10*(3), 213–227.

Lim, E., et al. (2008), Longitudinal study of the profile and predictors of left ventricular mass regression after stentless aortic valve replacement, *The Annals of Thoracic Surgery*, *85*(6), 2026–2029.

Long, J. S., and L. H. Ervin (2000), Using heteroscedasticity consistent standard errors in the linear regression model, *The American Statistician*, *54*(3), 217–224.

Maziarz, M., P. Heagerty, T. Cai, and Y. Zheng (2017), On longitudinal prediction with time-to-event outcome: Comparison of modeling options, *Biometrics*, *73*(1), 83–93.

Nicolaie, M., J. Houwelingen, T. Witte, and H. Putter (2013), Dynamic prediction by landmarking in competing risks, *Statistics in Medicine*, *32*(12), 2031–2047.

Njagi, E. N., G. Molenberghs, D. Rizopoulos, G. Verbeke, M. G. Kenward, P. Dendale, and K. Willekens (2016), A flexible joint modeling framework for longitudinal and time-to-event data with overdispersion, *Statistical Methods in Medical Research*, *25*(4), 1661–1676.

Parast, L., and T. Cai (2013), Landmark risk prediction of residual life for breast cancer survival, *Statistics in Medicine*, *32*(20), 3459–3471.

Peng, L., and Y. Huang (2007), Survival analysis with temporal covariate effects, *Biometrika*, *94*(3), 719–733.

Philipson, P., I. Sousa, P. J. Diggle, P. Williamson, R. Kolamunnage-Dona, R. Henderson, and G. L. Hickey (2017), *joineR: Joint modelling of repeated measurements and time-to-event data*, R package version 1.2.2.

Pitt, M., D. Chan, and R. Kohn (2006), Efficient Bayesian inference for gaussian copula regression models, *Biometrika*, *93*(3), 537–554.

Prenen, L., R. Braekers, and L. Duchateau (2017), Extending the Archimedean copula methodology to model multivariate survival data grouped in clusters of variable size, *Journal of the Royal Statistical Society: Series B (Statistical Methodology)*, *79*(2), 483–505.

Putter, H. (2015), dynpred: Companion package to "Dynamic prediction in clinical survival analysis.", *R package version 0.1*, *2*.

Putter, H., and H. C. Van Houwelingen (2015), Dynamic frailty models based on compound birth–death processes, *Biostatistics*, *16*(3), 550–564.

Putter, H., and H. C. van Houwelingen (2016), Understanding landmarking and its relation with time-dependent Cox regression, *Statistics in Biosciences*, pp. 1–15.

Rizopoulos, D. (2011), Dynamic predictions and prospective accuracy in joint models for longitudinal and time-to-event data, *Biometrics*, *67*(3), 819–829.

Rizopoulos, D., G. Verbeke, E. Lesaffre, and Y. Vanrenterghem (2008a), A two-part joint model for the analysis of survival and longitudinal binary data with excess zeros, *Biometrics*, *64*(2), 611–619.

Rizopoulos, D., G. Verbeke, and G. Molenberghs (2008b), Shared parameter models under random effects misspecification, *Biometrika*, *95*(1), 63–74.

Rizopoulos, D., M. Murawska, E.-R. Andrinopoulou, G. Molenberghs, J. J. Takkenberg, and E. Lesaffre (2013), Dynamic predictions with time-dependent covariates in survival analysis using joint modeling and landmarking, arXiv:1306.6479 [stat.AP].

Rizopoulos, D., L. A. Hatfield, B. P. Carlin, and J. J. Takkenberg (2014), Combining dynamic predictions from joint models for longitudinal and time-to-event data using bayesian model averaging, *Journal of the American Statistical Association*, *109*(508), 1385–1397.

Rizopoulos, D., G. Molenberghs, and E. M. Lesaffre (2017), Dynamic predictions with time-dependent covariates in survival analysis using joint modeling and landmarking, *Biometrical Journal*, *59*(6), 1261–1276.

Shi, M., J. M. Taylor, and A. Muñoz (1996), Models for residual time to AIDS, *Lifetime Data Analysis*, *2*(1), 31–49.

Shih, J. H., and T. A. Louis (1995), Inferences on the association parameter in copula models for bivariate survival data, *Biometrics*, pp. 1384–1399.

Sklar, A. (1959), Fonctions de répartition à n dimensions et leurs marges, *Publications de l'Institut de Statistique de l'Université de Paris*, *8*, 229–231.

Song, P. X.-K., M. Li, and Y. Yuan (2009), Joint regression analysis of correlated data using Gaussian copulas, *Biometrics*, *65*(1), 60–68.

Song, X.-K. (2007), *Correlated data analysis: Modeling, analytics, and applications*, Springer Science & Business Media.

Spiekerman, C. F., and D. Lin (1998), Marginal regression models for multivariate failure time data, *Journal of the American Statistical Association*, *93*(443), 1164–1175.

Suresh, K., J. M. Taylor, D. E. Spratt, S. Daignault, and A. Tsodikov (2017), Comparison of joint modeling and landmarking for dynamic prediction under an illness-death model, *Biometrical Journal*, *59*(6), 1277–1300.

Taylor, J. M., W. Cumberland, and J. Sy (1994), A stochastic model for analysis of longitudinal AIDS data, *Journal of the American Statistical Association*, *89*(427), 727–736.

Taylor, J. M., M. Yu, and H. M. Sandler (2005), Individualized predictions of disease progression following radiation therapy for prostate cancer, *Journal of Clinical Oncology*, *23*(4), 816–825.

Taylor, J. M., Y. Park, D. P. Ankerst, C. Proust-Lima, S. Williams, L. Kestin, K. Bae, T. Pickles, and H. Sandler (2013), Real-time individual predictions of prostate cancer recurrence using joint models, *Biometrics*, *69*(1), 206–213.

Thompson, I. M., P. J. Goodman, C. M. Tangen, H. L. Parnes, L. M. Minasian, P. A. Godley, M. S. Lucia, and L. G. Ford (2013), Long-term survival of participants in the prostate cancer prevention trial, *New England Journal of Medicine*, *369*(7), 603–610.

Thompson, I. M., et al. (2003), The influence of finasteride on the development of prostate cancer, *New England Journal of Medicine*, *349*(3), 215–224.

Touraine, C., P. Joly, and T. Gerds (2013), SmoothHazard: Fitting illness-death model for interval-censored data, *R package version*, *1*(9).

Tsiatis, A. A., and M. Davidian (2004), Joint modeling of longitudinal and time-to-event data: An overview, *Statistica Sinica*, pp. 809–834.

van Houwelingen, H., and H. Putter (2011), *Dynamic prediction in clinical survival analysis*, CRC Press.

van Houwelingen, H. C. (2007), Dynamic prediction by landmarking in event history analysis, *Scandinavian Journal of Statistics*, *34*(1), 70–85.

Vaupel, J. W., K. G. Manton, and E. Stallard (1979), The impact of heterogeneity in individual frailty on the dynamics of mortality, *Demography*, *16*(3), 439–454.

Wang, Y., and J. M. G. Taylor (2001), Jointly modeling longitudinal and event time data with application to acquired immunodeficiency syndrome, *Journal of the American Statistical Association*, *96*(455), 895–905.

Yashin, A. I., and K. G. Manton (1997), Effects of unobserved and partially observed covariate processes on system failure: A review of models and estimation strategies, *Statistical Science*, pp. 20–34.

Zeger, S. L., and K.-Y. Liang (1986), Longitudinal data analysis for discrete and continuous outcomes, *Biometrics*, pp. 121–130.

Zheng, Y., and P. J. Heagerty (2005), Partly conditional survival models for longitudinal data, *Biometrics*, *61*(2), 379–391.